Membrane-targeting antimicrobials as promising resistance-breaking antibiotic candidates.

Jessica Alice Buttress

Thesis submitted in partial fulfilment of the requirements of the regulation
for the degree of Doctor of Philosophy

Newcastle University

Faculty of Medical Sciences

Biosciences Institute

Centre for Bacterial Cell Biology

June 2022

Abstract

Antimicrobial resistance has rapidly become one of the biggest threats to global health; a crisis only exacerbated by a lack of new antibiotic development. Currently, the bacterial cell envelope is a primary target of several antibiotics. This structure differs between Gram-positive and Gram-negative organisms; the most striking variation being the presence of an additional Gram-negative outer membrane. However, developing antimicrobial agents with similar modes of action to current cell envelope-targeting antimicrobials such as β-lactams and vancomycin may remain susceptible to pre-existing bacterial resistance mechanisms. Therefore, there is the urgent need for agents acting on thus far unexploited targets.

Two such emerging strategies are targeting of the bacterial cytoplasmic membrane in both Gram-positive and Gram-negative bacteria and disrupting the outer membrane in Gram-negative bacteria to improve efficacy of already approved antibiotics. Therefore, the aim of this thesis was to develop multiple fluorescence-based assays to screen for these effects in both novel natural product compounds and current clinically used antibiotics.

Through this, I was able to develop fluorescence-based assays for the detection of both inner membrane depolarisation and permeabilisation in the Gram-positive and Gram-negative model organisms, *Bacillus subtilis* and *Escherichia coli* respectively, and techniques investigating outer membrane permeabilisation and multidrug efflux inhibition in *E. coli*. Implementation of these screens allowed for the identification of several *Actinomycete*-derived antimicrobial extracts with cytoplasmic membrane effects in *B. subtilis*. Preliminary mode of action studies of these were also performed using further microscopic experimentation. Finally, I utilised these techniques to further elucidate the mode of action of two clinically relevant membrane-targeting antimicrobials: daptomycin and octenidine, and investigate the membrane effects of PanT toxins identified from various bacteria and bacteriophages.

Acknowledgements

Firstly, I would like to thank my supervisor Henrik Strahl. I know (and I say this with 100% confidence) that I would not have completed a PhD without you as a PI. Your commitment and passion for science, as well as your utter patience and endless encouragement have built my confidence as a researcher and helped me excel both in and out of the lab. My thanks also go to all members of our group, past and present: Sandra Laborda Anadón, Maria Dakes Stavrakakis, Alan Koh, Maddie Humphrey, Laura Dobby and Jamie Grimshaw. You are all the most supportive and caring people I have ever met, and friends I know I have made for life. Special thanks go to Maddie, who has been a constant source of laughter, reassurance and necessary pub trips.

I would also like to thank my friends Dan, Grace and Calum, who welcomed me with open arms from the very beginning and made me feel so at home in both a new workplace and city.

Of course, I would like to thank my family: my brother James, for telling me not to do a PhD in the first place, but if I did, to take as much holiday as possible, and my Mum and Dad, Viv and Pete, who are my whole world. Thank you for believing in me even when I don't believe in myself, and being the most patient, loving and supportive parents. I owe everything and more to the both of you.

Finally, I wish to dedicate this thesis to my beautiful cousin Charlotte, who was taken from this world far too soon. Your memory will live on forever.

Research output

Publications

Buttress, J.A., Halte, M., te Winkel, J.D., Erhardt, M., Popp, P.F. and Strahl, H. (2022). A guide for membrane potential measurements in Gram-negative bacteria using voltage-sensitive dyes. *Microbiology. 168(9)*. https://doi.org/10.1099/mic.0.001227

Malanovic, N., **Buttress, J.A.**, Vejzovic, D., Ön, A., Piller, P., Kolb, D., Lohner, K. and Strahl, H. (2022). Disruption of the Cytoplasmic Membrane Structure and Barrier Function Underlies the Potent Antiseptic Activity of Octenidine in Gram-Positive Bacteria. *Applied and Environmental Microbiology*. https://doi.org/10.1128/aem.00180-22

Kurata, T., Saha, C.K., **Buttress, J.A.**, Mets, T., Brodiazhenko, T., Turnbull, K.J., Awoyomi, O.F., Oliveira, S.R.A., Jimmy, S., Ernits, K., Delannoy, M., Persson, K., Tenson, T., Strahl, H., Hauryliuk, V. and Atkinson, G.C. (2022). A hyperpromiscuous antitoxin protein domain for the neutralization of diverse toxin domains. *Proceedings of the National Academy of Sciences of the United States of America. 119*(6). https://doi.org/10.1073/pnas.2102212119

Gohrbandt, M., Lipski, A., Grimshaw, J.W., **Buttress, J.A.**, Baig, Z., Herkenhoff, B., Walter, S., Kurre, R., Deckers-Hebestreit, G. and Strahl, H. (2022). Low membrane fluidity triggers lipid phase separation and protein segregation in living bacteria. *The EMBO Journal. 41*(5). https://doi.org/10.15252/embj.2021109800

Oral presentations

"Daptomycin-induced autolysis and membrane depolarisation in *Bacillus subtilis*", Subtillery Virtual Conference, 14th -18th June 2021.

Poster presentations

"Daptomycin-induced autolysis in *Bacillus subtilis*: *in vivo* evidence against membrane pore formation as its principal mode of action", 75th Microbiology Society Annual Conference, 4th – 7th April 2022.

Table of Figures

x

Table of Tables

List of abbreviations

ADP	adenosine diphosphate
ATP	adenosine triphosphate
ATPase	ATP hydrolase
a.u.	arbituary units
B. subtilis	*Bacillus subtilis*
BGC	biosynthetic gene cluster
Ca^{2+}	calcium
CCCP	carbonyl cyanide m-chlorophenyl hydrazone
CL	cardiolipin
Da	dalton
DAPI	4',6-diamidino-2-phenylindole
DiI-C12	1,1'-didodecyl-3,3,3',3'-tetramethylindocarbocyanine perchlorate
DMF	dimethyl formamide
DMSO	dimethyl sulphoxide
E. coli	*Escherichia coli*
ECF	extracytoplasmic function
EDTA	ethylenediaminetetra-acetic acid disodium salt dihydrate
FM5-95	N-(3-trimethylammoniumpropyl)-4-(6-(4-(Diethylamino)phenyl) hexatrienyl)pyridinium dibromide
GFP	green fluorescent protein
GlcNAc	N-acetylglucosamine
GTP	guanosine triphosphate
GYM	glucose-yeast extract-malt extract
H^+	proton
HEPES	4-(2-hydroxyethyl)-1-piperazineethanesulfonic acid
K^+	potassium
LB	Lysogeny broth
LPS	lipopolysaccharide
LTA	lipoteichoic acid
Mg^{2+}	magnesium
MIC	minimal inhibitory concentration
mRNA	messenger RNA
msfGFP	monomeric superfolded GFP

MSM	magnesium-sucrose-maleic acid
MurNAc	N-acetylmuramic acid
mV	millivolt
NA	nutrient agar
Na$^+$	sodium
NB	nutrient broth
NPN	1-N-phenylnaphthylamine
PBS	phosphate buffered saline
PE	phosphatidylethanolamine
PG	phosphatidylglycerol
PMF	proton motive force
(p)ppGpp	guanosine pentaphosphate
RIF	region of increased fluidity
rpm	revolutions per minute
sfGFP	superfolded GFP
SIM	structured illumination microscopy
TCS	two-component system
WT	wild type
WTA	wall teichoic acid

Table of Contents

Chapter 1 – Introduction

1.1 – The bacterial cell envelope

The bacterial cell envelope is a complex multi-layered structure that serves to provide structural integrity to the cell, and protect it from both internal osmotic pressures and stressors from the external environment. The cell envelopes of most bacteria fall under two main categories. Gram-negative bacteria are surrounded by a cytoplasmic membrane, a thin peptidoglycan cell wall and an additional outer membrane. Gram-positive bacteria, on the other hand, lack an outer membrane but are surrounded by a thicker peptidoglycan cell wall (Fig. 1). Another difference is the presence of cell surface polymers known as teichoic acids in the Gram-positive cell envelope. These can be either cytoplasmic membrane-bound, lipoteichoic acids (LTAs), or anchored to peptidoglycan, wall teichoic acids (WTAs). For this thesis, I will discuss all components of the bacterial cell envelope as both *B. subtilis* and *E. coli* (the model Gram-positive and Gram-negative organism respectively) are used throughout this study.

1.1.1 – *The Gram-negative outer membrane*

Starting from the outside of the cell and proceeding in, the outer membrane is a unique asymmetric lipid bilayer. The inner leaflet is composed of phospholipids, whilst the outer leaflet consists almost exclusively of large glycolipids termed lipopolysaccharides [LPSs; (Kamio and Nikaido, 1976)]. The phospholipid composition of the inner leaflet is similar to that of the Gram-negative cytoplasmic membrane, which is discussed in detail below, but in short contains three main phospholipid species: phosphatidylethanolamine (PE), phosphatidylglycerol (PG) and cardiolipin (CL). Embedded within this membrane environment are also a large proportion of integral membrane proteins called outer membrane proteins, or OMPs; examples of which will be expanded upon later.

LPS is a complex molecule that consists of three distinct units: (i) the hydrophobic lipid A formed from phosphorylated glucosamine disaccharide, attached to up to seven acyl chains, (ii) a relatively short oligosaccharide core, which contains anionic groups and (iii) a distal O-antigen region containing varying numbers of oligosaccharide repeats (Fig. 1) (Nikaido, 2003). LPS synthesis occurs at the cytoplasmic membrane, with lipid A and the core oligosaccharide produced on the cytoplasmic side whilst the O antigen is synthesised independently on both faces of the cytoplasmic membrane (Bertani and Ruiz, 2018). The core-lipid A molecule is flipped to the periplasmic side by the ATP-binding cassette (ABC) transporter, MsbA (Zhou *et al.*, 1998), where it is subsequently
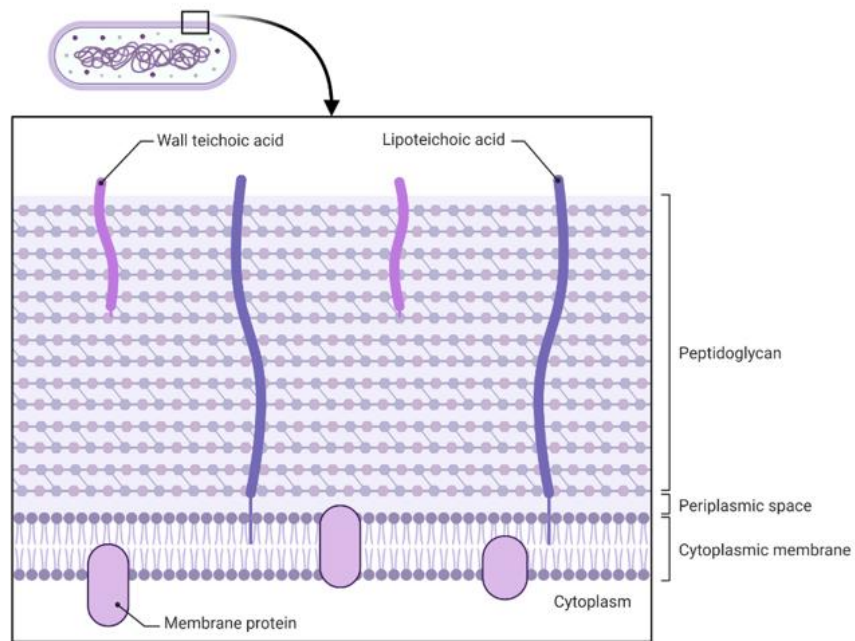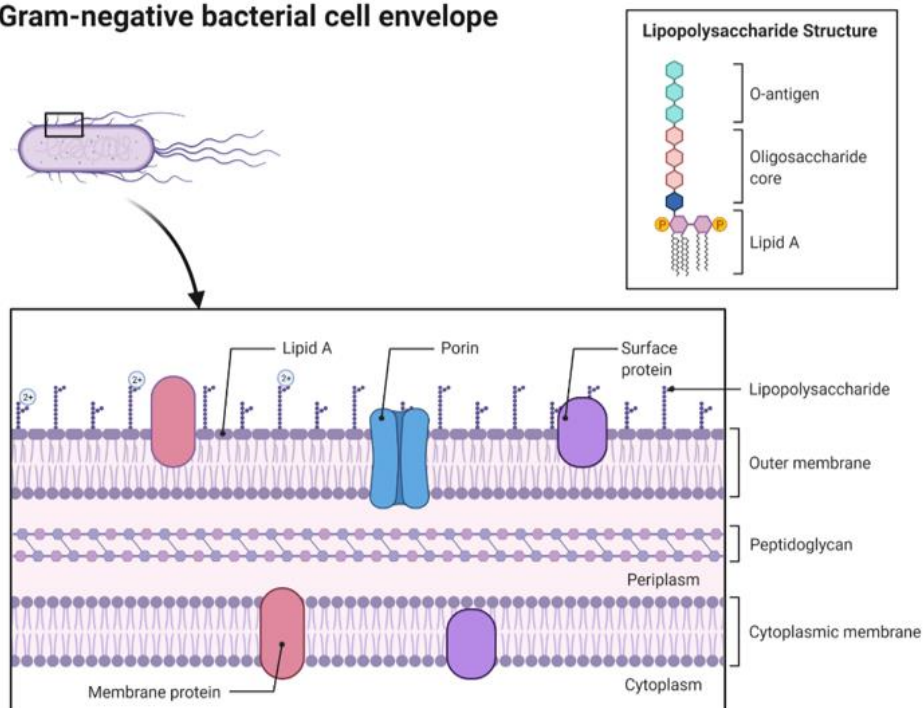
Figure 1: Graphical representations of the Gram-positive (top panel) and Gram-negative (bottom panel) bacterial cell envelopes, featuring the generic structure of a lipopolysaccharide molecule (insert). Both are expanded upon in the text, but note the presence of an additional outer membrane in Gram-negatives; whilst the Gram-positive cell envelope contains many more layers of peptidoglycan and anionic polymers known as teichoic acids. Created with BioRender.com.

joined to the O-antigen portion by the ligase WaaL (Raetz and Whitfield, 2002). Transport of LPS to the outer membrane is mediated by the LPS transport (Lpt) system, which involves seven essential and conserved proteins (LptA-G). This complex spans all compartments of the cell and is responsible for extracting LPS from the cytoplasmic membrane, transporting it across the periplasmic space, and inserting it into the outer leaflet of the outer membrane (Okuda *et al.*, 2016).

In contrast, how phospholipids are transported between the inner and outer membrane is less well-studied; however, it is known that movement is bidirectional (Jones and Osborn, 1977; Donohue-Rolfe and Schaechter, 1980; Langley, Hawrot and Kennedy, 1982). One proposed system is the Mla pathway, which commonly consists of 6 proteins, MlaA-F. *E. coli* mutants defective in this complex have been shown to exhibit increased sensitivity to detergents and hydrophobic compounds (a hallmark of outer membrane destabilisation) (Malinverni and Silhavy, 2009) and it has been demonstrated that phospholipids readily bind 3 Mla proteins: MlaA, MlaC, and MlaD (Thong *et al.*, 2016; Abellón-Ruiz *et al.*, 2017; Ekiert *et al.*, 2017). Despite this, the directionality of phospholipid transport mediated by the Mla system is still heavily debated, with reports of both anterograde (from the cytoplasmic membrane to the outer membrane; Hughes *et al.*, 2019; Kamischke *et al.*, 2019) and retrograde transport (from the outer membrane to the cytoplamsic membrane; Malinverni and Silhavy, 2009; Powers, Simpson and Stephen Trent, 2020) (Fig. 2).
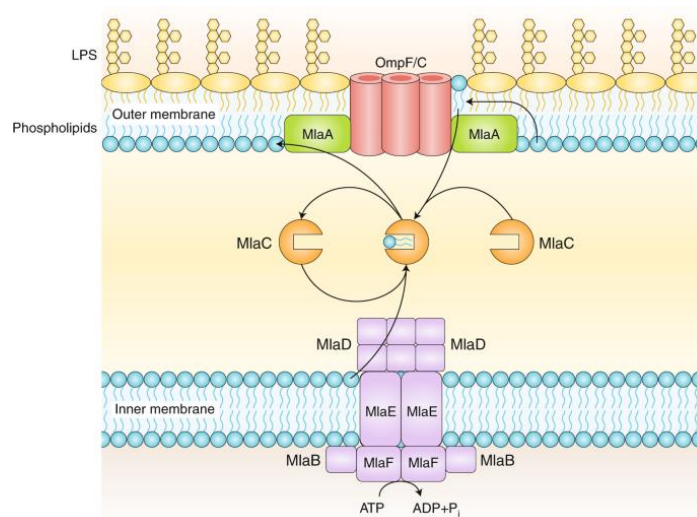
Figure 2: Graphical schematic of Mla-mediated phospholipid transport in Gram-negative bacteria. In brief, phospholipids that have migrated to the outer leaflet of the outer membrane can translocate back to the periplasm via MlaAC in a retrograde transport process. In contrast, cytoplasmic membrane phospholipids can also be transported from MlaD to MlaC in the anterograde direction. From Bishop (2019).

A known pathway of retrograde transport, however, is the Tol-Pal complex. Again, loss of Tol-Pal function was shown to perturb the outer membrane permeability barrier (Cascales *et al.*, 2000; Llamas, Ramos and Rodriguez-Herva, 2000). It was subsequently discovered that this caused defects in outer membrane lipid asymmetry due to accumulation of phospholipids in the outer membrane outer leaflet (Shrivastava, Jiang and Chng, 2017), implicating the role of Tol-Pal in retrograde phospholipid transport and maintaining outer membrane lipid homeostasis.

LPS is well-known for its role in activating the host innate immune system in response to Gram-negative infection, however its major function is to produce an effective bacterial permeability barrier, preventing the entry of inhibitory compounds such as antibiotics. Under normal growth conditions, the acyl chains of LPS are all saturated. This facilitates tight packing, creating a gel-like state of low fluidity mostly impermeable to hydrophobic molecules (Labischinski *et al.*, 1985). Furthermore, strong lateral interactions exist between neighbouring LPS molecules due to the cross-bridging action of divalent cations such as Mg^{2+} and Ca^{2+} (Takeuchi and Nikaido, 1981). Nevertheless, LPS can be targeted by antibacterial agents that perturb the organisation of the outer membrane bilayer. For example, polymyxins (the class of antibiotics that includes the last-resort agents polymyxin B and colistin) compete for binding to LPS with divalent cations. The displacement of the lateral interactions results in destabilisation of the LPS outer leaflet, allowing penetration of polymyxins into the periplasm and for the fatty acid tail region to interact with and permeabilise the cytoplasmic membrane (Band and Weiss, 2015). Polymyxin derivatives such as polymyxin B nonapeptide, which lack the fatty acid tail (Fig. 3), are less bactericidal or not inhibitory at all, but interestingly retain a notable outer membrane-permeabilising action (Vaara and Vaara, 1983) and can sensitise bacteria to hydrophobic antibiotics such as rifampin; otherwise restricted by the LPS leaflet of the outer membrane. Therefore design of such permeabiliser compounds could be of therapeutic value to widen the spectrum of already approved antibiotics.

Furthermore, due to their limited permeability for hydrophilic solutes, Gram-negative outer membranes contain non-specific pore forming OMPs termed porins, which allow the influx and efflux of small (<600 Da) water-soluble nutrients and waste respectively (Nikaido, Rosenberg and Foulds, 1983). Therefore, another mechanism by which
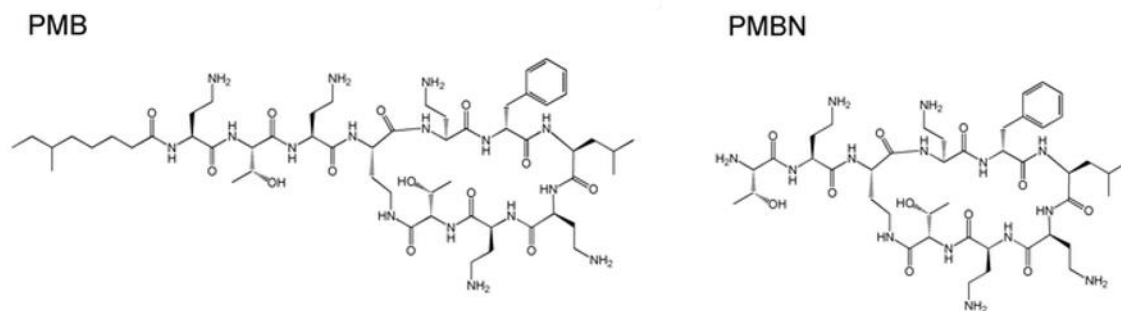
Figure 3: The chemical structures of the last-resort antibiotic polymyxin B (PMB) and its derivative polymyxin B nonapeptide (PMBN). Note the absence of the fatty acid tail in PMBN, which abolishes its bactericidal activity.

compounds can overcome cell envelope integrity is diffusion through the outer membrane porins. This is the case for small hydrophilic antibiotics such as the cell-wall targeting β-lactams (Harder, Nikaido and Matsuhashi, 1981; Jaffe, Chabbert and Semonin, 1982).

Finally, antibiotics may gain access to Gram-negative organisms if their multidrug efflux systems, that actively extrude compounds from the cell, are defective. I will expand on these complexes later in this thesis, but efflux pump inhibitors are thus another focus of research attention as a method of potentiating the entry of currently used antibiotics (Lomovskaya *et al.*, 2001; Vargiu *et al.*, 2014; Plé *et al.*, 2022).

1.1.2 – The peptidoglycan cell wall

The bacterial cell wall is integral to cell physiology and survival and thus is responsible for a number of roles, including maintaining cell shape (Höltje, 1998; Scheffers and Pinho, 2005), anchoring other Gram-positive surface components such as enzymes (Dramsi *et al.*, 2008) and teichoic acids (which I will discuss in more detail later in this chapter), but most crucially protecting the cell against lysis by withstanding the outward pressure imposed by the high osmolarity of the cytoplasm.

In both Gram-negative and Gram-positive bacteria, the cell wall comprises a mesh-like peptidoglycan sacculus that surrounds the cytoplasmic membrane. Peptidoglycan is composed of long glycan strands formed from alternating N-acetylglucosamine (GlcNAc) and N-acetylmuramic acid (MurNAc) residues. Attached to the MurNAc group is a species-dependent series of of L- and D-amino acids, most commonly a pentapeptide with the sequence L-Ala-γ-D-Glu-L-lysine (or -meso-diaminopimelic acid)-D-Ala-D-Ala (Al-Dabbagh, Mengin-Lecreulx and Bouhss, 2008), which can be cross-linked with each other.

Peptidoglycan synthesis begins in the cytoplasm, with the synthesis of UDP-GlcNAc from fructose-6-phosphate by the Glm enzymes (Rani and Khan, 2016) and UDP-N-acetylmuramyl-pentapeptide (UDP-MurNAc-5P) from UDP-GlcNAc by the Mur enzymes (Fig. 4) (Lovering, Safadi and Strynadka, 2012). UDP-MurNAc-5P is then coupled to membrane-embedded undecaprenyl phosphate (UP) by the integral membrane enzyme phospho-MurNAc-pentapeptide translocase, or MraY, yielding the product undecaprenyl-pyrophosphoryl-MurNAc-pentapeptide, more commonly known as lipid I (Higashi, Strominger and Sweeley, 1967). To form UP, undecaprenyl pyrophosphate (UPP) synthase (UppS) catalyses eight sequential condensations of isopentenyl pyrophosphate with farnesyl pyrophosphate to produce UPP (Apfel *et al.*, 1999), which is then dephosphorylated by UPP phosphatase (UppP) (El Ghachi *et al.*, 2004). Lipid I is then coupled with UDP-GlcNAc by the glycosyltransferase MurG, forming undecaprenyl-pyrophosphoryl-MurNAc-pentapeptide-GlcNAc, typically referred to as lipid II (Bouhss *et al.*, 2008). The now mature cell wall precursor lipid II is subsequently translocated to the outer leaflet of the membrane by a flippase, postulated to be MurJ (Butler *et al.*, 2013). It is then incorporated into existing peptidoglycan by penicillin binding proteins (PBPs), which can possess both glycosyltransferase and transpeptidase activities, or SEDS (shape, elongation, division and sporulation) proteins such as FtsW and RodA, which are membrane-bound glycosyltransferases (Meeske *et al.*, 2016; Emami *et al.*, 2017). The remaining UPP is then released and dephosphorylated back to UP where it can be further reloaded with peptidoglycan precursors. This recycling is critical, not only for cell wall synthesis, but for other cellular processes that share the lipid carrier, such as teichoic acid synthesis in Gram-positives (Watkinson, Hussey and Baddiley, 1971) and lipid A phosphorylation and O-antigen synthesis in Gram-negatives (Wright *et al.*, 1967; Touzé *et al.*, 2008). UPP recycling can therefore be exploited by antibacterial compounds, an example of which is bacitracin, which binds as a complex with metallic ions to UPP, sequestering it and preventing its dephosphorylation (Siewert and Strominger, 1967; Storm and Strominger, 1973).
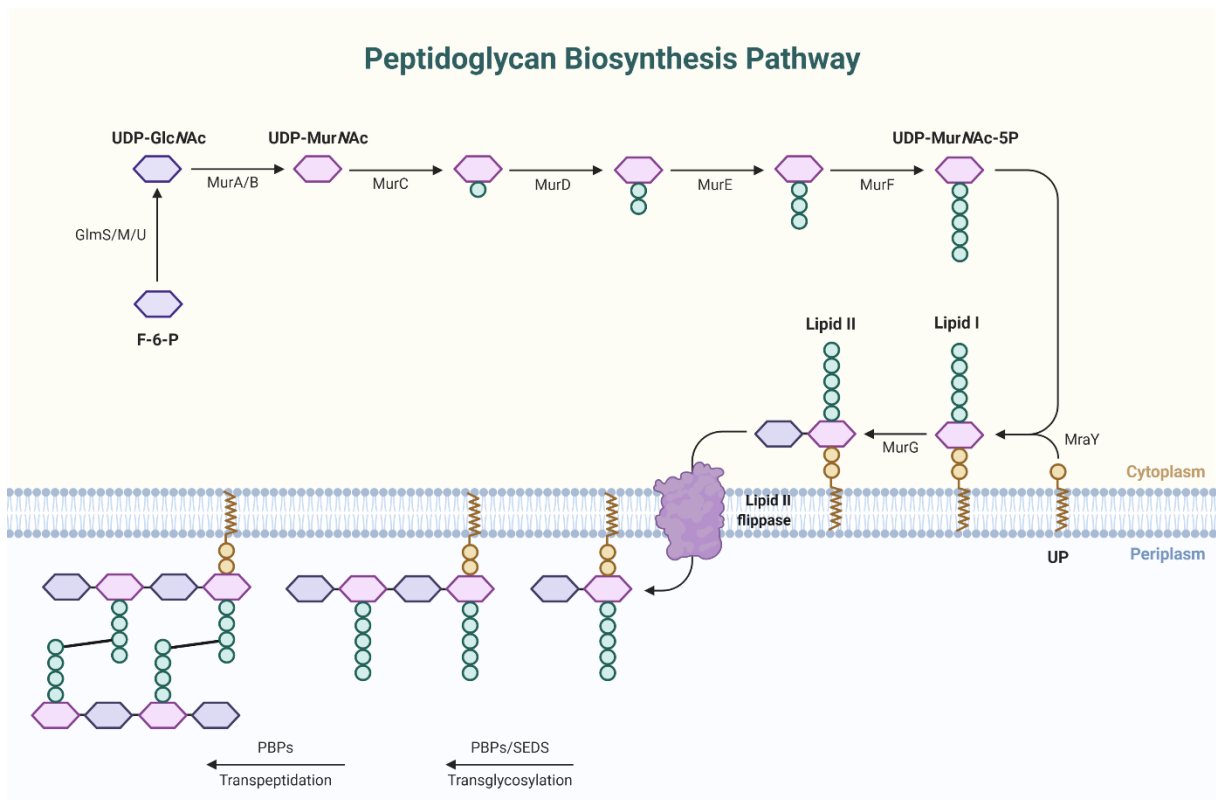
Figure 4: Simplified schematic of peptidoglycan biosynthesis. In brief, UDP-MurNAc-5P is formed by the sequential addition of amino acids to UDP-MurNAc by the Mur ligases. It is then coupled to membrane-embedded undecaprenyl phosphate (UP) by MraY and joined to UDP-GlcNAc by MurG, forming lipid I and II respectively. Lipid II is flipped across the cytoplasmic membrane, where it is added to the exisiting glycan strand (transglycosylation) and the pentapeptides are cross-linked (transpeptidation) by penicillin binding proteins (PBPs) or SEDS proteins. Created with BioRender.com.

Peptidoglycan synthesis and insertion are regulated by distinct components of the bacterial cytoskeleton at different phases in the cell cycle. Actin-like MreB proteins assemble a large multi-protein complex, known as the Rod complex or elongasome, in several rod-shaped bacteria including *B. subtilis* and *E. coli,* which is responsible for lateral cell wall synthesis. Later in the cell cycle, orientation of peptidoglycan synthesis is shifted by the tubulin-like protein FtsZ, which is conserved in all bacteria and recruits proteins to midcell to form a structure called the divisome; as discussed in depth below.

Finally, to facilitate expansion of the cell wall during cell elongation and division, it is necessary to break bonds in the existing peptidoglycan network, allowing insertion of newly synthesised material. This function is performed by peptidoglycan hydrolases, or autolysins, which are universal among bacteria that possess a peptidoglycan cell wall. Autolysins of importance to this project will be described later in this chapter.

1.1.3 – The cytoplasmic membrane

One of the hallmarks of eukaryotic cells are membrane-bound organelles, which are absent from bacteria. Consequently all membrane-associated processes, including energy production, lipid biosynthesis, protein secretion and transport are performed in bacteria at the cytoplasmic membrane. The bacterial cytoplasmic membrane exhibits a classical lipid bilayer structure in which proteins are integrally or peripherally embedded, first described by Singer and Nicolson in 1972 as "The fluid mosaic model". Membranes are primarily formed from phospholipids, which are highly polar molecules, containing a hydrophilic glycerophosphate head group and two hydrophobic fatty acid tails. Bacteria synthesise a number of phospholipids that can vary in fatty acid chain length, saturation, branching and the structure, size, and charge of head groups. Localisation and content of phospholipid variants can subsequently alter biologically relevant membrane properties, eliciting direct effects on membrane-associated proteins and processes (Strahl and Errington, 2017). In particular, determination of both transmembrane potential and membrane fluidity will be reviewed later in this chapter.

The phospholipid composition of the cytoplasmic membrane differs between bacterial species and variations even occur within the same species when exposed to different environmental conditions including temperature, osmolality and pH (Marr and Ingraham, 1962; Catucci *et al.*, 2004; Ohniwa, Kitabayashi and Morikawa, 2013). Both the outer and cytoplasmic membranes of *E. coli* are predominately composed of the zwitterionic PE (~80%), but *E. coli* additionally synthesises the anionic lipids PG and CL [~15% and 5% respectively; (Raetz and Dowhan, 1990)]. In contrast, the membrane of *B. subtilis* is more complex than that of *E. coli*, containing PE (~49%), PG (~25%) and CL (~8%), but also other lipid species including glucolipids (mono-, di- and triglucosyldiacylglycerol) and positively charged lysyl-phosphatidylglycerol (lysyl-PG) (López *et al.*, 1998; Lopez *et al.*, 2006). Other essential lipids include undecaprenyl carriers, as discussed in depth in the previous section. The fatty acid composition of the cytoplasmic membrane also differs between *E. coli* and *B. subtilis*: the former primarily producing saturated (SFA), unsaturated (UFA) and cyclopropane fatty acids (CFA) (Magnuson *et al.*, 1993; Wang and Cronan, 1994); whilst the latter predominantly synthesises branched chain saturated fatty acids (BCFA; Fig. 5) (Kaneda, 1977). Modulation of the ratio between lipids carrying these fatty acids is the

most common mechanism by which bacteria maintain stable levels of membrane fluidity in response to changes in their environment.
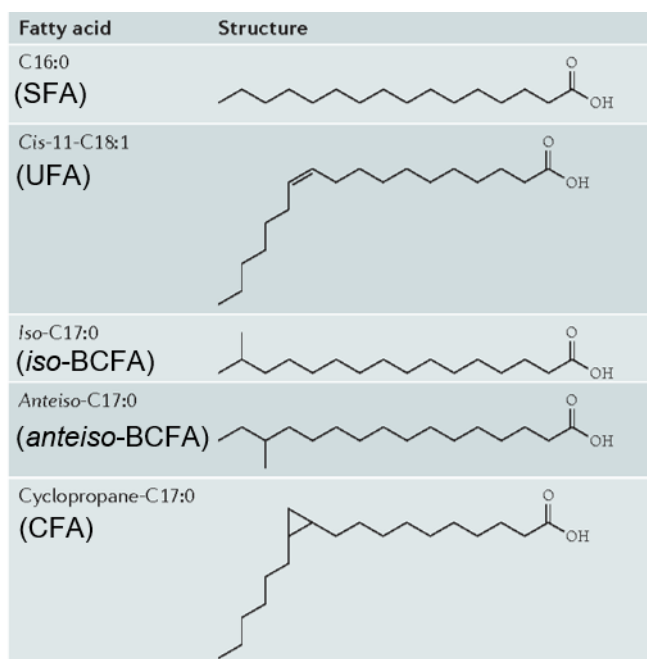
Figure 5: Chemical structures of membrane phospholipid fatty acids found in *B. subtilis* and *E. coli*. SFA: saturated fatty acid, UFA: unsaturated fatty acid, BCFA: branched chain fatty acid, CFA: cyclopropane fatty acid. Adapted from Zhang and Rock (2008).

1.1.4 – Teichoic acids

Threaded through the layers of peptidoglycan in Gram-positive bacteria are long anionic polymers, known as teichoic acids. In *B. subtilis*, these are composed from repeating units of glycerol-phosphate linked via phosphodiester bonds, to which glycosyl and D-alanyl ester residues are attached (Neuhaus and Baddiley, 2003). One class of these polymers, wall teichoic acids (WTAs), are covalently bound to the MurNAc residues of peptidoglycan by a linkage unit, whereas lipoteichoic acids (LTAs) intercalate into the cytoplasmic membrane via a glycolipid anchor (Fig. 6). Collectively, these polymers constitute up to 60% of the mass of the Gram-positive cell wall, and thus are implicated in a number of cell envelope functions, for example determination of cell shape and cell wall porosity, cation homeostasis and acquisition of metal cations for cellular function, protection against antibiotics and modulation of the activity of

autolysins (Cole *et al.*, 1970; Boylan *et al.*, 1972; Heckels, Lambert and Baddiley, 1977; Wecke, Madela and Fischer, 1997).
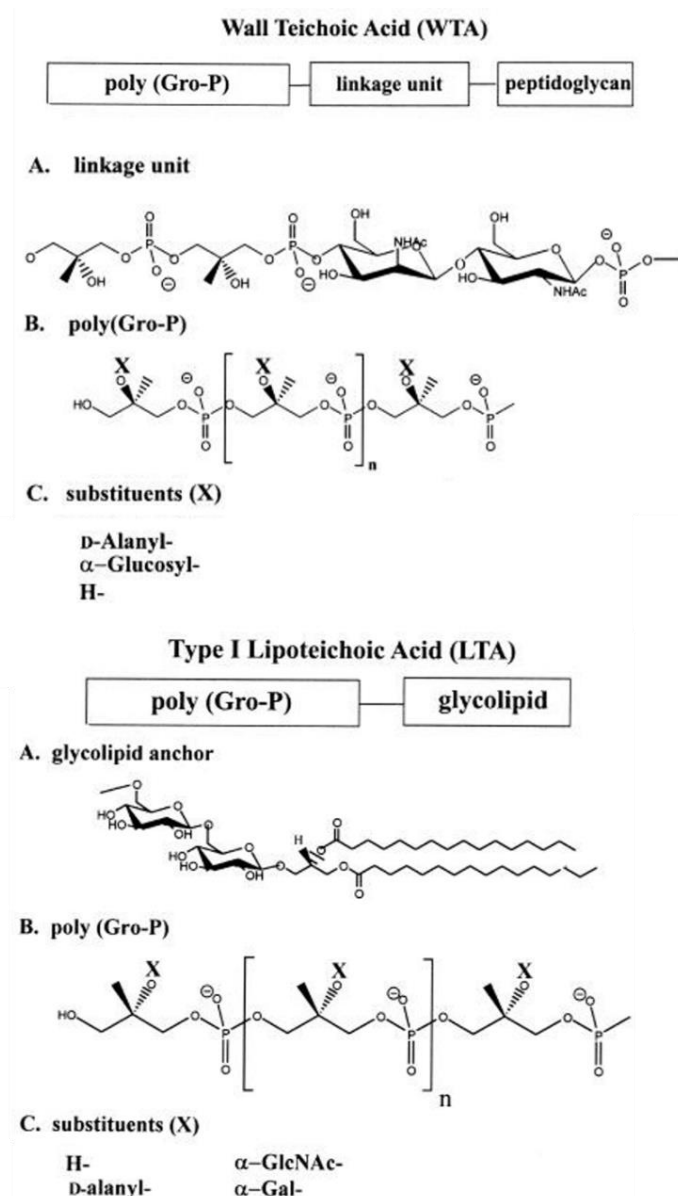
Figure 6: The structures of wall teichoic acids (WTA) and lipoteichoic acids (LTA) in *B. subtilis*. Top panel: Wall teichoic acids are formed from a linkage unit and repeating glycerol phosphate (Gro-P) units, which can be D-alanylated, α-glucosylated and protonated. Bottom panel: *B. subtilis* lipoteichoic acids are composed of a glycolipid anchor (derived from the membrane lipid diacylglycerol) and a Gro-P polymer, onto which protons, D-alanyl esters and α-GlcNAc and α-galactose residues are added. Adapted from Neuhaus and Baddiley (2003).

Synthesis of WTAs begins intracellularly on the cytoplasmic face of the membrane, with the transfer of GlcNAc-1-P from UDP-GlcNAc to a membrane-embedded UP carrier by the enzyme TagO (Soldo, Lazarevic and Karamata, 2002). TagA and TagB catalyse the addition of N-acetylmannosamine and a single glycerol-phosphate unit to the existing structure respectively (Bhavsar, Truant and Brown, 2005; D'Elia *et al.*,

14

2009), thus completing synthesis of the linkage unit. Thirty five to sixty glycerol-phosphate repeats are then added to this product, by the TagF enzyme, to assemble the polymer (Pereira *et al.*, 2008). As stated above, sugars are attached to the final WTA; in *B. subtilis*, this is performed by the glycosyltransferase TagE (Allison *et al.*, 2011), and subsequently it is exported to the external surface of the membrane by the two-component ABC transporter TagGH (Lazarevic and Karamata, 1995). Finally, a phosphodiester bond is formed between the polymer and the peptidoglycan MurNaC unit, proposed to be catalysed by the TagTUV enzymes in *B. subtilis* (Kawai *et al.*, 2011). Only then are WTAs modified by cationic D-alanyl esters (facilitated by the *dltABCD* operon); a key mechanism by which Gram-positive bacteria modulate their cell surface charge (Perego *et al.*, 1995).

For lipoteichoic acids, the glycolipid anchor is initially synthesised in the cytoplasm from diacylglycerol and UDP-glucose by the glycosyltransferase UgtP (Jorasch *et al.*, 1998). This is then transported to the outer leaflet of the membrane by an as yet undetermined membrane protein in *B. subtilis*. Here, glycerol-phosphate repeat units are assembled on the glycolipid anchor, derived from the head group of the membrane phospholipid PG, catalysed by LtaS and its three homologues YqgS, YvgJ and YfnI (Schirner *et al.*, 2009). It is proposed that expression and activity of these proteins is tightly regulated to adjust LTA synthesis in response to different growth and stress conditions, and even sporulation (Wörmann *et al.*, 2011). Again, similarly to WTAs, LTAs are modified with D-alanine esters by the *dltABCD* operon. LTAs can also be glycosylated, however, in contrast to WTAs, this is commonly with α-GlcNAc or α-Gal residues (Iwasaki, Shimada and Ito, 1986; Iwasaki *et al.*, 1989).

B. subtilis mutants defective in glycolipid synthesis (i.e. Δ*ugtP*) are viable, and LTA synthesis still occurs with the polymer linked to another membrane lipid; however, cells exhibit a reduction in length (Salzberg and Helmann, 2008). This is due to the absence of UgtP-dependent inhibition of FtsZ assembly and thus there is a disrupted ratio of FtsZ rings to cell length (Weart *et al.*, 2007). Additionally, mutants lacking *ltaS* demonstrated a chainy phenotype caused by incomplete Z ring formation (Schirner *et al.*, 2009). Deleting all 4 LtaS homologues (thereby inhibiting all LTA synthesis) produced chaining and even more severe morphological defects. The mechanism by which this reduction or lack of LTAs affects cell division requires further research, however it may be that LTAs recruit metallic cations essential for the activity of certain divisome enzymes.

Deleting *tagO* or *tagA* in *B. subtilis* leads to a complete lack of WTA polymers. These bacteria exhibit growth defects, a nonuniform thickening of the peptidoglycan layer and a spherical morphology, however they remain viable (D'Elia *et al.*, 2006). In contrast, deletion of genes involved downstream in the WTA synthetic pathway are lethal. This may be due to intracellular accumulation of toxic precursors, such as activated sugars or incomplete polymer, or sequestration of the carrier lipid UP, which is also essential for cell wall synthesis (described above).

1.1.5 – Membrane potential

The bacterial cytoplasmic membrane is first and foremost a permeability barrier, shielding the cytoplasmic content from the extracellular environment. Uptake and secretion of ions as well as the internalisation of charged molecules, such as proteins and nucleic acids, produces a sharp electrical gradient across the cytoplasmic membrane, which is the basis of membrane potential. The overall membrane potential of *B. subtilis* is estimated to be approximately -110 mV from exterior to interior (Hosoi *et al.*, 1980; te Winkel *et al.*, 2016), whilst *E. coli* is reported to exhibit a membrane potential of ~-150 mV (Feile *et al.*, 1980; Zilberstein *et al.*, 1984). In bacteria, the membrane potential is generally dominated by the H^+ gradient due to the pumping of protons across the membrane by the electron transport chain (Mitchell, 1961). This gradient, known as the proton motive force (PMF), is subsequently used in ion and metabolite transport and to power other cellular systems. Other ions, such as Na^+, K^+ and Ca^{2+}, are transported across the membrane, usually in symport or antiport with protons (Fujisawa *et al.*, 2005, 2009; Tascón *et al.*, 2020). However, K^+ can also move out of the cell through mechanosensitive channels, which are essential in the bacterium's survival to hypoosmotic shock (Booth and Blount, 2012).

As stated above, a number of bacterial processes are associated with membrane potential; the most well-studied and crucial being the synthesis of ATP. Here, protons flow down their gradient through membrane-bound ATP synthases, causing a clockwise rotation and the conversion of ADP and inorganic phosphate to ATP. On the other hand, under conditions of low PMF, the synthases can function as ATPases, hydrolysing ATP to generate a proton gradient (Deckers-Hebestreit and Altendorf, 1996). Motility also requires membrane potential, and flagellar motor rotation is driven by H^+ translocation across the membrane, similarly to the ATP synthase (Nakamura and Minamino, 2019). In addition, multidrug efflux systems are influenced by the PMF; either directly, as the major facilitator superfamily (MFS), the small multidrug resistance

(SMR) family, and the resistance/nodulation/cell division (RND) family of pumps function as multidrug/proton antiporters (Paulsen, Brown and Skurray, 1996), or indirectly as the ABC superfamily is driven by ATP hydrolysis (which is of course synthesised via the proton gradient) (Lubelski, Konings and Driessen, 2007). Finally, bacteria can modulate their membrane potential to limit uptake of positively charged antibiotics such as aminoglycosides (Damper and Epstein, 1981), to enter a "persister" state tolerant to antibacterial attack (Verstraeten *et al.*, 2015), or to even enable cell-cell electrical communication within biofilms (Prindle *et al.*, 2015; Martinez-Corral *et al.*, 2019).

Furthermore, it has been identified that membrane potential is crucial for the normal localisation of several membrane-associated proteins involved in cell morphogenesis; many of which will be discussed later in this thesis due to their roles in division and elongation. MinD, and its interaction partner MinC, which are responsible for correct positioning of the septum prior to cell division, lose their membrane binding and polar localisation upon depolarisation (Strahl and Hamoen, 2010). This is due to the C-terminal amphipathic helix of MinD no longer associating with the lipid bilayer. This is likely the case for the division protein FtsA as well, which also binds the membrane via a C-terminal amphipathic helix and becomes mislocalised upon dissipation of membrane potential (Strahl and Hamoen, 2010). Other proteins involved in cell division (FtsZ, ZapA, SepF, and PBP2B) exhibit a reduction in septal localisation, further affecting formation and site of the Z ring (Strahl and Hamoen, 2010). Lastly, MreB, Mbl, MreBH, MreC and MreD, all components of the elongasome, lose their localisation when PMF was dissipated (Strahl and Hamoen, 2010).

1.1.6 – Membrane fluidity and domains
Membrane fluidity is postulated to be a key parameter of cell viability and that changes can dramatically affect membrane protein movement and activity and membrane permeability (Haest *et al.*, 1972; Kurita, Kato and Shiomi, 2020); thus a number of membrane-associated processes including transport and morphogenesis. Therefore, bacterial membranes undergo quick adaptation in response to environmental challenges, such as changes in temperature, that disturb membrane fluidity. This is known as homeoviscous adaptation and is achieved by bacteria actively altering their membrane lipid composition. It was recently shown, however, that both *E. coli* and *B. subtilis* can tolerate dramatically large changes in membrane fluidity with no effect on growth, and the tight temperature-dependent regulation of membrane

lipid composition in these organisms may instead have evolved to maintain membrane thickness; another important feature of biological membranes (Gohrbandt *et al.*, 2022).

The first mechanism of homeoviscous adaptation in *B. subtilis* involves a rapid fluidisation of the membrane, in response to cold shock, increased membrane thickness or increased saturated fatty acid chains (Porrini *et al.*, 2014; Saita, Albanesi and De Mendoza, 2016). Under any of these conditions, DesK, a transmembrane dimeric histidine kinase switches from a phosphatase-active to a kinase-dominant state (Aguilar *et al.*, 2001) (Fig. 7). It undergoes autophosphorylation and activates DesR, a transcriptional regulator of the *des* gene. This drives expression of the Δ5-lipid desaturase encoded by *des*, converting SFA chains to UFA ones. Unsaturated acyl chains exhibit a kinked shape, therefore the lipids pack with lower densities and form a more fluid bilayer. Upon this increase in newly synthesised UFAs, DesK shifts back to its phosphatase-active state, dephosphorylating DesR-P and halting transcription of the desaturase.
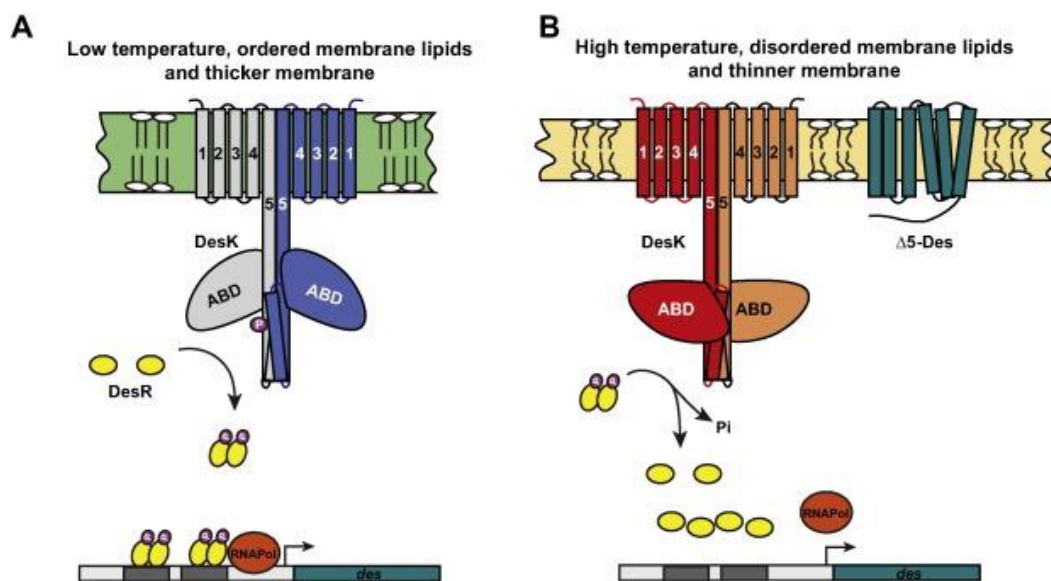
Figure 7: Regulation of membrane fluidity in *B. subtilis* by the Des pathway. (A) Reduced membrane fluidity promotes a kinase-dominant state of DesK, which autophosphorylates and activates DesR, resulting in transcriptional upregulation of des. (B) Δ5-Des is expressed and desaturates the membrane phospholipid SFA chains, increasing membrane fluidity. From Saita, Albanesi and De Mendoza (2016).

The second mechanism in *B. subtilis* involves a longer-term adaptation to changes in temperature, since it is achieved by the *de novo* synthesis of *iso* or *anteiso*-BCFAs. How the ratio between these two isomers is regulated is far from fully understood, however it is thought that upon temperature downshift, the sigma factor σ^L interacts with the transcriptional regulator BkdR, activating expression of the *bkd* operon

(Wiegeshoff *et al.*, 2006). This operon encodes 7 enzymes [*ptb*, *bcd*, *buk*, *lpd*, *bkdAA*, *bkdAB*, and *bkdB* (Debarbouille *et al.*, 1999)], which are responsible for the conversion of isoleucine to α-keto acids, precursors for *anteiso*-BCFA synthesis. The melting point of *anteiso*-BCFAs is significantly lower than their *iso*- counterpart [e.g., 51.7°C for C15:0 *iso* and 23.0°C for C15:0 *anteiso* (Kaneda, 1991)], thus an increased proportion of *anteiso*-BCFAs in the membrane increases its fluidity.

In *E. coli*, membrane fluidity is regulated by adjusting the incorporation of SFAs and UFAs. FabA is a key enzyme in UFA synthesis, introducing a double bond into a 10-carbon acyl chain intermediate (Bloch, 1963) (Fig. 8). FabB and FabF then elongate this intermediate to form the UFAs most abundantly found in the membrane phospholipids (Garwin, Klages and Cronan, 1980; De Mendoza, Klages Ulrich and Cronan, 1983). In particular, the activity of FabF is increased at lower temperatures, which is responsible for the synthesis of *cis*-vaccenic acid, an unsaturated fatty acid that is found in increased amounts upon cold shock (Marr and Ingraham, 1962).
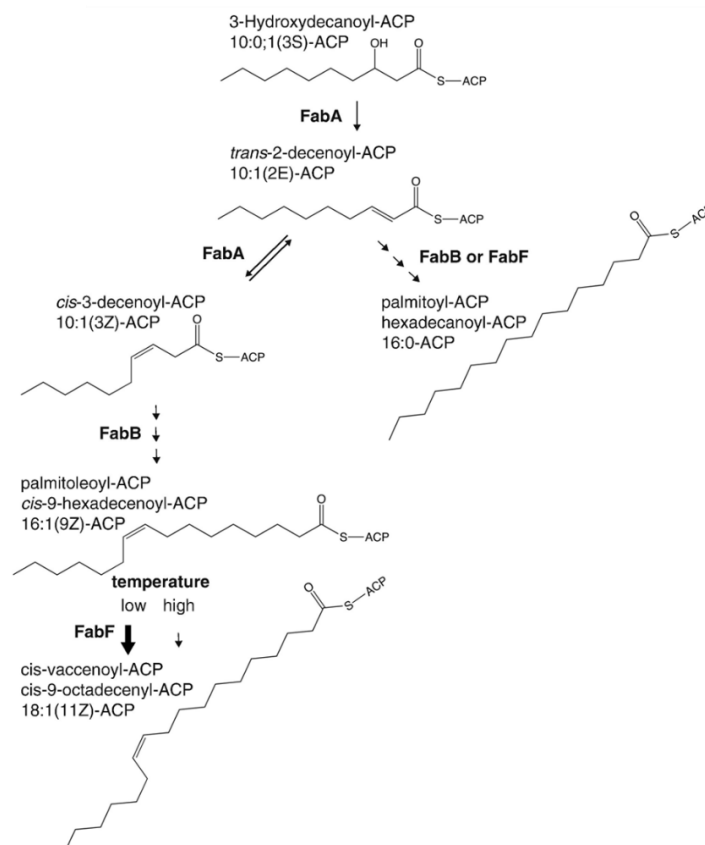
Figure 8: The synthesis of UFAs in *E. coli*. In brief, the key enzyme FabA introduces a *cis* double bond into a 10-carbon chain intermediate bound to an acyl carrier protein (ACP) and catalyses its *trans* isomerisation. FabB and FabF then elongate this intermediate. The FabF-dependent synthesis of *cis*-vaccenic acid (18:1[11Z]-ACP) is particularly increased in response to low temperatures. Adapted from Ernst, Ejsing and Antonny (2016).

Until recently, the lipid bilayer was thought to be a largely homogenous structure, however much speculation and discussion has emerged regarding the existence of membrane areas that differ in their composition and physiochemical characteristics, so called lipid domains. The most well-studied example of these are lipid rafts in eukaryotic membranes, which are low-fluidity areas rich in cholesterol and sphingolipids, such as sphingomyelin (Simons and Ikonen, 1997). Although less investigated, bacterial cytoplasmic membranes can also exhibit heterogeneity and formation of specific lipids domains, such as those with high or low membrane fluidity. Areas of increased membrane fluidity have been identified in *B. subtilis* and since named regions of increased fluidity, or RIFs (Strahl, Bürmann and Hamoen, 2014). These were initially observed when investigating how membrane depolarisation is associated with delocalisation of the bacterial actin homolog MreB and consequently the lateral cell wall synthetic machinery (Strahl and Hamoen, 2010; Strahl, Bürmann and Hamoen, 2014). This resulted in the formation of membrane foci preferentially stained by the uncharged membrane dye Nile red; that were subsequently defined by increased membrane fluidity through staining with the fluidity-sensitive dyes Laurdan and Dil-C12 (Fig. 9a) (Parasassi and Gratton, 1995; Baumgart *et al.*, 2007). A later study by Oswald *et al.* in 2016 independently confirmed the existence of MreB-dependent microdomains and additionally demonstrated that they can induce a temporal confinement of membrane protein mobility (Oswald *et al.*, 2016). The authors also showed that the MreB-associated membrane domain organisation is conserved in *E. coli*, suggesting that domains are a feature of both Gram-positive and Gram-negative bacteria beyond *B. subtilis*. The mechanism by which MreB recruits fluid lipids remains unclear, but in general membrane fluidity can be increased by (i) the binding of charged proteins such as cationic peptides (Mbamala *et al.*, 2005 and see below) or (ii) accumulation of lipids that promote local membrane disorder (Zhao, Wu and Veatch, 2013). One possible candidate that may be responsible for the formation of RIFs is the undecaprenyl-coupled cell wall synthesis precursor lipid II. Lipid II partitions into membrane regions of high fluidity and can induce local membrane disorder (Janas *et al.*, 1994; Ganchev *et al.*, 2006). Furthermore, MreB organises the biosynthetic elongasome thereby directly interacting with MurG and MraY; proteins involved in the synthesis of lipid II (Mohammadi *et al.*, 2007; Favini-Stabile *et al.*, 2013). Finally, it should be noted that lipid domains with elevated fluidity can exist in the absence of MreB (Müller *et al.*, 2016; Wenzel *et al.*, 2018), indicating that MreB dissociation is not the only mechanism by which such domains can emerge.

High-fluidity membrane microdomains

GFP-MreB   Dil-C12

Low-fluidity membrane microdomains

Flotillin-GFP
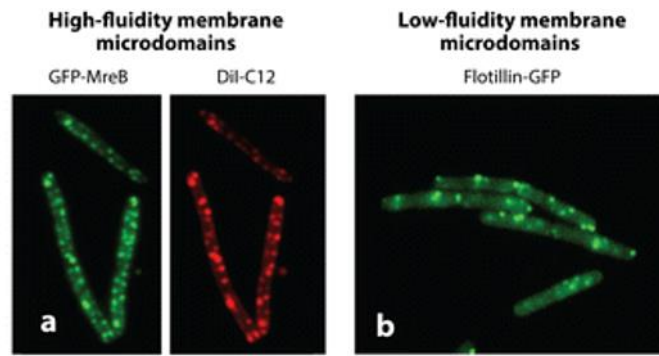
Figure 9: Lipid domains in the bacterial cytoplasmic membrane. (a) MreB-associated high-fluidity membrane microdomains, as demonstrated by the co-localisation of GFP-tagged MreB and Dil-C12 foci (which preferentially stains membrane regions of increased local fluidity). (b) Low-fluidity membrane microdomains, as shown by the focalised localisation pattern of GFP-tagged FloT. From Strahl and Errington (2017).

Cholesterol is absent from the membranes of most bacteria, so it was therefore assumed that rigidified membrane areas, such as lipid rafts, were limited to eukaryotes. This was disputed, however, by the discovery that KinC, a sensory kinase involved in biofilm formation, was not functional upon deletion of the farnesyl diphosphate phosphatase, YisP (López and Kolter, 2010). YisP catalyses the synthesis of farnesol (Feng *et al.*, 2014), a compound that is required for the production of other isoprenoids, such as squalene, carotenoids, and hopanoids. These molecules play a role in inducing membrane rigidification (Gruszecki and Strzałka, 2005; Spanova *et al.*, 2012; Sáenz *et al.*, 2015), and therefore may be analogous to eukaryotic cholesterol. Such membrane regions can be purified as they resist detergent solubilisation (Brown, 2002). Using this technique, KinC was present only in the detergent-resistant membrane (DRM) fraction, and only if functional YisP was present (López and Kolter, 2010). In addition, proteins homologous to eukaryotic flotillins, which localise exclusively to lipid rafts (Langhorst, Reuter and Stuermer, 2005), named FloT and FloA, were found in abundance in the DRM fraction (Donovan and Bramkamp, 2009; López and Kolter, 2010). Absence of flotillins in bacterial membranes reduces membrane heterogeneity and leads to a coalescence of regions of lower fluidity (Bach and Bramkamp, 2013). Overall, this provides strong evidence that domains of increased rigidity do exist in bacterial membranes, however since they do not contain cholesterol, they were termed functional membrane microdomains. These domains are visible microscopically through the use of fluorescent protein fusions (Fig. 9b); however FloT and FloA localise to different areas along the cytoplasmic membrane (Schneider *et al.*, 2015; Dempwolff *et al.*, 2016), implying that there may be two distinct microdomain systems. In contrast, another recent study demonstrated that flotillins are

essential for maintaining membrane fluidity in *B. subtilis*, and their absence notably decreased MreB mobility and, as a consequence, lateral cell wall synthesis (Zielińska *et al.*, 2020).   Ergo, more research is required into how flotillins organise the bacterial cytoplasmic membrane and how this affects protein movement and associated cellular processes.

1.2 – Antibiotic-relevant cell-envelope associated proteins and processes

1.2.1 – The bacterial divisome

Cell division is critical to the viability of bacteria, and as stated above, in almost all bacteria this is governed by a large and highly dynamic molecular machine, known as the divisome. The cell division, or *fts*, genes, so named because thermosensitive mutants of these genes conferred a filamentous temperature-sensitive phenotype, were first observed by François Jacob's group in the 1960s (Hirota, Ryter and Jacob, 1968). At the non-permissive temperature, these mutants elongate in the absence of cell division, forming filaments longer than 150 μm, compared to ~3 μM long for wild type daughter cells. This was followed by the identification of FtsZ in both *E. coli* and *B. subtilis*, a tubulin-like protein that co-ordinates divisome assembly (Lutkenhaus, Wolf-Watz and Donachie, 1980; Beall, Lowe and Lutkenhaus, 1988), and of the cell division regulators, MinCD and E (de Boer, Crossley and Rothfield, 1989). Finally, perhaps the biggest breakthrough came in 1991, when Erfei Bi and Joe Lutkenhaus determined that FtsZ forms a ring-like structure at the site of division, now termed the Z ring (Bi and Lutkenhaus, 1991). This was of particular significance, as it demonstrated that, similarly to eukaryotes, bacteria utilise cytoskeletal proteins for cell morphogenesis.

Bacterial cell division begins with positioning of the nascent division site, a highly precise and regulated process, that in *E. coli* and *B. subtilis* takes place within approximately 2% of the cell's midcell (Yu and Margolin, 1999; Migocki *et al.*, 2002). This involves both positive regulation that promotes FtsZ assembly in the correct position, and negative regulation that prevents mislocalisation of the Z ring i.e., at the cell poles or through the nucleoid. Since cytokinesis follows bacterial DNA replication, it was proposed that initiation of DNA replication prepares the midcell for FtsZ assembly (Moriya *et al.*, 2010). However, it was more recently shown that, instead, the chromosome organisation protein, Spo0J, and Noc act collectively to ensure Z rings do not form too early in the cell cycle, before most of the chromosome has cleared midcell (Hajduk *et al.*, 2019). Other regulatory proteins include EzrA in *B. subtilis*, which

prevents aberrant Z ring formation at cell poles, whilst maintaining correct FtsZ assembly at midcell (Haeusser *et al.*, 2007), and MatP and ZapB in *E. coli*, which co-ordinate interactions between chromosome segregation and the cell division machinery (Espéli *et al.*, 2012). Perhaps the most well-known regulatory mechanisms are the Min system, which inhibits Z ring formation at the cell poles, and the nucleoid occlusion system (NO), SlmA in *E. coli* and Noc in *B. subtilis,* which blocks Z ring assembly on portions of the membrane surrounding the nucleoid (Wu and Errington, 2004; Bernhardt and De Boer, 2005). However, despite what is commonly thought, precise placement of the Z ring at midcell still occurs in the absence of both the Min and NO systems (Migocki *et al.*, 2002; Rodrigues and Harry, 2012), reiterating that these systems are additional safety mechanisms and not essential for establishing the medial division site.
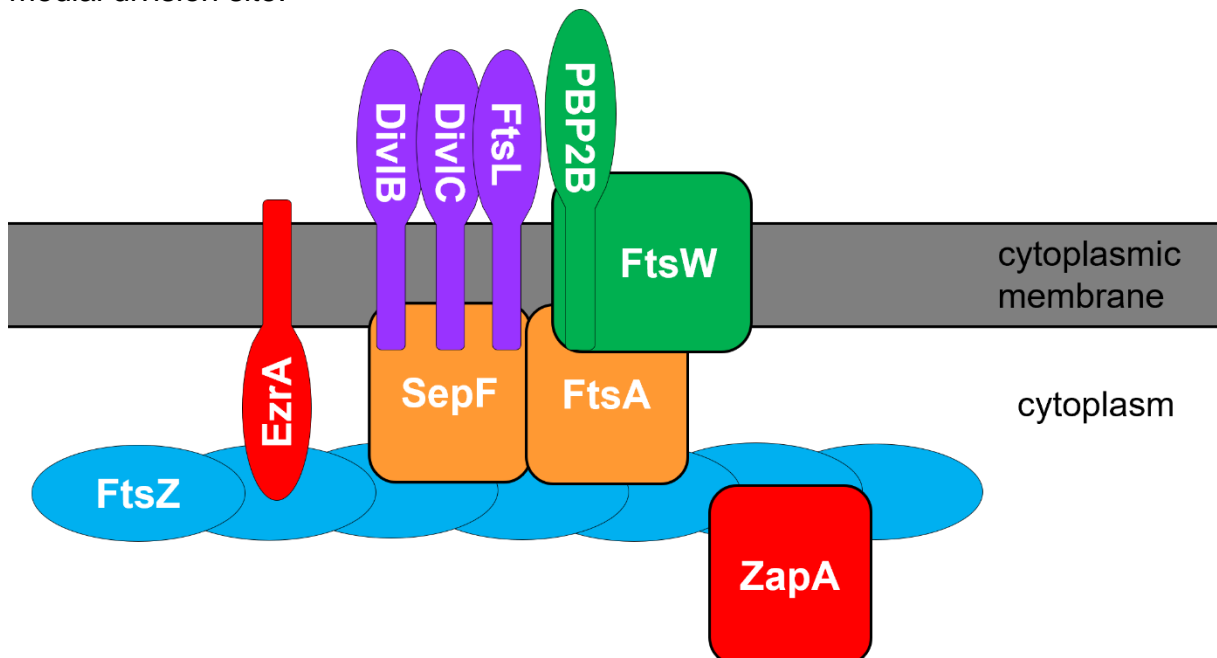
Figure 10: A simplified schematic of the *B. subtilis* divisome. FtsZ polymers are tethered to the cytoplasmic membrane via the functionally redundant anchors FtsA and SepF. They also interact with the regulatory proteins, EzrA and ZapA, and the essential glycosyltransferase and transpeptidase for cell division, FtsW and PBP2B respectively.

After division site selection, divisome assembly is initiated by recruitment of the "early" division proteins which include FtsZ and its membrane anchor, FtsA, both of which are highly conserved among bacteria, as well as other less conserved proteins such as SepF, EzrA and the Zaps (Rico, Krupka and Vicente, 2013). This forms the proto-ring, or Z ring, onto which more than 30 "late" division proteins are assembled, including the glycosyltransferase FtsW and the transpeptidase PBP2B (Gamba *et al.*, 2009) (Fig. 10). Upon completion of the divisome, it constricts and synthesises septal peptidoglycan to allow for septum formation and eventually cell division.

To form the Z ring, FtsZ polymerises at the intracellular face of the cytoplasmic membrane. Recent studies using super-resolution and single-molecule imaging have demonstrated that FtsZ polymers exhibit GTP-dependent treadmilling, in which polymerisation occurs at one end of the filament and depolymerisation at the other, with the central monomers remaining stationary (Bisson-Filho *et al.*, 2017; Yang *et al.*, 2017). These dynamics ensure the spatial and temporal distribution of the septal cell wall synthesis machinery, allowing for smooth septum morphogenesis and correct polar morphology.

1.2.2 – The bacterial elongasome

In contrast, the bacterial elongasome directs lateral insertion of peptidoglycan along the long axis of the cell and is organised by the membrane associated actin homologue MreB. MreB was first identified to determine cell shape in *E. coli* (Wachi *et al.*, 1987), but it has since been discovered that almost all rod-shaped bacteria encode one or more actin homologues. The exception are rod-shaped or filamentous bacteria such as Actinobacteria, which grow by tip extension: a mechanism independent of MreB (Flärdh, 2010). *B. subtilis* carries three *mreB* paralogous genes: *mreB, mbl* (MreB like) and *mreBH* (MreB homologue). MreB is expressed as part of the *mre* operon, upstream of MreC and MreD, other components of the elongasome (Levin *et al.*, 1992), whilst Mbl and MreBH are expressed as standalone proteins (Abhayawardhane and Stewart, 1995; Carballido-López *et al.*, 2006). It initially appeared that an *mreB* deletion led to loss of rod shape and cell lysis in *B. subtilis*; however, it was subsequently demonstrated that high concentrations of magnesium in the growth medium rescue viability and morphological defects (Formstone and Errington, 2005). Why magnesium saves this phenotype remained unknown for many years, until recently when Tesson *et al.* discovered that MreB depletion disrupts the tightly controlled balance between peptidoglycan synthesis and degradation, which is restored by the Mg^{2+}-dependent inhibition of autolysin activity (Tesson *et al.*, 2022). Several reports have shown that the three paralogues exhibit partially redundant functions, and overexpression of any of the MreB isoforms rescues defects in lateral peptidoglycan synthesis and cell shape of a triple deletion mutant (Kawai *et al.*, 2009). It is also possible to construct a strain carrying deletions of all three actin homologues if *rsgI*, the anti-sigma factor of σ^I, is also deleted (Schirner and Errington, 2009). The cells grow well, but exhibit spherical morphology, further emphasising the role of MreB and its homologues in lateral cell wall synthesis.
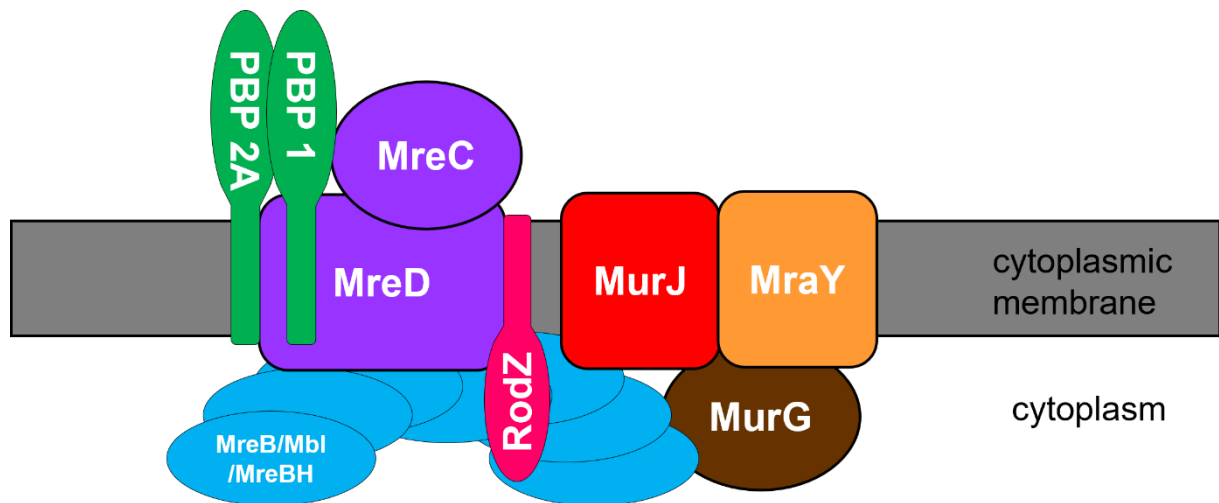
Figure 11: A simplified schematic of the _B. subtilis_ elongasome. The bacterial actin homologues MreB, Mbl and MreBH form short filaments that move around the cell width driven by peptidoglycan synthesis. These filaments interact with the cell wall synthetic machinery via the other _mre_ proteins, MreC and MreD, and RodZ. PBP 1 and PBP 2A are major peptidoglycan synthases both involved in cell elongation. The membrane-associated enzymes MraY and MurG synthesise the peptidoglycan precursors Lipid I and Lipid II respectively; whilst MurJ is a potential lipid II flippase.

MreB paralogues form antiparallel double filaments that can polymerise in the presence of either ATP or GTP (Dempwolff _et al._, 2011; van den Ent _et al._, 2014). This arrangement ensures that the hydrophobic membrane-binding loop of both protofilaments can interact with the membrane (a process that is enhanced by an amphipathic helix in _E. coli_; Salje _et al._, 2011) and in particular the membrane-bound proteins MreC, MreD and RodZ, which mediate MreB's contact with the cell wall synthetic machinery (Fig. 11). MreB was initially thought to form static helical structures running the length of the cell (Jones, Carballido-López and Errington, 2001); however recent high-resolution imaging demonstrated that MreB assembles in discrete shorter filaments that move circumferentially around the width of the cell (Domínguez-Escobar _et al._, 2011; Garner _et al._, 2011; van Teeffelen _et al._, 2011). Furthermore, the curved structure of MreB filaments allows them to align and translocate along the direction of greatest membrane curvature, inserting cell wall in that direction and maintaining the rod shape (Hussain _et al._, 2018). Finally, motility of MreB filaments and the associated elongasome appears to be driven by peptidoglycan synthesis, as movement is rapidly halted upon treatment with cell wall synthesis-inhibiting antibiotics or depletion of PBPs (Garner _et al._, 2011; van Teeffelen _et al._, 2011).

Aside from their role in cell shape determination and lateral cell wall synthesis, MreB isoforms have been shown to have differentiated roles in regulating autolytic activity (Carballido-López _et al._, 2006; Domínguez-Cuevas _et al._, 2013). Linked to this, I

described earlier that correct MreB localisation is dependent on membrane potential (Strahl and Hamoen, 2010). Delocalisation, induced by membrane depolarisation, leads to aberrant autolytic degradation of the cell wall (as their activity is no longer regulated, and the elongasome is not present to insert newly synthesised material), ultimately resulting in cell lysis (Scheinpflug *et al.*, 2017; Seistrup, 2018). This process may be an overlooked component of the mode of action of several membrane-targeting antimicrobials.

1.2.3 – Autolysins

Previously, I have described peptidoglycan synthesis and in addition, the importance of the tight regulation between this and its breakdown by enzymes called autolysins, to facilitate bacterial growth. In importance to this project, the major autolysins of *B. subtilis* are: the N-acetylmuramoyl-L-alanine amidase LytC (the activity of which is regulated by its operon partners LytA and LytB), the glucosaminidase LytD and the endopeptidases LytE and LytF (Smith, Blackman and Foster, 2000). These all cleave at different locations in the peptidoglycan matrix (Fig. 12), and have been implicated in elongation, division, vegetative cell separation and motility (Rashid, Kuroda and Sekiguchi, 1993; Ohnishi, Ishikawa and Sekiguchi, 1999).
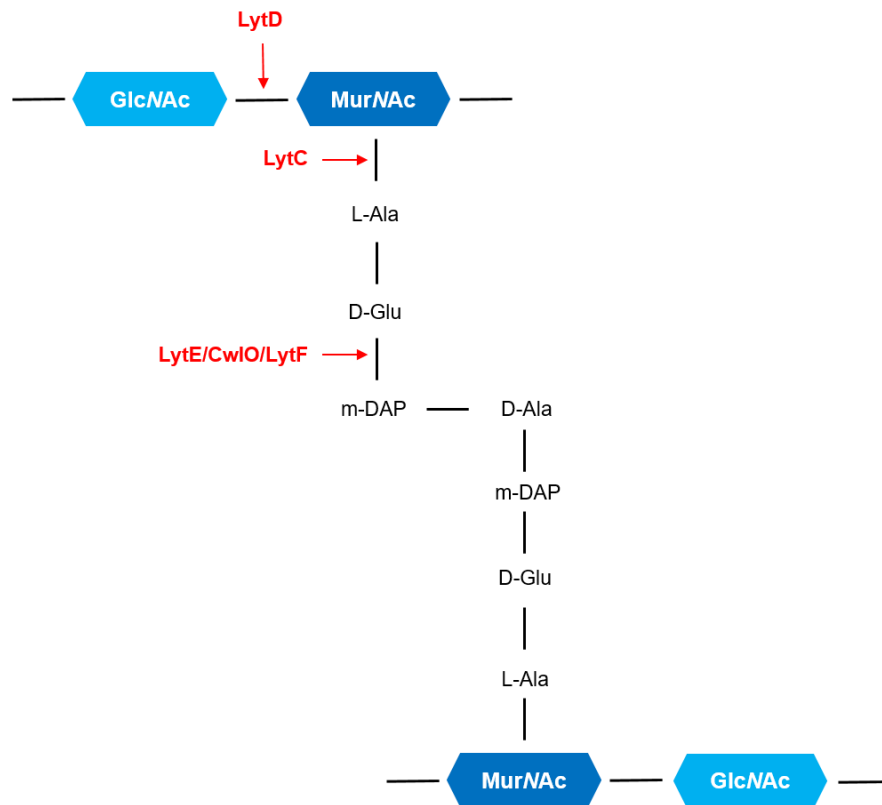
Figure 12: Simplified schematic structure of peptidoglycan, formed from alternating GlcNAc and MurNAc subunits, crosslinked by short peptides. An example of the type of bond attacked by each autolysin discussed in this thesis is shown. LytC cleaves the MurNAc-L-Ala bond, LytD cleaves the GlcNAc-MurNAc bond, whilst LytE and LytF cleave the D-Glu-*m*-DAP bond. *m*-DAP: *meso*-diaminopimelic acid

LytC (or CwlB) is a 50-kDa amidase, secreted during vegetative growth, that cleaves the MurNAc-L-ala bond in peptidoglycan. It is expressed in the *lytABC* operon, along with the acidic, low-molecular mass protein, LytA, as well as its modifier, LytB, under control of the sigma factors σ^D and σ^A (Lazarevic *et al.*, 1992). LytA plays a role in the secretion of LytB and LytC, whilst LytB is a membrane-bound regulator of LytC, enhancing its activity by a factor of two to three (Herbold and Glaser, 1975; Margot and Karamata, 1992). LytC has been shown to localise uniformly on the entire cell surface, suggesting that it is a major autolysin not essential for cell separation (Yamamoto, Kurosawa and Sekiguchi, 2003). Instead, since σ^D also controls expression of the flagellar regulon (Marquez *et al.*, 1990) and swarming motility is abolished in *lytC* mutants (Chen *et al.*, 2009), LytC appears to also be important for proper flagellar function.

LytD is a 95-kDa N-acetylglucosaminidase which cleaves the covalent bonds between the GlcNAc and MurNAc residues of glycan strands. It is expressed as a monocistronic operon, again under the regulation of a σ^D-dependent promoter. *B. subtilis* mutants

deficient of LytD show no changes to cell separation, motility, autolysis, cell wall turnover or growth (Margot, Mauël and Karamata, 1994); therefore its specific role remains unclear.

LytE is a 35-kDa DL-endopeptidase which hydrolyses the bond between D-Glu and *meso*-diaminopimelic acid of the stem peptide, and is expressed under the control of 3 sigma factors, σ^A, σ^H and σ^I. LytE localises at the cell septa, poles, and lateral sidewall (Hashimoto, Ooiwa and Sekiguchi, 2012), implying that it functions as a major autolysin in cell separation and elongation. Furthermore, localisation and regulation of LytE is specifically dependent on the MreB homologues, MreB and MreBH (Carballido-López *et al.*, 2006; Domínguez-Cuevas *et al.*, 2013), and consequently both *lytE* and *mreBH* mutants show similar morphological, cell wall-related defects (a thinning of cells for as yet unknown reasons). As I also mentioned previously, an excess of divalent cations leads to inhibition of DL-endopeptidases, such as LytE (Tesson *et al.*, 2022). Finally, LytE was proposed to be functionally redundant with the other cell elongation autolysin in *B. subtilis*, CwlO (Bisicchia *et al.*, 2007), and deletion of both blocks cell elongation and triggers lysis (Hashimoto, Ooiwa and Sekiguchi, 2012). However, as mutants in each exhibit distinct phenotypes, it was recently suggested that they may have more differentiated roles in cell morphogenesis than initially expected (Domínguez-Cuevas *et al.*, 2013).

LytF is a 50-kDa γ-D-glutamate-*meso*-diaminopimelate muropeptidase, which also cleaves the bond between D-Glu and *meso*-diaminopimelic acid in the peptide bridge (Margot, Pagni and Karamata, 1999), and is homologous to LytE, differing mainly in the number of their LysM peptidoglycan-binding repeats (Fukushima *et al.*, 2006). It is encoded by the monocistronic *lytF* operon, and similarly to other autolysins, is under the control of the σ^D promoter. LytF localises to cell septa and poles (Yamamoto, Kurosawa and Sekiguchi, 2003), and mutants grow predominantly as chains (Chen *et al.*, 2009), implicating its role as a major cell separation autolysin. Finally, expression and localization of LytF is reduced in mutants of the LTA synthesis pathway, implying that teichoic acids may regulate autolysin activity (Kiriyama *et al.*, 2014); however the mechanism by which this occurs remains unclear.

1.2.4 – Cell envelope stress responses

Bacteria are often exposed to harsh environments, microbial competition and the attack of antibiotics, and have therefore developed efficient stress response systems in order to survive. Due to its important physiological role and common exploitation as

an antibacterial target, it is crucial for bacteria to maintain integrity of their cell envelope. Of importance to this thesis, I will be discussing two cell envelope-associated stress responses in *B. subtilis,* which involve two different regulatory systems: extracytoplasmic function (ECF) σ factors or two-component systems (TCS). Both are functionally analogous as they comprise a membrane-embedded sensor (anti-σ factor or histidine kinase, respectively) and a cytoplasmic transcriptional regulator, in the form of an ECF σ factor or response regulator. Subsequently, the systems differ by how the sensor and regulator communicate upon encountering envelope stress. In the case of ECF σ factors, the σ factor is released from the anti-σ factor, due to a conformational change or degradation of the anti-σ factor. The σ factor is then free to bind RNA polymerase and direct transcription to the promoters of target genes (Fig. 13b) (Helmann, 2002). In contrast, for TCSs, the intracellular domain of the histidine kinase phosphorylates the N-terminal receiver domain of the response regulator under inducing conditions. This causes dimerization, eliciting enhanced DNA-binding capacity and the response regulator can subsequently act as a transcription factor (Fig. 13a) (Parkinson, 1993).
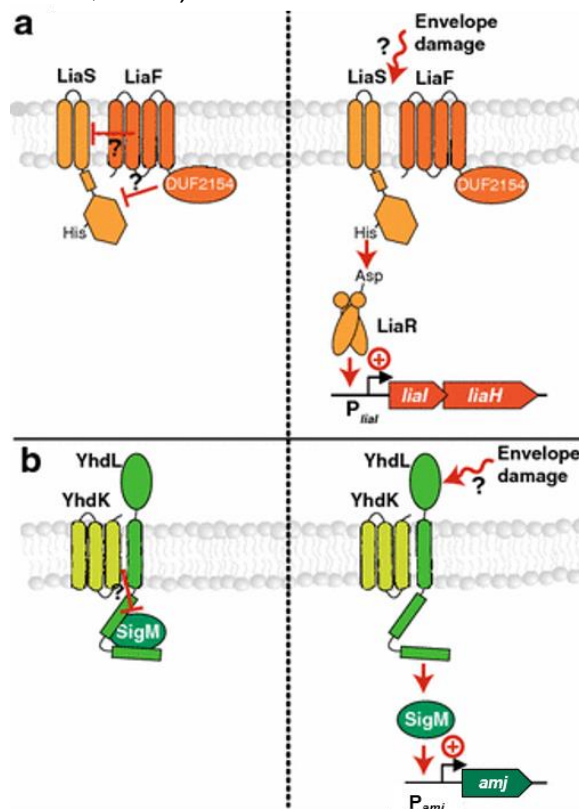
Figure 13: Mechanism of signal transduction of the LiaRS two-component system and the ECF σ factor σ^M. (a) Under resting conditions, the membrane-bound inhibitor LiaF regulates LiaS activity. Upon cell envelope stress, LiaS phosphorylates the response regulator LiaR, causing its dimerisation and induction of *liaIH*. (b) In the absence of stress, the anti-σ factor YhdKL sequesters the ECF σ factor σ^M. Under

inducing conditions, σ^M is released, where it recruits RNA polymerase to its target promoters, including P$_{amj}$. Adapted from Radeck, Fritz and Mascher (2017).

B. subtilis encodes seven ECF σ factors (Helmann and Moran, 2014), at least four of which are involved in the cell envelope stress response and one of these is σ^M. σ^M is co-transcribed with its cognate anti-σ factors encoded by *yhdL* and *yhdK.* The three are proposed to form a tripartite complex, as σ^M binds to the N-terminal domain of YhdL, whilst YhdK specifically interacts with YhdL (Yoshimura *et al.*, 2004). The role of σ^M was first determined during a screen for genes involved in endospore outgrowth. *B. subtilis* strains in which the then σ factor of unknown function had been insertionally inactivated produced aberrantly shaped cells, which swelled and lysed in medium containing elevated levels of different salts (Horsburgh and Moir, 1999). Indeed, it is induced by high salt, acidic pH and heat stress (Thackray and Moir, 2003). However, as the σ^M regulon (which comprises 30 distinct promoter regions regulating the expression of over 60 genes) mainly facilitates the expression of genes involved in cell wall synthesis and cell division, it is thought that the common theme of these environmental stresses is impairment of peptidoglycan synthesis. Further evidence for this is that σ^M is strongly activated by antibiotics that target the peptidoglycan biosynthetic pathway, including both early stage (for example, fosfomycin, which inhibits MurA) and late stage (such as β-lactams and vancomycin, which prevent transglycosylation and transpeptidation) inhibitors (Cao *et al.*, 2002; Thackray and Moir, 2003). The σ^M regulon, characterised by its vancomycin-induced activation, can be categorised into 3 classes. The first involves promoters that directly upregulate genes encoding proteins in the cell envelope biosynthetic pathway, such as the *mreBCD* operon (Eiamphungporn and Helmann, 2008) which is essential in the bacterial elongasome and thus, lateral cell wall synthesis. The second category involves promoters that induce expression of stress-activated replacement enzymes. For example, σ^M can upregulate *amj*, which encodes a lipid II flippase, redundant with MurJ (Meeske *et al.*, 2015). The third class are promoters that activate expression of regulatory proteins. This includes the *sigMyhdLK* operon itself, to allow for positive autoregulation and to also increase levels of the anti-σ factors, ensuring rapid sequestration of σ^M once the stress has been overcome. Finally, there are other regulon members with as yet undefined functions; one of which is *ypuA*. Despite this, its σ^M-dependent promoter has been fused to a reporter gene in *B. subtilis*, to act as a biosensor for cell envelope stress (Urban *et al.*, 2007).

Four TCSs associated with cell envelope stress have been identified in *B. subtilis*; one of which is the LiaRS system. LiaRS was originally characterised as part of the regulatory network activated in response to the antibiotic bacitracin (Mascher *et al.*, 2003). Indeed, it strongly responds to other antibiotics that interfere with the lipid II cycle in the cytoplasmic membrane, such as nisin and cationic antimicrobial peptides (cAMPs) (Mascher *et al.*, 2004; Pietiäinen *et al.*, 2005). In support of this membrane-dependent induction, several other triggers of the LiaRS response, such as alkaline shock, detergents and organic solvents, also perturb the cytoplasmic membrane (Petersohn *et al.*, 2001; Wiegert *et al.*, 2001). LiaRS is expressed, with its membrane-bound inhibitor LiaF, as part of the *liaIH-liaGFSR* operon (Jordan *et al.*, 2006). LiaG is proposed to be a putative membrane-embedded hypothetical protein, with an as yet elusive function. In contrast to σM, there are only 2 LiaR-dependent promoters: the *liaI* promoter (P_{liaI}) and the *yhcY* promoter. LiaI, expressed alongside LiaH, a member of the phage-shock protein family, is a small hydrophobic protein with two putative transmembrane helices (Jordan *et al.*, 2007). It is proposed to act as a membrane anchor for LiaH and both proteins colocalise in discrete foci in response to cell envelope stress, presumably to maintain cytoplasmic membrane integrity and counteract antibiotic-induced damage (Domínguez-Escobar *et al.*, 2014). Meanwhile, LiaR-dependent P_{yhcY} upregulation was only observed in a *liaF* mutant, therefore when LiaRS activity is not regulated by its inhibitor.

1.2.5 – Multidrug efflux

The general mechanisms that contribute to antimicrobial resistance include target alteration, drug inactivation, decreased bacterial permeability and increased drug efflux. Therefore, overexpression of multidrug efflux pumps, which actively extrude toxic compounds from the cell, is a common factor of pathogens resistant to multiple clinically relevant antibiotics. Efflux pumps have been identified in almost all bacteria, and the genes that encode them can be located on the chromosome (expressed constitutively or following mutation), or on plasmids (where they can be readily transmissible to other bacteria) (Piddock, 2006). Depending on their structural characteristics, energy sources and substrates, bacterial efflux pumps are classified into 6 families (Du *et al.*, 2018). Of importance to this thesis, I will discuss in detail the resistance-nodulation-cell division (RND) family, which includes the multidrug efflux pump AcrAB-TolC.

RND family efflux pumps are mainly expressed by Gram-negative bacteria, however genes encoding proteins with homology to RND pump monomers have been identified in Gram-positive organisms such as *Corynebacterium glutamicum* and *Staphylococcus aureus* (Schindler *et al.*, 2014; Yang *et al.*, 2014; Alnaseri *et al.*, 2015). These efflux pumps organise as tripartite systems: (i) a transporter (efflux) protein located in the cytoplasmic membrane, (ii) a periplasmic "adaptor" protein, also known as a membrane-fusion protein and (iii) an outer membrane protein channel. Using the *E. coli* AcrAB-TolC system as an example, this constitutes AcrB, AcrA and TolC respectively. Importantly, each of these proteins is essential for efflux, and the absence of any renders the whole complex non-functional (Ma *et al.*, 1993, 1995). AcrB is a homotrimer, in which 2 main binding pockets exist. These are enriched in aromatic, polar and charged amino-acid residues, which would favour interactions with a number of substrates and may contribute to the "polyspecificity" of the pump. The protomers of AcrB each exhibit a distinct conformation upon drug binding, designated the loose (L), tight (T) and open (O) states (Murakami *et al.*, 2006; Seeger *et al.*, 2006). In brief, the model of AcrB drug transport hypothesises that the drug accesses the trimer via the L state, moves further into the drug-binding pocket in the T state and is finally expelled in the O state, through the periplasmic AcrA hexamer and eventually out of the cell via the outer membrane TolC channel (Fig. 14). Furthermore, RND efflux pumps are driven by the PMF and it is proposed that protonation of AcrB triggers transition from the 'binding' (T) state to the 'extrusion' (O) state (Seeger *et al.*, 2009).

AcrB can transport a wide range of substrates, including a number of antimicrobial compounds such as tetracycline, chloramphenicol, β-lactams, fusidic acid and fluoroquinolones (Nishino, Nikaido and Yamaguchi, 2009), detergents, cationic dyes and organic solvents (Tsukagoshi and Aono, 2000; Poole, 2004). There is therefore an emerging area of drug discovery to identify efflux pump inhibitors (EPIs). One such experimental compound is phenyl-arginine β-naphthylamide (PAβN), which inhibits efflux systems in both *Pseudomonas aeruginosa* and *E. coli* (Lomovskaya *et al.*, 2001; Kourtesi *et al.*, 2013). It acts as a competitive inhibitor of substrate binding; however, its use as an EPI is debated as it additionally affects outer membrane integrity, thereby
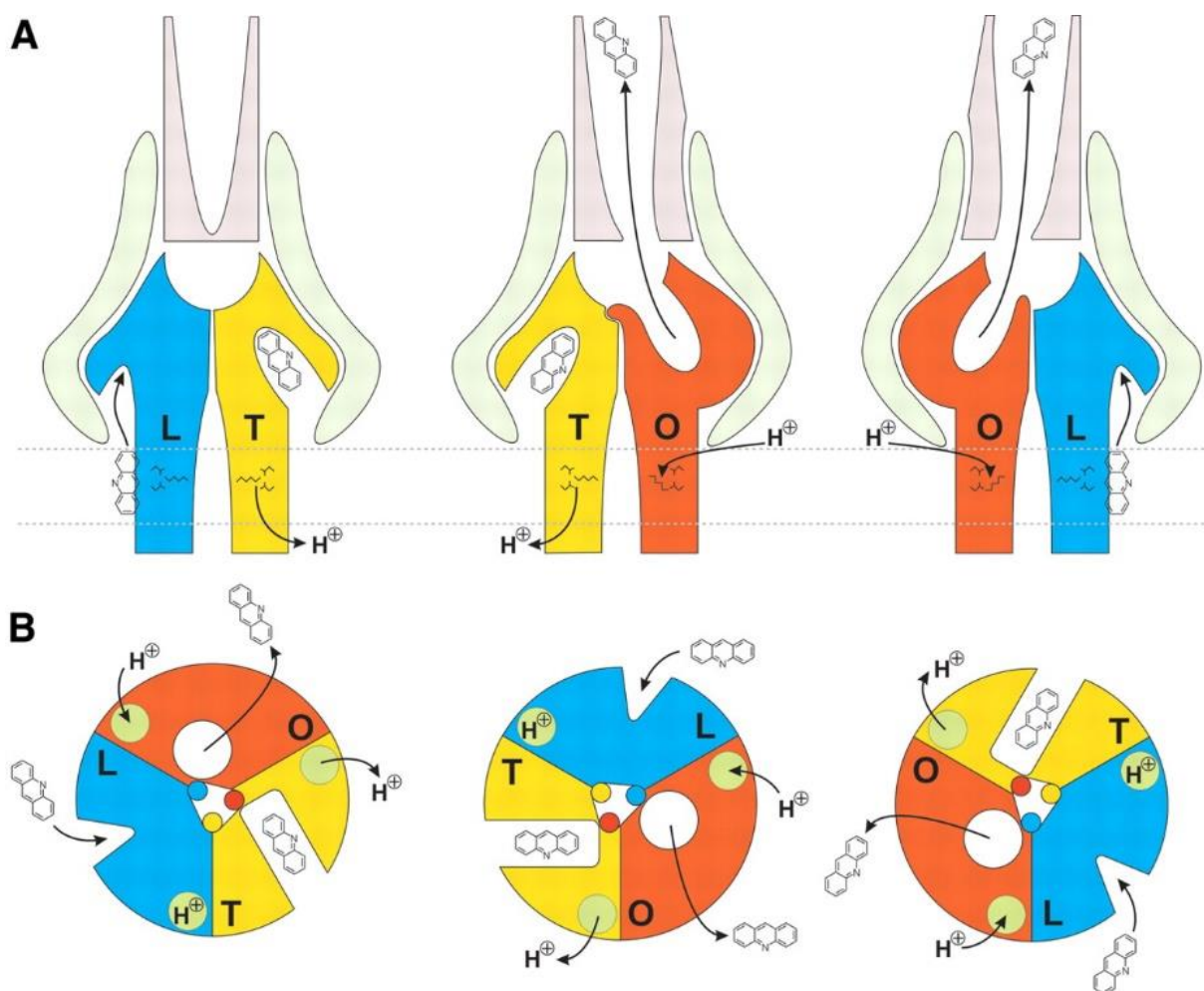
Figure 14: Graphical representation of the AcrAB-TolC multidrug efflux mechanism. AcrB monomer confirmations, loose (L), tight (T) and open (O), are represented as blue, yellow and red respectively. (A) Simplified schematic featuring two of the three AcrB protomers, the AcrA adaptor protein (light green) and the outer membrane TolC channel (light purple). (B) The cycling of conformational states upon access, binding and extrusion of the substrate. Note protonation of AcrB induces efflux of the compound from the O state. From Seeger *et al.* (2006).

reducing drug penetration. Another method to inhibit efflux pumps is to dissipate the PMF which energises them. This is commonly achieved by the protonophore CCCP, which has been shown to potentiate the activity of tetracycline (Anoushiravani, Falsafi and Niknam, 2009), however its toxicity towards mammalian cells limits its use to the laboratory. One promising candidate is IITR08027, which reverses resistance against fluoroquinolones, is not antibacterial on its own (which could give rise to mutants conferring resistance), and is non-toxic in animal cells at its minimum effective concentration (Bhattacharyya *et al.*, 2017).

1.3 – Antimicrobial resistance

The discovery of the sulfonamides and penicillin in the early 20th century marked the beginning of the modern "antibiotic era" where previously deadly bacterial infections

could be easily treated. The next decades witnessed the "golden age" of antibiotic discovery, as one half of the compounds commonly used today were discovered in this period. However, soon after, resistance mechanisms (i.e., modifications in bacteria that cause the antibiotics used to treat infections to become less effective) plagued their clinical use. Sulfonamide resistance was first reported in the late 1930s, and similar resistance mechanisms are still prevalent in bacteria nowadays (MacLeod, 1940). Interestingly, a bacterial β-lactamase was identified several years before the use of penicillin as an antibiotic (Abraham and Chain, 1940), emphasising that antibiotic resistance genes were found in bacterial populations even before the selection pressure of antimicrobials. Nowadays, the rampant use, misuse and abuse of antibiotics in both medical and agricultural settings has accelerated the incidence of antibiotic resistance, and led to the emergence of multidrug resistant bacteria, or "superbugs": pathogens that cause increased morbidity and mortality due to several mutations and/or acquired genes that confer resistance to a wide range of antibiotics. Unsurprisingly then, antibiotic resistance is rapidly becoming one of the biggest threats to global health and the Review on Antimicrobial Resistance, commissioned by the UK Government, estimated that AMR could kill 10 million people worldwide per year by 2050 (note, however, that this estimation also includes viral and parasitic pathogens) (O'Neill, 2014). In addition, more recent data has suggested that in 2019 alone, there were 1.27 million deaths attributable to bacterial antimicrobial resistance (Murray *et al.*, 2022). Just 6 pathogens accounted for 73.4% of these deaths: *E. coli*, followed by *Staphylococcus aureus*, *Klebsiella pneumoniae*, *Streptococcus pneumoniae*, *Acinetobacter baumannii*, and *Pseudomonas aeruginosa*; all of which have been identified as priority pathogens by WHO (World Health Organization (WHO), 2017). The severity of this situation is only exacerbated by the lack of new antibiotic development as demonstrated by the almost linear decrease in antibacterial new molecular entities over the past 30 years (Infectious Diseases Society of America (IDSA), 2011) (Fig. 15).
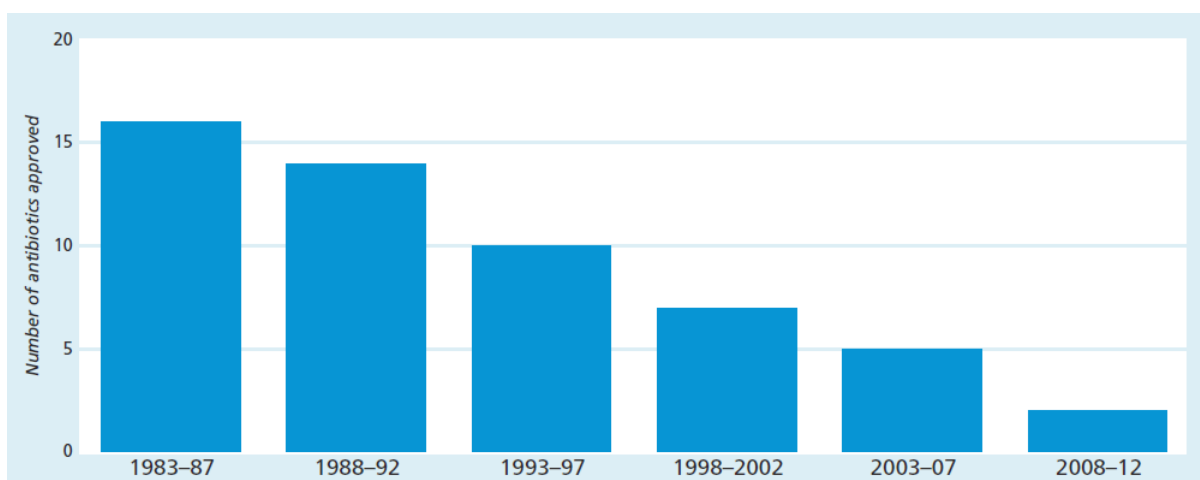
Figure 15: The number of new molecular entity systemic antibiotics approved by the US FDA per five-year period up to March 2011. From Infectious Diseases Society of America (IDSA) (2011).

Intervention strategies to combat antibiotic resistance include infection prevention and control (both in hospitals and communities), enrolment and development of vaccination programmes, reducing agricultural antibiotic use, minimising inappropriate clinical antibiotic use and finally promoting investment into the development of new antibiotics. The latter would allow for the potential discovery of new classes of antibiotics with novel targets or mechanisms of action that would not be susceptible to pre-existing bacterial resistance mechanisms. One such emerging strategy is targeting the bacterial cytoplasmic membrane.

1.4 – Membrane-targeting antimicrobials

1.4.1 – Structure and function

Membrane-targeting antimicrobials target an essential macromolecular structure, which, as described previously, is the site for many crucial cellular processes. These agents also exhibit a reduced incidence of resistance as (i) they target a non-DNA encoded structure and are therefore less susceptible to resistance conferred by simple point mutations or horizontal gene transfer, (ii) they can simultaneously inhibit multiple membrane-associated processes including bacterial respiration, cell division and cell wall synthesis and (iii) they trigger de-energisation of the bacterium, thereby impeding cellular stress responses. This attractive characteristic is well demonstrated by the membrane-targeting lantibiotic nisin, which has been used in the food industry for over four decades without significant resistance development (Draper *et al.*, 2015). Additionally, they resemble host defence peptides, such as LL-37 and thrombocidins (Henzler Wildman, Lee and Ramamoorthy, 2003; Barns and Weisshaar, 2013; Riool *et al.*, 2020), displaying similar structures and activity against various human

pathogens, further validating the cytoplasmic membrane as an antibacterial target site. The clinical efficacy of targeting the bacterial cytoplasmic membrane is also demonstrated by the recent success of existing membrane-active antibiotics polymyxin B, daptomycin and colistin as last resort agents against multi-drug resistant infections (Sauermann *et al.*, 2008; Vaara, 2019; Sabnis *et al.*, 2021). Finally, they may even prove a promising strategy for treating persistent bacterial infections caused by dormant bacteria. For example, the lipoglycopeptides telavancin and oritavancin, which disrupt membrane potential, eradicate enterococcal and staphylococcal biofilms *in vitro* (Belley *et al.*, 2009; LaPlante and Mermel, 2009).

Membrane-targeting antimicrobials are usually cationic, amphipathic peptides and demonstrate selectivity for bacterial cells due to strong electrostatic interactions with negatively charged phospholipids on the surface of the bacterial cytoplasmic membrane [compared to an abundance of zwitterionic phosphatidylcholine present on the outer leaflet of mammalian cells (Vance, 2015)]. Moreover, such compounds can be sensitive to other membrane properties aside from charge. For instance, magainin 2 (a membrane-targeting antimicrobial peptide) acts more effectively against liposomes composed of PG, which due to its cylindrical shape, affects the curvature of the membrane (Matsuzaki *et al.*, 1998).

To date, the prevailing mechanism by which membrane-active antibiotics act is pore formation resulting in cytoplasmic leakage and thus, cell lysis. After initial interaction with the bacterial membrane, various models have been proposed to describe how membrane-targeting antimicrobials induce pore formation in bacteria (Fig. 16A). In the barrel-stave model, compounds insert perpendicularly in the lipid bilayer, creating a circular pore stabilised by lateral interactions, similar to that of membrane ion channels. In the toroidal pore, insertion of the antibiotic induces a local curvature of the lipid bilayer and pores are formed between compound molecules and phospholipid head groups. The final mechanism is the carpet/detergent-like model. In this case, the peptides accumulate at the membrane surface, creating a "carpet", which eventually disintegrates the membrane by forming micelles (Kumar, Kizhakkedathu and Straus, 2018). However, more recently, alternate mechanisms of action have been identified, which involve changes to bulk membrane properties (Fig. 16B). These include disruption of membrane potential, changes to curvature of the membrane, clustering of specific phospholipids, packing defects affecting bilayer order and fluidity, or

targeting specific components of the membrane such as undecaprenyl-coupled cell wall precursors or teichoic acids (Epand *et al.*, 2016).
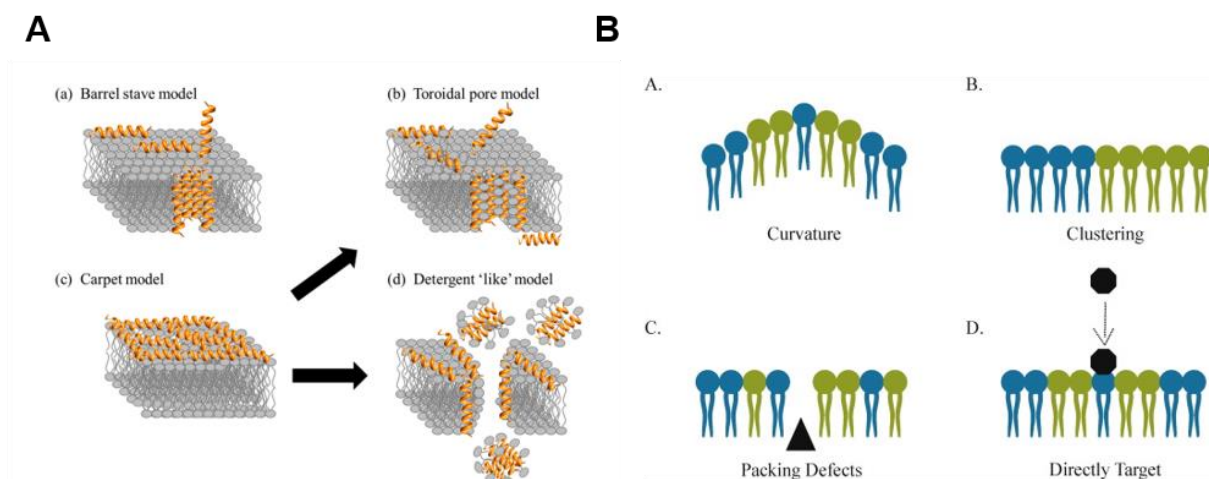
Figure 16: Proposed models for membrane disruption in bacteria. (A) Proposed models for membrane pore formation in bacteria. See text for further description of each model. From Kumar, Kizhakkedathu and Straus (2018). (B) Graphical representation of the effects that membrane-targeting antibiotics can have on the physical properties of the bacterial cell membrane. From Epand *et al.* (2016).

1.4.2 – Clinical limitations

Despite the promising outlook of membrane-targeting antimicrobials as a novel class of antibiotic, there are several limitations to their use as therapeutic agents. The first is that they exhibit low bioavailability resulting from proteolytic degradation and limited solubility. Moreover, since they rely on electrostatic interactions with the bacterial membrane, their antibacterial activity can be attenuated by physiological concentrations of divalent cations such as Mg^{2+} and Ca^{2+}. Currently, there are efforts to overcome these drawbacks through structure-activity relationship studies and subsequent introduction of chemical modifications. For example, D-amino acid substitution and fatty acid conjugation of CopW, an antimicrobial peptide derived from the insect defensin coprisin, enhanced its serum stability and antibacterial activity respectively (Lee *et al.*, 2019).

The mechanism of action of membrane-active compounds is also responsible for their relatively frequent cytotoxic effects. One example is the nephrotoxicity of polymyxins, which results in acute kidney injury in up to 50 to 60% of patients receiving colistin or polymyxin B (Nation, Velkov and Li, 2014; Kelesidis and Falagas, 2015). This is caused by their ability to induce apoptosis in renal proximal tubular cells (Azad *et al.*, 2013); and is currently managed by strict monitoring of renal function and rigorous dosing protocols (Nation *et al.*, 2019).

The most common and problematic side effect however is haemolysis, the permeabilisation of red blood cells, via membrane disruption similar to that which occurs at bacterial cells. This is due to negative surface charge of erythrocyte membranes (Eylar *et al.*, 1962; Jan and Chien, 1973) which, as mentioned previously, is the main selectivity determinant of membrane-targeting antimicrobials. One example is the cyclic decapeptide antibiotic gramicidin S, which demonstrates broad spectrum activity but unfortunately, due to its haemolytic activity, has been restricted to topical applications only (Dimick, 1951). Although it has been proved possible to design analogues of gramicidin S that exhibit reduced haemolytic activity (Kondejewski *et al.*, 1996), an in-depth understanding of the physico-chemical features that contribute to selectivity would be required to perform this for all membrane-active compounds. This uncovers an alternative approach: to identify and pursue membrane-targeting antimicrobials that do not act through pore formation.

1.4.3 – *Daptomycin*

Several recent studies have demonstrated that membrane-active compounds can act in the absence of pore formation; of which I will discuss two in detail. The first is daptomycin, a lipopeptide antibiotic that displays excellent activity against Gram-positive pathogens and is often implemented as a last resort agent to combat multi-drug resistant bacterial infections (Baltz, Miao and Wrigley, 2005). Despite its clinical use since 2003, the precise mechanism of action of daptomycin is still heavily debated. In particular, much controversy is centred on whether daptomycin forms large pores in the cytoplasmic membrane of target cells; with many discrepancies transpiring from differences between *in vivo* and *in vitro* studies.

Daptomycin, originally isolated from the Gram-positive soil bacterium *Streptomyces roseosporus* (Eliopoulos *et al.*, 1986; Debono *et al.*, 1987), is a lipodepsipeptide consisting of a 10-membered cyclic lactone core and three exocyclic amino acids linked to a decanoyl fatty acid tail (Allen, Hobbs and Alborn, 1987; Huber, Pieper and Tietz, 1988). Unlike other common lipopeptides, daptomycin is negatively charged and its antimicrobial activity depends on the presence of Ca^{2+} ions, which reduce the negative charge of the peptide and stimulate its oligomerisation (Ball *et al.*, 2004; Jung, *et al.*, 2004; Rotondi and Gierasch, 2005; Scott *et al.*, 2007). The resulting daptomycin-calcium complex therefore has an increased affinity for anionic phospholipids, such as PG. PG is particularly abundant in Gram-positive cell membranes (Epand, Savage and

Epand, 2007), thereby promoting daptomycin selectivity for bacterial over mammalian membranes (Hachmann *et al.*, 2011).

Daptomycin mode of action studies have provided controversial results for several decades, with the earliest data demonstrating that daptomycin inhibits peptidoglycan synthesis (Allen, Hobbs and Alborn, 1987; Mengin-Lecreulx *et al.*, 1990). Recent work from our group demonstrated, using fluorescent lipid probes and GFP-protein fusions, that daptomycin induces clustering of fluid lipids (RIFs; Fig. 17A), causing an overall rigidification of the cytoplasmic membrane (Müller *et al.*, 2016). This change in membrane organisation impairs the attachment of several peripheral membrane proteins, most prominently the lipid II synthase MurG (Fig. 17B), which is required for peptidoglycan synthesis (Kobayashi *et al.*, 2003). Despite this, a direct interaction between daptomycin and the cell wall had not been identified, until a very recent study by Grein *et al.* (2020) showed that daptomycin forms a tripartite complex with PG and the undecaprenyl-coupled cell wall precursor lipid II. This is consistent with the detachment of the cell wall synthesis machinery and massive membrane rearrangements, observed previously (Müller *et al.*, 2016). The question still remains, however, as to why daptomycin is still active against both *Enterococcus faecium* protoplasts and cell wall-less *B. subtilis* L-forms (Boaretti *et al.*, 1993; Wolf *et al.*, 2012). Several *in vitro* studies using model liposomes have shown that daptomycin forms cation-selective membrane pores (Zhang *et al.*, 2014; Zhang, Scoten and Straus, 2016). However when tested *in vivo*, high daptomycin concentrations and prolonged treated times were required to observe membrane depolarisation and ion leakage (Silverman, Perlmutter and Shapiro, 2003; Seydlová *et al.*, 2018); phenomena that occur near-instantaneously with other known pore forming molecules *(Wenzel et al.*, 2012; Wenzel *et al.*, 2018).

Finally, preliminary data using *B. subtilis* strains deficient for key autolysins and MreB homologues demonstrated that daptomycin induces MreB-dependent autolysis (Seistrup, 2018). Further investigation into the mechanism by which this occurs is required but this process may have been misinterpreted as pore formation in previous mode of action studies.
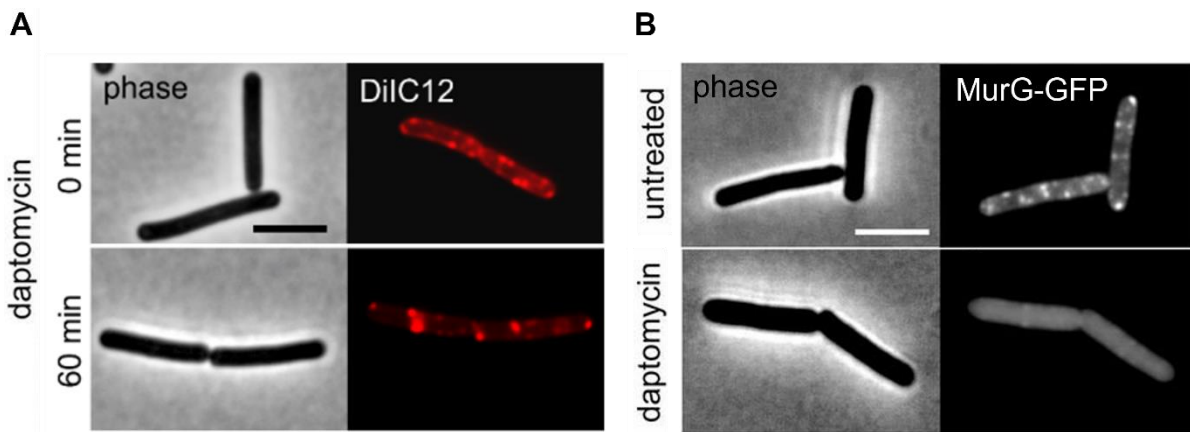
Figure 17: Daptomycin-induced fluid membrane microdomain reorganisation triggers delocalisation of MurG. (A) Daptomycin alters the native fluid microdomain organisation in the membranes of *B. subtilis* as shown by staining with the fluid membrane-sensitive dye DilC12. (B) Daptomycin causes complete dissociation of the lipid II synthase MurG from the membrane into the cytosol, demonstrated by *B. subtilis* cells expressing MurG-GFP. From Müller *et al.* (2016).

1.4.4 – cWFW

Membrane-targeting in the absence of pore formation was also proved true for cWFW (cyclo-RRRWFW), an arginine- and tryptophan-rich cyclic hexapeptide. This class of peptides, due to their cationic and hydrophobic nature, exhibit the ideal structural characteristics for interaction with anionic bacterial cytoplasmic membranes (Appelt *et al.*, 2008). cWFW was first identified during a library screen of small synthetic peptides derived from the human antimicrobial peptide lactoferricin (Blondelle, Pérez-Payá and Houghten, 1996); where it was shown to be active against both Gram-positive and Gram-negative bacteria at low micromolar concentrations, with limited toxicity towards mammalian cells (Scheinpflug *et al.*, 2013). The cytoplasmic membrane was confirmed as its target; however it did not induce formation of large pores (Scheinpflug *et al.*, 2015). Instead, *in vitro* studies demonstrated that cWFW causes clustering of anionic lipids in model membrane vesicles (Arouri, Dathe and Blume, 2009; Finger *et al.*, 2015). Later, using proteomic profiling, fluorescence microscopy and membrane analysis, it was concluded that cWFW neither permeabilises nor depolarises the cytoplasmic membrane *in vivo* (Scheinpflug *et al.*, 2017). In contrast, it triggers a rapid reduction of membrane fluidity and the formation of large-scale lipid domains which differ in local fluidity (Fig. 18A). This disrupts membrane protein localisation, in particular of MurG and the MreB-homologues (Fig. 18B), efficiently inhibiting cell wall synthesis. Finally, similarly to daptomycin, use of a *B. subtilis* mutant deficient for the

major autolysins LytABCDEF demonstrated that cWFW-induced lysis is autolytic in nature. Although not tested yet, this may also be dependent on the MreB cytoskeleton.
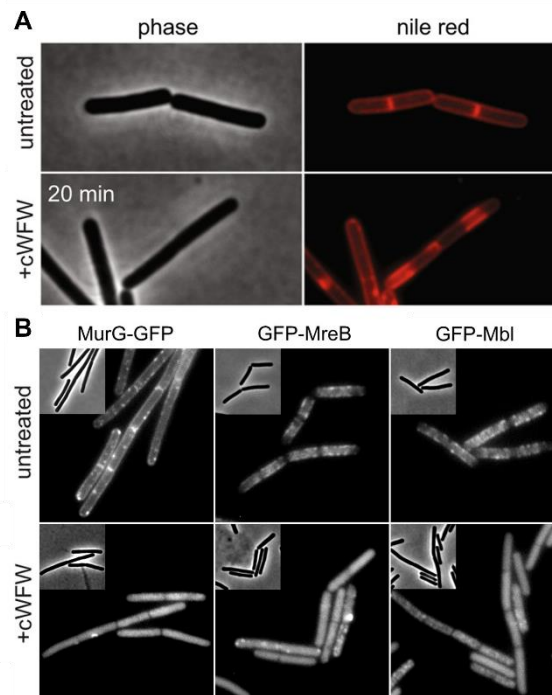
Figure 18: cWFW-induced large-scale lipid domain formation causes delocalisation of MurG and MreB-homologues. (A) cWFW triggers formation of large membrane domains, differing in local fluidity, as shown by changes in staining with the fluidity-sensitive membrane dye Nile red. (B) cWFW causes dissociation the bacterial actin homologs MreB and Mbl, and the lipid II synthesis protein MurG from the cytoplasmic membrane, demonstrated by GFP-protein fusions. From Scheinpflug *et al.* (2017).

1.5 – *Actinomycetes*

1.5.1 – *Ecology and characteristics*

Actinomycetes (members of the order *Actinomycetales*) are Gram-positive, filamentous, spore-forming bacteria with a high guanosine and cytosine content. The order is further divided into several suborders, including *Actinomyceineae*, *Micromonosporineae* and *Streptomycineae*. Whilst *Actinomycetes* are commensals in the human body (from skin to mucosal surfaces) and are important members of a normal microbiota (although in rare cases these bacteria can cause disease i.e., actinomycosis caused by *Actinomyces israelii*), they constitute a significant component of the microbial population in most soils and counts of over 1 million per gram are commonly obtained (Goodfellow and Williams, 1983). Here, they play a major role in degradation of organic polymers by production of hydrolytic enzymes, for example lignocelluloses from various grasses and woods (Antai and Crawford, 1981; McCarthy, 1987), and chitin from the exoskeletons of insects (Gomes *et al.*, 2000). *Actinomycetes*

are also involved in nitrogen fixation in soil. This is the ability to reduce dinitrogen to ammonium, which is bioavailable to plants and other organisms, unlike the dinitrogen molecule because of its stable triple bond. *Actinomycetes* can establish symbiotic relationships with non-leguminous plants, such as the *Frankia* genus that can colonise the roots of over 200 plant species (referred to as actinorhizal plants) (Normand *et al.*, 2007).

Aside from the soil, *Actinomycetes* are widely distributed in aquatic habitats. Although they exist in both freshwater and marine environments, they are thought to form only a small fraction of the bacterial flora in the latter, compared to their prevalence in terrestrial and freshwater sites (Goodfellow and Haynes, 1984). Similarly to those in soil habitats, aquatic *Actinomycetes* are involved in the decomposition of various materials, including cellulose, alginates, and other hydrocarbons (Erikson, 1941; Mulkins Phillips and Stewart, 1974; Imada *et al.*, 2014). There remains the possibility, however, that these organisms wash-in from surrounding terrestrial habitats, as the number of species observed decreases with increasing distance from land (Okazaki and Okami, 1972; Attwell and Colwell, 1981). On the other hand, species are found notably at lower depths (Johnston and Cross, 1976) and are well-adapted to this environment i.e., exhibit a greater tolerance to high salinity and pressure (Helmke, 1981).

Actinomycetes are morphologically similar to fungi, due to their mycelial growth, and this is attributed to adaptation to the same habitats. The life cycle alternates between sporulation and vegetative growth, and upon favourable environmental conditions, the "free spore" starts the germination process by forming a germ tube. This promotes the formation of branching filaments known as hyphae, which either anchor the organism (substrate mycelium) or grow upwards (aerial hyphae). Under adverse conditions, the aerial hyphae coil, initiating septation and chromosome segregation. A thick cell wall then forms around the spore (spore maturation) and it is released into the environment where it can remain dormant (Klieneberger-Nobel, 1947; Hamedi, Poorinmohammad and Papiran, 2017).

1.5.2 – Antibiotic discovery

Of importance to this thesis is the ability of *Actinomycetes* to produce a range of bioactive molecules. In fact, approximately two-thirds of all known antibiotics are produced by *Actinomycetes*, predominantly the genus *Streptomyces* (Takahashi and Nakashima, 2018). The production of such a vast number of compounds is due to a

process known as secondary metabolism, which occurs upon the onset of morphological differentiation (i.e., formation of aerial hyphae in solid cultures or transition to stationary phase during liquid growth). The trigger for these changes, and therefore the synthesis of secondary metabolites, is a depletion of growth nutrients, and likely an accumulation of the stringent response alarmone (p)ppGpp and activation of the phosphate starvation-dependent TCS PhoRP (Bibb, 2005; Van Wezel and McDowall, 2011; Van Der Heul *et al.*, 2018). The genes that encode the synthetic machinery for secondary metabolites, typically alongside resistance gene(s) and transcriptional autoregulators, are clustered together in biosynthetic gene clusters, or BGCs. Sequencing of the genome of the *Streptomyces* model organism *Streptomyces coelicolor* revealed that it harboured more than 20 BGCs (Bentley *et al.*, 2002), with many so-called "cryptic" or "silent" natural products, or those only synthesised under specific growth conditions (Pawlik *et al.*, 2007). Moreover, with the rapid advancement of genome sequencing, it appeared that the capacity of *Actinomycetes* as gifted natural chemists had been underestimated; with some species exhibiting over 50 different BGCs (Oliynyk *et al.*, 2007; Ohnishi *et al.*, 2008; Cao *et al.*, 2016), and an indication that the number of potential antimicrobial compounds from *Streptomyces* alone may be in the order of 100,000 (Watve *et al.*, 2001). Therefore, this led to the development of methods to induce their biosynthesis under laboratory conditions, such as eliciting stress responses or co-cultivation with other micro-organisms (Yoon and Nodwell, 2014; Rutledge and Challis, 2015), and bioinformatics tools to specifically identify BGCs, including antiSMASH [antibiotics and secondary metabolite analysis shell; (Medema *et al.*, 2011)]. antiSMASH identifies BGCs from previously characterised proteins or protein domains and compares them with all currently known BGCs throughout the tree of life to accurately predict chemical structure and function. Finally, novel species are being increasingly discovered from underexplored and extreme habitats (Bull *et al.*, 2016). It is crucial to maintain libraries of such isolates to be sequenced, in the hope that silent BGCs can be "awakened" and prompt the synthesis of as yet undiscovered natural product antibiotics.

1.6 – Research aims and objectives

The first objective of this research project was to optimise *in vivo* fluorescence-based techniques to rapidly detect disturbances to the cytoplasmic membrane in both the Gram-positive and Gram-negative model organisms, *B. subtilis* and *E. coli*, respectively. Such assays are of importance to screen for novel membrane-targeting

antimicrobials, in addition to other mode of action and physiological studies. Secondly, I aimed to optimise similar fluorescence-based assays to distinguish between multidrug efflux inhibition and outer membrane permeabilisation in *E. coli*. Identifying EPIs or outer membrane permeabilisers to potentiate the activity of currently used antibiotics is another emerging strategy to combat antimicrobial resistance. In collaboration with Demuris Ltd, the third aim was to screen a library of *Actinomycete* strains for those producing compounds with membrane-targeting effects, and perform preliminary mode of action analyses on aqueous and methanolic extracts derived from them. The final objective was to utilise techniques optimised in this thesis to perform comprehensive mode of action analyses of two clinically relevant membrane-targeting antimicrobials: daptomycin and octenidine, and investigate the membrane effects of PanT toxins identified from various bacteria and bacteriophages.

Chapter 2 – Materials and Methods

2.1 – Bacterial strains

The strains used throughout this thesis, including their names, species, genotypes and origins, can be found in Table 1.

Table 1: Strains used throughout this thesis.

Strain	Species	Genotype	Reference
168	*B. subtilis*	*trpC2*	(Anagnostopoulos and Spizizen, 1960)
MG1655	*E. coli*	*λ⁺ F⁻ ilvG- rfb-50 rph-1 (wild type)*	(Blattner *et al.*, 1997)
BW25113	*E. coli*	*λ⁻ F⁻ rph-1 hsdR514 Δ(araD-araB)567 ΔlacZ4787(::rrnB-3) Δ(rhaD-rhaB)568*	(Datsenko and Wanner, 2000; Baba et al., 2006)
JW5503-1	*E. coli*	*λ⁻ F⁻ rph-1 hsdR514 ΔtolC732::kan Δ(araD-araB)567 ΔlacZ4787(::rrnB-3) Δ(rhaD-rhaB)568*	(Baba *et al.*, 2006)
YvQI	*B. subtilis*	*lial::pMUTIN4 lial-lacZ ermC*	(Mascher *et al.*, 2004)
YuPA	*B. subtilis*	*ypuA::pMUTIN4 ermC ypuA'-lacZ*	(Urban *et al.*, 2007)
KS19	*B. subtilis*	*lytABC::neo lytD::tet lytE::cat lytF::spc*	(Scheinpflug *et al.*, 2017)
HS553	*B. subtilis*	*mreB::msfGFP-mreB*	(Donahue, unpublished)

KS60V	*B. subtilis*	*Ωneo3427 ΔmreB, mbl::cat, mreBH::erm, Ω(neo::spec) rsgI*	(Seistrup, 2018)
KS109	*B. subtilis*	*Pspac-ftsZ ble*	(Seistrup, 2018)
BS23	*B. subtilis*	*atpA-gfp Pxyl-'atpA cat*	(Johnson, van Horck and Lewis, 2004)
ARK3	*B. subtilis*	*clsA(ywnE)::tet clsB(ywjE)::spc ywiE::kan*	(Pogmore, Seistrup and Strahl, 2018)
KS119	*B. subtilis*	*psd::MLS*	(Pogmore, Seistrup and Strahl, 2018)
AK0117B-A	*B. subtilis*	*ugtP::MLS*	(Koh, unpublished)
AK0118B-A	*B. subtilis*	*mprF::kan*	(Koh, unpublished)
AK0119B-A	*B. subtilis*	*pssA::spc*	(Koh, unpublished)
AK066B	*B. subtilis*	*yfnI::erm yqgS::spc ltaS::cat (ΔLTA)*	(Koh, unpublished)
AK094B	*B. subtilis*	*tagO::MLS (ΔWTA)*	(Koh, unpublished)
AK199B	*B. subtilis*	*ispA(D92E)::spec mreB::msfGFP-mreB uppS::kan pLOSS (Pspac-uppS) (mls)*	(Koh, unpublished)
bSS421	*B. subtilis*	*amyE::spc PrpsD-sfGFP*	(Syvertsson, unpublished)
AK001E	*E. coli*	BW25113 pBAD33	(Koh, unpublished)
JB021	*E. coli*	BW25113 pBAD33-phRel2$_{Bac.\ sub.}$	This work. BW25113 transformed with VHp303.

JB022	*E. coli*	BW25113 pBAD33-*panT*$_{Bif. rum.}$	This work. BW25113 transformed with VHp464.
JB023	*E. coli*	BW25113 pBAD33 SD-*panT*$_{Esc. col.}$	This work. BW25113 transformed with VHp515.
JB024	*E. coli*	BW25113 pBAD33 SD-*capRel*$_{Vib. har..}$	This work. BW25113 transformed with VHp517.
JB026	*E. coli*	BW25113 pBAD33 SD-*panT*$_{Bar. api.}$	This work. BW25113 transformed with VHp518.
JB027	*E. coli*	BW25113 pBAD33 SD-*panT*$_{Bur. phage}$	This work. BW25113 transformed with VHp545.
JB028	*E. coli*	BW25113 pBAD33 SD-*panT*$_{Hel. sp.}$	This work. BW25113 transformed with VHp578.
JB029	*E. coli*	BW25113 pBAD33 SD-*panT*$_{Pse. mor.}$	This work. BW25113 transformed with VHp580.

2.2 – Media and growth conditions

The media and buffers used throughout this thesis, including their names, components and manufacturers, can be found in Table 2. In general, *B. subtilis* strains were grown at 30°C and supplemented with 0.2% glucose to minimise sporulation, whilst *E. coli* were grown at 37°C, both overnight in Lysogeny Broth (LB) under vigorous shaking, before sub-culturing the next day for utilisation in experiments. All studies involving the

antimicrobial daptomycin were performed in the presence of 1.25 mM $CaCl_2$, unless otherwise stated.

For generation of *B. subtilis* L-forms, strains were grown in LB with any appropriate antibiotics or inducers to mid-logarithmic phase at 37°C with shaking. Cells were then washed in fresh LB and resuspended in Nutrient Broth (NB) with the MSM supplement and lysozyme (2 mg/ml) for an hour with gentle shaking to create the protoplasts. L-forms were then propagated by diluting the protoplasts in NB/MSM supplemented with penicillin G (200 µg/ml) and growing at 30°C.

Table 2: Media and buffers used throughout this thesis.

Name	Component(s) and manufacturers
Lysogeny Broth (LB)	10 g/l tryptone (Oxoid)
	5 g/l yeast extract (Oxoid)
	10 g/l NaCl (VWR)
Nutrient Broth (NB)	Preparation from Oxoid:
	1 g/l `Lab-Lemco' powder
	2 g/l yeast extract
	5g/l peptone
	5 g/l NaCl
LB Agar	10 g/l tryptone (Oxoid)
	5 g/l yeast extract (Oxoid)
	10 g/l NaCl (VWR)
	15 g/l agar (Oxoid)
Nutrient Agar (NA)	Preparation from Oxoid:
	1 g/l `Lab-Lemco' powder
	2 g/l yeast extract
	5 g/l peptone
	5 g/l NaCl
	15 g/l agar
GYM agar	4 g/l glucose (VWR)
	4 g/l yeast extract (Oxoid)
	10 g/l malt extract (Sigma-Aldrich)
	10 g/l agar (Oxoid)
Valinomycin medium	10 g/l tryptone (Oxoid)

	5 g/l yeast extract (Oxoid)
	50 mM HEPES (Sigma-Aldrich)
	300 mM total KCl + NaCl (VWR)
Phosphate-buffered saline (PBS)	Preparation from Oxoid:
	8 g/l NaCl
	0.2 g/l KCl
	1.15 g/l Na_2HPO_4
	0.2 g/l KH_2PO_4
MSM supplement	20 mM maleic acid (Sigma-Aldrich)
	20 mM $MgCl_2$ (Sigma-Aldrich)
	0.5 M sucrose (Millipore)

2.3 – Minimal inhibitory concentration (MIC) determination and growth curves

The MICs of antimicrobial compounds were established to determine appropriate concentrations for subsequent growth curves and fluorescence-based experiments, and to observe whether antibacterial activity varied in mutant strains. Overnight cultures were diluted 1:100 in appropriate growth medium and grown to mid-logarithmic phase. Cells were then diluted to give a final concentration of 5×10^5 cells/ml in a pre-warmed 96-well clear, flat-bottomed microtiter plate (Falcon). This plate was prepared with an initial high concentration of the desired compound followed by a standard serial dilution. After addition of the cells, the plate was incubated at 37°C for 16 hours with shaking at 700 rpm. MIC was defined as the lowest compound concentration able to inhibit visible bacteria growth.

To observe the effect of studied compounds on cells in logarithmic growth phase, they were also added to growing cultures and optical density was monitored. For this, overnight cultures were diluted and grown to mid-logarithmic phase. Cells were then diluted to an OD_{600nm} (OD_{600}) of 0.05 and transferred to a 96-well clear, flat-bottomed microtiter plate (Falcon) in triplicate, to a final volume of 200 µl per well. Absorbance measurements were taken every 5 minutes using the BMG SPECTROstar Nano, until an OD_{600} of 0.2-0.6 (exact optical densities are stated in individual experiments) was reached, then compounds were added.

2.4 – Fluorescence microscopy

2.4.1 – General fluorescence microscopy

For standard fluorescence microscopy, cells were grown to early logarithmic phase in appropriate growth medium, including any inducers required for fluorescent protein

expression. 100 µl of culture was transferred to a 2 ml round bottomed Eppendorf tube with a perforated lid. Cells were incubated with appropriate dyes and/or antibiotics (see Tables 3 and 4) at the concentrations specified in individual experiments, with vigorous shaking at 37 °C unless stated otherwise. Teflon-coated multi-spot microscope slides were covered with a thin layer of deionised H_2O/1.2% agarose and warmed to room temperature prior to use. 0.5 µl of cell culture was applied to the exposed agarose surface and, after the liquid had evaporated, covered with a microscopy coverslip. Due to a gradual loss of membrane potential as a result of oxygen starvation, images were taken within 10 minutes of placing the coverslip. Microscopy was performed using Nikon Eclipse Ti (Nikon Plan Apo 100×/1.40 Oil Ph3 objective and CoolLED pE-300 or pE-4000 light source) equipped with the excitation/emission filters in Table 3, and images were acquired with either a Prime 4.2sCMOS or BSI camera (Photometrics) and Metamorph 7.7 (MolecularDevices).

Table 3: Fluorophores used throughout this thesis, including their functions and excitation and emission wavelengths for fluorometric measurements and fluorescence microscopy

Fluorophore	Function	Plate reader Ex/Em filters (nm)	Microscopy Ex/Em filters (nm)	Manufacturer
Sytox Green	Membrane-impermeant dye	485-10/520-10	470-40/525-50	Thermo Fisher Scientific
$DiSC_3(5)$	Voltage-sensitive dye	610-10/660-10	628-40/692-40	Anaspec or Sigma-Aldrich
NPN	Membrane dye	340-10/415-10	-	Sigma-Aldrich
Nile red	Membrane dye	584-10/620-10	560-40/630-75	Sigma-Aldrich
FM5-95	Membrane dye	-	560-40/630-75	Thermo Fisher Scientific
Hoechst 33342	DNA dye	355-10/460-10		Thermo Fisher Scientific
DAPI	DNA dye	-	350-50/460-50	Sigma-Aldrich

NADA	Peptidoglycan label	-	470-40/525-50	From Professor Waldemar Vollmer
Propidium Iodide	Membrane-impermeant dye	544-10/620-10	-	Thermo Fisher Scientific
Laurdan	Membrane fluidity dye	360-20/spectral scan	-	Sigma-Aldrich

Specific concentrations used are stated in individual experiments.

Table 4: Function, solvent and manufacturer of commonly used antibiotics throughout this thesis.

Compound	Function	Solvent	Manufacturer
Nisin	Pore forming	H_2O	Sigma-Aldrich
Gramicidin	Channel forming	DMSO	Sigma-Aldrich
Polymyxin B	Pore forming	H_2O	Sigma-Aldrich
Polymyxin B nonapeptide	Outer membrane permeabilising	H_2O	Sigma-Aldrich
CCCP	Protonophore	DMSO	Sigma-Aldrich
Colicin N	Channel forming	50 mM sodium phosphate, pH 7, 300 mM NaCl	From Dr Jeremy Lakey
Daptomycin	Membrane-active	H_2O	Abcam
Valinomycin	Potassium ionophore	DMSO	Sigma-Aldrich
NF-DAP	Daptomycin variant	H_2O	From Dr Scott Taylor
Octenidine	Membrane-active	H_2O	From Dr Nermina Malanovic

2.4.2 – DiSC$_3$(5) and Sytox Green combined fluorescence microscopy

Overnight cultures were diluted 1:100 in growth medium and grown to an OD$_{600}$ of 0.3 whilst shaking. 100 µl was transferred to a 2 ml round bottomed Eppendorf tube with a perforated lid. Compounds of interest were added from the beginning, alongside 200 nM of the membrane permeability indicator Sytox Green; whilst 1 µM of the voltage-

sensitive dye DiSC$_3$(5) was added 5 min before imaging (any modifications to dye concentrations will be stated in individual experiments) and incubated at 37°C upon shaking with a thermomixer. Samples were then immobilised on microscope slides covered with a H$_2$O/1.2% agarose and imaged immediately. Microscopy was performed using the filter sets listed in Table 3 and single cell fluorescence intensities were quantified using ImageJ/Fiji (Schindelin *et al.*, 2012), as described below.

2.4.3 – Peptidoglycan labelling

Incorporation of fluorescent D-amino acids such as NADA into bacterial peptidoglycan allows the *in situ* analysis of cell wall synthesis in live cells (Kuru *et al.*, 2012). For experiments using NADA, cells were grown in LB supplemented with 0.2% glucose overnight at 37°C. The following day, samples were diluted in growth medium and grown at 37°C until an OD$_{600}$ of 0.3 was reached. 100 µl were transferred to a 2 ml round bottomed Eppendorf tube with a perforated lid and incubated with the desired compounds. NADA was then added to a final concentration of 250 µM and incubated for a further 20 minutes. Cells were washed and resuspended in fresh growth medium to remove the excess dye and immobilised and imaged on H$_2$O/1.2% agarose as before.

2.4.4 – B. subtilis L-form DiSC$_3$(5) fluorescence microscopy

Generation of L-forms is described in section 2.2. All experiments involving L-forms were performed in osmoprotective NB/MSM growth medium. For microscopy, L-forms were incubated with compounds of interest at 30°C, followed by addition of 1 µM DiSC$_3$(5) prior to imaging. 70 µl were then transferred to a slide containing a gene frame (1.7 cm X 2.8 cm; Thermo Fisher Scientific) and sealed with a plasma treated coverslip (20 mins plasma treatment in a plasma cleaner; Harrick Plasma). The sealed slide was allowed to stand for 5 min to allow L-forms to settle. Microscopy was performed using the microscope and camera setup stated above, and the filter set described in Table 3. Images were acquired with Metamorph 7.7 (MolecularDevices) and single cell fluorescence intensities were quantified using ImageJ/Fiji (Schindelin *et al.*, 2012), as described below.

2.4.4 – Structured Illumination Microscopy (SIM)

Cells were prepared and immobilised on H$_2$O/1.2% agarose slides as described above. To reduce binding of Nile red to the coverslip surface, which can distort the structured illumination pattern projections, the coverslips were coated with L-dopamine (Zhang *et al.*, 2013; te Winkel *et al.*, 2016). For this, L-dopamine (2 mg/ml freshly

solved in 1 mM Tris, pH 8.0) was added to the coverslip and incubated at room temperature for 30 minutes. The excess L-dopamine and Tris were then removed by aspiration and submersion in H_2O, before evaporation at 37°C for 30 minutes. Dual-colour 2D-SIM was performed using Nikon N-SIM equipped with 488 and 561 nm lasers, Nikon CFI SR HP Apochromat TIRF 100x/1.49 oil objective, and Andor iXon DU-897 camera. Image capture and reconstruction was carried out using NIS Elements 5.21 (Nikon).

2.4.5 - Analysis and quantification of microscopy images

For general fluorescent microscopy, images were analysed using ImageJ/Fiji (Schindelin *et al.*, 2012). Quantification of $DiSC_3(5)$-fluorescence for individual cells was performed in a semi-automated manner. In brief, any background fluorescence was first subtracted, originating from unincorporated dye and medium. Individual cells were then selected as regions of interest (ROIs) by thresholding of corresponding phase contrast images. If cells adhered to each other or grew as chains, they were manually separated by a thin line with an appropriate pixel prior to automated cell detection. Finally, the mean fluorescence values for individual cells across the population were obtained.

2.5 – Fluorometric experiments

2.5.1 – General fluorometric experiments

For general fluorometric measurements, overnight cultures were prepared followed by 1:100 dilution in appropriate growth medium and growth to the OD_{600} stated in individual experiments. Fluorescent dyes were then either pre-added to cells or directly added to cells in black, polystyrene, flat-bottomed microtiter plates (Porvair Sciences). Fluorescence intensity was monitored until stable levels were obtained, followed by the addition of compounds. Fluorescence measurements were taken using a BMG Clariostar multimode plate reader, equipped with the excitation and emission filters listed in Table 3. All media, plates and instruments were warmed to 37°C prior to use.

2.5.2 - Laurdan-based membrane fluidity measurements

For observation of changes to the fluorescent spectra of cells unstained or stained with fluorescent membrane fluidity probe Laurdan, overnight cultures were diluted and grown in LB supplemented with 0.2% glucose at 30°C until an OD of 0.35. Here, samples were either unstained or stained with Laurdan, at a final concentration of 10 µM in 1% DMF, for 5 minutes with vigorous shaking at 30°C. Cells were washed four times with PBS supplemented with 0.2% glucose in the absence or presence of 1.25

mM CaCl$_2$ prior to transfer to black, polystyrene, flat-bottomed microtiter plates (Porvair Sciences). Compounds were then added to appropriate wells and shaken for 20 seconds at 30°C prior to measurement of emission spectra upon excitation at 360±20 nm using a BMG Clariostar multimode plate reader.

2.6 – *Bacillus subtilis* reporter strain screening

B. subtilis reporter strains were analysed in agar plug and Kirby Bauer disc diffusion assays. For this, cylinders were cut from GYM-agar cultures of the strain of interest or filter paper discs were impregnated with antimicrobial compounds. These were then placed and incubated on nutrient agar plates, supplemented with X-Gal (200 µg/ml) and erythromycin (3 µg/ml) and seeded with the *B. subtilis* reporter strains (either P$_{ypuA}$-*lacZ* or P$_{liaI}$-*lacZ*), that had been grown overnight in NB supplemented with erythromycin (3 µg/ml). 125 µg cefotaxime and 750 µg bacitracin were used as positive controls respectively. Plates were incubated overnight at 30°C and the following day, blue halos and zones of inhibition were determined.

2.7 – *Actinomycete* aqueous and methanolic extractions

Actinomycete strains that tested positive against the reporter strain panel were streaked on GYM-agar plates and grown to the day at which they most strongly activated σ^M or LiaRS. The cell material was then obtained and incubated at -20°C overnight. Following thawing, the cell mass was removed by centrifugation and the remaining supernatant was sterile filtered and stored at -20°C. For the methanolic extraction, 100% MeOH was incubated with the cell mass for 20 minutes at room temperature, with rotation. The supernatant was again collected by centrifugation and filtered into glass tubes. The samples were then evaporated to dryness and the crude extract resuspended in 100% DMSO. These were also stored at -20°C for future screening.

2.8 – Transformation of *E. coli*

For preparation of calcium competent *E. coli*, an overnight culture of the desired strain was diluted 1:100 in 50 ml LB and grown to mid-logarithmic phase. Cells were then incubated on ice for 20 minutes followed by centrifugation at 3000 rpm at 4°C for 10 minutes. The pellet was resuspended in 10 ml ice-cold 100 mM CaCl$_2$ and incubated on ice for a further 20 minutes. These steps were repeated; however, in 5 ml CaCl$_2$ and for 10 minutes. Again, the cells were centrifuged and then resuspended in 1.5 ml ice-cold 100 mM CaCl2 supplemented with 15% glycerol. Competent cells were then either snap frozen in liquid nitrogen or used for downstream transformation.

For heat-shock transformation, 0.5 µl of plasmid (10 – 30 ng DNA) was incubated with competent cells on ice for 30 minutes. Plasmids used throughout this thesis are listed in Table 5. Cells were then heat-shocked for 45 seconds in a 42°C water bath, before being placed on ice again for 5 minutes. Pre-warmed growth medium was then added, and samples were shaken at 37°C and 200 rpm for 1 hour. Samples were plated on appropriate selective plates and incubated overnight at 37°C. Single colonies were clean streaked onto selective plates and grown overnight. A single colony was then grown overnight in liquid culture supplemented with any relevant antibiotics and glycerol stocks were prepared from this with a final glycerol concentration of 25%.

Table 5: Plasmids, including their genotype and source, used throughout this thesis.

Plasmid	Genotype	Reference
pBAD33	pBAD33	(Guzman *et al.*, 1995)
VHp303	pBAD33-*phRel2*$_{Bac. sub.}$	(Jimmy *et al.*, 2020)
VHp464	pBAD33-*panT*$_{Bif. rum.}$	(Kurata *et al.*, 2022)
VHp515	pBAD33 SD-*panT*$_{Esc. col.}$	(Kurata *et al.*, 2022)
VHp517	pBAD33 SD-*capRel*$_{Vib. har.}$	(Kurata *et al.*, 2022)
VHp518	pBAD33 SD-*panT*$_{Bar. api.}$	(Kurata *et al.*, 2022)
VHp545	pBAD33 SD-*panT*$_{Bur. phage}$	(Kurata *et al.*, 2022)
VHp578	pBAD33 SD-*panT*$_{Hel. sp.}$	(Kurata *et al.*, 2022)
VHp580	pBAD33 SD-*panT*$_{Pse. mor.}$	(Kurata *et al.*, 2022)

2.9 – Statistical analysis

All statistical analysis was performed using Graphpad Prism 9, utilising either an unpaired, two-sided t-test, or an ordinary one-way, unpaired ANOVA with a Tukey's multiple comparisons post hoc test.

Chapter 3 – Optimising *in vivo* fluorescence-based techniques to identify membrane-disrupting antimicrobial compounds

3.1 – Introduction

Due to their misuse and overuse in both clinical and agricultural settings, antibiotic resistance is one of the biggest threats to global health today (World Health Organization (WHO), 2020). This crisis is exacerbated by a deficit in antibiotic innovation, as demonstrated by the linear decline in antibacterial new molecule entities over the past 30 years (Infectious Diseases Society of America (IDSA), 2011). There is, therefore, the urgent need for compounds with novel targets and modes of action. One emerging strategy is targeting the bacterial cytoplasmic membrane. This essential macromolecular structure, already exploited by known host defence peptides (Henzler Wildman, Lee and Ramamoorthy, 2003; Barns and Weisshaar, 2013; Riool *et al.*, 2020), is not only the site for crucial cellular processes, but is also non-DNA encoded, making the development of resistance less likely. Their clinical efficacy is also proven by the recent success of existing membrane-active antibiotics polymyxin B, daptomycin and colistin as last resort agents against multi-drug resistant infections (Sauermann *et al.*, 2008; Vaara, 2019; Sabnis *et al.*, 2021).

Membrane-targeting antibiotics commonly perturb membrane integrity by increasing permeability to ions or larger molecules, or by inducing more subtle changes such as forming or disturbing lipid domains, altering membrane fluidity, or delocalising membrane-associated proteins (Wiedemann *et al.*, 2004; Müller *et al.*, 2016; Wenzel *et al.*, 2018). Large membrane-impermeable fluorescent dyes, such as Propidium Iodide and Sytox Green, are often implemented to investigate antibiotic-induced changes in membrane permeability *in vivo*. These probes are ~600 Da and can only enter the cell when large pores are formed in the cytoplasmic membrane. Subsequently, they intercalate with DNA, causing a large enhancement of dye fluorescence (Roth *et al.*, 1997; Barns and Weisshaar, 2013; Stiefel *et al.*, 2015). However, due to their size, these probes are unable to detect smaller-sized channels, increased ion permeability, or inhibition of respiration; all of which can still be lethal to the cell through dissipation of the transmembrane potential (Jolliffe, Doyle and Streips, 1981; Strahl and Hamoen, 2010; Müller *et al.*, 2016; Bruni and Kralj, 2020). Therefore, membrane depolarisation can be followed as a reporter for antibiotic-induced membrane disturbances using a number of voltage-sensitive fluorescent probes. These include fast-response probes (usually styrylpyridinium dyes, such as di-4-

ANEPPS) which undergo an electronic charge shift, and consequently a spectral shift, in response to changes in the voltage across the membrane (Fluhler, Burnham and Loew, 1985). Although they are able to detect millisecond changes in membrane potential, their voltage-dependent change in fluorescence intensity is usually small: ~2–10% per 100 mV. In contrast, slow-response probes (carbocyanines and oxonols such as $DiOC_2(3)$ and $DiBAC_4(3)$, respectively), which exhibit voltage-dependent changes in transmembrane location, demonstrate a much larger fluorescence change: typically 1% per mV, and are more suitable for detecting drug-induced changes in the membrane potential of bacteria. Another example of a voltage-sensitive carbocyanine dye is 3,3′-Dipropylthiadicarbocyanine iodide, or $DiSC_3(5)$. Due to its hydrophobic and cationic nature, it can penetrate the lipid bilayer and accumulate in polarised cells, causing a self-quenching of fluorescence. Upon depolarisation, the dye is rapidly released from the cells, resulting in a de-quenching which can be followed fluorometrically (Waggoner, 1976; te Winkel *et al.*, 2016).

WHO have identified 3 "critical priority" antibiotic-resistant pathogens (*Acinetobacter baumannii*, *Pseudomonas aeruginosa* and *Enterobacteriaceae)*, all of which are Gram-negative and resistant to multiple antibiotics (Tacconelli *et al.*, 2018). However, due to exclusion of fluorescent probes by the outer membrane, it has proved difficult to monitor disturbances to the cytoplasmic membrane in these organisms. The use of $DiSC_3(5)$ has been reported in mechanism of action studies in Gram-negative bacteria (Wu *et al.*, 1999; Silvestro, Weiser and Axelsen, 2000; French *et al.*, 2020); but measurements are frequently taken in buffers of various compositions, in the presence of chelating agents such as EDTA or in strains with hyperpermeable outer membranes. Thus, a robust protocol for using $DiSC_3(5)$ to measure perturbations of transmembrane potential in Gram-negative bacteria is missing. Results from this chapter investigating such methods were the basis of a collaborative publication with Dr Philipp Popp from Humboldt-Universität zu Berlin (Buttress *et al.*, 2022).

The higher-throughput use of $DiSC_3(5)$ (i.e., a cell-based assay in a 96-well plate format) in Gram-positive bacteria has been previously optimised by our group (te Winkel *et al.*, 2016); whereas determining membrane pore formation with Sytox Green has only been performed by fluorescence microscopy or flow cytometry (Kepplinger *et al.*, 2018; Kurata *et al.*, 2022; Malanovic *et al.*, 2022). Furthermore, the use of DNA-intercalating and voltage-sensitive fluorescent dyes has been combined to

simultaneously investigate membrane pore-formation and depolarisation (Clementi *et al.*, 2014; McAuley *et al.*, 2018; Boix-Lemonche, Lekka and Skerlavaj, 2020), however to the best of our knowledge, a higher-throughput screen has not yet been developed using both DiSC$_3$(5) and Sytox Green, and such assays have only been tested with known antibacterial compounds and not extracts derived from bacterial origin. This provides an easily accessible method to detect membrane disturbances as part of antibiotic mode of action studies.

3.2 – Results

3.2.1 – Fluorometric detection of membrane disruption in the Gram-positive *Bacillus subtilis*

I first aimed to develop a high-throughput screen for cytoplasmic membrane pore formation in the Gram-positive model organism *B. subtilis*, using the large membrane-impermeable fluorescent dye Sytox Green. To begin, I performed a MIC assay to confirm our candidate for positive control, nisin, was growth inhibitory against our test strain *B. subtilis* 168. Nisin is a lantibiotic derived from *Lactococcus lactis* (Mattick, Hirsch and Berridge, 1947), which binds to and polymerises with the membrane-bound peptidoglycan precursor lipid II, allowing its insertion into the membrane and the formation of pores (Breukink and de Kruijff, 2006). It was determined that nisin was highly toxic against *B. subtilis* 168 (Table 6).

Table 6: Minimum inhibitory concentrations (MICs) of nisin and gramicidin against the Gram-positive model organism *B. subtilis* 168.

Compound	*B. subtilis* 168
	MIC (µM)
Nisin	0.625
Gramicidin	2.5

N=3.

The next step was to verify whether this peptide could interact with the fluorescence of Sytox Green, as it was previously shown that the protonophore CCCP interfered with the voltage-sensitive dye DiSC$_3$(5) (te Winkel *et al.*, 2016). Sytox Green fluorescence,

in the absence of cells, was therefore monitored over time. No change was observed upon addition of nisin (Fig. 19A), validating its compability with Sytox Green.
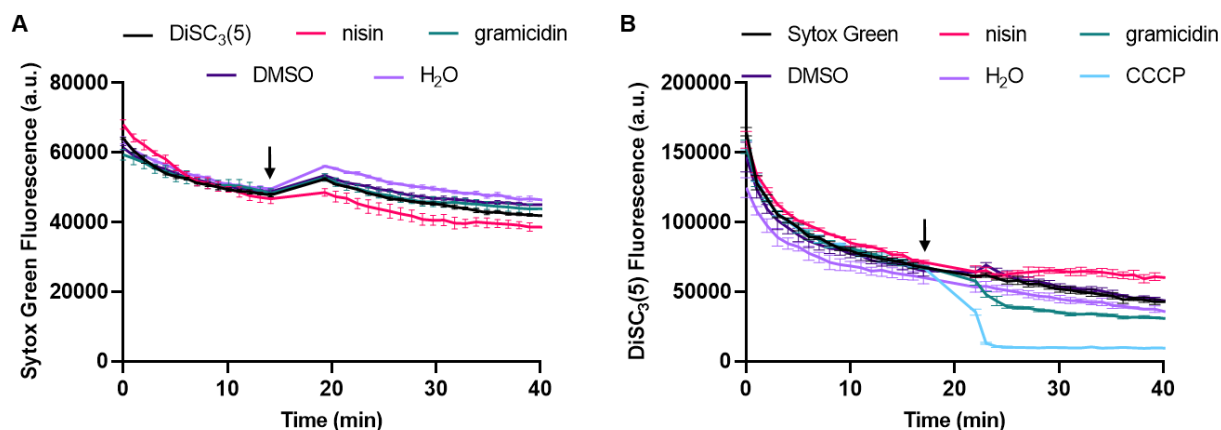
Figure 19: Interactions between DiSC$_3$(5) and Sytox Green, antimicrobial compounds and solvents. Fluorescence intensity of (A) 1 µM Sytox Green and (B) 1 µM DiSC$_3$(5) in LB medium upon addition of the other dye, the lantibiotic nisin, the channel-forming peptide gramicidin and the solvents, DMSO and H$_2$O. The time point of compound addition is indicated by a black arrow. Note, although not used in these assays, addition of the protonophore CCCP is included as a representation of strong dye interference. Data are represented as mean±SD (n=3).

During their study, te Winkel et al. (2016) noted the importance of first determining the optimal cell density and dye concentration when adapting fluorometric assays for new fluorescent dyes. Therefore a range of Sytox Green concentrations was tested, and as shown in Fig. 20, only a concentration of 1 µM demonstrated a detectable increase in fluorescence upon nisin addition.
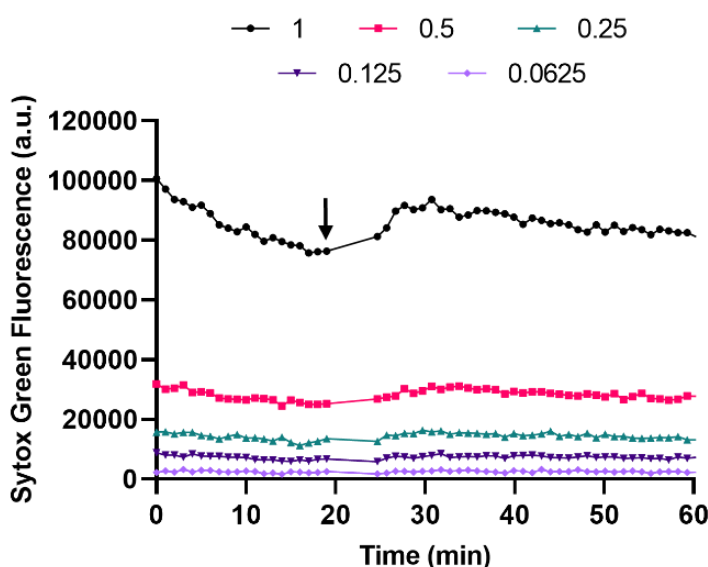
Figure 20: Effect of dye concentration on nisin-induced Sytox green fluorescence in *B. subtilis*. Fluorescence intensity changes of different Sytox Green concentrations (all µM) in *B. subtilis* cells at an OD$_{600}$ of 0.2 following addition of 10 µM nisin. Sytox Green was added from 0 min and nisin addition is indicated by a black arrow. Strain used: *B. subtilis* 168 (wild type).

To optimise this response, I experimented with different optical densities of cells, and determined that an OD_{600} of 0.6 produced the optimal difference pre- and post-nisin treatment (Fig. 21). However, to ensure the cells were in a logarithmic phase of growth,
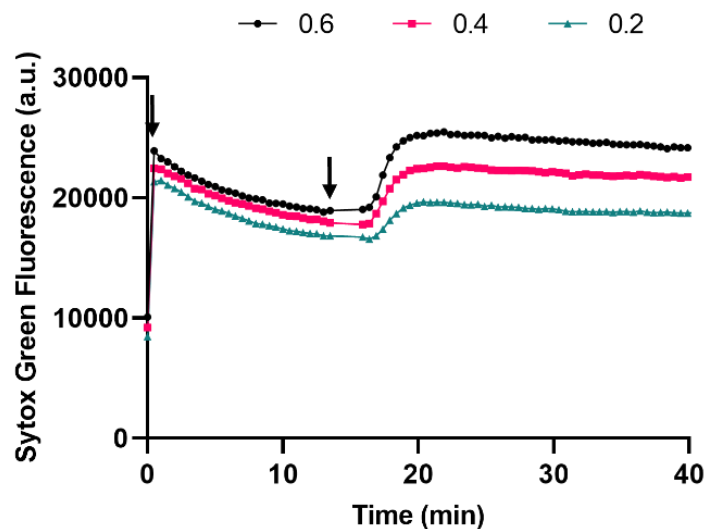
Figure 21: Effect of cell density on nisin-induced Sytox green fluorescence in *B. subtilis*. Fluorescence intensity changes of 1 µM Sytox Green in *B. subtilis* cells at different OD_{600} values following addition of 10 µM nisin. Sytox Green addition is represented by the first arrow and nisin-treatment by the second. Strain used: *B. subtilis* 168 (wild type).

I proceeded with a slightly lower cell density of OD_{600} 0.5. This combined with a Sytox Green concentration of 1 µM provided a good fluorescence intensity difference between intact and membrane-compromised cells (Fig. 22).
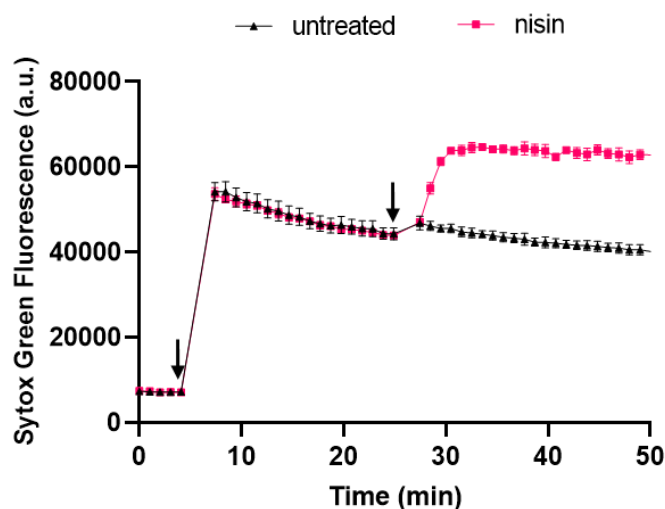
Figure 22: Fluorometric detection of membrane pore formation in *B. subtilis*. Fluorescence intensity changes of 1 µM Sytox Green in *B. subtilis* at an OD_{600} of 0.5, in the absence or presence of 10 µM nisin. Sytox Green addition is indicated by the first arrow and nisin addition by the second. Data are represented as mean±SD (n=3). Strain used: *B. subtilis* 168 (wild type).

Due to the far-red fluorescence of DiSC$_3$(5), it should be compatible with simultaneous detection of green fluorescent dyes such as Sytox Green. Therefore, I next began to develop a combined Sytox Green and DiSC$_3$(5) assay to simultaneously investigate membrane pore formation and depolarisation, respectively. This would allow for the identification of membrane-targeting compounds that act without pore formation, and thus might exhibit improved safety profiles due to predicted reduced haemolytic activity (see 1.4.2). For membrane depolarisation, the positive control was gramicidin ABCD, from here on referred to as "gramicidin", which was growth inhibitory against *B. subtilis* at low micromolar concentrations (Table 6). Gramicidin is a highly hydrophobic linear antibiotic isolated from *Bacillus brevis* (Sarges and Witkop, 1965)*,* which forms monovalent and cation specific channels in the cytoplasmic membrane (Hladky and Haydon, 1972), impeding the bacterium's ability to maintain its membrane potential. Again, I tested whether gramicidin or its solvent, DMSO, affected either Sytox Green or DiSC$_3$(5) fluorescence, and moreover whether there was interference between both dyes. No interactions existed between any peptides, solvents or dyes (Fig. 19).

The optimal Sytox Green conditions (1 µM and OD$_{600}$ 0.5) in conjunction with the previously optimised DiSC$_3$(5) concentration in *B. subtilis*, 1 µM in 1% DMSO, provided strong fluorescence intensity increases of both dyes in response to nisin-treatment (Fig. 23); whilst gramicidin only increased DiSC$_3$(5) fluorescence (as the channels it forms are not large enough to allow Sytox Green entry). Furthermore, experiments were performed in LB medium supplemented with 0.5 mg/ml BSA and 10 µg/ml chloramphenicol to reduce absorption of DiSC$_3$(5) to the polystyrene surface of the plate and prevent shifts in fluorescence due to cell growth, respectively (te Winkel *et al.*, 2016). These conditions were applied to all subsequent plate reader experiments measuring DiSC$_3$(5) fluorescence intensity.
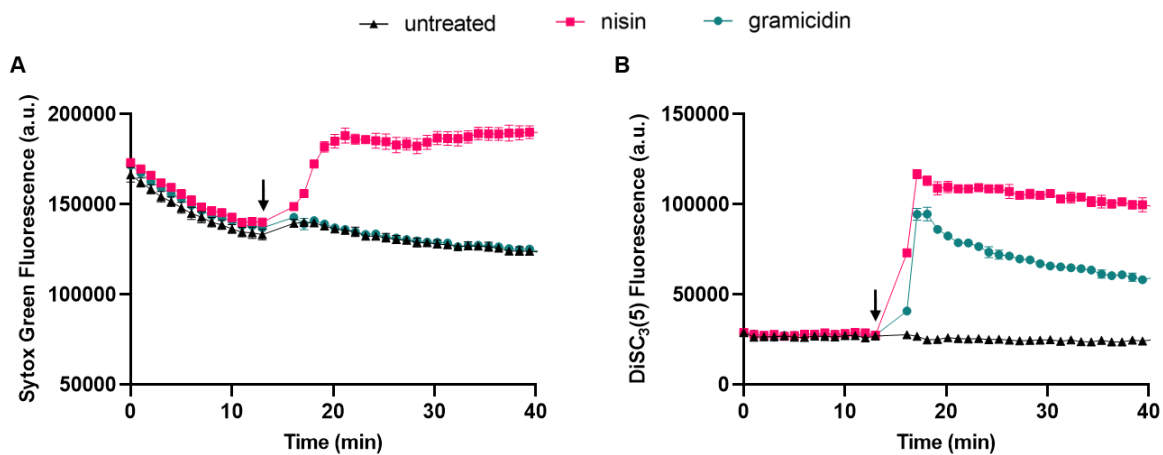
Figure 23: A combined screen simultaneously investigating membrane pore formation and depolarisation is viable in *B. subtilis*. Fluorescence intensity changes of (A) 1 µM Sytox Green and (B) 1 µM $DiSC_3(5)$ in *B. subtilis* cells at an OD_{600} of 0.5, untreated or treated with 10 µM nisin or 10 µM gramicidin, in the presence of 0.5 mg/ml BSA and 10 µg/ml chloramphenicol. The time point of antibiotic addition is highlighted by an arrow. The kinetics of each dye are shown in separate graphs for clarity. Data are represented as mean±SD (n=3). Strain used: *B. subtilis* 168 (wild type).

Finally, maintaining sufficient aeration during measurement is crucial to provide stable energisation, and thus fluorescence levels for polarised cells (te Winkel *et al.*, 2016). Therefore, I performed the combined screen in a full microtiter plate to determine the length of shaking required to ensure untreated cells remained energised despite the prolonged measurement time. Measurements taken every 150 s with 75 s vigorous
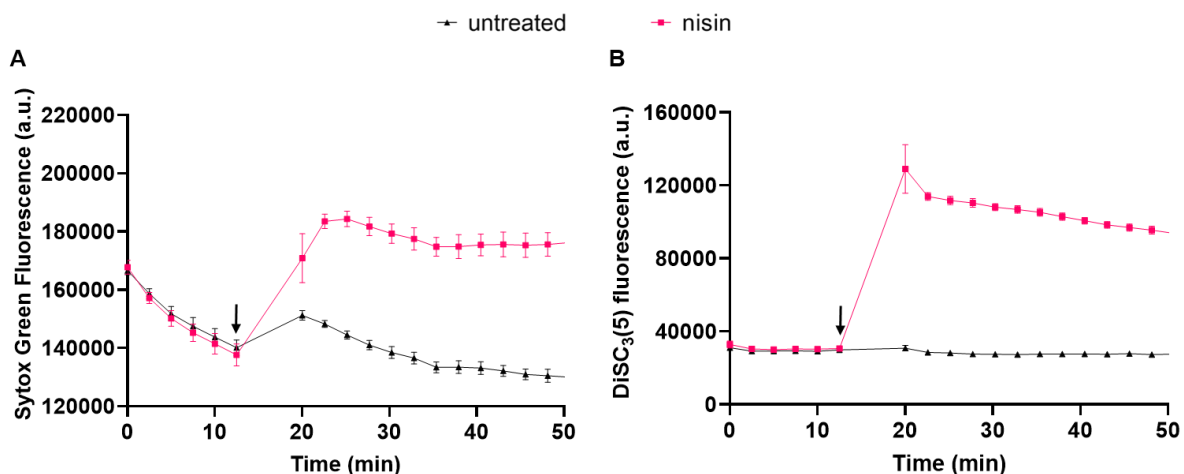
Figure 24: The combined *B. subtilis* membrane pore formation and depolarisation screen is compatible in a 96-well plate format. Changes in (A) 1 µM Sytox Green and (B) 1 µM $DiSC_3(5)$ fluorescence intensity in *B. subtilis*, untreated or treated with 10 µM nisin. The time point of nisin addition is indicated by an arrow. Untreated cells remain energised despite the prolonged measurement time, as demonstrated by no upward shift in $DiSC_3(5)$ fluorescence. Data are represented as mean±SD (n=24). The kinetics of each dye are shown in separate graphs for clarity. Strain used: *B. subtilis* 168 (wild type).

shaking at 200 rpm resulted in the minimal cycle time with maximal shaking in which untreated cells remained energised (demonstrated by no upward shift in $DiSC_3(5)$ fluorescence; Fig. 24). It should be noted that the increase in Sytox Green fluorescence observed in untreated cells is due to the duration of time the plate is removed from the reader between measurements for compound addition, as demonstrated in Fig. 25. Thus, a fluorescence-based assay that allows the rapid identification and differentiation between membrane pore forming and depolarising compounds has been developed in a 96-well plate format. Use of this assay to screen *Acintomycete*-derived extracts will be detailed in Chapter 5.
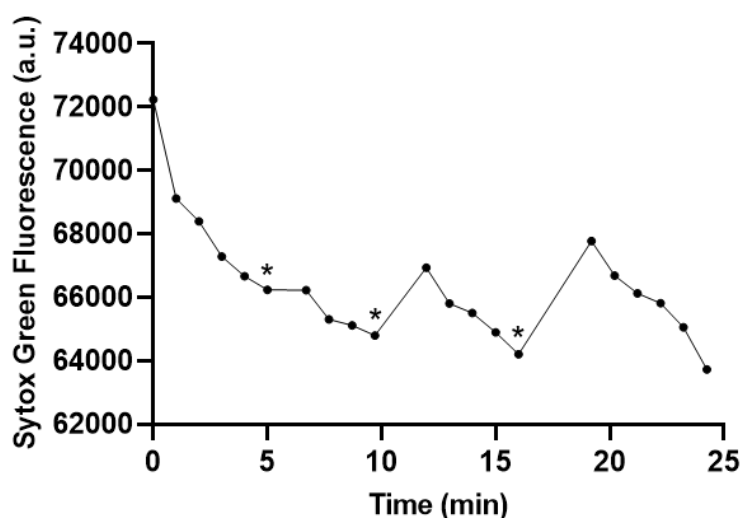
Figure 25: Sudden increases in Sytox Green fluorescence are dependent on the length of time that the plate is removed from the plate reader. Fluorescence kinetics of *B. subtilis* cells stained with 1 μM Sytox Green. Asterisks indicate when the plate was removed from the plate reader; the first for 1 min, the second for 2 min and the third for 3 min. Strain used: *B. subtilis* 168 (wild type).

3.2.2 – Detection of cytoplasmic membrane depolarisation in the Gram-negative *Escherichia coli*

As discussed previously, for both fundamental cell biology and antibiotic discovery, it is becoming more crucial to detect disturbances at the cytoplasmic membrane of Gram-negative bacteria. Therefore, I wished to develop techniques to analyse cytoplasmic membrane depolarisation in the Gram-negative model organism, *E. coli*. I began by investigating the toxicity of $DiSC_3(5)$ [as its prolonged incubation in *B. subtilis* can impair growth (te Winkel *et al.*, 2016)] and antimicrobial peptides in the strain used throughout these experiments, *E. coli* MG1655. Results in Table 7 show that polymyxin B (PMB) displayed high antibacterial activity. This, along with its well-documented ability to permeabilise the cytoplasmic membrane (see 1.1.1) confirmed its validity as a positive control in this study. As expected, due to absence of the fatty acid tail (Fig.

2), the nonapeptide derivative (PMBNP) was not growth inhibitory at any concentration tested.

Table 7: Minimum inhibitory concentrations (MICs) of PMB, PMBNP and DiSC$_3$(5) against *E. coli* MG1655 in the absence and presence of the outer membrane permeabilising agent PMBNP.

Compound	*E. coli* MG1655	
	MIC (µM)	MIC in the presence of PMBNP (µM)
Polymyxin B	0.2	NA
Polymyxin B nonapeptide	>100	NA
DiSC$_3$(5)	>100	10

PMB: Polymyxin B, PMBNP: Polymyxin B nonapeptide, NA: not applicable, n=3.

I also observed that DiSC$_3$(5) was not toxic at any concentration tested in intact bacteria, however when the outer membrane was permeabilised by nonapeptide treatment, it was growth inhibitory at 10 µM (Table 7). Although this is interesting, as it suggests that the outer membrane provides additional protection against the toxicity of DiSC$_3$(5), this concentration was higher than applied in subsequent experiments. I verified this by applying 1 µM of DiSC$_3$(5) to cells in logarithmic growth phase and observed no effect on growth even in the presence of PMBNP (Fig. 26). Therefore, the inhibitory effect of DiSC$_3$(5) appears to be a peculiarity of *B. subtilis,* as it does also not occur in the close relative *Staphylococcus aureus* (unpublished data, Sandra Laborda Anadón)*.*
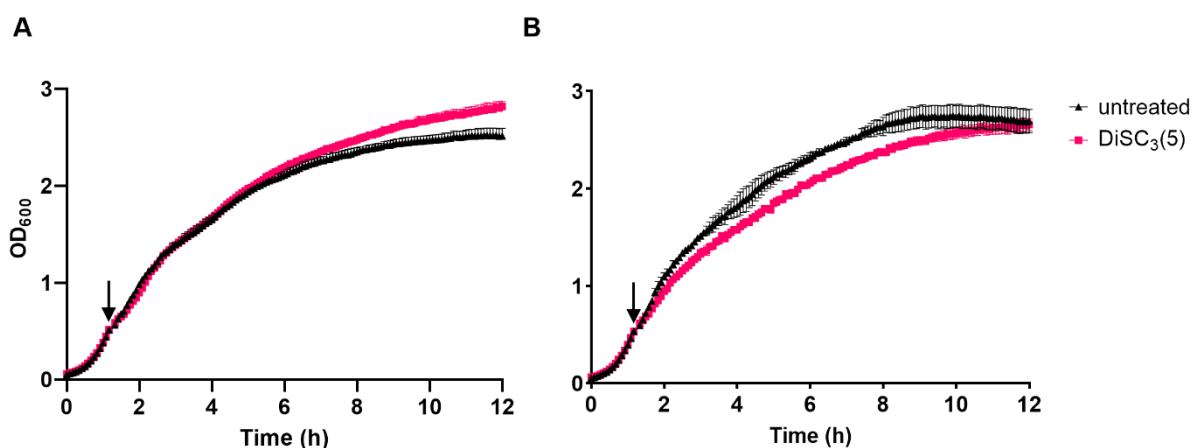
Figure 26: At experimental concentrations, DiSC$_3$(5) does not inhibit *E. coli* growth. Growth kinetics of *E. coli* cells grown to an OD$_{600}$ of 0.5 and then treated with 1 µM DiSC$_3$(5), in (A) the absence and (B) presence of 30 µM PMBNP. DiSC$_3$(5) addition is shown by a black arrow and data are represented as mean±SD (n=3). Strain used: *E. coli* MG1655 (wild type).

It has already been shown that single cell DiSC$_3$(5) fluorescence microscopy provides a simple and rapid method to measure membrane potential in the Gram-positive model organism *B. subtilis* (te Winkel *et al.*, 2016). To confirm whether this was also possible in Gram-negative bacteria, I probed the technique with *E. coli* cells, in the absence and presence of PMB and PMBNP. For this, I directly added DiSC$_3$(5) and the respective peptides to agarose pads, additionally supplemented with 10% LB, followed by addition of *E. coli* cells and rapid microscopy. This was to observe the coarse kinetics of membrane depolarisation upon the imaging process. In untreated cells, DiSC$_3$(5) fluorescence signals remained stable over 14 min (Fig. 27).
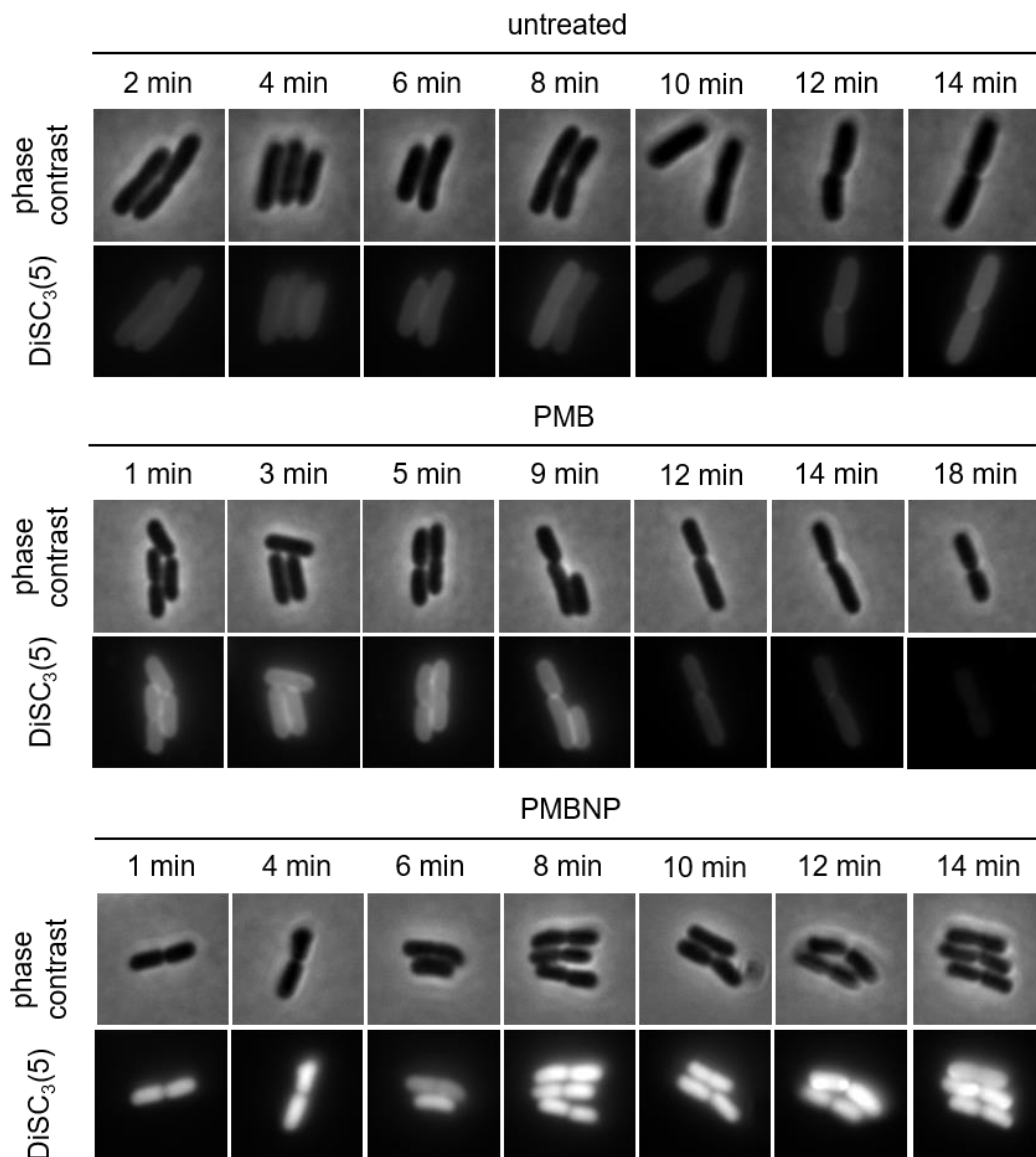
Figure 27: DiSC$_3$(5) staining is influenced by both outer membrane permeabilisation and (inner) membrane depolarisation in *E. coli*. Phase contrast and fluorescence microscopy of *E. coli* stained with 1 µM DiSC$_3$(5) in the absence and presence of 7 µM PMB or 30 µM PMNBNP at different time points. Note for this experiment, dyes and antibiotics were added directly to the agarose (supplemented with 10% LB) so that the immediate response could be visualised. Strain used: *E. coli* MG1655 (wild type).

Surprisingly, upon incubation with PMB, there was an immediate increase in $DiSC_3(5)$ fluorescence intensity for approximately 10 min prior to a loss $DiSC_3(5)$ signal, indicating cytoplasmic membrane depolarisation. This increase was even more apparent in PMBNP-treated *E. coli*, where cells remained highly stained for the entire time of the measurement (14 min). This demonstrates that whilst $DiSC_3(5)$ staining is sensitive to inner membrane potential levels and exhibits the expected loss of fluorescence upon depolarisation, the staining is also strongly influenced by outer membrane permeabilisation. It is therefore possible to use the voltage-sensitive fluorescent dye $DiSC_3(5)$ to observe single cell changes in membrane potential of wild type *E. coli* cells directly in growth medium. However, care should be taken when interpreting the results if used under conditions that compromise the integrity of the outer membrane, or when comparing strains that have outer membranes of different composition or structure.

Subsequently, as several studies amongst the literature perform membrane potential measurements of cells in buffer (Wu *et al.*, 1999; Silvestro, Weiser and Axelsen, 2000; Morin *et al.*, 2011), I aimed to investigate how washing and resuspending the cells in the commonly used buffer, PBS, with or without additional supplements affected $DiSC_3(5)$ signal levels compared to measurements directly in the growth medium. One important but frequently overlooked parameter when analysing membrane potential levels in buffer-suspended cells is the necessity to maintain a metabolisable carbon source. To test its effect on $DiSC_3(5)$ signal levels, I compared cells grown in LB supplemented with 0.2% glucose, and cells washed and resuspended in PBS with and without 0.2% glucose, followed by incubation for 15 min with shaking and staining. PMB-treatment was used as a positive control for complete depolarisation. Immediately, I observed that signals in PBS with glucose were higher compared to growth medium and extremely heterogeneous (Fig. 28A, B).
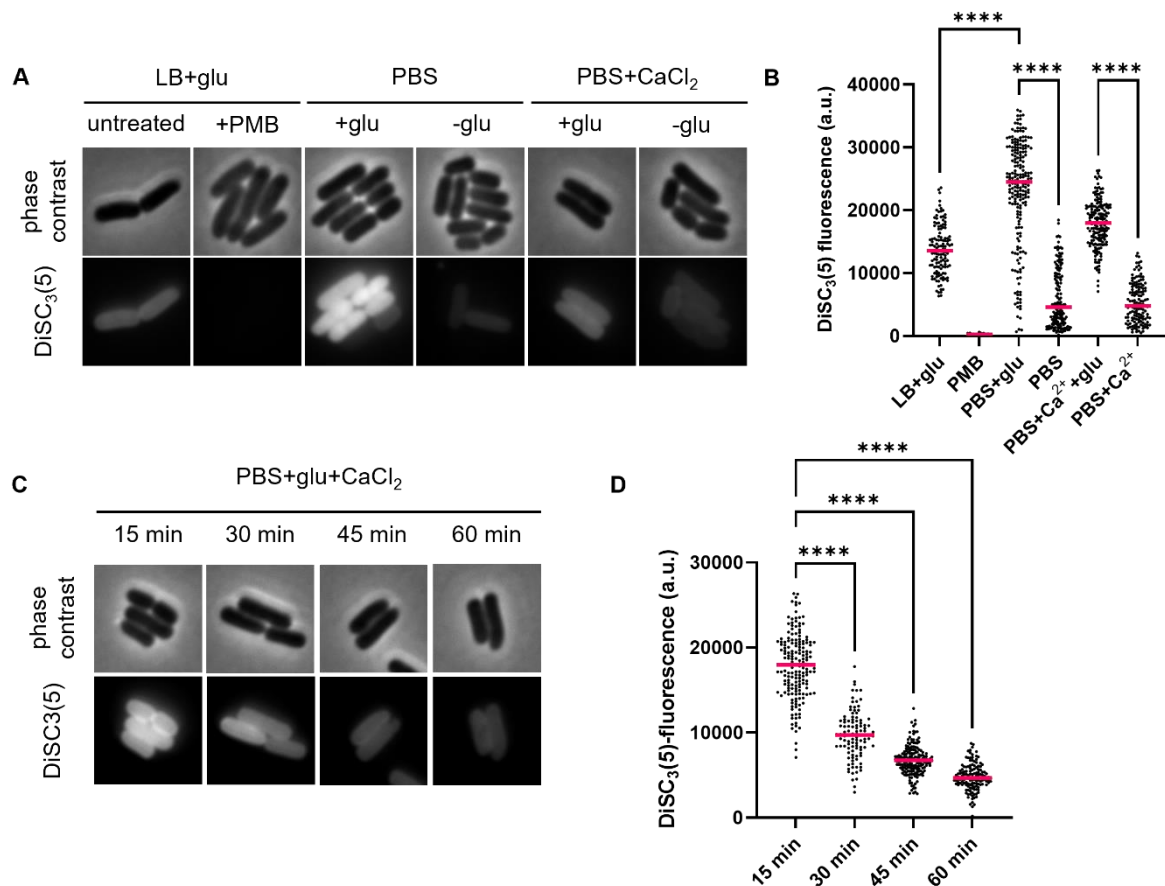
Figure 28: Calcium, glucose and rapid imaging are critical for measuring *E. coli* membrane potential in buffer. (A) Phase contrast and fluorescence microscopy images of *E. coli* in LB + 0.2% glucose or PBS in the presence or absence of 0.2% glucose and 1 mM CaCl₂, and stained with 1 µM DiSC₃(5). As a positive control, the transmembrane potential was disrupted by the pore forming antibiotic PMB (7 µM). (B) Quantification of DiSC₃(5)-fluorescence for individual cells from the dataset shown in panel A (n=128-211 cells). Median fluorescence intensity is indicated with a magenta line, together with P values of a one-way, unpaired ANOVA. **** represents p < 0.0001. (C) Phase contrast and fluorescence microscopy time course of *E. coli* in PBS supplemented with 0.2% glucose and 1 mM CaCl₂ and stained with 1 µM DiSC₃(5). (D) Quantification of DiSC₃(5)-fluorescence for individual cells from the dataset shown in panel C (n=106-176 cells). Median fluorescence intensity is indicated with a magenta line, together with P values of a one-way, unpaired ANOVA. **** represents p < 0.0001. Strain used: *E. coli* MG1655 (wild type).

In the absence of a carbon source, this heterogeneity still existed; however, as shown in both the microscopy images and quantification, the DiSC₃(5) staining was greatly reduced, indicating diminished membrane potential. Whilst the higher initial DiSC₃(5) levels in PBS may be due to differences in solubility of the dye between growth medium and buffer, I hypothesised that washing the cells could also remove divalent cations that bridge neighbouring LPS molecules in the outer membrane, thereby destabilising it and increasing DiSC₃(5) fluorescence, as I see with PMBNP-treatment. To test this,

I repeated the experiment washing and resuspending the cells in PBS additionally supplemented with 1 mM CaCl$_2$. Again, signals were reduced in the absence of a carbon source (Fig. 28A, B); however, supplementation with both glucose and CaCl$_2$ improved consistency of signals and gave rise to DiSC$_3$(5) fluorescence intensities more comparable to those measured in growth medium. This demonstrates that divalent cation removal, likely through destabilisation of the outer membrane, indeed affects DiSC$_3$(5) staining. I also performed a DiSC$_3$(5) fluorescence microscopy time course of cells washed and resuspended in PBS to investigate how long they would remain energised. As demonstrated by the loss of DiSC$_3$(5) fluorescence, *E. coli* cells gradually lose membrane potential in PBS buffer even when supplemented with both glucose and CaCl$_2$ (Fig. 28C, D). These findings highlight that if there are experimental reasons to perform membrane potential measurements in controlled buffers, it is necessary to include both a carbon source and Ca^{2+} followed by rapid imaging to maintain cell energisation and signal homogeneity.

Next, I aimed to confirm whether co-staining with DiSC$_3$(5) and Sytox Green was also possible in Gram-negative *E. coli*. As shown in Fig. 29, untreated cells exhibited strong DiSC$_3$(5) fluorescence, indicative of polarisation; whilst cells treated with the membrane pore forming lipopeptide PMB lost DiSC$_3$(5) fluorescence and gained a strong Sytox Green signal. Thus, this technique permits the identification and differentiation between membrane depolarising and membrane pore-forming antimicrobial compounds or stresses *in vivo*, on a single-cell level, and will be utilised for mode of action studies later in this thesis.
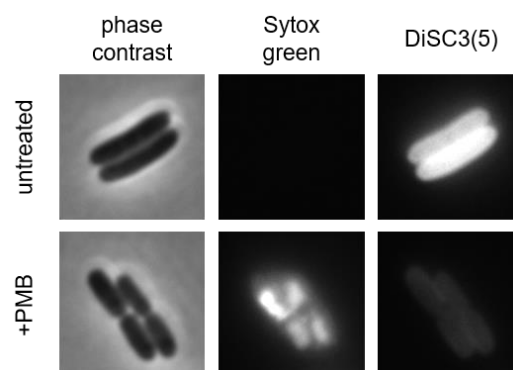
Figure 29: Simultaneous detection of membrane potential and pore formation in *E. coli*. Phase contrast and fluorescence microscopy of *E. coli*, co-stained with 200 nM Sytox Green and 1 µM DiSC$_3$(5) in the absence or presence of 7 µM PMB (15 min). Note that the loss of membrane potential in PMB-treated cells coincides with ability of Sytox Green to enter the cells, indicating pore formation. Strain used: *E. coli* MG1655 (wild type).

I then wanted to investigate whether membrane depolarisation in Gram-negative organisms could be analysed in a higher-throughput format (i.e., in the plate reader). Similarly to section 3.2.1, I verified that our control compounds (PMB and PMBNP) did not interfere with $DiSC_3(5)$ fluorescence (Fig. 30). Next, as I was optimising the dye concentration, I noticed that higher concentrations prolonged the quenching of $DiSC_3(5)$ fluorescence as it initially accumulated in polarised cells (Fig. 31). Therefore, I proceeded with 0.5 µM $DiSC_3(5)$ in 1% DMSO, as the fluorescence stabilised more rapidly.
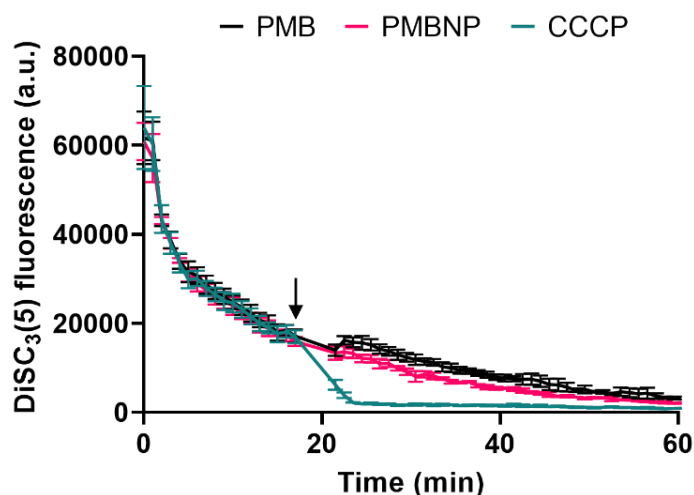
Figure 30: Interactions between DiSC₃(5) and antimicrobial compounds. Fluorescence intensity of 1 µM $DiSC_3(5)$ in LB upon addition of the pore forming antibiotic PMB and the outer membrane permeabilising agent PMBNP. The time point of compound addition is indicated by a black arrow. Note, although not used in these assays, I have included addition of the protonophore CCCP as a representation of strong dye interference. Data are represented as mean±SD (n=3).
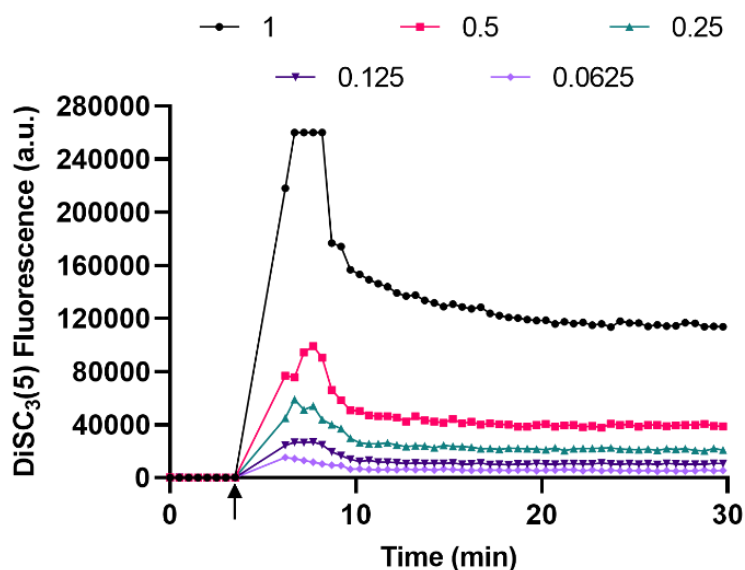
Figure 31: A lower DiSC₃(5) concentration is required to facilitate fluorescence quenching in *E. coli*. Fluorescence kinetics of *E. coli* cells stained with different

DiSC$_3$(5) concentrations (all μM in 1% DMSO). DiSC$_3$(5) addition is represented by a black arrow. Strain used: *E. coli* MG1655 (wild type).

Following optimisation, treatment with our control compounds mirrored our observations microscopically: an initial decrease in fluorescence due to increased accumulation of DiSC$_3$(5) within the cells as the outer membrane is destabilised, and an increase following approximately 10 min incubation with PMB, that corresponds to membrane depolarisation (Fig. 32). Therefore, DiSC$_3$(5)-based membrane potential assays are possible using fluorometry and, although sacrifice single-cell resolution, are more accessible and provide both higher throughput and better temporal resolution.
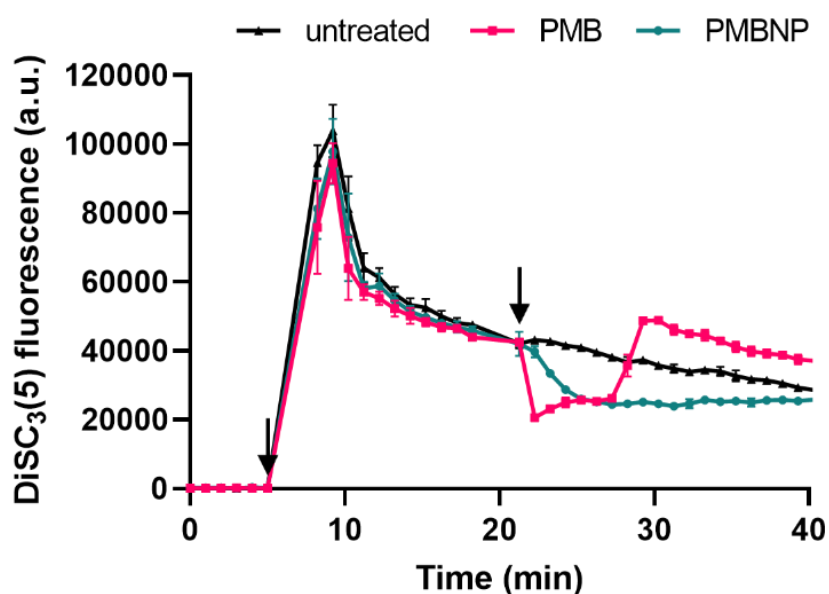
Figure 32: Fluorometric detection of outer membrane permeabilisation and inner membrane depolarisation in *E. coli*. Fluorescence intensity changes of 0.5 μM DiSC$_3$(5) in *E. coli* at an OD$_{600}$ of 0.5, in the absence or presence of 7 μM PMB or 30 μM PMBNP. DiSC$_3$(5) addition is indicated by the first arrow and compound addition by the second. Data are represented as mean±SD (n=3). Strain used: *E. coli* MG1655 (wild type).

Finally, I wished to determine whether membrane pore formation could be detected fluorometrically in *E. coli*, and ultimately lead to a combined screen, similarly to what I had optimised in *B. subtilis* (Fig. 23 and 24). However, as shown in Fig. 33A, polymyxin B-addition did not elicit a detectable change in Sytox Green fluorescence intensity at any concentration I tested. For this purpose, I also investigated another large membrane-impermeable nucleic acid stain, Propidium Iodide, which is frequently used to monitor changes in bacterial membrane permeability (Belley *et al.*, 2009; Müller *et al.*, 2016; Seydlová *et al.*, 2018; Wenzel *et al.*, 2018). Again, polymyxin B-treatment
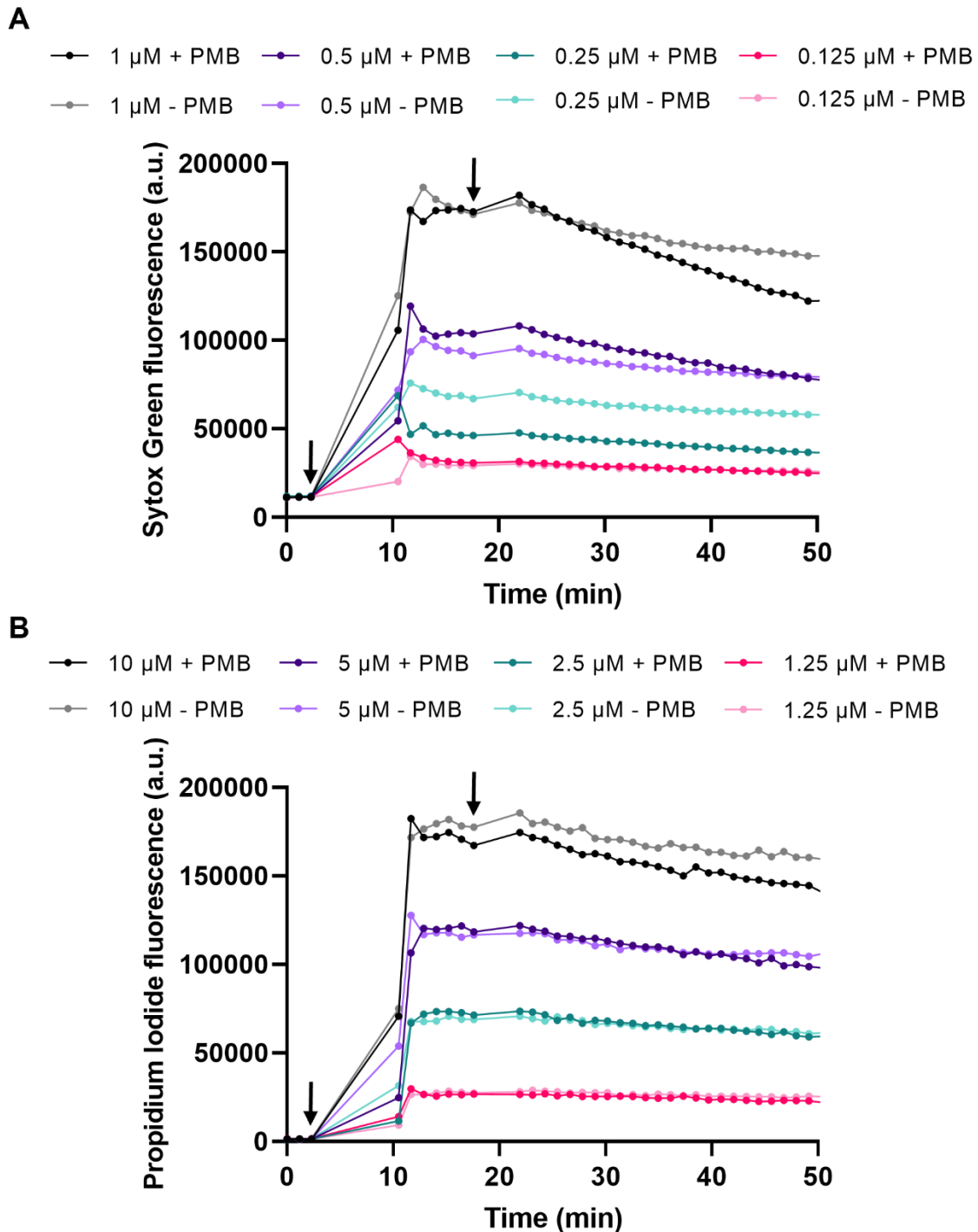
Figure 33: Fluorometric detection of inner membrane pore formation is not possible in *E. coli*. Fluorescence intensity changes of varying concentrations of (A) Sytox Green and (B) Propidium Iodide in *E. coli* cells at an OD_{600} of 0.5 in the absence or presence of 7 µM PMB. Dye addition is indicated by the first arrow and PMB addition by the second. Strain used: *E. coli* MG1655 (wild type).

did not affect fluorescence intensity compared to untreated cells at any concentration tested (Fig. 33B). From these experiments I concluded that an *in vivo* plate reader assay to detect inner membrane pore formation was not amenable in the Gram-negative model organism *E. coli*.

3.3 – Discussion

Due to the growing threat of antibiotic resistance, there are increasing efforts to identify antimicrobial compounds with novel targets and activities. One such target is the bacterial cytoplasmic membrane and hence, robust and reliable assays are required to detect damage to this important cellular structure, for the purpose of both mode of action and physiological studies, as well as target validation and identification of any off-target effects during the drug development process. Here, to the best of our knowledge, I have developed the first fluorometric assay utilising the nucleic acid stain Sytox Green and the voltage-sensitive dye $DiSC_3(5)$ to simultaneously monitor membrane pore formation and depolarisation in live bacteria.

As part of assay development, I have provided proof of concept with antimicrobial peptides of known function, such as nisin, which binds lipid II to form transmembrane pores (Wiedemann, Benz and Sahl, 2004), and gramicidin, which forms small cation specific channels in the cytoplasmic membrane (Smart, Goodfellow and Wallace, 1993; Kelkar and Chattopadhyay, 2007). Both have been used as positive controls for membrane pore formation and depolarisation, respectively, throughout this thesis and in many previous studies (te Winkel *et al.*, 2016; Kepplinger *et al.*, 2018; Omardien *et al.*, 2018; Popp *et al.*, 2020). In addition, these assays are implemented later in this thesis to unravel the mode of action of two known but poorly characterised membrane-targeting antimicrobials and screen for novel natural product compounds targeting the cytoplasmic membrane. To allow for this in a higher-throughput manner, the assay was set up in a 96-well plate format and in particular, I highlight the necessity of vigorous shaking to maintain cell energisation; an important factor that is frequently overlooked in previous reports of voltage-sensitive dye-based fluorometric assays. Finally, measurements were performed directly in growth medium rather than buffers of various compositions (Clementi *et al.*, 2014; Boix-Lemonche, Lekka and Skerlavaj, 2020), which as discussed in this chapter can have detrimental consequences on membrane potential levels. The next step would be translating this assay to other Gram-positive organisms, in particular those of clinical relevance such as *Enterococcus faecium* and *Staphylococcus aureus;* both of which are identified by WHO as antibiotic-resistant "priority pathogens" (Tacconelli *et al.*, 2018)*.* As reported previously and employed throughout this thesis, when adapting fluorometric assays to new bacterial species, re-optimisation of the cell density and dye concentration would first be required. Another parameter to be considered is that composition of the cell

envelope can differ between Gram-positive organisms, for example the presence of a bacterial capsule or S-layer (O'Riordan and Lee, 2004; Ravi and Fioravanti, 2021). In this case it would be advisable to first verify that cells can be stained microscopically prior to assay optimisation.

Although the use of DiSC$_3$(5) as a reporter for membrane potential in Gram-negative bacteria is not novel, this study provides guidance regarding the effects and problems associated with outer membrane permeabilisation and the use of buffers rather than growth media, which is prevalent amongst the literature (Wu *et al.*, 1999; Silvestro, Weiser and Axelsen, 2000; Morin *et al.*, 2011). Furthermore, in collaboration with Dr Philipp Popp from Humboldt-Universität zu Berlin we confirmed the robustness of the DiSC$_3$(5)-based fluorometric assay, as comparable results were obtained for another Gram-negative model organism, *Salmonella enterica*, in a different laboratory using different instrumentations. They also demonstrated that pre-incubation with the permeabiliser compound polymyxin B nonapeptide allows the confounding effects of outer membrane permeabilisation to largely be removed in logarithmic phase cells, rendering it easier to detect inner membrane-specific changes. Moreover, this eliminates the need for chelators such as EDTA, which can have detrimental effects on bacterial growth and on the cytoplasmic membrane itself, including membrane fluidisation and destabilisation (Prachayasittikul *et al.*, 2007); which are not observed for polymyxin B nonapeptide (Table 7). Finally, I believe these practices and advice could be easily translatable to use of DiSC$_3$(5) in flow cytometry, which could be verified by future work. As both Ca^{2+} and Mg^{2+} are required to maintain integrity of the LPS layer, it would also be beneficial to test whether supplementation of buffers with $MgCl_2$ also prevents destabilisation of the outer membrane during washing, and similarly, whether other carbon sources can be utilised to sustain central carbon metabolism and thus, cell energisation.

Chapter 4 – Determining *in vivo* fluorescence-based techniques to differentiate between multidrug efflux inhibition and outer membrane permeabilisation in *E. coli*

4.1 – Introduction

As several antibiotics are unable to access their target in Gram-negative organisms due to the presence of the additional outer membrane and effective multidrug efflux systems, one emerging strategy to combat antibiotic resistance in such pathogens is identifying compounds that either permeabilise the outer membrane or inhibit efflux, to be used in conjunction with existing antibiotics. Therefore, it is essential to develop reliable and reproducible assays that screen for changes in outer membrane permeability barrier function, as well as drug efflux, not only in the context of antibiotic discovery but to further our understanding of these systems and any interactions between them.

The outer membrane is an effective permeability barrier due to the unique asymmetric presence of LPS in the outer leaflet and strong lateral interactions between neighbouring molecules. Thus, outer membrane permeability can be selectively increased by two main mechanisms. Firstly, compounds such as EDTA trigger massive release of LPS into the extracellular environment. This results in the migration of phospholipids from the inner leaflet to the outer leaflet, producing phospholipid domains which exhibit increased permeability to lipophilic compounds (Leive, 1965). Alternatively, compounds such as polymyxin B and polymyxin B nonapeptide compete for binding to LPS with the divalent cations that normally cross bridge LPS molecules. This results in increased lateral diffusion of LPS and destabilisation of the outer leaflet (Band and Weiss, 2015).

Similarly to monitoring disturbances to the cytoplasmic membrane, fluorescent probes can be used to identify destabilisation of the Gram-negative outer membrane and one such is the commonly used lipophilic dye 1-N-phenylnaphthylamine (NPN). NPN is a small molecule that, under normal conditions, is unable to traverse the outer membrane, and is thus weakly fluorescent in aqueous environments. Upon the action of permeabilisers, such compounds that weaken stabilising interactions between components of the outer membrane, phospholipids of both the outer and inner membrane become accessible and NPN fluorescence strongly increases (Helander and Mattila-Sandholm, 2000; Muheim *et al.*, 2017).

Interestingly though, accumulation of similar hydrophobic fluorescent dyes is also used to investigate efflux in Gram-negative organisms. In fact, NPN itself was used to identify multidrug efflux inhibitors in *Pseudomonas aeruginosa* (Lomovskaya *et al.*, 2001)*,* since it is a known substrate of the MexA-MexB-OprM efflux pump (Ocaktan, Yoneyama and Nakae, 1997). In *E. coli*, the fluorescent probe Nile red is more commonly used, as it has been previously shown to be a substrate of the AcrAB-TolC pump complex (Bohnert, Karamian and Nikaido, 2010). Similarly to NPN, Nile red is almost non-fluorescent in aqueous solution, but undergoes a large fluorescence enhancement in lipid-rich environments (Greenspan and Fowler, 1985). Due to the characteristics of these dyes, it is therefore challenging to differentiate between outer membrane permeabilisation and inhibition of multidrug efflux in such Gram-negative uptake-based assays. An additional complication is the association between efflux pumps and the PMF, which commonly energises such systems (Nikaido, 1996), and thus any disruption to the PMF will also affect multidrug efflux and subsequently dye fluorescence. One alternate approach is to use nucleic acid stains, for example Hoechst 33342; which enter via porins and accumulation of which only occurs if its extrusion from the cell is being actively inhibited. Similarly to NPN and Nile red, Hoechst 33342 has been shown to be a substrate of several multidrug efflux pumps in *E. coli* and beyond (Van Den Berg Van Saparoea *et al.*, 2005; Coldham *et al.*, 2010; Richmond, Chua and Piddock, 2013).

4.2 – Results

4.2.1 – Investigating the interplay between outer membrane permeabilisation, efflux pump inhibition and inner membrane depolarisation using fluorescent probes

I first tested the effects of several antimicrobials with varying modes of action on the fluorescence of Nile red, which, as stated above, is commonly used as an indicator of multidrug efflux inhibition. I performed this in the strain *E. coli* BW25113, as this is the background of single-gene knockout mutants known as the "Keio collection" (Baba *et al.*, 2006), which will be utilised later. Similarly to previous dye-based fluorometric assays in this thesis, I first optimised the cell density and dye concentration to an OD_{600}

of 0.5 and 1 µg/ml in 1% DMSO respectively, and tested for any dye-compound interactions; of which there were none (Fig. 34).
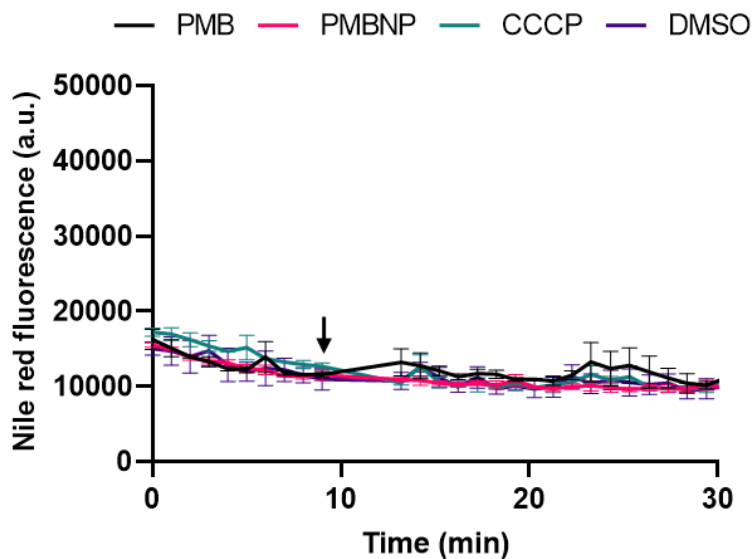
Figure 34: Interactions between Nile red and antimicrobial compounds. Fluorescence intensity of 1 µg/ml Nile red in LB medium upon addition of 7 µM polymyxin B (PMB), 30 µM polymyxin B nonapeptide (PMBNP), 100 µM CCCP or 1% of the solvent DMSO. Nile red was added from 0 min and the timepoint of compound addition is highlighted by an arrow. Data are represented as mean±SD (n=3).

As expected, the protonophore CCCP caused an increase in Nile red fluorescence intensity (Fig. 35A), as it dissipates the proton motive force which commonly energises multi-drug efflux pumps (Nikaido, 1996). Likewise, polymyxin B, which depolarises the cytoplasmic membrane through the formation of large pores, also increased Nile Red fluorescence intensity. To more directly confirm that Nile red fluorescence is influenced by efflux inhibition, I repeated this assay in the Keio collection *tolC*-deletion strain (Δ*tolC*) (Baba *et al.*, 2006). TolC is the outer membrane channel of the *E. coli* AcrAB-TolC efflux pump complex and is therefore required for effective multidrug efflux (Sharff *et al.*, 2001). As shown in Fig. 35B, there was a clear fluorescence increase upon addition of Nile red to *ΔtolC* cells. Perhaps most interestingly however, Nile red fluorescence also increased in response to addition of polymyxin B nonapeptide, which retains its ability to permeabilise the Gram-negative outer membrane but is unable to depolarise the cytoplasmic membrane (as shown in the previous chapter; Fig. 27).

These effects on Nile red fluorescence were also confirmed on a single-cell level by fluorescence microscopy (Fig. 32C).
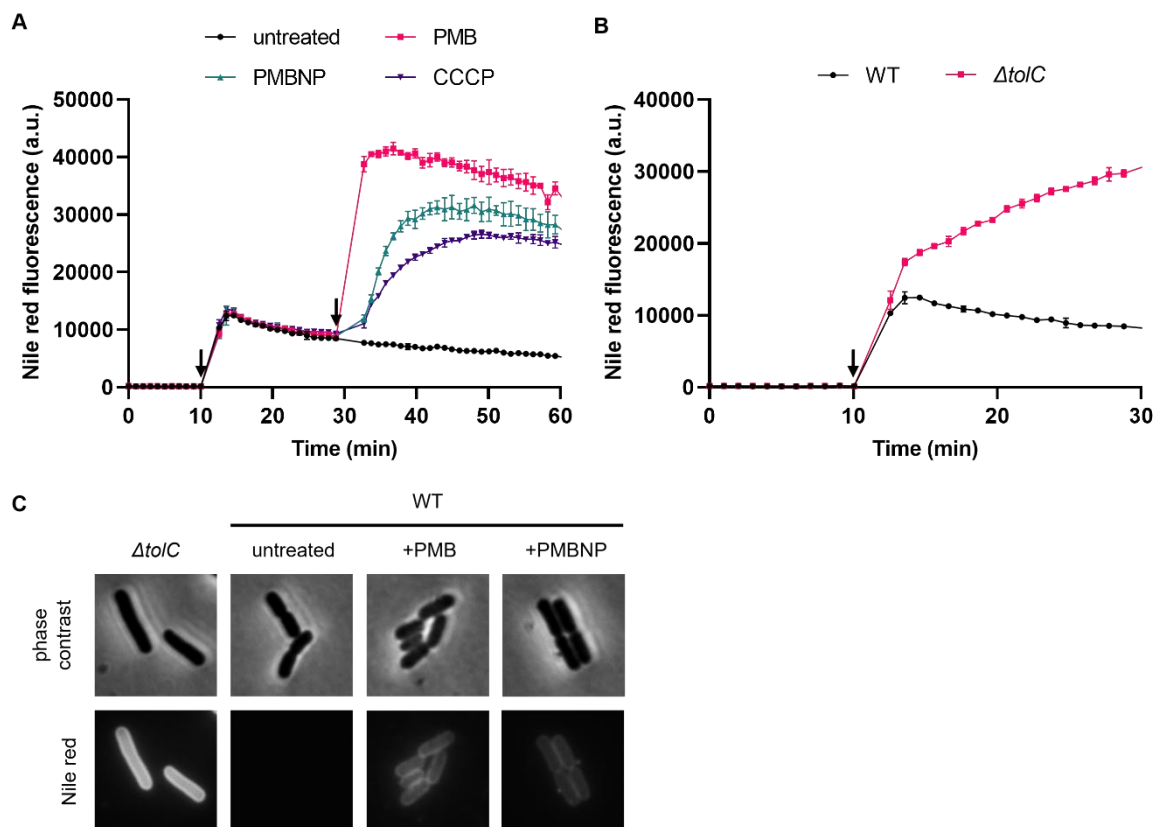
Figure 35: Nile red fluorescence is influenced by both outer membrane permeabilisation and efflux inhibition in *E. coli*. Fluorescence intensity changes of 1 µg/ml Nile red in (A) *E. coli* BW25113 or (B) *E. coli* BW25113 (WT) and *E. coli* BW25113 *ΔtolC* cells, all at an OD_{600} of 0.5, untreated or treated with 7 µM polymyxin B (PMB), 30 µM polymyxin B nonapeptide (PMBNP) or 100 µM CCCP. Dye and compound addition are indicated by black arrows respectively. Data are represented as mean±SD (n=3). (C) Phase contrast and fluorescence microscopy images of *ΔtolC* and WT *E. coli* BW25113, stained with 1 µg/ml Nile red and untreated or treated with 7 µM PMB or 30 µM PMBNP (15 min). Strains used: *E. coli* BW25113 (wild type) and JW5503-1 (*ΔtolC)*.

This raises two questions: (i) whether Nile red staining in fact reflects outer membrane permeabilisation rather than efflux inhibition or (ii) whether both processes are intrinsically linked. To investigate the former, I tested whether deletion of *tolC* caused the outer membrane to become phenotypically "leaky" by observing its sensitivity to the glycopeptide antibiotic vancomycin. Due to its large size (1.45 kDa), vancomycin cannot normally cross the *E. coli* outer membrane, resulting in full resistance. Changes in sensitivity to vancomycin are therefore commonly used to assess outer membrane integrity (Lam *et al.*, 1986; Vaara, 1993; Muheim *et al.*, 2017). As shown in Table 8, when the outer membrane of *E. coli* was permeabilised by polymyxin B nonapeptide, vancomycin inhibited growth at a concentration of 50 µM. In contrast, similarly to wild

type cells, vancomycin was not growth inhibitory at concentrations up to 100 μM against *ΔtolC* cells, implying that integrity of the outer membrane is not compromised in this strain.

Table 8: Minimum inhibitory concentrations (MICs) of vancomycin against *E. coli* BW25113 in the absence and presence of PMBNP and *E. coli* BW25113 *ΔtolC*.

Strain genotype	Vancomycin
	MIC (μM)
wild type	>100
wild type + PMBNP	50
ΔtolC	>100

N=3.

Another dye I have assessed for the purpose of such screens is NPN, which, as mentioned previously, has been used to detect both outer membrane permeabilisation and efflux pump inhibition in Gram-negatives (Helander and Mattila-Sandholm, 2000; Lomovskaya *et al.*, 2001; Mariano *et al.*, 2019). The cell density and dye concentration used were as described previously (Helander and Mattila-Sandholm, 2000; Muheim *et al.*, 2017): cells grown to an OD_{600} of 0.5 and resuspended to a final OD_{600} of 1 and 10 μM in 1% DMF, respectively. Interestingly, CCCP interfered with NPN fluorescence (Fig. 36), so instead colicin N was used as a positive control for membrane depolarisation in the absence of outer membrane permeabilisation; which did not interact with NPN. Colicin N is a bacteriocin produced by *E. coli*, which binds the porin OmpF and exploits the Tol system (energised by the PMF) to translocate the outer membrane (Jansen *et al.*, 2020). Subsequently, colicin N inserts its C-terminal domain into the inner membrane, forming ion-conductive channels which result in cell death (Wilmsen, Pugsley and Pattus, 1990).
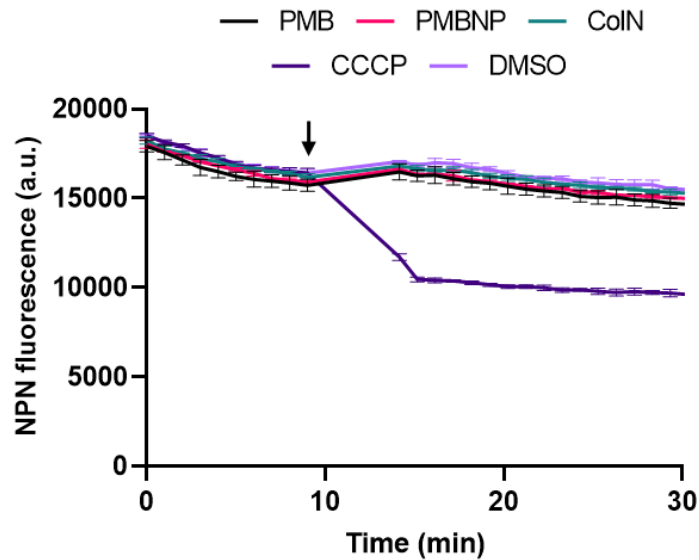
Figure 36: Interference between NPN fluorescence and the protonophore CCCP.
Fluorescence intensity of 10 µM NPN in LB medium upon addition of 7 µM polymyxin
B (PMB), 30 µM polymyxin B nonapeptide (PMBNP), 100 µM CCCP, 0.3 µM colicin N
(ColN) or DMSO. NPN was added from 0 min and the timepoint of compound addition
is highlighted by an arrow. Data are represented as mean±SD (n=3).

PMB and PMBNP, which both permeabilise the outer membrane, caused an increase
in NPN fluorescence (Fig. 37A); however, it also appeared to reflect inhibition of efflux
as, again, there was marked increase upon addition to the *ΔtolC* mutant (Fig. 34B).
Finally, colicin N triggered an increase in NPN fluorescence, similar to that of both PMB
and PMBNP. Unfortunately, I was unable to implement this dye for fluorescence
microscopy, but altogether this data raises concerns over the suitability of this dye to
distinguish between outer membrane permeabilisation and efflux inhibition and
highlights the potential links between not only these mechanisms, but also
depolarisation of the cytoplasmic membrane.
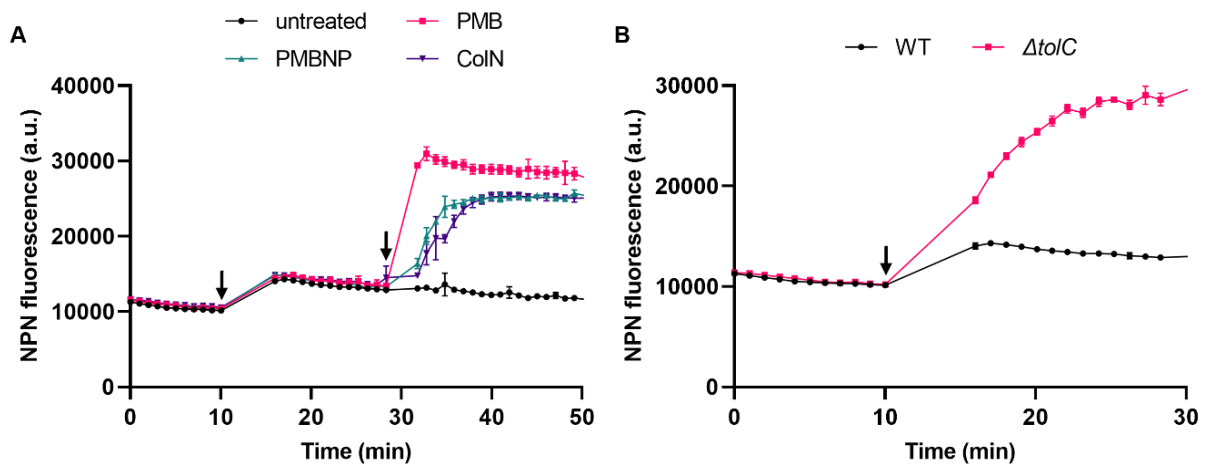
**Figure 37: NPN fluorescence is influenced by both outer membrane
permeabilisation and efflux inhibition in *E. coli*.** Fluorescence intensity changes of
10 µM NPN in (A) *E. coli* BW25113 or (B) *E. coli* BW25113 (WT) and *E. coli* BW25113

ΔtolC cells, all at an OD$_{600}$ of 1, untreated or treated with 7 µM polymyxin B (PMB), 30 µM polymyxin B nonapeptide (PMBNP) or 0.3 µM colicin N (ColN). Dye and compound addition are indicated by black arrows, respectively. Data are represented as mean±SD (n=3). Strains used: *E. coli* BW25113 (wild type) and JW5503-1 (*ΔtolC*).

Finally, I investigated the DNA dye Hoechst 33342 for the purpose of assaying efflux inhibition. Hoechst 33342 is a cell permeable fluorescent dye that fluoresces when bound to double-stranded DNA and is a known substrate of bacterial efflux systems (Van Den Berg Van Saparoea *et al.*, 2005; Richmond, Chua and Piddock, 2013; Marshall *et al.*, 2020). As before, I began by first optimising the cell density and dye concentration to an OD$_{600}$ of 0.5 and 1 µM in H$_2$O, respectively. Similarly to NPN, CCCP also clearly interfered with Hoechst 33342 fluorescence (Fig. 38), so again colicin N was used as a positive control for inner membrane depolarisation.
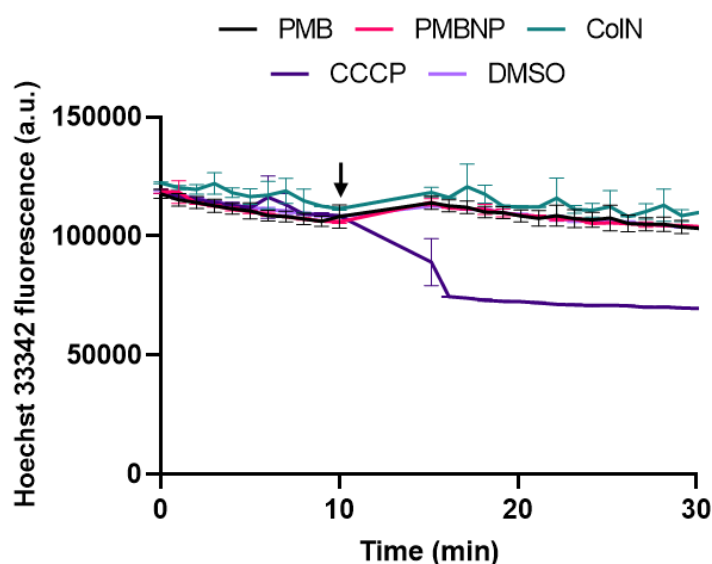
Figure 38: Interference between Hoechst 33342 fluorescence and the protonophore CCCP. Fluorescence intensity of 1 µM Hoechst 33342 in LB medium upon addition of 7 µM polymyxin B (PMB), 30 µM polymyxin B nonapeptide (PMBNP), 100 µM CCCP, 0.3 µM colicin N (ColN) or DMSO. Hoechst 33342 was added from 0 min and the timepoint of compound addition is highlighted by an arrow. Data are represented as mean±SD (n=3).

As expected, PMB, colicin N and deletion of TolC all triggered an increase in Hoechst 33342 fluorescence (Fig. 39A, B). However, in this case, permeabilisation of the outer membrane caused by PMBNP demonstrated no effect on Hoechst 33342 staining. This implies that Hoechst 33342 is the only probe from the ones tested that truly reflects specific changes in multidrug efflux.
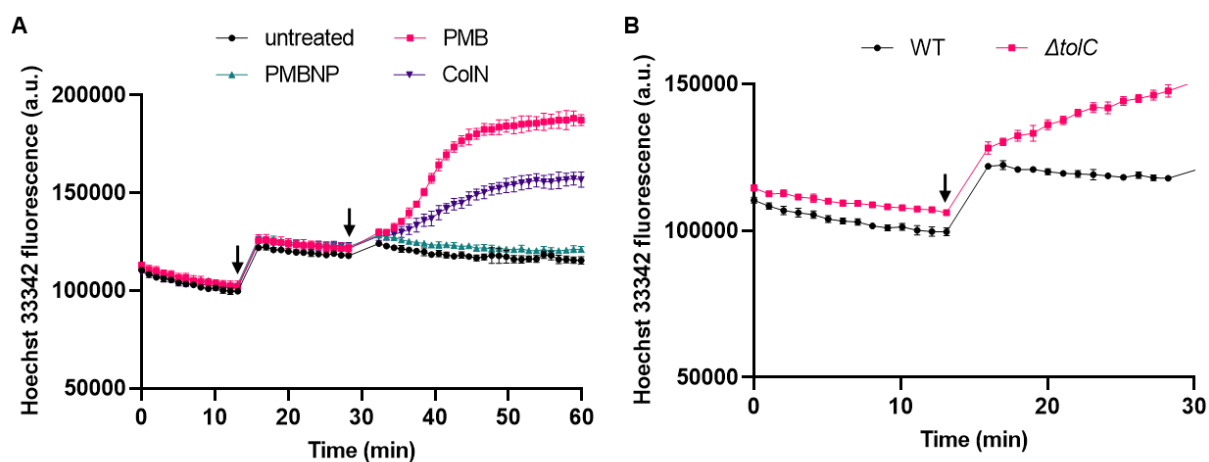
Figure 39: Hoechst 33342 fluorescence is only influenced by efflux inhibition in _E. coli_. Fluorescence intensity changes of 1 µM Hoechst 33342 in (A) _E. coli_ BW25113 or (B) _E. coli_ BW25113 (WT) and _E. coli_ BW25113 _ΔtolC_ cells, all at an OD$_{600}$ of 0.5, untreated or treated with 7 µM polymyxin B (PMB), 30 µM polymyxin B nonapeptide (PMBNP) or 0.3 µM colicin N (ColN). Dye and compound addition are indicated by black arrows, respectively. Data are represented as mean±SD (n=3). Strains used: _E. coli_ BW25113 (wild type) and JW5503-1 (_ΔtolC_).

4.3 – Discussion

Currently, outer membrane permeabilisers and efflux pump inhibitors (EPIs) are under investigation as "antibiotic resistance-breaking" compounds that can sensitise Gram-negative bacteria to the effects of already approved antibiotics. These molecules usually do not exhibit direct antibacterial activities themselves and are therefore less susceptible to resistance development. Such agents are of dire need, as in 2019 alone, over 200,000 deaths were attributable to antimicrobial-resistant _E. coli_; the most from any pathogen (Murray _et al._, 2022). Similarly to the previous chapter, fluorescent probes can be used to monitor changes in outer membrane permeability and multidrug efflux, and such techniques are not a novel concept (Helander and Mattila-Sandholm, 2000; Lomovskaya _et al._, 2001; Bohnert, Karamian and Nikaido, 2010; Muheim _et al._, 2017). Generally, the fluorescent dyes implemented fall under 2 categories: (i) hydrophobic dyes, such as NPN and Nile red, which strongly fluoresce in non-polar environments (e.g. phospholipids) or (ii) hydrophilic nucleic acid stains such as Hoechst 33342 that fluoresce upon intercalation with DNA. In this work, I have demonstrated that the efflux substrate Nile red is not only sensitive to TolC-deletion and de-energisation of efflux pumps through dissipation of the PMF, but surprisingly also to permeabilisation of the outer membrane caused by polymyxin B nonapeptide. On the other hand, fluorescence of the outer membrane permeability indicator NPN, whilst affected by polymyxin B nonapeptide, is also increased by membrane

depolarisation and the absence of TolC. This suggests that such lipophilic dyes may not specifically monitor either outer membrane integrity or multidrug efflux, but instead may be affected by changes in both, or that both processes are biologically connected.

This led us to speculate that outer membrane permeabilisation, efflux inhibition and inner membrane depolarisation may be intrinsically linked (Fig. 40). In our hypothetical
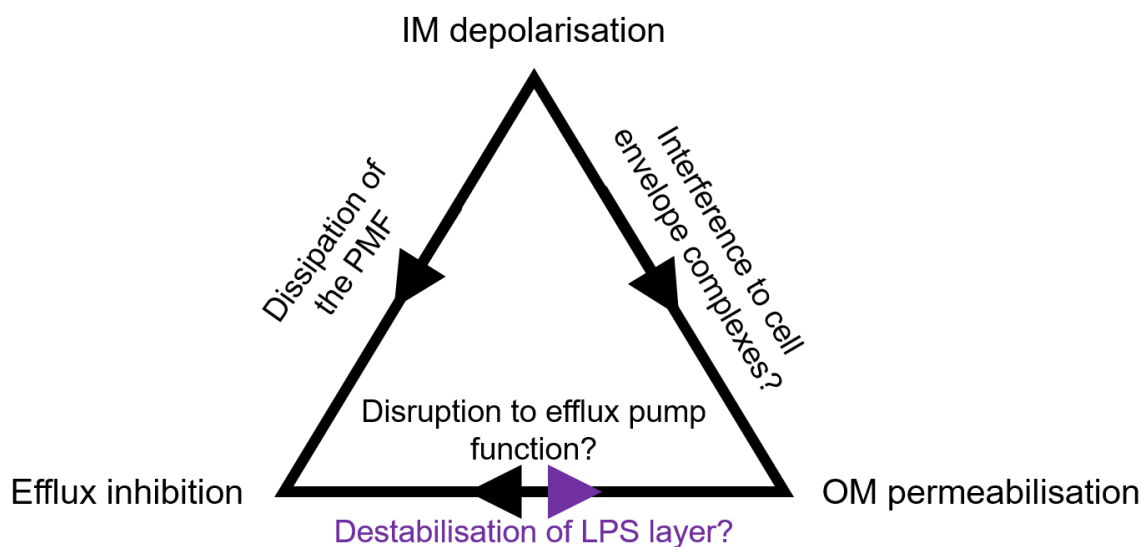
Figure 40: Schematic representation of the potential interplay between inner membrane depolarisation, outer membrane permeabilisation and efflux inhibition. In brief, dissipation of the proton motive force (PMF) de-energises multidrug efflux pumps and potentially also trans-cell envelope complexes, such as Tol-Pal and OmpC–Mla. Disturbances to the integrity of the outer membrane may also affect efflux via disruption or blockage of outer membrane channel proteins, such as TolC. Efflux inhibitors, such as PAβN, could additionally exhibit effects on outer membrane stabilisation.

model, there is a clear association between depolarisation and efflux through dissipation of the PMF, which commonly energises export pumps either directly or indirectly via the production of ATP (Paulsen, Brown and Skurray, 1996; Lubelski, Konings and Driessen, 2007). The other two links are less well-defined; however, it is well-known that dissipation of PMF de-energises cell envelope systems that span the inner and outer membrane. For example, the Tol-Pal complex, which plays a major role in constricting the outer membrane during cell division (Egan, 2018), is coupled to the PMF. Protonation of the inner membrane TolQ-TolR-TolA complex allows for binding and accumulation of TolB-Pal at division sites, which prevents blebbing and destabilisation of the outer membrane (Petiti *et al.*, 2019; Szczepaniak *et al.*, 2020). Tol-Pal has also been implicated in the retrograde transport of phospholipids from the outer to inner membrane, and *E. coli tol-pal* mutants retain phospholipids in the outer leaflet of their outer membranes (Shrivastava, Jiang and Chng, 2017; Shrivastava and

Chng, 2019). Whether this process is also linked to inner membrane energisation remains unknown; however, if it is, dissipation of the PMF could therefore lead to disruption of outer membrane asymmetry, and increased bilayer permeability. Moreover, the OmpC–Mla pathway also plays an important role in maintaining outer membrane lipid asymmetry in Gram-negative bacteria. Similarly to Tol-Pal, deletion of any component of the system results in abberant accumulation of phospholipids at the outer leaflet of the outer membrane (Malinverni and Silhavy, 2009; Chong, Woo and Chng, 2015). In contrast, the activity of this complex is coupled to ATP hydrolysis, which drives transfer of phospholipids from periplasm to inner membrane (Thong *et al.*, 2016). Therefore, dissipation of the PMF, which consequently inhibits ATP synthesis, could further trigger formation of these phospholipid domains in the outer leaflet via disruption of the Mla system and destabilise the outer membrane.

The final connection to discuss is that between permeabilisation of the outer membrane and inhibition of multidrug efflux. Firstly, colicins, and colicin fragments, have been shown to actually plug the TolC channel, inhibiting its function as a component of the AcrAB-TolC efflux pump (Zakharov *et al.*, 2004; Budiardjo *et al.*, 2022). It is also thought that the well-studied EPI PAβN, which acts as a competitive inhibitor of the AcrB substrate binding pocket, additionally affects outer membrane integrity through a mechanism distinct to that of PMBNP (Lamers, Cavallari and Burrows, 2013; Schuster *et al.*, 2019). However, as mutations in the LPS biosynthesis pathway and supplementation with Mg^{2+} restored resistance to large lipophilic drugs, its target site is still assumed to be within the LPS layer. Finally, another possibility is that changes to LPS packing or outer membrane asymmetry directly disrupt efflux pump function, or that the permeability of the outer membrane is increased to such an extent that it counteracts the active pumping of efflux systems.

Hoechst 33342, on the other hand, is a small (~560 Da), hydrophilic nucleic acid stain which can enter the cell via porins. In this work, I demonstrated that its fluorescence is not affected by outer membrane permeability, but instead appears to be specifically dependent on inhibition of the efflux pumps through depletion of TolC or dissipation of the PMF. Thus it appears unlikely that outer membrane destabilisation directly inhibits efflux pump activity, and more likely that it potentiates entry or re-entry of extruded compounds; of which Hoechst 33342 is not affected as it can already move in through porins.

This work highlights the possible connections between inner membrane depolarisation, outer membrane permeabilisation and efflux inhibition; the mechanisms of which require further elucidation. I also demonstrate that fluorescent probes, commonly used to detect changes in outer membrane integrity or multidrug efflux may not be specific for either, or such processes may be intrinsically linked. Developing assays to specifically measure efflux- or outer membrane-destabilising activities *in vivo* are therefore of great importance for the discovery of EPIs and permeabilisers, respectively, that will aid in combatting the global antibiotic resistance crisis.

Chapter 5 – Screening and extraction of *Actinomycetes* for novel membrane-targeting antibiotics

5.1 – Introduction

As mentioned previously, *Actinomycetes* are well-known for the production of a range of bioactive compounds, and, in particular, are responsible for the synthesis of around two-thirds of all used antibiotics. This is mainly due to their genomes containing a large number of distinct biosynthetic gene clusters (BGCs; ~20-50), which encode enzymes to synthesise specialised metabolites. Despite this, only a minority have been chemically explored; with two major challenges being the rediscovery of known compounds or "cryptic" or "silent" BGCs that have only been predicted through advancements in genome sequencing techniques. Moreover, in relation to this thesis, many membrane-active compounds would have been discarded during the drug discovery process as a result of assumed poor safety profiles. This is due to the relatively frequent occurrence of cytotoxic effects; the most common of which is haemolysis, the permeabilisation of red bloods cells, caused by similarities between the erythrocyte and bacterial cell surface charges. Of course, several commonly used antimicrobials trigger membrane pore formation; examples of which are nisin and the polymyxins, however these usually exhibit an additional layer of bacterial-specificity such as targeting of lipid II or LPS, respectively (Wiedemann, Benz and Sahl, 2004; Sabnis *et al.*, 2021). Thus, an alternate approach is to identify *Actinomycete*-derived membrane-targeting antimicrobial compounds that act through mechanisms distinct to pore formation. This has now been observed for several antibacterial compounds, and includes depolarisation of the bacterial membrane, changes to membrane lipid domain organisation or targeting of specific membrane-embedded components (Müller *et al.*, 2016; Scheinpflug *et al.*, 2017; Wenzel *et al.*, 2018; Grein *et al.*, 2020).

This PhD was in collaboration with Demuris Ltd., an SME focussing on novel antibiotic discovery. They own a vast collection of *Actinomycete* strains, isolated from a range of extreme and neglected terrestrial and marine habitats. The collection also exhibits a well-documented high level of biological dereplication (i.e., eliminating strains that are identical or closely related) and thus reduces the likelihood of rediscovering current antibiotics. Finally, previous reporter guided screening performed by Demuris to indicate potential modes of action identified, of *Actinomycete* extracts active on the Gram-positive model organism *B. subtilis*, 14% appeared to activate the promoter of LiaI (a target of the TCS, LiaRS); indicative of targeting the cell envelope.

5.2 – Results

5.2.1 – Reporter-based screening of Actinomycetes

As part of my PhD, I completed a 3-month iCASE placement at the antibiotic discovery company Demuris Ltd. They own a unique and vast collection of *Actinomycete* bacteria; of which I pre-screened the subset that activated LiaI to confirm whether they produced compounds with membrane- or cell wall-associated antibacterial properties. To achieve this, I used *B. subtilis* reporter strains in which promoters of genes activated during cell wall damage and cell envelope stress are fused to LacZ (P$_{ypuA}$-*lacZ* and P$_{liaI}$-*lacZ* respectively). These were used on Nutrient Agar plates supplemented with X-gal so that LacZ activity could be visualised by the appearance of a blue halo. Although it is unknown what specifically induces *ypuA* and *liaI*, these reporters have been validated by antibiotics with well-known mechanisms of action (Fischer *et al.*, 2004). For example, *ypuA*, which is part of the σ^M regulon, is strongly activated by β-lactams and vancomycin (Urban *et al.*, 2007), indicating that it is responsive to cell wall synthesis inhibition. On the other hand, *liaI* is induced by direct interference with lipid II (compounds such as bacitracin and nisin) or compounds that perturb the cytoplasmic membrane including daptomycin and cWFW (Mascher *et al.*, 2004; Müller *et al.*, 2016; Scheinpflug *et al.*, 2017), implying its activation is more related to the membrane-associated steps of cell wall synthesis. Overall, I screened 70 *Actinomycete* strains and identified 28 and 40 that produce compounds inducing *ypuA* and *liaI* respectively (examples of which are shown in Fig. 41). Of these strains, I discovered approximately 20 secreting agents that activated both reporter strains (in Fig. 41, strain 2). This was of interest to my project, as these may represent daptomycin-like compounds in which membrane disruption triggers inhibition of cell wall synthesis. Unfortunately, due to lockdown restrictions, I was unable to grow and harvest 2 strains that produced *liaI*-positive compounds; however, I did successfully collect cell material for compound extraction from the remaining 38.
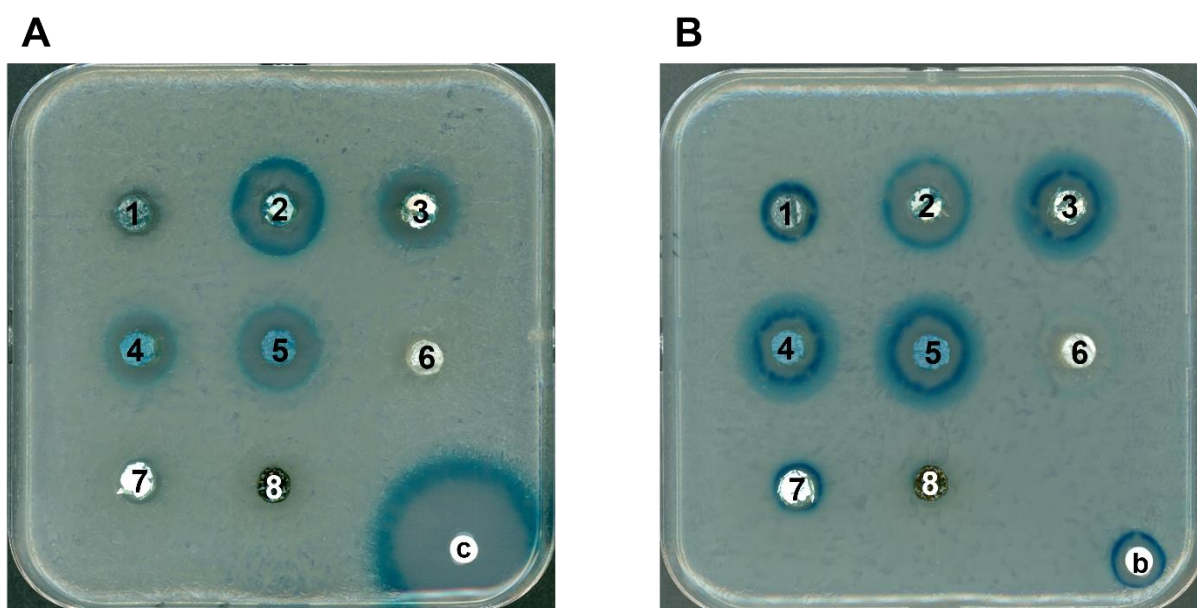
Figure 41: *Actinomycete* strains produce compounds that induce cell wall damage and/or cell envelope stress as shown by *B. subtilis* reporter strains. Representative images of *Actinomycete* agar plugs on Nutrient Agar plates supplemented with erythromycin and X-gal and seeded with either the cell wall P_{ypuA}-*lacZ* (A) or cell membrane P_{lial}-*lacZ* reporter (B). Discs impregnated with 125 µg of the β-lactam cefotaxime (c) or 750 µg of the undecaprenyl pyrophosphate inhibitor bacitracin (b) were used as positive controls for (A) and (B) respectively. Strains used: *B. subtilis* YuPA *(ypuA'-lacZ)* and *B. subtilis* YvQI *(lial-lacZ).*

5.2.2 – Extraction of relevant Actinomycetes and minimum inhibitory concentration determination

From the cell material obtained from the 38 *lial*-positive strains, I produced both aqueous and methanolic extracts by the protocol described in sub-chapter 2.7. Following evaporation, the methanolic-extracted residue was suspended in 100% DMSO as we know that this solvent is compatible with our assays (eg. Fig. 19). The extracts were then again subject to *lial* reporter screening to determine whether they had retained their membrane-associated activities. A representative experiment is shown (Fig. 42), but overall 17 aqueous and 19 methanolic extracts activated the *lial* reporter (as demonstrated by the appearance of a blue halo). As several lipopeptide antibiotics are calcium-dependent (Wood and Martin, 2019), I also repeated these assays in the presence of 1.25 mM $CaCl_2$. One methanolic extract exhibited Ca^{2+}-dependent induction of LiaI, whilst three others produced a larger zone of bacterial growth inhibition, indicating that their activities are potentiated in the presence of calcium (Appendix I).
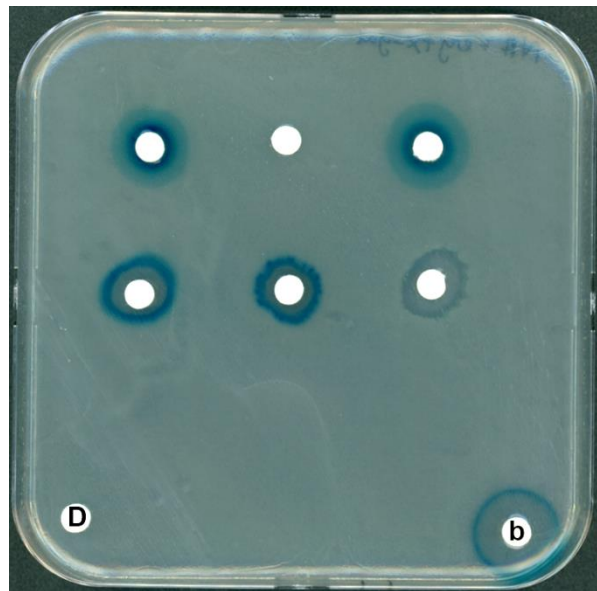
Figure 42: Methanolic *Actinomycete* extracts that induce cell envelope stress using a *B. subtilis* reporter strain. An example image of discs impregnated with different methanolic extracts on Nutrient Agar plates supplemented with erythromycin and X-gal and seeded with the cell membrane P$_{lial}$-*lacZ* reporter. Discs impregnated with 750 µg bacitracin (b) and the solvent DMSO (D) were used as positive and negative control respectively. *Strain used: B. subtilis* YvQI (*lial-lacZ*).

I then tested the minimum inhibitory concentration (MIC) for all extracts in the Gram-positive model organism *B. subtilis* 168 and found that 4 aqueous and 14 methanolic extracts were growth inhibitory at a concentration of 1% v/v or below (again an example MIC assay is displayed; Fig. 43). From an antibiotic discovery point of view and guided from these results, I subjected these 18 to a more comprehensive mode of action analysis.
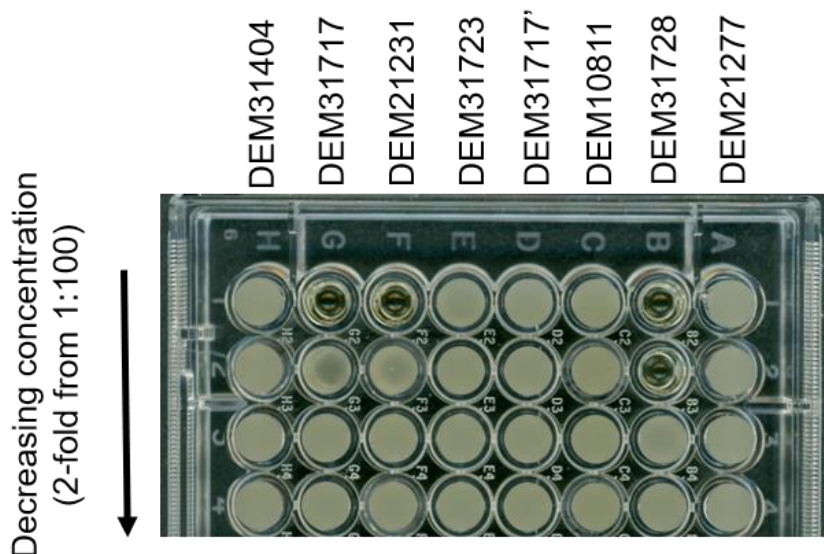
Figure 43: Minimum inhibitory concentrations (MICs) of several methanolic *Actinomycete* extracts in *B. subtilis* 168. Extracts were assayed over a 4-point, 2-fold serial dilution curve, from 1% to 0.125% (v/v). All tests were performed in technical

triplicate (not shown here), with two biological replicates. Strain used: *B. subtilis* 168 (wild type).

5.2.3 – Preliminary mode of action experiments of growth inhibitory extracts

First, I investigated the effect of all 18 extracts upon addition to B. subtilis 168 cells in logarithmic growth phase. Their activities varied from no effect on growth at all to both inhibitory and lytic, and again example extracts are shown in Fig. 44. Interestingly, for
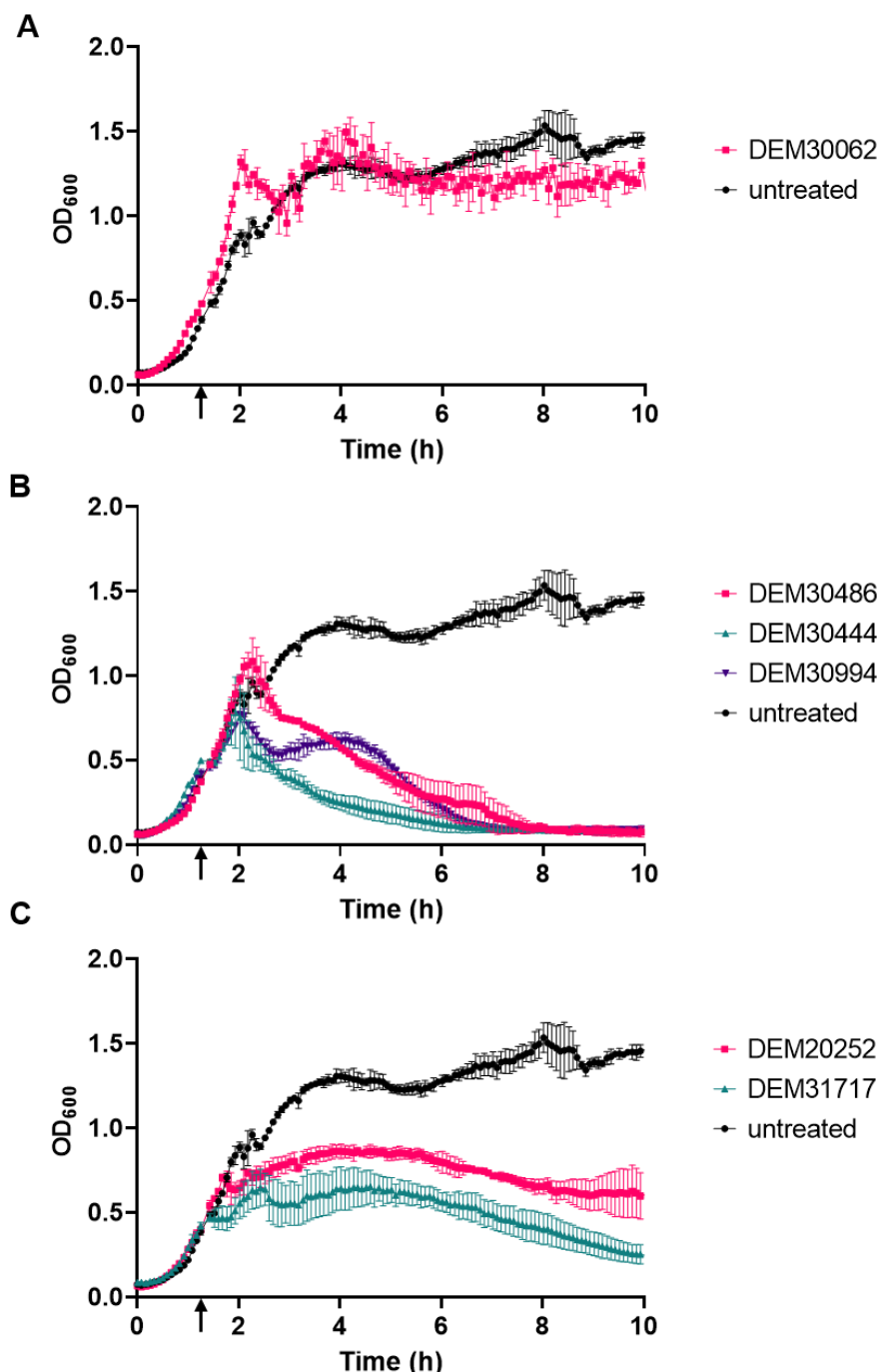
Figure 44: The effect of methanolic extracts derived from several *Actinomycetes* strains on growth of *B. subtilis* 168. Growth kinetics of *B. subtilis* 168 grown in LB to an OD_{600} of 0.5 and then treated with different extracts at 1% v/v. Arrows indicate the time point of extract addition. Data are shown as mean±SD (n=3) and are grouped as (A) not growth inhibitory, (B) lytic and (C) growth inhibition prior to delayed lysis. Strain used: *B. subtilis* 168 (wild type).

several extracts (e.g., DEM30994, DEM30444 and DEM30486), optical density initially increased following addition prior to lysis. This behaviour has also been observed for the cell-wall targeting antibiotics, including vancomycin (unpublished data, Sandra Laborda Anadón).

I then performed my combined membrane pore formation and depolarisation screen from Chapter 3 on all growth inhibitory extracts to determine any cytoplasmic membrane-disrupting effects. This identified 2 methanolic extracts, from strains DEM30444 and DEM30486, that triggered an increase in $DiSC_3(5)$ fluorescence intensity (Fig. 45A), indicative of a loss in membrane potential. There appeared to be no change in Sytox Green fluorescence intensity upon addition of extracts from both strains (Fig. 45B), however it is unclear due to the jump in fluorescence which is explained in 3.2.1. Therefore, to verify these effects, I also tested all 18 extracts with simultaneous Sytox Green and $DiSC_3(5)$ fluorescent microscopy, which, although lower throughput, is more sensitive and changes to the bacterial cell envelope can be observed on a single-cell level.
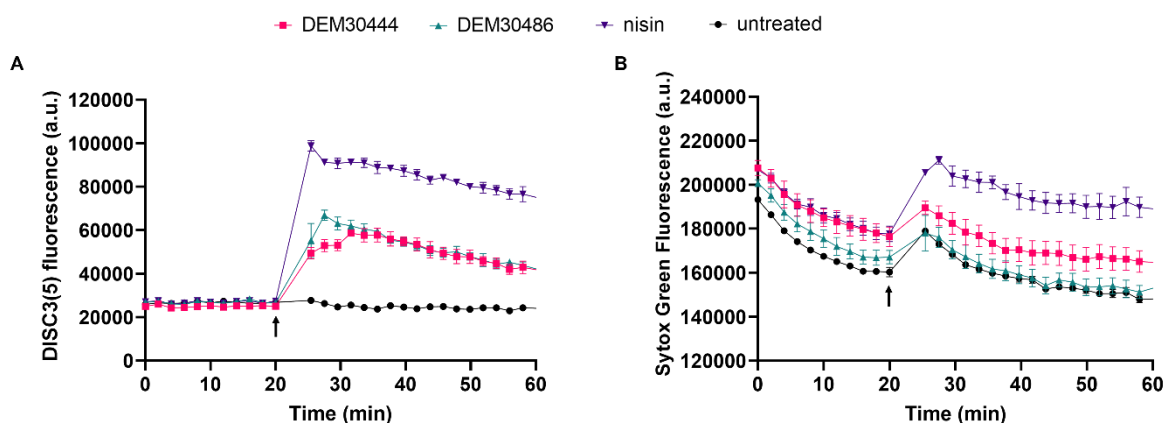
Figure 45: Fluorometric measurement of membrane depolarisation and pore formation triggered by *Actinomycete* extracts in *B. subtilis*. Fluorescence intensity changes of (A) 1 µM $DiSC_3(5)$ and (B) 1 µM Sytox Green in *B. subtilis* cells at an OD_{600} of 0.5, untreated or treated with methanolic extracts from strains DEM30444 and DEM30486. The pore forming lantibiotic nisin (10 µM) was used for positive control. The time point of compound addition is indicated by an arrow. Data are represented as mean±SD (n=3). Strain used: *B. subtilis* 168 (wild type).

As expected from the initial screen, extracts from both DEM30444 and DEM30486 depolarised the cytoplasmic membrane (Fig. 46), and this is triggered by the formation of large pores as indicated by the intracellular Sytox Green staining. This also occurred for the extract derived from strain DEM31717. Interestingly, although they demonstrated no effect on membrane integrity or potential, incubation with both the aqueous and methanolic extract of DEM30994 resulted in this "bulging" phenotype,

shown in Fig. 46. The cause of this will be further investigated later in this chapter. Finally, the methanolic extract from DEM30062 did not depolarise the cytoplasmic membrane, but instead caused a "spotty" DiSC$_3$(5) stain, which is commonly observed with several membrane dyes as indication of changes in lipid domain organisation (Strahl, Bürmann and Hamoen, 2014).
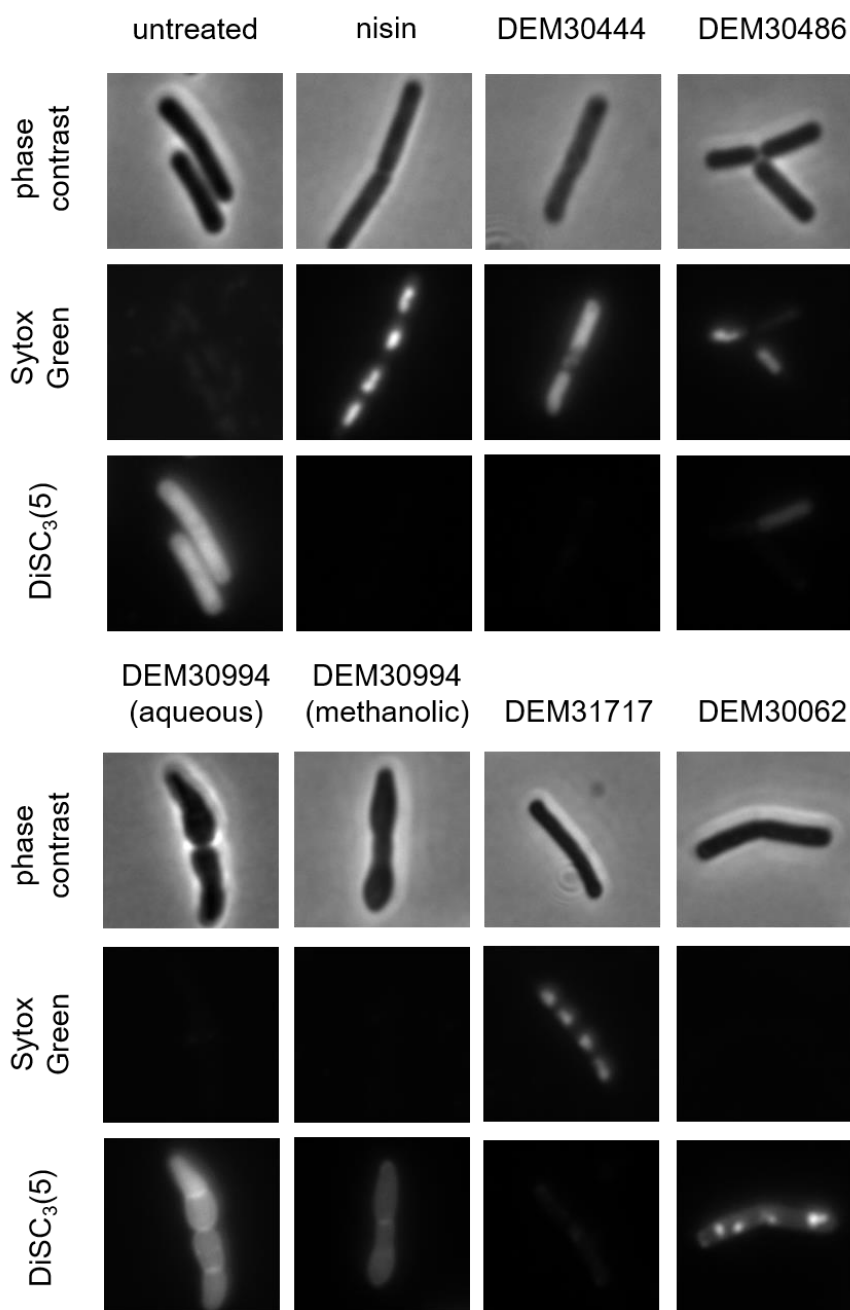
Figure 46: Effects of extracts on *B. subtilis* membrane integrity and potential on a single-cell level. Phase contrast and fluorescence microscopy of *B. subtilis* stained with 200 nM Sytox Green and 1 μM DiSC$_3$(5), and untreated or treated with extracts from different DEM strains (methanolic unless stated) for 100 min. As a positive control, the transmembrane potential and the membrane barrier functions were disrupted by the pore forming lantibiotic nisin (10 μM). Strain used: *B. subtilis* 168 (wild type).

To test this, I performed Nile red fluorescence microscopy, which preferentially stains areas of increased local membrane fluidity, of a *B. subtilis* strain constitutively expressing msfGFP-MreB. Previously, our group demonstrated that formation of fluid lipid domains can be associated with delocalisation of the cytoskeletal protein MreB, and postulated it to be caused by clustering of undecaprenyl-coupled cell wall precursors, such as lipid II (Strahl, Bürmann and Hamoen, 2014). As shown in Fig. 47,
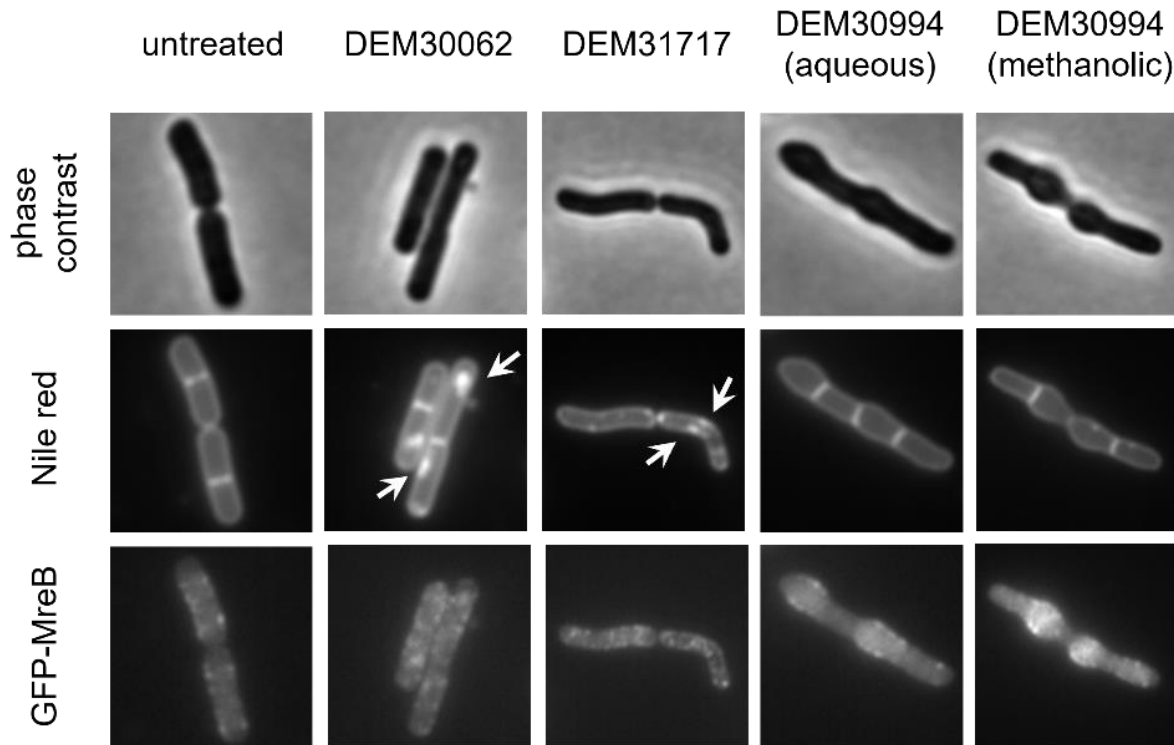
Figure 47: Effect of several extracts on membrane organisation and localisation of the bacterial actin homolog MreB in *B. subtilis*. Phase contrast and fluorescence microscopy images of *B. subtilis* cells expressing msfGFP-MreB stained with 0.5 µg/ml Nile red untreated or treated with extracts from different DEM strains (methanolic unless stated) for 100 min. Some of the Nile red foci appearing with extract treatment are highlighted with white arrows. Strain used: *B. subtilis* HS553 (*msfGFP-mreB*).

treatment with extracts from DEM30062 and DEM31717 caused the emergence of brightly stained Nile red foci, which developed into large membrane patches for the former. Interestingly, these did not correlate with the localisation of MreB. Finally, for those extracts that triggered a "bulging" morphology, there was no change in the Nile red membrane staining. There was, however, a brighter GFP signal associated with the bulging cell areas (Fig. 47).

To confirm that the Nile red foci were not dependent on the presence of MreB, I repeated this microscopy in *B. subtilis* cells lacking MreB and its two other homologues, Mbl and MreBH. Deletion of all three genes results in a spherical morphology due to

inhibition of lateral cell wall synthesis (Schirner and Errington, 2009). Despite this, the triple mutant cells (ΔmreB, Δmbl, ΔmreBH) still displayed Nile red foci when treated with extracts from both DEM30062 and DEM31717 (Fig. 48), demonstrating that the formation of these lipid patches is not associated with the MreB cytoskeleton, or its clustering.
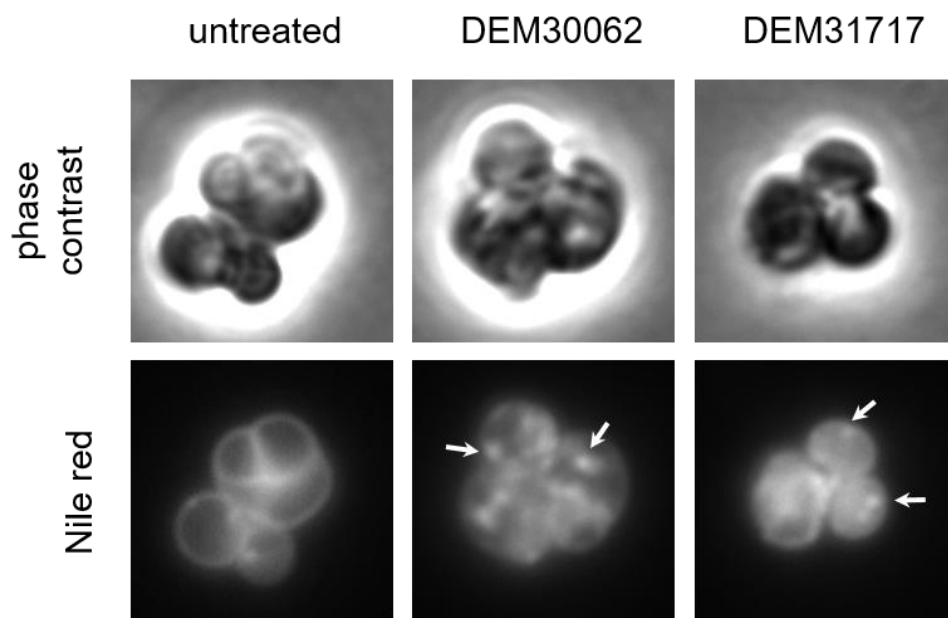
Figure 48: DEM30062 and DEM31717 *extract*-induced Nile red foci are not dependent on MreB. Phase contrast and fluorescence microscopy images of B. subtilis cells lacking all three MreB homologues (ΔmreB Δmbl ΔmreBH) stained with 0.5 µg/ml Nile red, and untreated or treated with DEM30062 and DEM31717-derived extracts for 100 min. Extract-induced foci are indicated by white arrows. Strain used: B. subtilis KS60V (ΔmreB Δmbl ΔmreBH).

Lastly, I further investigated the mode of action of the extracts that triggered the "bulging" phenomenon, derived from strain DEM30994. Both the methanolic and aqueous extracts did not induce the *lial* reporter; however, they did activate *ypuA*, indicative of inhibition of cell wall synthesis (Appendix I). This, in conjunction with the change in morphology and altered recruitment of MreB, led us to investigate whether these extracts impaired lateral peptidoglycan incorporation. To achieve this, I performed a microscopy time course with the fluorescent D-amino acid NADA, which allows the analysis of real-time peptidoglycan biosynthesis in growing cells (Kuru *et al.*, 2012). As shown in Fig. 49, untreated cells were labelled with NADA but treatment with vancomycin (which binds the D-Ala-D-Ala residues of peptidoglycan monomers preventing transglycosylation and transpeptidation) completely abolished incorporation of NADA. Interestingly, peptidoglycan synthesis continued upon treatment with the DEM30994 extracts; however, this resulted in the emergence of

NADA foci (Fig. 49). These foci were particularly prominent at one cell pole during short incubation times (20 min; white arrows) and migrated to the width of the cell where the bulges developed upon longer treatment (40 and 60 min).
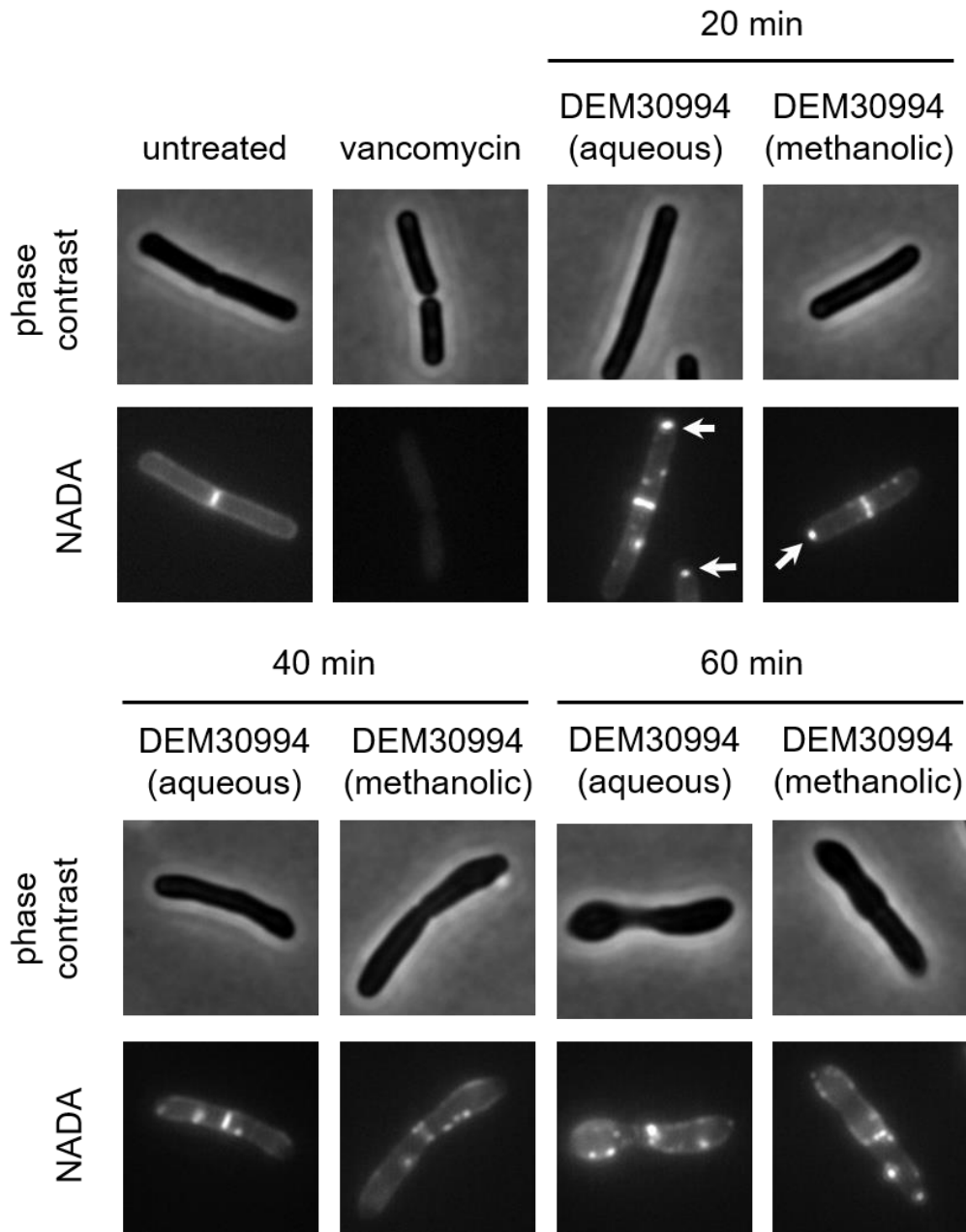
Figure 49: DEM30994 extracts induce aberrant peptidoglycan synthesis in *B. subtilis.* Phase contrast and fluorescence microscopy images of *B. subtilis* untreated or treated with DEM30994 extracts for different incubation times and stained with 250 µM NADA. White arrows indicate polar localisation of peptidoglycan incorporation. Vancomycin (3 µM) was used as a control for inhibition of cell wall synthesis. Strain used: *B. subtilis* 168 (wild type).

Next, to observe whether this misguided peptidoglycan synthesis aligned with MreB localisation, I performed a fluorescence microscopy time course of *B. subtilis* cells expressing msfGFP-MreB and treated with the extracts. Immediately, I noted that overall GFP levels were strongly increased in cells treated with the extracts (Fig. 50A).
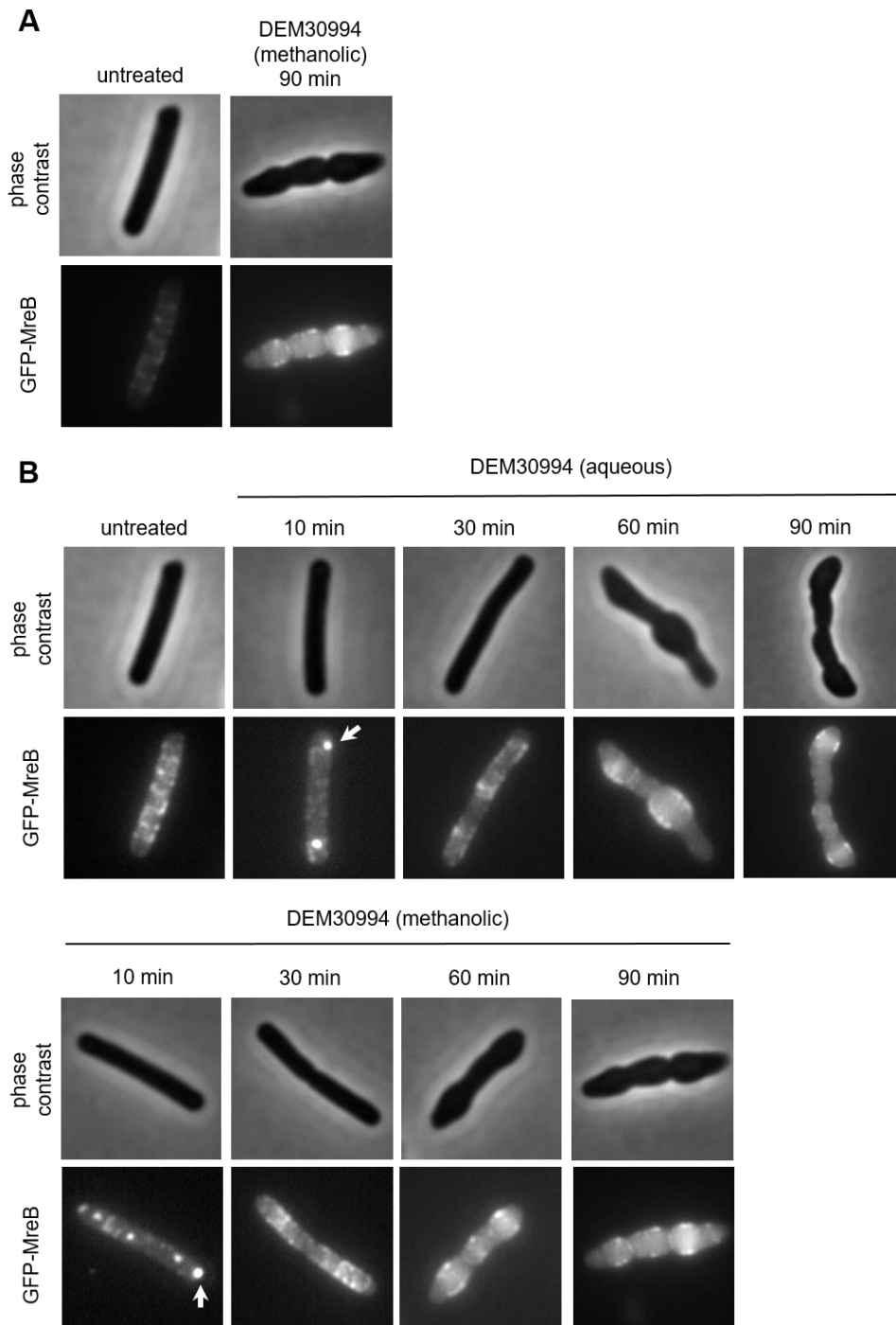
Figure 50: DEM30994 extracts cause changes to MreB localisation in _B. subtilis_.
Phase contrast and fluorescence microscopy of _B. subtilis_ cells expressing msfGFP-
MreB untreated or treated with DEM30994 extracts for different times. In (A),
fluorescence images retain identical contrast settings to allow intensity comparison;
whilst in (B), contrast settings have been altered between images to allow enhanced
visualisation of MreB localisation. Polar localisation of MreB is indicated by white
arrows. Strain used: _B. subtilis_ HS553 (_msfGFP-mreB_).

We postulate that as MreB is part of the σM regulon (Eiamphungporn and Helmann,

2008), which is induced by these extracts, there is also increased expression of the

fusion protein. Despite this, I did observe polar localisation of MreB within 10 minutes

(Fig. 50B), that dispersed to areas where the cells began to bulge during longer incubation times, mirroring the labelling with NADA. We therefore hypothesise that these extracts induce an abnormal localisation of the elongasome, as indicated by MreB, via an as yet undefined mechanism, which results in misdirected lateral peptidoglycan synthesis, changes to cell morphology and ultimately lysis.

A full list of strains and extracts screened and their various effects can be found in Appendix I.

5.3 – Discussion

Natural product compounds have been used as antibacterials since the "golden age" of antibiotic discovery during the 1950s. However, more recently, there is the necessity to identify agents with novel targets and modes of action to overcome the resistance mechanisms evolved by bacteria. Here, I pre-screened a subset of *Acintomycetes*, previously shown by Demuris Ltd to induce a P$_{lial}$-*lacZ* membrane damage reporter and identified 38 strains that produced *lial*-positive compounds. From these, I generated 76 aqueous and methanolic extracts, that, due to the crude methodology, could potentially contain 1 or more active product. Subsequent to the extraction process, 36 extracts retained their ability to activate the LiaRS response and 18 exhibited a MIC of 1% v/v or less against the Gram-positive model organism *B. subtilis*. Following preliminary MoA testing, we identified 3 that depolarised the cytoplasmic membrane through formation of large pores, 2 that formed MreB-independent fluid lipid domains and finally, 2 that induced changes to MreB localisation and subsequently lateral peptidoglycan synthesis. I will now discuss each of these in more detail.

Firstly, all 3 extracts that depolarised the cytoplasmic membrane (DEM30444, DEM30486 and DEM31717) were also bacteriolytic in *B. subtilis,* as determined by addition of extracts to logarithmic growth phase cultures. Since it is known that many membrane disrupting compounds can kill via triggered autolysis (Jolliffe, Doyle and Streips, 1981; Falk, Noah and Weisblum, 2010; Lacriola, Falk and Weisblum, 2013; Scheinpflug *et al.*, 2017; Seistrup, 2018), it would be interesting to test whether these extracts also act through membrane depolarisation-induced autolysis by using strains deficient for the major autolytic enzymes in *B. subtilis* (LytABCDEF). The extract from DEM31717 also induced MreB-independent fluid lipid microdomains (Fig. 47 and 48). This was similarly observed for the membrane-active antibiotic daptomcyin (although in the absence of membrane pore formation) and clustering of such fluid lipid-daptomycin complexes resulted in complete dissociation of MurG and PlsX, proteins

involved in cell wall and lipid synthesis respectively, from the membrane (Müller *et al.*, 2016). Using fluorescent protein fusions, we could determine whether extract DEM31717 also causes detachment of peripheral membrane proteins and thus, may have pleiotropic effects on other cellular processes. Furthermore, incubation of extracts from DEM30444 and DEM30486 with *B. subtilis* caused an increase in optical density prior to lysis. Recent unpublished observations from our group have demonstrated that cell wall targeting antibiotics such as vancomycin trigger an immediate inhibition of cell envelope expansion, whilst production of intracellular biomass continues; resulting in an initial increase in optical density prior to membrane depolarisation and cell death (unpublished data, Laborda Anadón). As I only performed microscopy at one time point, a combined DiSC$_3$(5) and Sytox Green fluorescence microscopy time course experiment would therefore be of benefit to determine whether membrane depolarisation occurs only after this rise in optical density and may instead be caused by accumulation of cytoplasmic biomass as a result of cell wall synthesis inhibition, prior to pore formation.

Extracts derived from DEM30994 also triggered this initial increase in *B. subtilis* optical density, as observed from growth curves. However, due to activation of the cell wall damage reporter P$_{ypuA}$-*lacZ* and changes to staining with the fluorescent D-amino acid NADA, it can be hypothesised that this is instead due to aberrant peptidoglycan synthesis. From localisation of NADA and the bacterial actin homologue MreB, it appears that there is increased, mislocalised lateral cell wall synthesis that causes the bulging phenotype. Despite this, cells continue to grow, accounting for the increase in the optical density, before ultimately, misdirection of the elongasome leads to weakening of the cell wall in certain areas and lysis. Interestingly, in a previous study, a similar change in morphology was associated with abnormal localisation of the major bi-functional penicillin-binding protein PBP1 at the cell poles (Kawai, Daniel and Errington, 2009); recruitment of which is dependent on MreB. GFP-tagging of this protein could therefore be implemented to investigate whether PBP1 also exhibits polar localisation upon treatment with these extracts and is responsible for the excess cell wall synthetic activity. Nevertheless, although not dependent on membrane potential [as previous delocalisation of MreB has been found to be (Strahl and Hamoen, 2010; Seistrup, 2018)] the mechanism by which MreB and the elongasome is recruited to these membrane regions remains unknown, and requires further elucidation.

Finally, the methanolic extract from DEM30062 induced membrane lipid domains of increased local fluidity, as demonstrated by the emergence of foci brightly stained with the fluidity-sensitive dye Nile red. Such fluid lipid domains have been observed before (Strahl *et al.*, 2014; Müller *et al.*, 2016; Wenzel *et al.*, 2018) and are usually triggered by membrane depolarisation or delocalisation of MreB. However, those induced by extract DEM30062 occurred in the absence of both membrane depolarisation and all three bacterial actin homologues (MreB, Mbl and MreBH). Therefore, to the best of our knowledge, this is a novel and more direct mechanism of fluid microdomain formation, and the extract derived from DEM30062 provides a useful tool to investigate this mechanism independent of membrane depolarisation, MreB dissociation and their pleiotropic effects. The next stages would be to confirm that the strongly fluorescent Nile red foci are not caused by membrane invaginations, which also results in increased dye signal due to excess membrane material, as has been previously observed for the membrane-active antimicrobials tyrocidines and octenidine (Wenzel *et al.*, 2018; Malanovic *et al.*, 2022). If not, we could also more directly determine the local fluidity of these membrane regions using fluorescent probes that analyse phospholipid packing within the bilayer such as Laurdan (Jay and Hamilton, 2017) and DPH (Fox and Delohery, 1987).

As mentioned in 5.2.2 and shown in Appendix I, one extract also gained LiaI-inducing properties in the presence of calcium, whilst three others exhibited larger areas of bacterial growth inhibition. These, therefore, resemble calcium-dependent lipopeptide antibiotics, such as daptomycin and friulimicin (Debono *et al.*, 1987; Aretz *et al.*, 2000), which are rapidly emerging as a novel class of antibacterial agents. The next stages would be to repeat the preliminary experiments performed in the presence of calcium to observe the calcium-dependent effects of these extracts on bacterial growth and morphology, membrane integrity and organisation, and localisation of MreB and the cell wall synthetic machinery.

Moreover, these preliminary mode of action studies have been performed on crude extracts derived from solid *Actinomycete* cultures. Due to the rudimentary extraction process, a combination of several active compounds could therefore be present within each solution. To more definitively determine the specific membrane-active agent(s), it would be necessary to perform high-performance liquid chromatography (HPLC) fractionation, as has been previously described (Eldridge *et al.*, 2002; Tu and Yan,

2012), and subsequent large-scale purification for structural and more detailed mode of action analyses.

As mentioned previously, the work described in this chapter was performed in conjunction with the SME, Demuris Ltd. My placement there was not only affected by the beginning of the global Covid-19 pandemic, but also by the subsequent acquisition of Demuris by the larger biotechnology company, Odyssey Therapeutics. Both of these were accompanied by logistical and contractual reasons why I unfortunately could not continue with my research on these strains and their extracts. Nevertheless, the project could be continued by the sequencing and phylogenetic analysis of the producer strains to ensure dereplication and provide insight into other characteristics of the organism such as its ecology and evolutionary ancestors. Finally, the implementation of further bioinformatics processes such as antiSMASH would allow the identification of BGCs and their products (Medema *et al.*, 2011), and thus an indication of the organism's secondary metabolites and any potential antimicrobials.

Chapter 6 – Further elucidating the mode of action of clinically relevant membrane-targeting antimicrobials and other membrane-active proteins

6.1 – Introduction

Using methods that I had optimised, in addition to other fluorescent-based techniques, I worked on further elucidating the mechanism of action of two currently used membrane-active antimicrobials, daptomycin and octenidine, and of PanT toxins identified from various bacteria and bacteriophages. The results from the latter 2 formed part of collaborative publications with Dr Malanovic's group from University of Graz and Dr Atkinson's group from Lund University, respectively (Kurata *et al.*, 2022; Malanovic *et al.*, 2022).

As discussed previously, daptomycin is a last resort antibiotic used for the treatment of multidrug resistant Gram-positive bacterial infections (Baltz, Miao and Wrigley, 2005). Despite this important clinical role, its precise mechanism of action is poorly understood; however, it is known to inhibit cell wall synthesis [through interaction with the peptidoglycan precursor lipid II and delocalisation of the elongasome components, MurG and MreB (Müller *et al.*, 2016; Grein *et al.*, 2020)], and preliminary data from our group suggested that daptomycin-induced lysis may be autolytic in nature (Seistrup, 2018). In particular, much controversy is centred on whether this membrane disruption is caused by formation of large pores or autolysis. I aimed to further elucidate the mechanism of action of daptomycin in the Gram-positive model organism *Bacillus subtilis*, in particular investigating whether *in vivo* permeabilisation is due to membrane pore formation or autolysis, and whether partial membrane depolarisation at low concentrations is sufficient to inhibit growth, or additional effects on the cell well are required. In addition, doubts have been raised regarding daptomycin-induced membrane rigidification (see 1.4.3), as measured by the membrane fluidity fluorescent probe Laurdan, due to daptomycin's intrinsic fluorescent properties. This shall also be discussed and tested within this chapter.

Octenidine is an antiseptic molecule, used for over 30 years for skin, mucous membrane and wound antisepsis and patient decolonisation (Hübner, Siebert and Kramer, 2010; Jeans *et al.*, 2018; Pichler *et al.*, 2018), due to its broad spectrum activity against multidrug resistant Gram-positive and Gram-negative pathogens (Conceição, de Lencastre and Aires-de-Sousa, 2016; Alvarez-Marin *et al.*, 2017), and

even fungi (Koburger *et al.*, 2010). Its cationic and hydrophobic nature (owing to ammonium and octanyl groups respectively) allows for octenidine's interaction with the bacterial cytoplasmic membrane (Assadian, 2016), and recently, it was shown that the molecule induces membrane depolarisation and changes in membrane fluidity, due to a dramatic rearrangement of phospholipid packing, in the Gram-negative *E. coli* (Malanovic *et al.*, 2020). In collaboration with Dr Malanovic, we planned to expand this mode of action study to Gram-positive bacteria, and whilst their group observed the biophysical effects of octenidine, I investigated its membrane effects using fluorescence microscopy against the model organism *B. subtilis*.

Finally, toxin-antitoxin systems are widespread in bacterial and bacteriophage genomes. The toxin proteins act by inhibiting essential cellular processes, including targeting DNA polymerase, cleaving tRNAs and mRNAs or compromising integrity of the cytoplasmic membrane (Jurėnas *et al.*, 2022). In the collaborative publication (Kurata *et al.*, 2022), Dr Atkinson's group discovered that the antitoxin domain DUF4065 is found as the cognate to dozens of different toxic domains across Bacteria, Archaea, and Bacteriophages, and experimentally characterised 9 PanAT pairs (DUF4065-containing antitoxin proteins and their toxin proteins respectively). Our role was to investigate the membrane effects of such PanT toxins in *E. coli*, using fluorescence microscopy.

6.2 – Results

6.2.1 – Daptomycin mode of action

6.2.1.1 – Membrane pore formation and autolysis

To investigate whether daptomycin forms large pores in the cytoplasmic membrane of *B. subtilis*, I performed my optimised Sytox Green membrane pore formation assay. Indeed, daptomycin treatment induced an increase in Sytox Green fluorescence; however, this was a delayed event, occurring approximately 30 minutes following addition (Fig. 51A). Due to this delay and recent preliminary data from our group that implied daptomycin's autolytic activities (Seistrup, 2018), I tested whether this fluorescence was instead due to autolysis by repeating the assay on a *B. subtilis* strain deficient for the major autolysins and their regulators (*ΔlytABCDEF).* Interestingly, there was a reduction in daptomycin-induced Sytox Green fluorescence (Fig. 51B); an effect that was not observed for the known pore forming lantibiotic nisin.
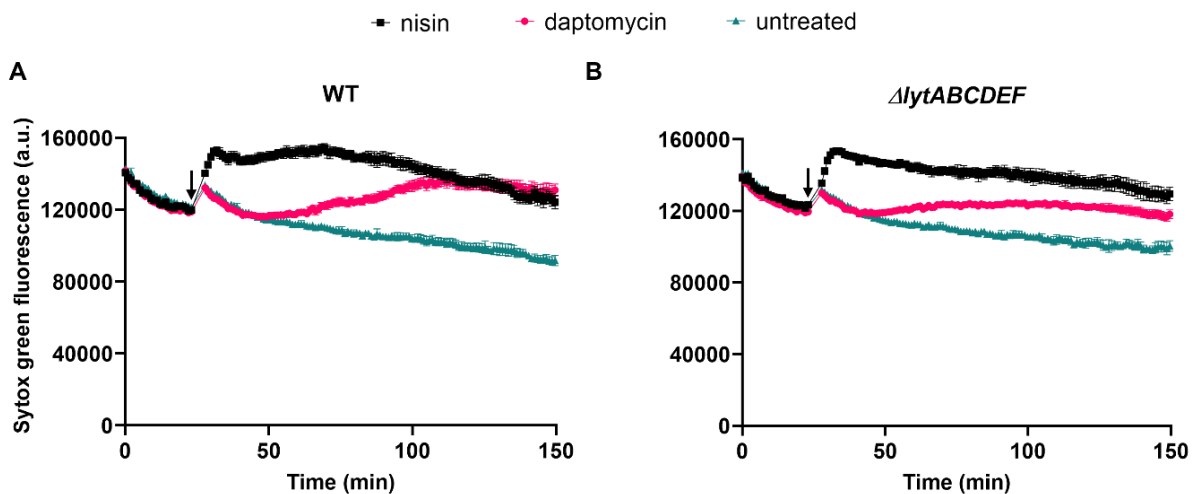
Figure 51: Daptomycin-induced Sytox Green fluorescence is reduced in an autolysin deficient *B. subtilis* mutant. The effect of 10 µg/ml daptomycin on the fluorescence intensity of 1 µM Sytox Green in (A) *B. subtilis* wild type cells and (B) *B. subtilis* cells deficient for cell wall autolytic proteins, LytA-F, at an OD_{600} of 0.5. The pore-forming lantibiotic nisin (10 µM) was used for positive control. The time point of antibiotic addition is indicated by an arrow. Data are represented as mean±SD (n=3). Strains used: *B. subtilis* 168 (WT) and *B. subtilis* KS19 (*ΔlytABCDEF*).

To observe this on a single-cell level, I performed phase contrast and Sytox Green fluorescence microscopy of *B. subtilis* wild type cells treated with two concentrations of daptomycin (the minimum concentration to inhibit *B. subtilis* growth at an OD_{600} of 0.2 and two-fold greater than this), and at two time points to observe the early and late stages of its action. During these experiments, it became immediately apparent, especially at the later time point (25 min), that many of the cells had lysed as indicated by phase light cells (white arrows; Fig. 52A). In fact, when the proportion of phase light cells was quantified, at both concentrations over half of all cells had lysed by 25 minutes (Fig. 52B). I then determined the individual Sytox Green fluorescence intensities of the remaining phase dark cells, defining a signal of 2000 a.u. or greater as Sytox Green positive, due to the residual staining of untreated cells, and therefore exhibiting membrane pores. As shown in Fig. 52B, the majority of phase dark cells were not stained with Sytox Green when compared to our pore forming positive control nisin. We therefore hypothesise that the delayed Sytox Green fluorescence observed in the plate reader is due to staining of extracellular DNA released during autolysis. A representative image of this is shown in Fig. 52C, compared to the intracellular Sytox Green staining of nisin-treated cells, indicative of pore formation.
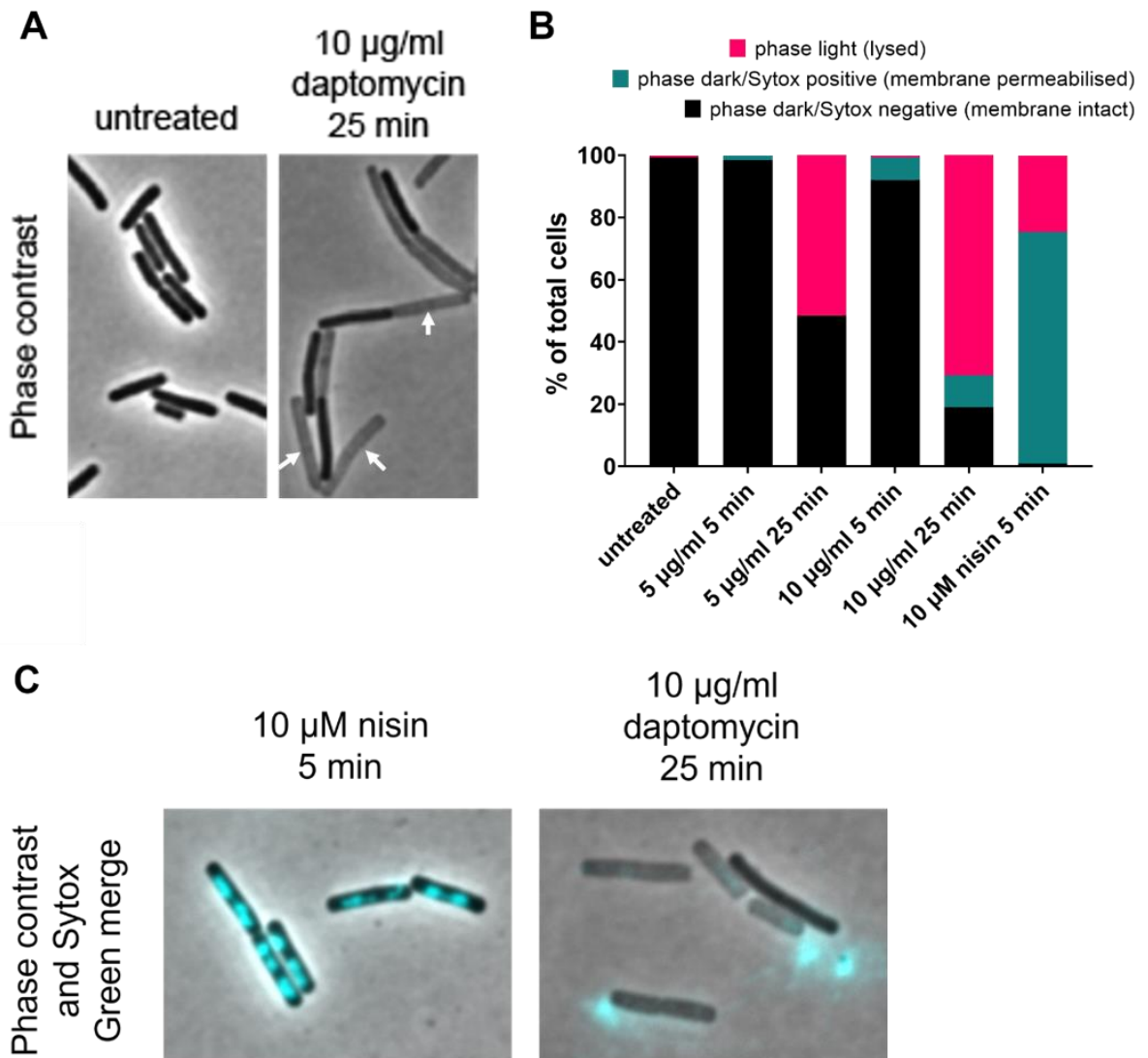
Figure 52: Daptomycin induces lysis without significant membrane pore formation. (A) Phase contrast microscopy images of *B. subtilis* wild type cells untreated or treated with 10 µg/ml daptomycin for 25 minutes. Fully lysed (phase light) cells are highlighted with white arrows. (B) *B. subtilis* wild type cells were stained with 200 nM Sytox Green and treated with either 5 µg/ml or 10 µg/ml daptomycin for 5 and 25 minutes. Percentage of total cells phase light (lysed), phase dark/Sytox positive (membrane permeabilised) or phase dark/Sytox negative (membrane intact) are shown. Sytox positive was defined as a fluorescence intensity of 2000 a.u. or greater. 10 µM of the lantibiotic nisin was used as a positive control for pore formation. N=107-142. (C) Phase contrast and fluorescent microscopy merge of *B. subtilis* wild type cells stained with 200 nM Sytox Green (shown in cyan) and treated with either 10 µM nisin or 10 µg/ml daptomycin. Strain used: *B. subtilis* 168 (wild type).

As the majority of cells were subject to lysis at the later time point, I then investigated how the action of daptomycin was affected in cells incapable of autolysis. Therefore, I performed phase contrast and Sytox Green fluorescence microscopy of daptomycin-treated *B. subtilis ΔlytABCDEF* cells. Deletion of the major autolysins in *B. subtilis* results in a chaining defect; where individual cells possess a separated cytoplasm but

are connected via a continuous peptidoglycan sacculus (Chen *et al.*, 2009). Therefore, to distinguish individual cells, this strain was co-stained with the membrane dye FM5-95 (Fig. 53A). As shown in Fig. 53, the majority of daptomycin-induced autolysis was abolished in this strain. Crucially, the majority of cells remained free from Sytox Green staining at both daptomycin concentrations and time points, compared to ~100% of nisin-treated cells exhibiting a Sytox Green signal. These results demonstrate that, even in the absence of autolysis, we do not observe increased levels of membrane pore-formation as a result of daptomycin treatment.
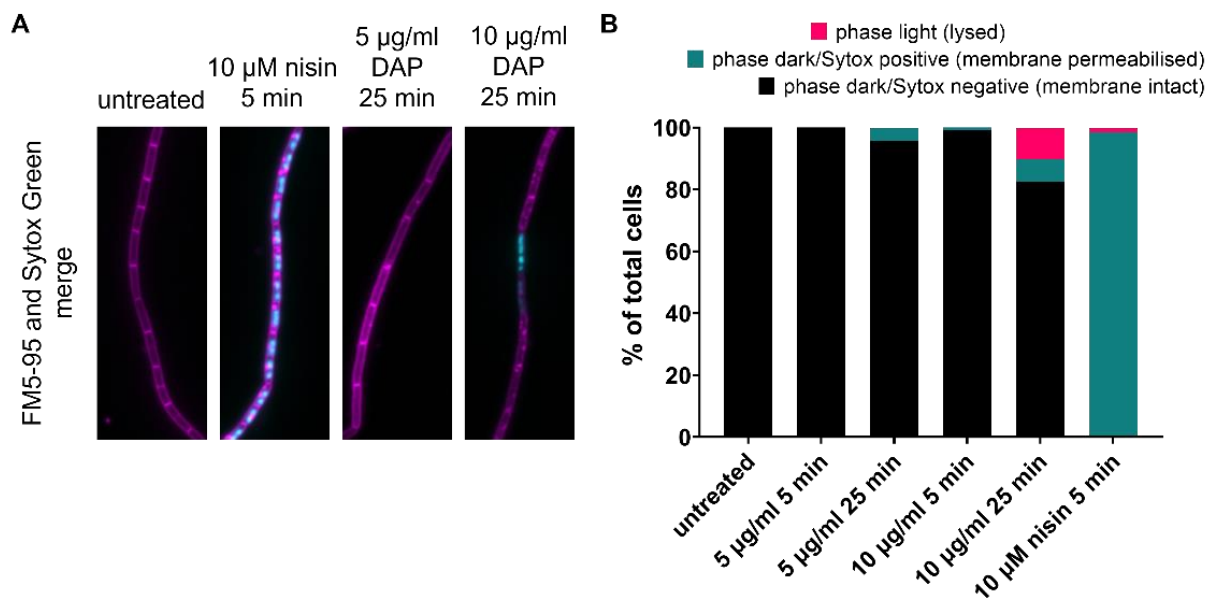
Figure 53: Daptomycin does not cause membrane pore formation even in the absence of autolysis. (A) Fluorescent microscopy images of *B.subtilis ΔlytABCDEF* cells co-stained with 2 µg/ml FM5-95 (shown in magenta) and 200 nM Sytox Green (shown in cyan), in the absence or presence of either 5 µg/ml or 10 µg/ml daptomycin for 5 and 25 minutes (only the later timepoint shown). (B) Quantification of the percentage of phase light (lysed), phase dark/Sytox positive (membrane permeabilised) or phase dark/Sytox negative cells (membrane intact) is shown. 10 µM of the lantibiotic nisin was used as a positive control for pore formation. N=118-230. Strain used: *B. subtilis* KS19 (*ΔlytABCDEF*).

6.2.1.2 – Membrane depolarisation and correlation to growth inhibition

It was previously shown that growth inhibitory concentrations of daptomycin only cause a partial depolarisation of the cytoplasmic membrane (Müller *et al.*, 2016); however, as a calibration of the DiSC$_3$(5) assay had not yet been established, the degree of depolarisation was not directly quantified. Therefore, to achieve this, I reproduced the calibration, previously set up by our group (te Winkel *et al.*, 2016), to specifically associate DiSC$_3$(5) fluorescence intensities with pre-defined membrane potential levels. Under normal conditions, due to the high H$^+$ transport activity of the respiratory

chain, the membrane potential is dominated by the H^+ gradient (Mitchell, 1961; Saraste, 1999). This, however, changes upon addition of the K^+-specific ionophore valinomycin, allowing the membrane permeability for K^+ to be exclusively increased to such an extent that membrane potential is now determined by the K^+ gradient. Using this and the Nernst equation, I calculated (with an online Nernst Potential Calculator [PhysiologyWeb, 2005]) the extracellular K^+ concentrations necessary to achieve different K^+ equilibrium potentials (assuming an intracellular concentration of 300 mM and ~6 mM present in yeast extract) and subsequently prepared HEPES-KCl growth media using these calculations (Table 9).

Table 9: K+ equilibrium potentials and the extracellular K+ concentration required to achieve them, assuming an intracellular concentration of 300 mM.

$V_{Eq.}$ (mV)	$[K^+]_{in}$ (mM)	$[K^+]_{out}$ (mM)
0	300	300
-50	300	46.2
-60	300	31.8
-70	300	21.9
-80	300	15
-90	300	10.3
-100	300	7.1
-105	300	6

I then performed the $DiSC_3(5)$ membrane depolarisation assay with *B. subtilis* cells grown in these media, dissipating the membrane potential with valinomycin (Fig. 54A). The resulting measurements were then used to calculate the mean $DiSC_3(5)$ fluorescence associated with each equilibrium potential, as well as the 95% confidence interval of the mean (Fig. 54B). These were plotted alongside the dissipation of membrane potential trigged by different concentrations of daptomycin in the HEPES-NaCl growth medium. As shown in Fig. 55, the minimum concentration of daptomycin to inhibit growth of *B. subtilis* at an OD_{600} of 0.2 (5 µg/ml) only caused a depolarisation of the cytoplasmic membrane down to ~-70 mV. This prompted the question of whether this degree of depolarisation alone would be sufficient to inhibit *B. subtilis* growth.
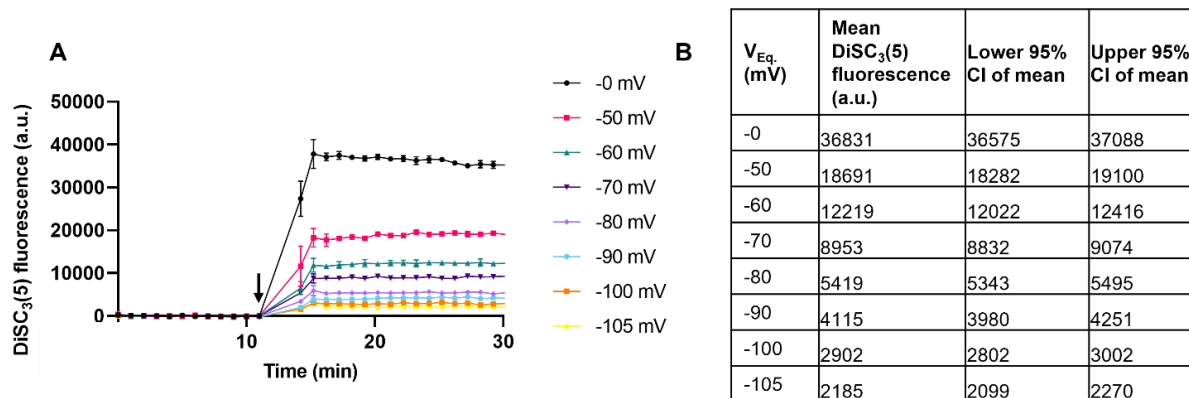
Figure 54: Calibration of the DiSC₃(5) membrane depolarisation assay in *B. subtilis*. (A) Fluorescence kinetics of *B. subtilis* cells grown to an OD_{600} of 0.2 in HEPES medium of varying K^+ concentrations, stained with 1 µM DiSC₃(5) and treated with 5 µM valinomycin to dissipate the membrane potential to a pre-defined level. Data are show as mean±SD (n=3) and the time point of valinomycin addition is indicated by an arrow. (B) The mean DiSC₃(5) fluorescence and 95% confidence interval of the mean calculated from the plateau for each K^+ equilibrium potential (n=30). Strain used: *B. subtilis* 168 (wild type).
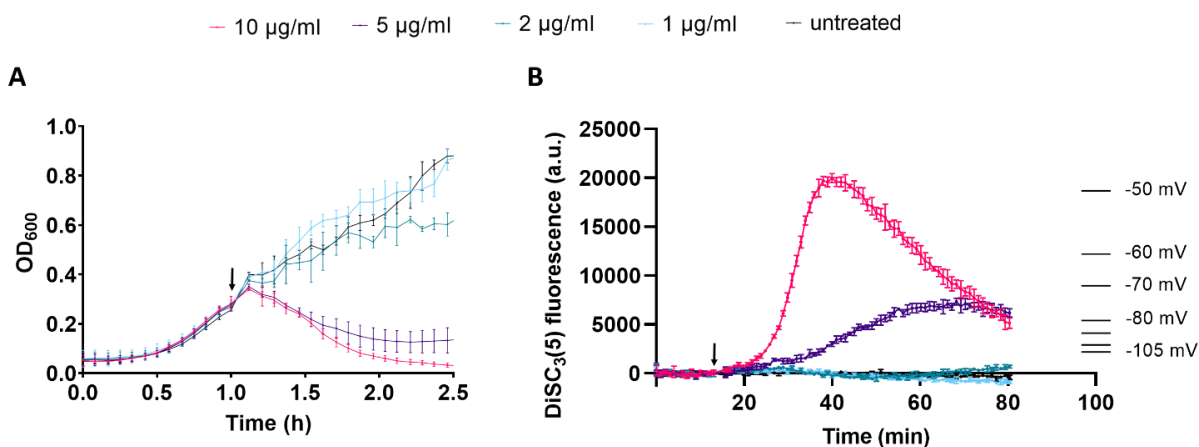
Figure 55: Correlation between daptomycin-induced growth inhibition and membrane depolarisation in *B. subtilis*. (A) Growth kinetics of *B. subtilis* cells grown in HEPES-NaCl medium to an OD_{600} of 0.2, in the absence and presence of different daptomycin concentrations. (B) Dissipation of the membrane potential by different daptomycin concentrations in *B. subtilis* cells grown to an OD_{600} of 0.2 in HEPES-NaCl medium. The calibration depicted to the right represents the mean DiSC₃(5) fluorescence intensities from cells with predefined membrane potential levels, as calculated from Fig. 51A. All data are show as mean±SD (n=3) and the time points of daptomycin addition are indicated by arrows. Strain used: *B. subtilis* 168 (wild type).

Therefore, I observed the growth kinetics of valinomycin-treated cells in the presence of varying extracellular K^+ concentrations to determine the effect that membrane potential exhibited on the ability of *B. subtilis* to grow. We believe that this is the first time an experiment has directly linked degree of membrane potential and growth in *B. subtilis*, and as demonstrated in Fig. 56, there is a clear threshold at which growth is

still supported (~-80 mV). Thus, the partial membrane depolarisation induced by growth inhibitory concentrations of daptomycin (~-70 mV) is capable of inhibiting growth in *B. subtilis* on its own.
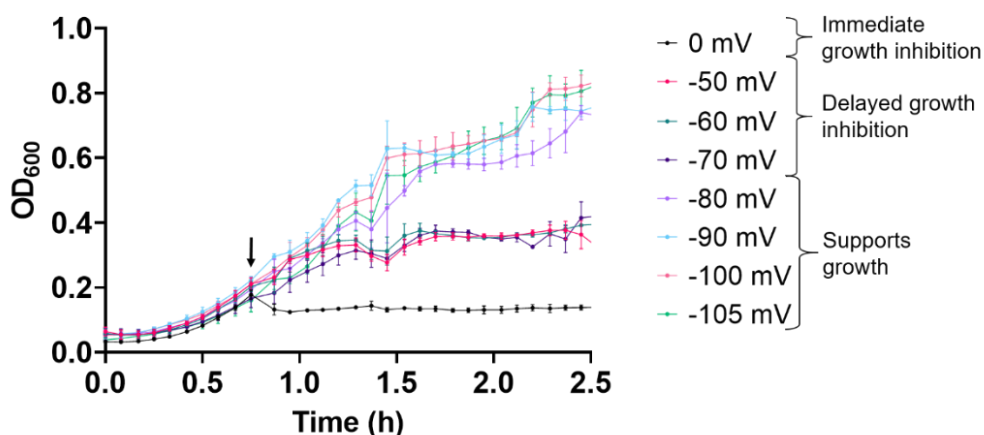
Figure 56: Correlation between membrane potential and growth in *B. subtilis*. Growth kinetics of *B. subtilis* cells grown to an OD_{600} of 0.2 in HEPES medium of varying K^+ concentrations and treated with 5 µM valinomycin to dissipate the membrane potential to a pre-defined level. Growth is supported at membrane potentials of -80 mV and below. The time point of valinomycin addition is indicated by an arrow. Data are represented as mean±SD (n=3). Strain used: *B. subtilis* 168 (wild type).

6.2.1.3 – Intrinsic calcium-dependent fluorescence of membrane-bound daptomycin

Daptomycin possesses a kynurenine residue that is intrinsically fluorescent, and maximally fluoresces upon insertion into the phospholipid bilayer, facilitated by the presence of Ca^{2+}, with an approximate maximum emission wavelength of 450 nm (Lakey and Ptak, 1988; Jung *et al.*, 2004). Since the emission wavelength of the fluorescent probe Laurdan shifts to ~440 nm upon decreases in membrane fluidity, this casted doubts on whether the Laurdan-based membrane fluidity measurements previously performed by our group (Müller *et al.*, 2016) observed daptomycin-induced membrane rigidification or the intrinsic fluorescent properties of daptomycin. To investigate this, I first confirmed that Laurdan exhibited a shift in peak fluorescence upon addition of daptomycin to stained-*B. subtilis* (Fig. 57A). Then to observe the effect of daptomycin fluorescence alone, I repeated this in the absence of Laurdan (Fig. 57B). Similarly to previous studies, in the absence of Ca^{2+}, daptomycin was only weakly fluorescent with an emission peak of ~465 nm, however addition of Ca^{2+} led to a ~20 nm blue shift and a 5-fold increase in fluorescence intensity, directly overlapping with the spectral shift of Laurdan.
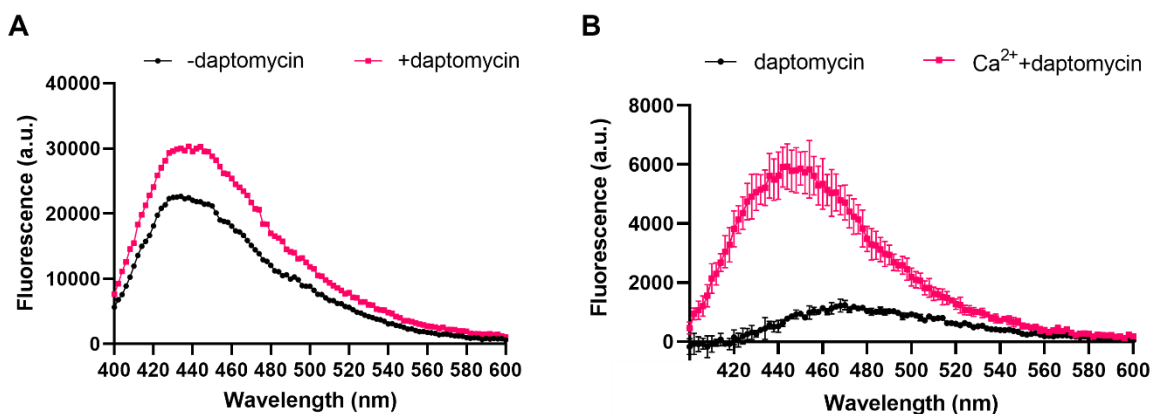
Figure 57: Laurdan-independent increase in daptomycin fluorescence upon addition of calcium. (A) Fluorescence emission spectra of *B. subtilis* stained with 10 µM Laurdan in the presence of 1.25 mM CaCl₂, following addition of 2 µg/ml daptomycin, at an excitation wavelength of 360±20 nm. (B) Fluorescence emission spectra of *B. subtilis* treated with 2 µg/ml daptomycin, in the absence and presence of 1.25 mM CaCl₂, at an excitation wavelength of 360±20 nm. Strain used: *B. subtilis* 168 (wild type).

To circumvent the issue of daptomycin's intrinsic fluorescence, we obtained a variant of daptomycin (from here on, referred to as NF-DAP) from Dr Scott Taylor's group at the University of Waterloo, with 3 amino acid substitutions: O6K, mE12E, but most importantly the kynurenine at position 13 changed to tryptophan (Kyn13W), thereby abolishing daptomycin's natural fluorescence. I first performed a MIC assay to determine whether the antibacterial activity of this variant differed compared to wild type daptomycin, and as shown in Table 10, NF-DAP exhibited an 8-fold higher MIC. Therefore, in experiments directly testing daptomycin's activity, I included NF-DAP at a concentration 8-times higher.

Table 10: Minimum inhibitory concentrations (MICs) of daptomycin and a variant, NF-DAP, against *B. subtilis* 168.

Compound	*B. subtilis* 168
	MIC (µg/ml)
Daptomycin	1.56
NF-DAP	12.5

N=3.

First, I observed the spectra of both types of daptomycin in *B. subtilis* in the absence of Laurdan (Fig. 58A). As expected, in both the absence and presence of Ca²⁺, NF-DAP exhibited no fluorescence at any wavelength. Therefore, since this variant would have no effect on its spectral shift, I used Laurdan to investigate whether NF-DAP induced changes to *B. subtilis* membrane fluidity. Even at 8-times the concentration of

normal daptomycin, NF-DAP demonstrated no effect on Laurdan fluorescence (Fig. 58B), implying that it does not cause a rapid rigidification of the membrane. Hence, previous daptomycin mode of action studies utilising Laurdan as a membrane fluidity probe cannot be relied upon, due to interference by the intrinsic fluorescence of daptomycin.
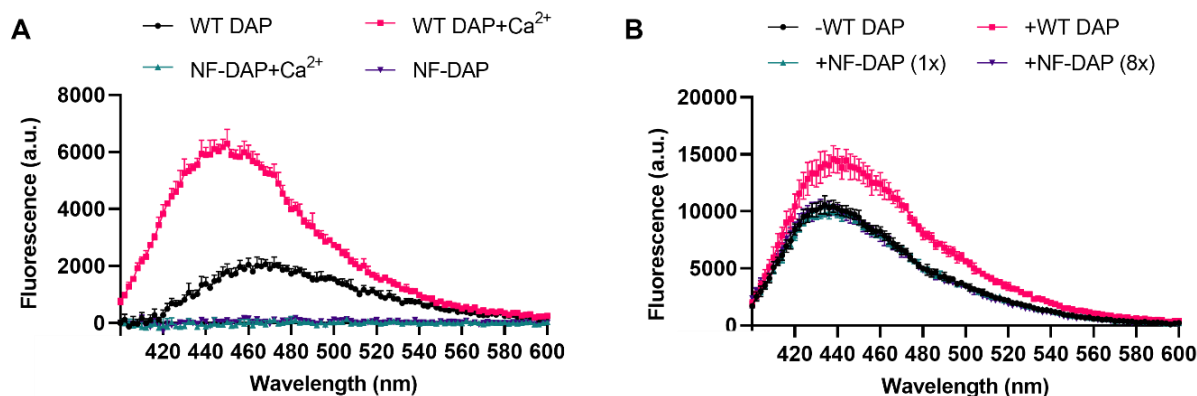
Figure 58: NF-DAP has no effect on membrane fluidity in *B. subtilis*, as measured by the fluorescent probe Laurdan. (A) Fluorescence emission spectra of *B. subtilis* treated with 2 µg/ml daptomycin (WT DAP) or 2 µg/ml NF-DAP, in the absence and presence of 1.25 mM CaCl$_2$, at an excitation wavelength of 360±20 nm. (B) Fluorescence emission spectra of *B. subtilis* stained with 10 µM Laurdan in the presence of 1.25 mM CaCl$_2$, following addition of WT DAP (2 µg/ml) or NF-DAP (2 or 16 µg/ml), at an excitation wavelength of 360±20 nm. Strain used: *B. subtilis* 168 (wild type).

6.2.1.4 – Dependency on undecaprenyl-coupled cell wall precursors in vivo

Next, I aimed to investigate whether daptomycin exhibits a dual mode of action, or instead whether its abilities to inhibit cell wall synthesis and depolarise the cytoplasmic membrane are inherently linked. As mentioned previously, a recent paper demonstrated that daptomycin inhibits cell wall synthesis through its interaction with undecaprenyl-coupled peptidoglycan precursors (Grein *et al.*, 2020). We therefore wanted to determine whether daptomycin-induced membrane depolarisation was also dependent on this interaction. To achieve this, we used L-forms, which are cell wall deficient bacterial variants and permit deletion of genes in the peptidoglycan biosynthesis pathway; that would otherwise be lethal (Kawai, Mercier and Errington, 2014). Using this system, we deleted the *upps* gene which encodes undecaprenyl pyrophosphate synthase, thereby preventing the synthesis of any undecaprenyl-coupled cell wall precursors, including lipid II. To prevent cell lysis by osmotic shock, L-forms are cultured in an osmoprotective medium composed of Nutrient Broth, magnesium, sucrose and maleic acid (NB-MSM). As shown in Fig. 59, DiSC$_3$(5)

fluorescence intensities were lower in this medium compared to LB in wild type *B. subtilis* rods. Despite this, there was still a detectable difference in DiSC$_3$(5) staining between polarised and depolarised cells (caused by the channel forming peptide gramicidin) in NB-MSM.
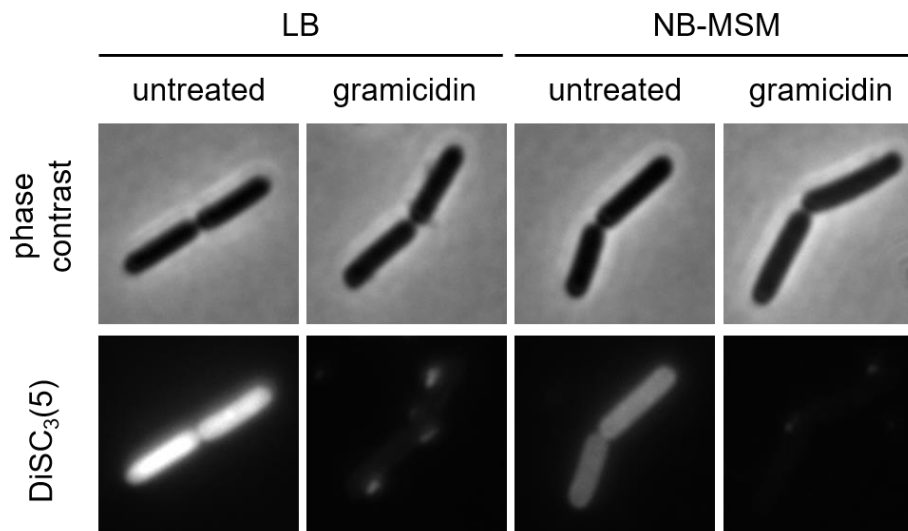
Figure 59: The effect of osmoprotective medium on DiSC$_3$(5) fluorescence intensities in *B. subtilis* 168. Phase contrast and fluorescence microscopy images of *B. subtilis* 168 grown in LB or NB-MSM, stained with 1 µM DiSC$_3$(5), in the absence and presence of 10 µM of the channel forming peptide gramicidin (5 min). Strain used: *B. subtilis* 168 (wild type).

We therefore performed DiSC$_3$(5) fluorescence microscopy of *B. subtilis* Δ*upps* L-forms in NB-MSM, and as demonstrated in both the microscopy images and quantification of single-cell fluorescence levels, daptomycin still induced membrane depolarisation (Fig. 60A, B), suggesting that it is not dependent on interaction with lipid II or any other undecaprenyl-coupled precursors.

Moreover, as discussed earlier, daptomycin triggers formation of fluid lipid microdomains (Müller *et al.*, 2016), which we speculated to be due to its interaction with lipid II (Strahl, Bürmann and Hamoen, 2014), and is now consistent with the recent findings from Grein et al. (2020). In addition, due to the intrinsic fluorescence of the kynurenine residue in daptomycin, we were able to directly observe the colocalisation

between daptomycin and these fluid membrane regions, which are preferentially stained by FM5-95 (Fig. 61).
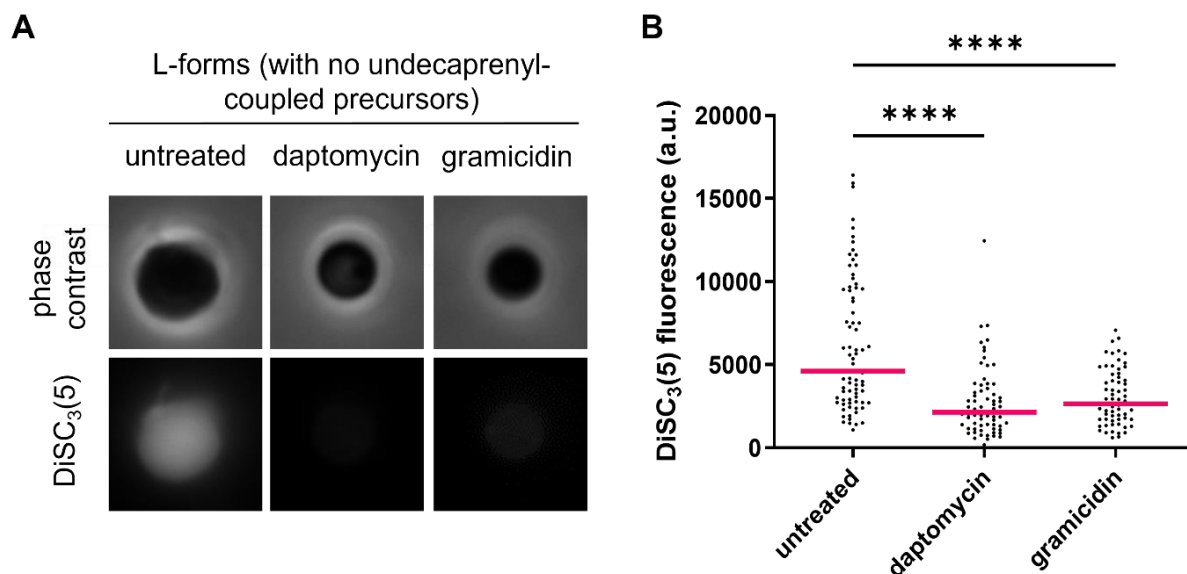
Figure 60: Daptomycin still induces membrane depolarisation in *B. subtilis* L-forms lacking cell wall precursors. (A) Phase contrast and fluorescence microscopy of *B. subtilis Δupps* L-forms stained with 1 µM DiSC$_3$(5), in the absence and presence of 10 µg/ml daptomycin (25 min). The channel forming peptide gramicidin was used as a positive control for membrane depolarisation (10 µM, 5 min). (B) Quantification of DiSC$_3$(5)-fluorescence for individual cells from the dataset shown in panel A (n=65-78 cells). Median fluorescence intensity is indicated with a magenta line, together with P values of a one-way, unpaired ANOVA. **** represents p < 0.0001. Performed in collaboration with Alan Koh. Strain used: *B. subtilis* AK199B (*Δupps*).
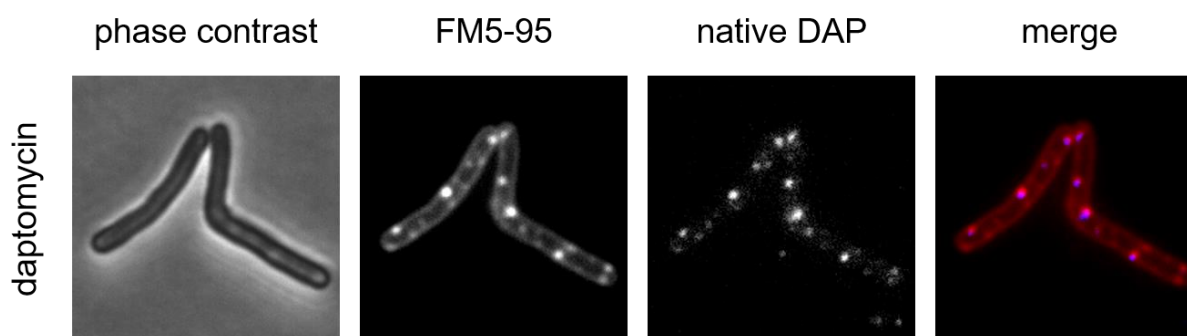
Figure 61: Daptomycin colocalises with fluid lipid microdomains in *B. subtilis*. Phase contrast and fluorescence microscopy of *B. subtilis* cells stained with 2 µg/ml FM5-95 (shown in red) and treated with 2 µg/ml daptomycin (shown in blue) for 60 min. Due to the intrinsic fluorescence of daptomycin, its localisation can be directly observed. Strain used: *B. subtilis* 168 (wild type).

Further evidence to support a lipid II-independent mechanism of action is that this domain formation is not observed upon incubation with NF-DAP (Fig. 62A), which, as stated previously, possesses 3 amino acid substitutions, suggesting that this variant no longer binds lipid II. Despite this, NF-DAP still caused an extensive depolarisation

of the cytoplasmic membrane in *B. subtilis* (Fig. 62B, C), reiterating that lipid II interaction is not required for daptomycin-induced membrane depolarisation.
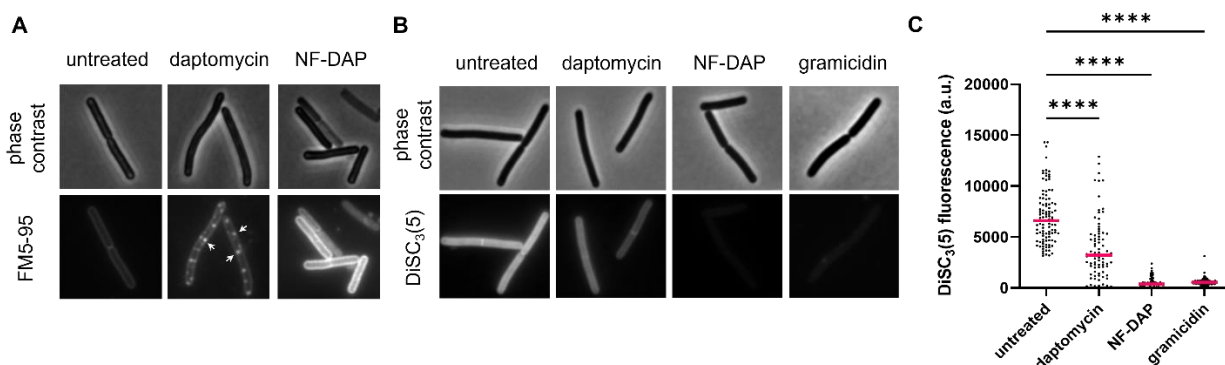
Figure 62: A daptomycin variant does not induce formation of fluid lipid microdomains, but still causes membrane depolarisation in *B. subtilis*. Phase contrast and fluorescence microscopy of *B. subtilis* stained with (A) 2 µg/ml FM5-95 or (B) 1 µM DiSC$_3$(5), in the absence and presence of 2 µg/ml native daptomycin or 16 µg/ml NF-DAP (8-fold concentration due to higher MIC; see above, 60 and 25 min for (A) and (B), respectively). The channel forming peptide gramicidin was used as a positive control for membrane depolarisation (10 µM; 5 min). Representative fluid domains are highlighted with white arrows. (C) Quantification of DiSC$_3$(5)-fluorescence for individual cells from the dataset shown in panel B (n=83-149). Median fluorescence intensity is indicated with a magenta line, together with P values of a one-way, unpaired ANOVA. **** represents $p < 0.0001$. Strain used: *B. subtilis* 168 (wild type).

6.2.2 – Octenidine mode of action

6.2.2.1 – Octenidine-induced membrane depolarisation and pore formation

To ascertain the mode of action of octenidine (OCT) in the Gram-positive *B. subtilis*, I first determined its susceptibility against cells in logarithmic growth at the concentrations used previously by the Malanovic group (Malanovic *et al.*, 2020). In contrast to the Gram-negative *E. coli*, both 0.001% and 0.0004% were rapidly lytic in *B. subtilis* and whilst 0.0001% is initially lytic, growth does start to reoccur approximately one hour after addition (Fig. 63).

I then performed combined Sytox Green and DiSC$_3$(5) fluorescent microscopy to simultaneously investigate the effect of OCT on membrane integrity and membrane potential. At the lowest concentration tested, OCT caused a heterogeneous depolarisation of *B. subtilis* (as demonstrated by a reduction in DiSC$_3$(5) fluorescence; Fig. 64A, B). With increasing OCT concentration, the depolarisation became more homogenous and extensive. At higher concentrations, OCT also permeabilised the cytoplasmic membrane, as indicated by staining with Sytox Green.
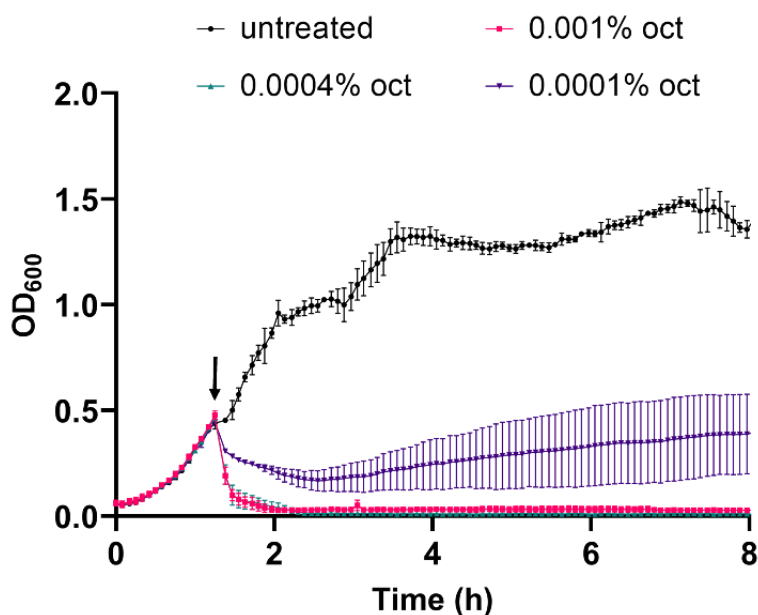
Figure 63: Effect of OCT on the growth of *B. subtilis* 168. Growth kinetics of *B. subtilis* 168 grown in LB to an OD_{600} of 0.5 then treated with different OCT concentrations. An arrow indicates the time point of compound addition. Data are shown as mean±SD (n=3). Strain used: *B. subtilis* 168 (wild type).

6.2.2.2 – Octenidine-induced changes to membrane organisation and fluidity

To further investigate the effect of OCT on the membrane, I performed combined Nile red and DAPI fluorescence microscopy. As shown in Fig. 65A, Nile red stains untreated *B. subtilis* membranes in a homogeneous manner without a visible preference for certain membrane areas. Upon incubation with OCT, however, I observed the emergence of brightly stained Nile red foci, which developed into larger membrane areas at the highest concentration. Interestingly, overall Nile red fluorescence levels were strongly increased in cells treated with OCT (Fig. 65B), and when quantified, fluorescence of 0.001% OCT-treated cells was significantly higher compared to untreated (Fig. 65C). It has been previously shown that Nile red fluorescence intensity is influenced by changes in fluidity of the membrane (Kucherak *et al.*, 2010; Strahl, Bürmann and Hamoen, 2014); therefore it is likely that this increase in Nile red fluorescence correlates to an increase in overall membrane fluidity. I also observed membrane areas with very low Nile red staining, and at the highest concentration, fully lysed cells (highlighted by white and red arrows respectively; Fig. 65A).
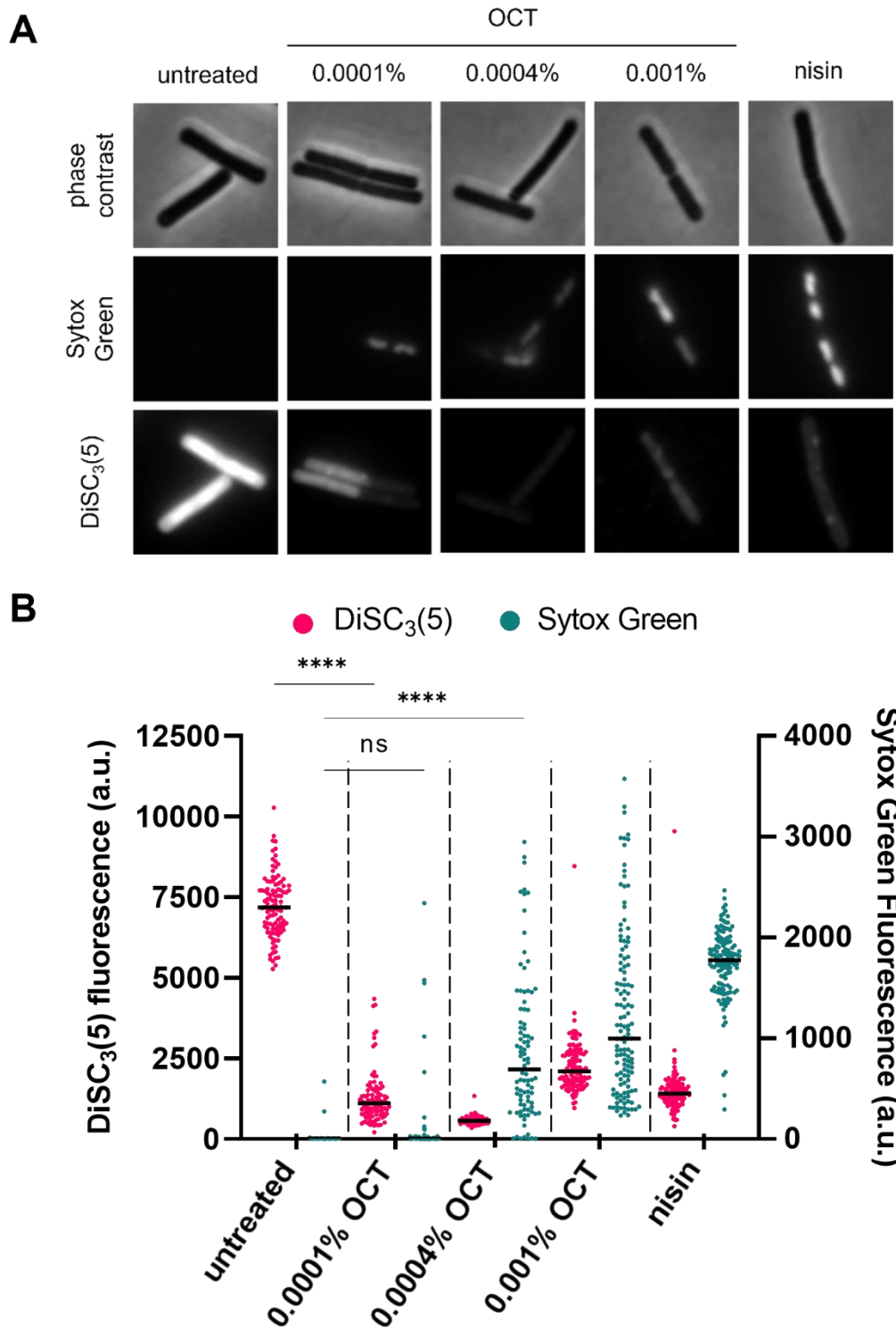
Figure 64: OCT disrupts the membrane barrier function in *B. subtilis*. (A) Phase contrast and fluorescence microscopy images of *B. subtilis* cells co-stained with the DiSC$_3$(5) and Sytox Green, and incubated in the absence and presence of different OCT concentrations for 5 min. The pore forming lantibiotic nisin was used as a positive control (10 µM). (B) Quantification of DiSC$_3$(5) and Sytox Green-fluorescence for individual cells from the dataset shown in panel A (n=90-130 cells). Median fluorescence intensity is indicated with a black line, together with P values of unpaired, two-sided t-tests. **** represents $p < 0.0001$ whereas ns indicates a non-significant difference. Strain used: *B. subtilis* 168 (wild type).
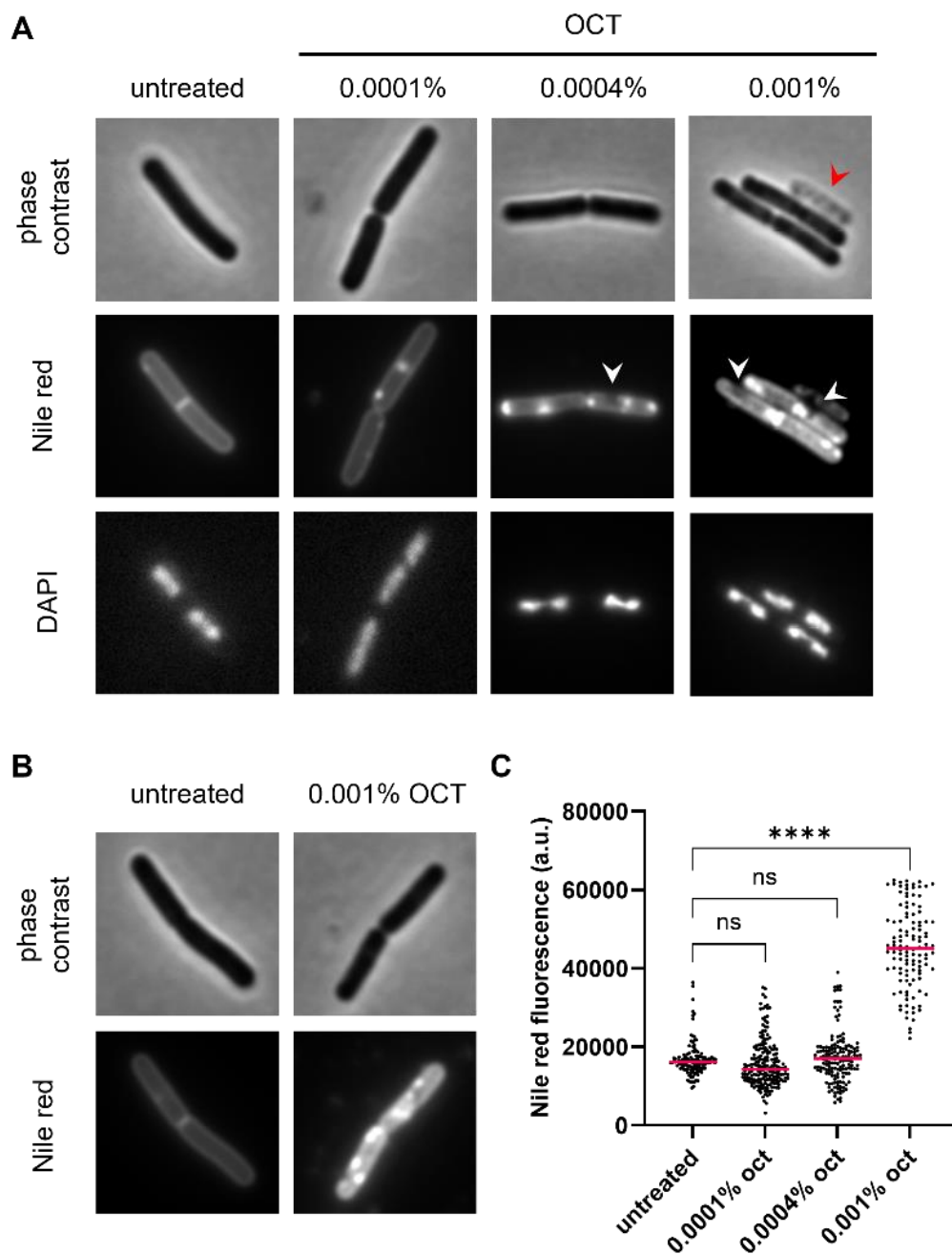
Figure 65: OCT disrupts membrane organisation and fluidity in *B. subtilis*. (A) Phase contrast and fluorescence microscopy images of *B. subtilis* cells co-stained with the membrane dye Nile red and the DNA dye DAPI, in the absence and presence of different OCT concentrations (5 min). Contrast settings have been altered between images to allow enhanced visualisation of fluorescent membrane patches. Membrane areas weakly stained by Nile red and fully lysed cells are highlighted with white and red arrows, respectively. (B) Phase contrast and fluorescence microscopy images of *B. subtilis* stained with Nile red in the absence and presence of 0.001 % OCT (5 min). Here, the fluorescence images retain identical contrast settings to allow intensity comparison. (C) Quantification of Nile red-fluorescence for individual cells from the same imaging dataset shown in panels A and B (n=118-199 cells). Median cell Nile red-fluorescence intensities are indicated with magenta lines, together with P values of unpaired, two-sided t-tests. **** represents p < 0.0001 whereas ns indicates a non-significant difference. Strain used: *B. subtilis* 168 (wild type).

To investigate whether the weakly-stained membrane areas were due to OCT-induced membrane disturbances, or linked to the ongoing cell lysis process, I repeated the Nile red fluorescent microscopy in a *B. subtilis* strain deficient of its major autolysins (*ΔlytABCDEF*). As expected, no lysis was observed microscopically, even when the cells were treated with the highest dose of OCT for 30 minutes (Fig. 66). Whilst incubation of *ΔlytABCDEF* cells with OCT still induced a spotty Nile red membrane stain, the weakly-stained membrane areas were absent in this strain, indicating that this phenomenon is not a direct consequence of OCT. Rather, the emergence of such areas is a secondary phenomenon associated with the developing cell lysis process.
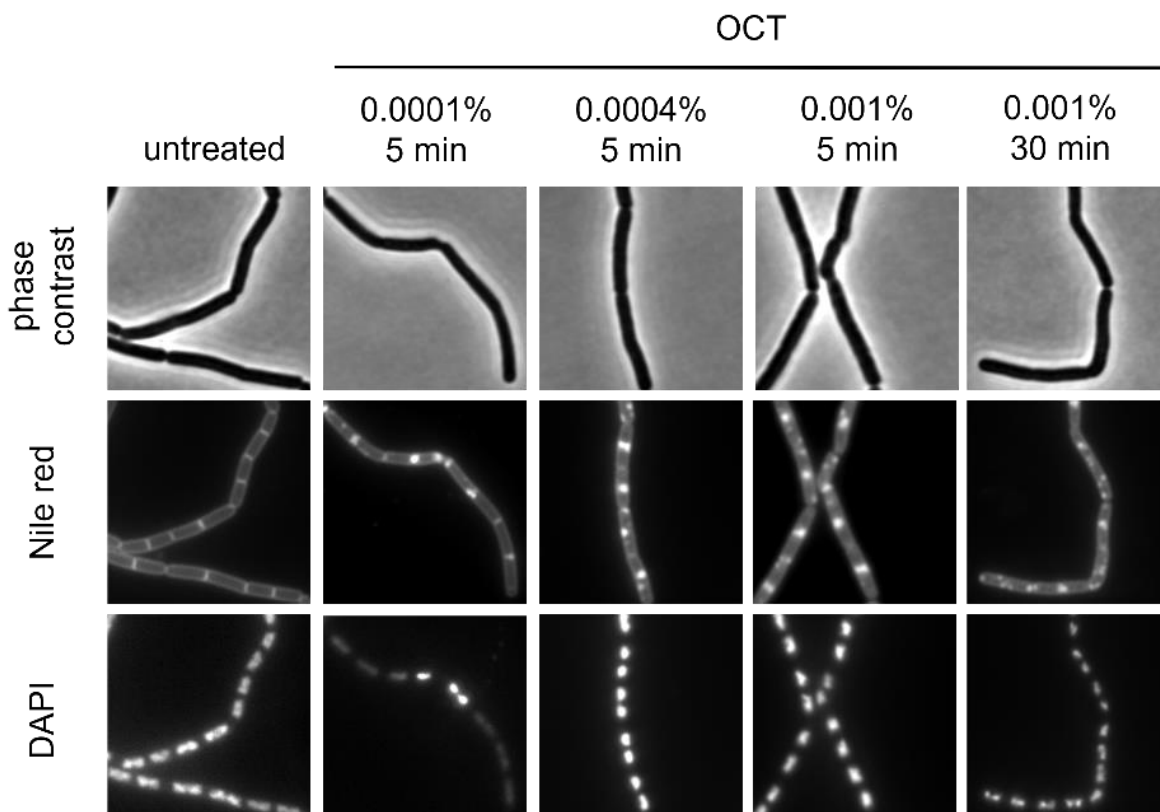
Figure 66: OCT-induced weakly Nile red-stained membrane areas are a manifestation of cell lysis. Phase contrast and fluorescence microscopy images of *B. subtilis* cells deficient for cell wall autolytic enzymes LytA-F, co-stained with the membrane dye Nile red and the DNA dye DAPI, in the absence and presence of different OCT concentrations (5 or 30 min). Note the lack of weakly Nile red-stained membrane areas, as observed in lysing wild type cells, whilst the brightly stained foci are still present. Due to the lack of cell wall hydrolase activity, these cells exhibit a chainy cell morphology as they cannot complete septal cleavage. Strain used: *B. subtilis* KS19 (*ΔlytABCDEF*).

Finally, it has been previously reported that antimicrobial peptides induce demixing in PG/PE bilayers, forming distinct domains enriched with either phospholipid (Arouri, Dathe and Blume, 2009; Finger *et al.*, 2015) and that the anionic phospholipid CL forms

polar localised domains in a number of bacterial species, including *B. subtilis* (Mileykovskaya and Dowhan, 2000; Matsumoto *et al.*, 2006). Therefore, to investigate whether these OCT-induced membrane disturbances were due to aberrant clustering of specific phospholipid species, I used strains incapable of producing CL (*ΔclsA, ΔclsB, ΔywiE*), PE (*Δpsd*), glucolipids (*ΔugtP*), lysyl-PG (*ΔmprF*) and phosphatidylserine (*ΔpssA*). I also observed what effect depleting wall- and lipoteichoic acids had in this context, *ΔtagO* and *ΔyfnI, ΔyqgS, ΔltaS* strains, respectively. I first performed MIC experiments to ensure that these strains remained susceptible to OCT treatment, and as shown in Table 11, all strains exhibited the same or 2-fold lower MIC compared to wild type.

Table 11: Minimum inhibitory concentrations (MICs) of octenidine against various *B. subtilis* 168 strains incapable of producing different phospholipid and teichoic acid species.

Strain genotype	OCT
	MIC (% w/v)
wild type	0.0001
ΔclsA, ΔclsB, ΔywiE	0.00005 - 0.0001
Δpsd	0.00005 - 0.0001
ΔugtP	0.00005 - 0.0001
ΔmprF	0.00005 - 0.0001
ΔpssA	0.00005 - 0.0001
ΔtagO	0.00005
ΔyfnI, Δ yqgS, ΔltaS	0.00005

N=3. Strains used: *B. subtilis* 168 (WT), ARK3 *(ΔclsA, ΔclsB, ΔywiE)*, KS119 *(Δpsd)*, AK0117B-A *(ΔugtP)*, AK0118B-A *(ΔmprF)*, AK0119B-A *(ΔpssA)*, AK094B *(ΔWTA) and* AK066B *(ΔLTA)*.

Next, I repeated Nile red staining with these strains, and the emergence of brightly stained Nile red foci still occurred in the absence of all phospholipid species and teichoic acids (Fig. 67), demonstrating that the action of OCT is not phospholipid- or teichoic acid-specific.
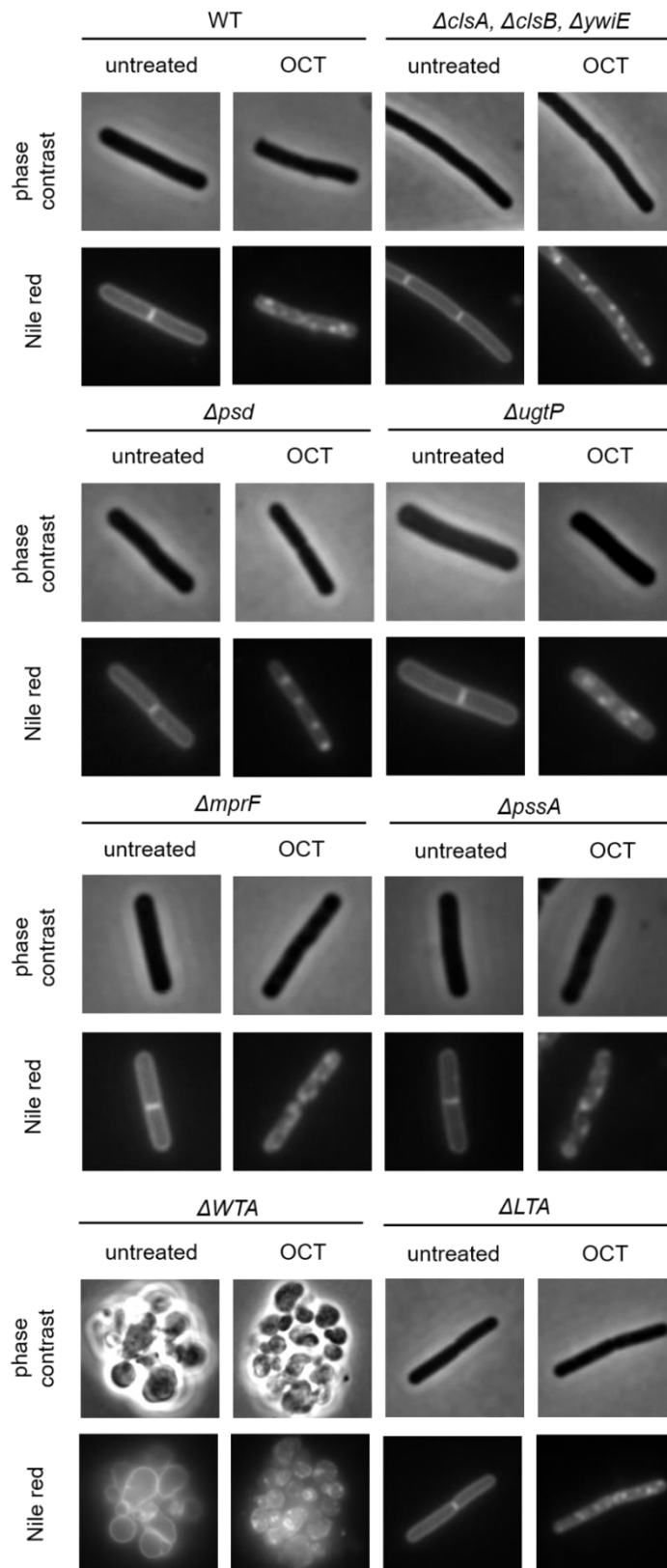
Figure 67: The activity of OCT in *B. subtilis* is not phospholipid or teichoic acid specific. Phase contrast and fluorescence microscopy images of *B. subtilis* cells deficient for certain phospholipids and teichoic acids, stained with the membrane dye Nile red in the absence and presence of 0.001% OCT (5 min). Strains used: *B. subtilis* 168 (WT), ARK3 *(ΔclsA, ΔclsB, ΔywiE),* KS119 *(Δpsd),* AK0117B-A *(ΔugtP),* AK0118B-A *(ΔmprF),* AK0119B-A *(ΔpssA),* AK094B *(ΔWTA) and* AK066B *(ΔLTA).*

6.2.2.3 – Octenidine-induced membrane invaginations

Finally, one potential cause of strongly fluorescent Nile red foci are membrane invaginations, which, due to excess membrane material, result in an increased membrane dye signal. To test whether OCT generates membrane invaginations, I observed the co-localisation between the Nile red signal and the FoF1 ATP synthase, which under normal conditions exhibits a uniform localisation pattern along the membrane (Strahl, Bürmann and Hamoen, 2014). As shown in Fig. 68A, treatment with OCT induced strong clustering of the ATP synthase subunit AtpA, which clearly co-localised with the fluorescent Nile red foci. Hence, these foci are indeed associated with a local folding of the membrane. In contrast, this is not observed for the control CCCP, which induces areas of high local membrane fluidity that are also preferentially stained by Nile red but are not associated with membrane invaginations (Strahl, Bürmann and Hamoen, 2014).
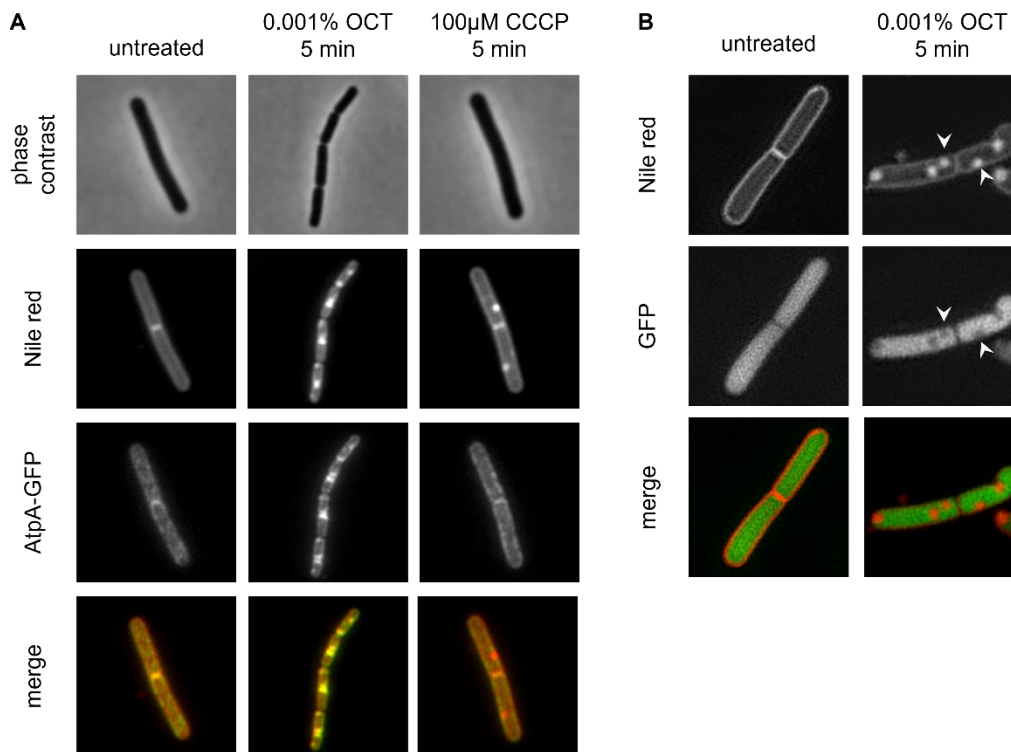
Figure 68: OCT-induced Nile red foci are due to membrane invaginations in *B. subtilis.* (A) Phase contrast and fluorescence microscopy images of Nile red-stained *B. subtilis* cells expressing AtpA-GFP, in the absence and presence of 0.001 % OCT (5 min). Note the co-localisation of OCT-induced Nile red and AtpA-GFP foci, which indicates membrane invaginations as the cause for high local Nile red intensity. The protonophore CCCP was used as a control, which induces invagination-independent Nile red foci associated with high local membrane fluidity, that do not influence AtpA-GFP localisation pattern. (B) SIM images of *B. subtilis* cells expressing sfGFP from a strong ribosomal promoter (PrpsD) and stained with Nile red in the absence and presence of 0.001% OCT. Note that the OCT-induced membrane invaginations exclude soluble, cytoplasmic GFP (white arrows). Strains used: *B. subtilis* BS23 (*atpA-gfp*) and bSS421 (*PrpsD-sfGFP*). SIM performed in collaboration with Henrik Strahl.

To confirm these findings through a more direct approach, I performed dual-colour SIM of Nile red-stained *B. subtilis* PrpsD-sfGFP cells, which constitutively express high levels of cytoplasmic GFP under control of the promoter for ribosomal protein S4. In untreated cells, I observed a uniform staining of the membrane and the cytoplasm was flooded with GFP (Fig. 68B). However, upon treatment with OCT, the Nile red foci were clearly associated with exclusion of the GFP signal (white arrows). This provides strong, direct evidence that OCT indeed induces membrane invaginations. Whilst likely, due to the presence of local membrane folds, we unfortunately cannot conclude whether the brightly stained Nile red membrane areas are also altered in local fluidity and disorder.

6.2.3 – Mode of action of membrane-active PanT toxins

6.2.3.1 – Generation of PanT mutants

Recently, Dr Aktinson and her group identified a domain of antitoxin function, DUP4065, that was able to neutralise a number of distinct toxins without conserved homology (Kurata *et al.*, 2022). We were involved in deciphering the activity of 8 experimentally characterised toxins associated with this domain (known as PanT toxins), in particular determining whether they disrupt the *E. coli* cytoplasmic membrane. Therefore, pBAD33 vectors containing the PanT toxins from various bacterial and bacteriophage origins (listed in Table 12) were constructed and sent to us by Dr Atkinson. I first transformed these into *E. coli* BW25113 and used *E. coli* BW25113 transformed with the empty vector as a control strain.

Table 12: Experimentally characterised PanT toxins, including their origin organism and description.

Organism	Toxin description
Escherichia coli STEC O31	PanT$_{Esc. col.}$
Bartonella apis	PanT$_{Bar. api.}$
Helicobacter sp. 13S00482-2	PanT$_{Hel.sp.}$
Bifidobacterium ruminantium	PanT$_{Bif. rum.}$
Pseudomonas moraviensis	PanT$_{Pse. mor.}$
Bacillus subtilis Ia1a	PhRel2$_{Bac. sub.}$
Vibrio harveyi	CapRel$_{Vib. har.}$
Burkholderia prophage phi52237	PanT$_{Bur. phage}$

I then tested that this had been successful by growing the transformants on agar plates supplemented with both chloramphenicol and glucose, and chloramphenicol and

arabinose. Arabinose induces PanT toxin expression; thus growth of the mutants was not observed on these plates (Fig. 69).
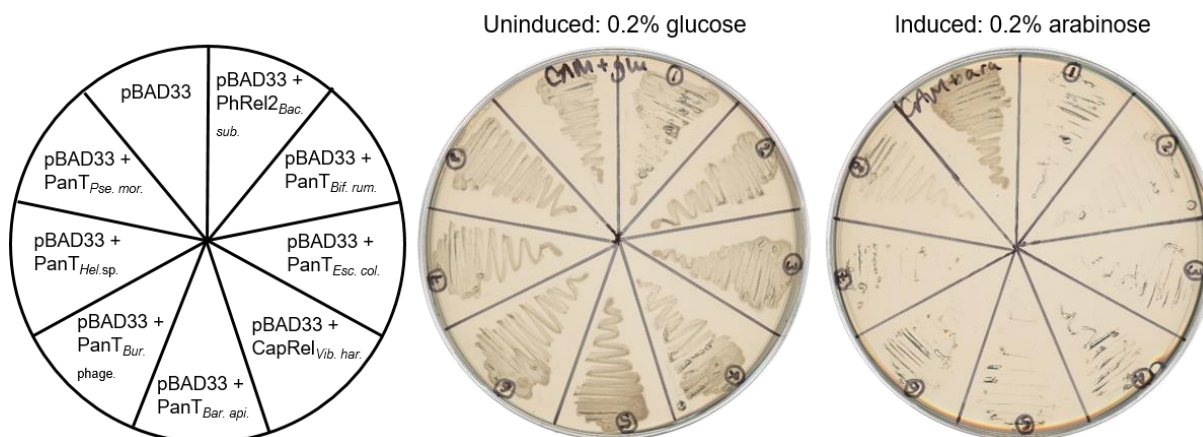
Figure 69: Induction of PanT toxins inhibits growth of *E. coli*. *E. coli* BW25113 was transformed with a pBAD33-based plasmid (either empty vector or L-arabinose inducible PanT expression plasmid) and transformants were streaked on uninducing (0.2% glucose) or inducing (0.2% arabinose) NA plates supplemented with 34 µg/ml chloramphenicol for plasmid maintenance. The plates were scored after an overnight incubation at 37 °C and no strains grew under inducing conditions.

6.2.3.2 – PanT toxin-induced membrane depolarisation and pore formation

It was observed that several PanT toxins caused an unspecific inhibition of transcription, translation and DNA replication, more representative of a general metabolic shutdown caused by targeting of the cytoplasmic membrane (Kurata *et al.*, 2022). To directly investigate this, we performed simultaneous DiSC$_3$(5) and Sytox Green fluorescence microscopy upon toxin induction. As shown in Fig. 70, PanT$_{Esc. col.}$, PanT$_{Bar. api.}$ and PanT$_{Hel. sp.}$ all act through membrane depolarisation which, in the case of PanT$_{Esc. col.}$ and PanT$_{Bar. api.}$, is caused by formation of large pores. Induction of PanT$_{Bif. rum.}$ and PanT$_{Pse. mor.}$ caused a weaker membrane depolarisation, and since these toxins are predicted to be RNases, it is more likely that this is due to an indirect effect on respiration or central carbon metabolism. Finally, no changes in membrane integrity were observed upon induction of PhRel2$_{Bac. sub.}$, CapRel$_{Vib. har.}$ and PanT$_{Bur. phage}$; and the latter two are proposed to predominantly target translation and transcription, respectively.

	phase	DiSC₃(5)	Sytox Green	phase	DiSC₃(5)	Sytox Green	predicted membrane	depolarising	pore forming
		uninduced			induced				
PhRel2$_{Bac. sub.}$									
CapRel$_{Vib. har.}$									
PanT$_{Bur. phage}$									
PanT$_{Bif. rum.}$									*	
PanT$_{Pse. mor.}$								*	
PanT$_{Esc. col.}$							✓	**	*
PanT$_{Bar. api.}$							✓	***	*
PanT$_{Hel. sp.}$							✓	***	
		untreated			Polymyxin B				
empty vector							✓	***	***
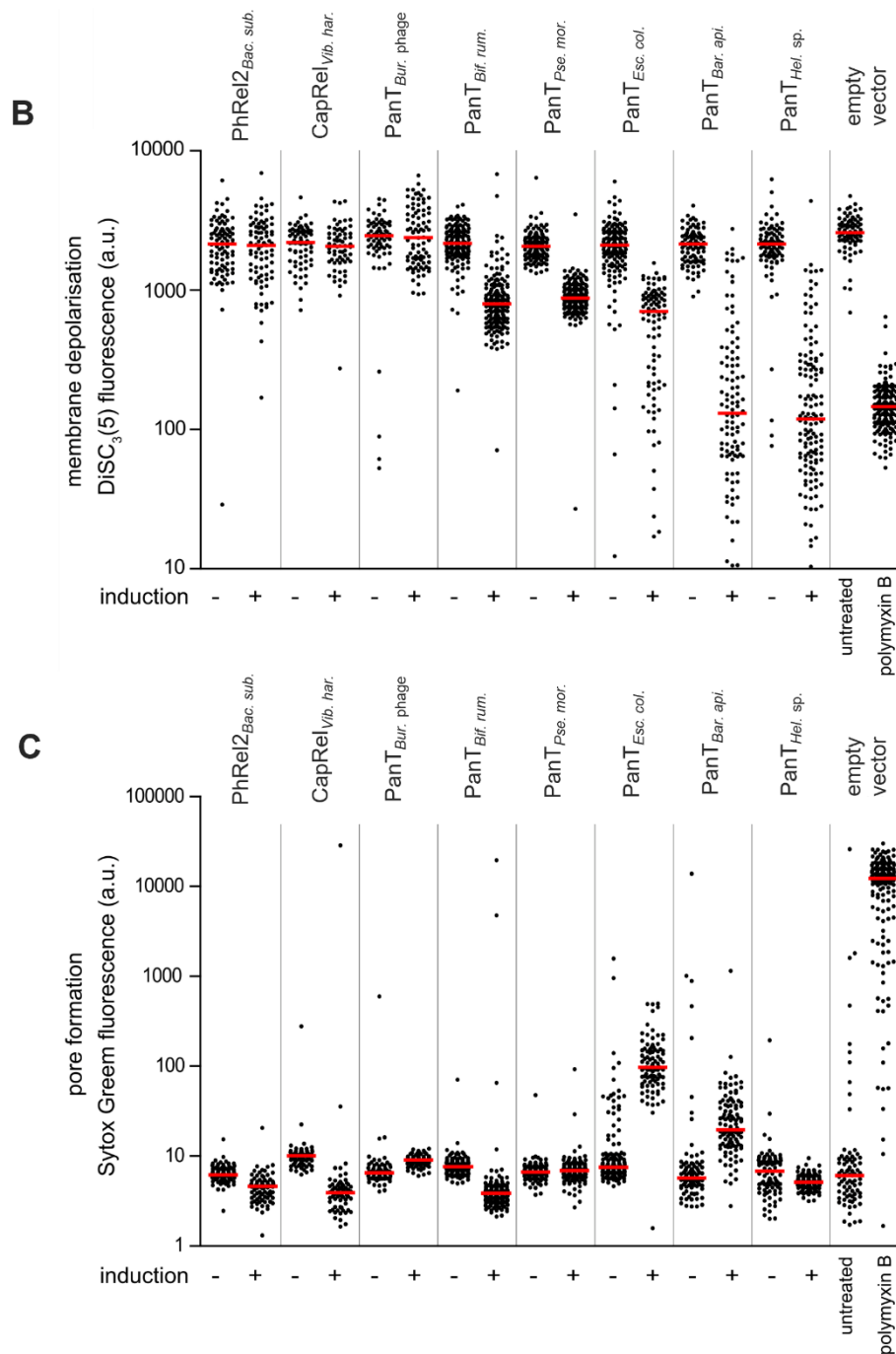
Figure 70: Cytoplasmic membrane integrity is a major target of PanT toxins. (A) Phase contrast and fluorescence microscopy images of *E. coli* BW25113 cells co-stained with 250 nM DiSC$_3$(5) and 200 nM Sytox Green, harbouring either an empty or PanT-expressing vector under uninducing (no arabinose) or inducing (30 min induction with 0.2% arabinose) conditions. As a positive control, the empty vector strain was treated with the membrane pore forming antibiotic polymyxin B (7 μM for 15 min). (B and C) Quantification of (B) DiSC$_3$(5) and (C) Sytox Green fluorescence for individual cells from the imaging dataset shown in panel A (n=92-65). Median fluorescence intensity is indicated with a red line. Strains used: *E. coli* AK001E (empty vector), JB021 (PhRel2$_{Bac. sub.}$), JB022 (PanT$_{Bif. rum.}$), JB023 (PanT$_{Esc. col.}$), JB024 (CapRel$_{Vib. har.}$), JB026 (PanT$_{Bar. api.}$), JB027 (PanT$_{Bur. phage}$), JB028 (PanT$_{Hel.sp.}$) and JB029 (PanT$_{Pse. mor.}$). Data was collected and analysed in collaboration with Henrik Strahl.

6.3 – Discussion

In this chapter, I have demonstrated that my previously optimised fluorescence-based techniques, including single-cell and fluorometric measurements, can be used to investigate the membrane disrupting properties of both antimicrobials and membrane-active proteins, such as bacterial and bacteriophage toxins. In particular, I have provided strong *in vivo* evidence that the membrane disruption induced by daptomycin is due to autolysis, and not membrane pore formation as has been shown in previous mode of action studies (Hover *et al.*, 2018; Seydlová *et al.*, 2018). This likely also explains why the fluorescence of permeability indicators, such as the nucleic acid stains Sytox Green and Propidium Iodide, demonstrates a gradual increase as it is dependent on degradation of the cell wall, and the subsequent release and staining of DNA. This is also in agreement with other studies, that only reported membrane depolarisation after the majority of the cell population had already lysed (Jung *et al.*, 2004; Hobbs *et al.*, 2008).

Furthermore, for the first time I have provided a method to directly link membrane potential levels and growth in *B. subtilis*, using the potassium ionophore valinomycin. The localisation of many membrane proteins, including MreB, FtsZ and SepF, is dependent on membrane potential (Strahl and Hamoen, 2010), and therefore important cellular processes such as cell wall synthesis and cell division. Using this technique, the membrane voltage could be set to predefined levels and the distribution of fluorescent protein fusions observed as a proxy for synthetic machineries. Moreover, I demonstrated using this calibration that growth inhibitory concentrations of daptomycin trigger only a partial depolarisation of the cytoplasmic membrane; however, this appears sufficient alone to explain the impairment of *B. subtilis* growth. Recent unpublished observations from our group have now also shown that antibiotics of other classes, including cell wall and protein synthesis inhibitors, may indirectly induce changes to membrane potential through inhibition of cell wall expansion or mistranslation of proteins and subsequent accumulation of intracellular biomass (unpublished data, Sandra Laborda Anadón). Therefore, similarly to daptomycin, we could use the calibrated DiSC$_3$(5) assay and its links to growth to determine whether membrane depolarisation caused by other antimicrobials would be growth inhibitory alone in *B. subtilis*.

Finally, I have shown that daptomycin likely exhibits a dual mode of action. Based on these experiments and those of others (Müller et al., 2016; Seistrup, 2018; Grein et al.,

2020), I propose that daptomycin demonstrates high potency against Gram-positive bacteria due to a combination of specific target binding and general membrane effects: i) formation of a tripartite complex of Ca2+-DAP with PG and undecaprenyl-coupled cell wall precursors leading to cell wall synthesis inhibition and ii) unspecific membrane binding resulting in loss of membrane potential and subsequent triggered autolysis (Fig. 71). This more general mode of action is also supported by previous evidence
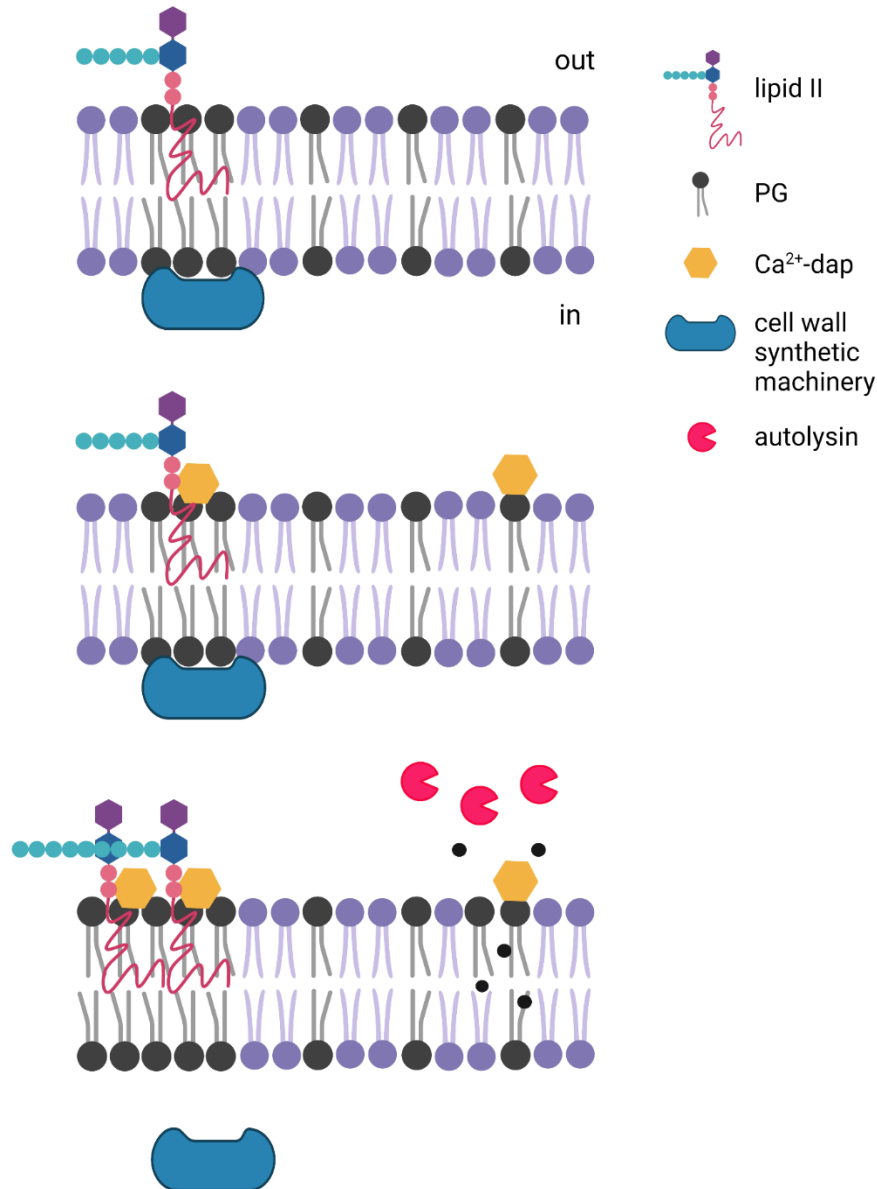
Figure 71: Proposed model of the dual mode of action of daptomycin. (Top panel) Peripheral membrane proteins associated with cell wall synthesis and the undecaprenyl-coupled peptidoglycan precursor lipid II localise to fluid microdomains under normal conditions. "In" and "out" represent the cytoplasmic and periplasmic faces of the membrane, respectively. (Middle panel) Calcium-daptomycin oligomers (Ca^{2+}-dap) either form a tripartite complex with phosphatidylglycerol (PG) and lipid II or bind directly to anionic phospholipids such as PG. (Bottom panel) Formation of these bulky complexes induces further clustering of fluid lipids and dissociation of the cell wall synthetic machinery. Meanwhile Ca^{2+}-dap also forms cation-selective channels independent of lipid II, depolarising the cytoplasmic and triggering autolysis.

that daptomycin is still active against cell wall-less *Mycoplasma orale* and *Mycoplasma arginine* (Tantibhedhyangkul *et al.*, 2019) and hypersensitive against *B. subtilis* L-forms (Wolf *et al.*, 2012). Here, we also demonstrated that in the absence of lipid II binding, daptomycin still induces depolarisation of the cytoplasmic membrane. We achieved this through two different methods: firstly, by use of a daptomycin variant, termed NF-DAP, that possesses three amino acid substitutions (O6K, mE12E and Kyn13W). As no fluid lipid clusters form upon incubation with this compound (as determined by staining with the membrane dye FM5-95), it can be assumed that these SNPs abolish daptomycin's interaction with lipid II. The other technique by which we abolished lipid II binding was by use of *B. subtilis* L-forms depleted for all undecaprenyl-coupled cell wall precursors. It would therefore be interesting to observe whether these cells also fail to form fluid lipid microdomains upon incubation with native daptomycin. This could be achieved with the probe DiIC12, which displays affinity for fluid membranes (Baumgart *et al.*, 2007), and a staining protocol of L-forms with which has already been set up by our group (unpublished data, Alan Koh). The lipid II-independent mechanism by which daptomycin induces membrane depolarisation is now consistent with previous *in vitro* studies, which have frequently been disputed as they do not resemble the biological membrane due to a lack of cell wall components. They show, in model bilayers, Ca^{2+}-dependent oligomerisation and association of daptomycin with anionic membrane phospholipids, such as PG, increases cation-selective conductivity (Muraih *et al.*, 2011; Zhang *et al.*, 2014; Zhang, Scoten and Straus, 2016). Zhang *et al.* (2016) argue that daptomycin-induced ion leakage is specific for K^+, however my data directly disputes this as daptomycin is still membrane-depolarising in conditions when the K^+-specific ionophore, valinomycin, is not (Fig. 54 and 55), implicating the role of other cations. Interestingly, one study by Taylor *et al.* (2017) also speculated that presence of the cell wall diminishes daptomycin's ability to permeabilise the membrane for sodium ions, which may underlie the partial depolarisation we observe *in vivo*.

Furthermore, when *B. subtilis* was incubated with NF-DAP, a strong increase in staining with the membrane dye FM5-95 was observed (Fig. 62A). This is most likely due to the changes in membrane permeability, caused by daptomycin's non-specific action, that consequently affect membrane dye binding or fluorescence, and not due to global effects on membrane fluidity, as NF-DAP caused no changes to Laurdan fluorescence (Fig. 58B). Nevertheless, a method to directly measure daptomycin-

induced changes in membrane fluidity would be of aid to this project. However, as documented in this thesis, the commonly used membrane fluidity fluorescent probe Laurdan cannot be implemented, as its intrinsic fluorescence directly overlaps with the spectral shift of Laurdan. Previously, our group also used Laurdan to analyse the local fluidity of daptomycin-lipid clusters (Müller *et al.*, 2016). They reported that these membrane areas exhibited a rigidification and predicted that it was due to restriction of lipid chain flexibility within these complexes. However, from data within this thesis, it is now more likely that the change in Laurdan signal was caused by accumulation of daptomycin's intrinsic fluorescence. They also stated that rigidity of these complexes may impair association of the cell wall synthetic machinery, but instead it can be speculated that daptomycin-Ca^{2+} oligomers just compete for binding with fluid lipids that are required for membrane association of such proteins (Fig. 71). An alternate technique to monitor membrane fluidity is another well-characterised probe 1,6-Diphenyl-1,3,5-hexatriene, or DPH. DPH differs from Laurdan, in that it is a rigid molecule that aligns itself parallel to the membrane fatty acids (Kaiser and London, 1998), and hence DPH polarisation is used as a direct measure of its rotational mobility within the membrane and therefore fluidity (Fox and Delohery, 1987). However, DPH is also not compatible for daptomycin mode of action studies, as it exhibits the same emission wavelengths as the antimicrobial (350 nm) and therefore polarisation measurements may be a combination of the rotational freedom of both DPH and membrane-bound daptomycin. Hence, only daptomycin-induced changes in fluid lipid domain organisation, as determined by DiIC12 staining and previously reported by our group (Müller *et al.*, 2016), are all that can currently be observed. The membrane dye Nile red has been shown to indicate changes in membrane fluidity (Kucherak *et al.*, 2010; Strahl, Bürmann and Hamoen, 2014; Malanovic *et al.*, 2022), but further work is required to fully establish this technique.

I also demonstrated that octenidine, a well-known synthetic antimicrobial molecule, induces changes to membrane potential, integrity and fluidity and formation of membrane invaginations in the model Gram-positive organism *B. subtilis*. Furthermore, it triggers lysis in *B. subtilis*, which is autolytic in nature, as shown by a full recovery upon depletion of the major autolytic enzymes, LytA-F. It is known that a number of compounds induce autolysis, including membrane-active antimicrobials, detergents and surfactants (Tsuchido *et al.*, 1990; Falk, Noah and Weisblum, 2010; Lacriola, Falk and Weisblum, 2013; Scheinpflug *et al.*, 2017). Although the precise mechanism by

which it occurs is not fully understood, it has frequently been linked to transmembrane potential (Jolliffe, Doyle and Streips, 1981; Penyige *et al*., 2002; Lamsa *et al.*, 2012; Seistrup, 2018), which is lost in the case of octenidine. I also observed membrane areas of very weak staining, which were determined to be part of the ongoing autolytic process, as they were abolished in the *ΔlytABCDEF* mutant. I speculate that these are associated with changes in the physical state of the membrane, forming distinct areas of high and low membrane fluidity, reminiscent of the lipid phase separation that has been previously observed (Scheinpflug *et al.*, 2017; Gohrbandt *et al.*, 2022). How membrane phase separation is linked to initiation of autolysis remains to be elucidated, but octendine could therefore provide a useful tool to investigate this process. Membrane fluidity probes, such as Laurdan and DPH (which were discussed above), could also be used to analyse changes in global membrane fluidity upon incubation with octenidine; however, similarly to Nile red staining, they could not be implemented to investigate the local fluidity of the distinct membrane regions observed due to the presence of invaginations and excess membrane material. Finally, I demonstrated that the action of octenidine is not dependent on binding to or clustering of any phospholipid or teichoic acid species. This non-specificity provides an explanation for octenidine's very broad spectrum of antimicrobial activity, even against both fungi and viruses, and identifying similar compounds may be of importance for hospital and community antisepsis, especially in a post-pandemic climate.

Chapter 7 – Concluding Remarks and Future Directions

The research within this thesis has focussed on optimising fluorescence-based techniques to monitor disturbances to membranes in both Gram-positive and Gram-negative model organisms, and using these to investigate the modes of action of natural products isolated as part of this project, clinically relevant antimicrobial compounds and membrane-active toxic proteins.

In Chapter 3, I described the development of an *in vivo* combined fluorometric screen in a 96-well plate format to simultaneously investigate membrane depolarisation and membrane pore formation in the Gram-positive model organism, *B. subtilis*. This assay was inspired by previous microscopic work from our group that demonstrated that cells could be co-stained with the voltage-sensitive and membrane-impermeable fluorescent dyes, DiSC$_3$(5) and Sytox Green (Kepplinger *et al.*, 2018), and establishment of the use of DiSC$_3$(5) in a plate reader-format in *B. subtilis* (te Winkel *et al.*, 2016). My results highlight the importance of vigorous shaking between measurements to maintain aeration of cells and that ideally such assays should be performed in growth media (as buffers can be detrimental to membrane potential); two key parameters that have been commonly overlooked in previous assay optimisation studies. Secondly, I investigated membrane depolarisation in the Gram-negative model organism *E. coli*; measurements of which are commonly more complex due to the presence of an additional outer membrane layer. Single-cell analysis of membrane potential using DiSC$_3$(5) is possible in *E. coli*; however, the dye exhibits initial increased accumulation within the cell upon conditions where the outer membrane is permeabilised. This confounding factor requires strong consideration when observing compounds or strains that have the potential to affect outer membrane integrity, or translating these experiments to organisms with different outer membrane compositions. Many studies commonly resuspend cells in various buffers prior to staining with voltage-sensitive dyes such as DiSC$_3$(5) (Wu *et al.*, 1999; Silvestro, Weiser and Axelsen, 2000; Morin *et al.*, 2011). I showed that, even in the presence of a carbon source and divalent cations to improve cell energisation and signal homogeneity respectively, cells begin to depolarise when washed and resuspended in the commonly-used buffer PBS. Similarly to *B. subtilis*, *E. coli* can also be successfully co-stained with DiSC$_3$(5) and Sytox Green, and outer membrane permeabilisation and inner membrane depolarisation can be followed fluorometrically using DiSC$_3$(5). This second body of work formed part of a first-author pre-print in conjunction with Dr Philipp

Popp from Prof Marc Erhardt's group at Humboldt-Universität zu Berlin (Buttress *et al.*, 2022). Unfortunately, it was not possible to fluorometrically detect membrane pore formation in *E. coli*, through use of either Sytox Green or another nucleic acid stain Propidium Iodide. An important next stage would be to translate these techniques and assays to species beyond model organisms. Due to potential differences in cell envelope composition and structure, this would require re-optimisation of both dye concentrations and cell densities, and verification microscopically with control compounds of known function prior to other mode of action or physiological studies.

The focus of Chapter 4 was using fluorescent probes to investigate outer membrane permeabilisation and efflux inhibition in the Gram-negative model organism, *E. coli*. I wished to establish a more direct, voltage-independent method to analyse outer membrane permeabilisation, after observing in the previous chapter that DiSC$_3$(5) is also sensitive to changes in its integrity. However, I quickly realised that lipophilic dyes, such as Nile red and NPN, appear to additionally reflect multidrug efflux, as demonstrated by staining upon addition to a *tolC*-deletion mutant. An alternate explanation was that membrane potential, outer membrane stability and multidrug efflux are all intrinsically interconnected, as depolarising compounds, such as the protonophore CCCP and the bacteriocin Colicin N, also affected fluorescence of both dyes. Certain links between these processes are well-known, for example that dissipation of the PMF will de-energise efflux pumps (Paulsen, Brown and Skurray, 1996; Lubelski, Konings and Driessen, 2007), however in this thesis, I have speculated connections between the others, postulating that dissipation of PMF disrupts cell envelope complexes involved in maintaining outer membrane asymmetry, or that outer membrane destabilisation may directly affect efflux OMP assembly or function. Future work would involve testing such assays with specific chemical efflux inhibitors and *E. coli* mutants deficient for components of these systems that span the inner and outer membrane, such as the Tol-Pal and Mla complexes. I also demonstrated that the small nucleic acid stain Hoechst 33342 seems to solely reflect multidrug efflux inhibition, as its fluorescence was not affected by outer membrane permeabilisation induced by polymyxin B nonapeptide. This may be because, due to its small and hydrophilic nature, it can enter the cells via porins, and thus its translocation of the outer membrane is not dependent on disruption of the outer membrane bilayer structure.

Chapter 5 focused on isolating membrane-active natural products from *Actinomycete* strains, which are a vast source of anti-infective compounds due to their large number

of secondary metabolite gene clusters in relation to their genome size. For this, I worked with the drug-screening SME, Demuris Ltd, and began by pre-screening a subset of strains for the production of cell wall- and cell membrane-targeting compounds using *B. subtilis* reporters. In the framework of this project, I produced crude aqueous and methanolic extracts from the strains that activated the *B. subtilis* membrane damage reporter when co-cultured. These are potentially a combination of several active compounds, highlighting the necessity of fractionation and purification for future work. Nevertheless, I performed preliminary mode of action analyses on these extracts, and most interestingly, identified four that acted similarly to calcium-dependent lipopeptides (Wood and Martin, 2019), three that caused membrane depolarisation through the formation of large pores, one that caused membrane potential- and MreB-independent fluid lipid domains and two that induced changes to localisation of the elongasome and consequently, cell morphology. Many also induced lysis of *B. subtilis* and future work could investigate whether this is due to misregulation of autolysins through use of strains deficient for the major autolytic enzymes. Fluorescence microscopy time courses could also be implemented to monitor the emergence of both fluid lipid domains and large membrane pores. This would further elucidate the time point of extract-induced membrane depolarisation, and whether it is linked to pore formation or is associated with a build-up of cytoplasmic biomass; a novel phenomenon recently identified by our group (unpublished data, Sandra Laborda Anadón). Another vital next stage would be to confirm that extract-induced Nile red foci are not a result of membrane invaginations, by investigating whether they co-localise with GFP-tagged AtpA, and using dual-colour SIM to observe changes to cytoplasmic GFP distribution (Malanovic *et al.*, 2022). If not, the local fluidity of these membrane areas could be more directly characterised using the membrane fluidity probes, Laurdan or DPH, as has been previously reported (Strahl, Bürmann and Hamoen, 2014). Finally, for extracts that induced changes to cell morphology, fluorescent protein-tagging could be used to identify which other components of the elongasome are recruited to these areas of "bulging", and whether depletion of any of these abolishes the phenotype. For example, the membrane protein RodZ is known to regulate MreB localisation and the insertion of cell wall material (Colavin, Shi and Huang, 2018). *B. subtilis* cells also depend on an intricate balance between elongasome activity, which reduces rod diameter, and class A PBPs, which increase it (Dion *et al.*, 2019); the tight regulation of which may have been perturbed in the case of these extracts. This could be tested by performing Total Internal Reflection

Fluorescence (TIRF) time lapse microscopy with tagged MreB and class A PBPs to follow their redirection. Finally, as NADA staining specifically shows active peptidoglycan synthesis, transmission electron microscopy (TEM) could be implemented to observe any changes to the peptidoglycan sacculus, including thickening or thinnening, or defects. If this project were to be continued, genomic techniques such as whole genome sequencing and antiSMASH should be employed to understand the phylogeny of the producer strains and uncover any predicted BGCs.

Finally, in Chapter 6, I implemented fluorescence techniques established within this thesis to further elucidate the modes of action of the commonly used but poorly characterised antimicrobials, daptomycin and octenidine, and membrane-active toxins derived from both bacteria and bacteriophages. The activity of daptomycin has been disputed for over three decades; in particular whether or not it forms large pores in the membrane of target cells (Zhang *et al.*, 2014; Müller *et al.*, 2016; Seydlová *et al.*, 2018). Recent preliminary data from our group also suggested that daptomycin induces membrane depolarisation-linked autolysis (Seistrup, 2018). In this work, I have indeed shown that daptomycin triggers autolysis in the absence of membrane pore formation, through the use of single-cell fluorescence microscopy and the autolysin deficient *B. subtilis* mutant strain. Thus, staining of DNA released during autolysis with permeability indicators may have been mistaken for pore formation in previous *in vivo* studies. I also developed a technique that allows well-controlled partial membrane depolarisation to be directly correlated with the ability of *B. subtilis* to grow, and utilising this, demonstrated that the partial depolarisation induced by growth inhibitory concentrations of daptomycin is sufficient alone to explain growth inhibition. This practice could prove useful to more directly determine which cellular processes are sensitive to reduced membrane potential, and at which levels membrane-associated proteins begin to delocalise, as has been shown previously (Strahl and Hamoen, 2010). I also concluded that Laurdan, a commonly used membrane fluidity probe, cannot be used in daptomycin mode of action studies as its emission wavelengths coincide with those of daptomycin's native fluorescence. It is therefore likely that previous reports from our group of daptomycin-induced membrane rigidification are incorrect; whilst its ability to interfere with fluid lipid domain organisation remains unaffected by this (Müller *et al.*, 2016). Moreover, I demonstrated that daptomycin-induced membrane depolarisation is not dependent on its recently identified interaction with lipid II (Grein *et al.*, 2020), and thus the antibiotic likely exhibits a dual mode of

action consisting of lipid II-independent membrane depolarisation, and inhibition of cell wall synthesis through its interaction with lipid II. Further work could involve investigating whether daptomycin still forms clusters with fluid lipids in L-forms depleted for undecaprenyl-coupled cell wall precursors, which our group is actively pursuing, and further elucidating the ions and phospholipids responsible for daptomycin-mediated membrane depolarisation in the absence of lipid II. Finally, I deciphered the membrane effects of octenidine, a commonly used antiseptic molecule, and toxins, demonstrating that these techniques can be implemented in mode of action studies of both antimicrobials and membrane-active proteins.

Lab Strain	DEM code	Lia induction	SigM induction	Extract	MIC (v/v)	Growth inhibitory (mid-log)	Lytic	Lia induction	SigM induction	Depolarisation	Permeabilisation	Lipid domain formation	Bulging	Oddities
ID5	DEM31724	Yes	Yes	MetOH	2 ul/200 ul	Yes	No	Yes	NT	No	No	NT	NT	NT
				H2O	>2 ul/200 ul	NT	NT	Yes	NT	NT	NT	NT	NT	NT
J95B	DEM110949	Yes	No	MetOH	>2 ul/200 ul	NT	NT	No	NT	NT	NT	NT	NT	NT
				H2O	>2 ul/200 ul	NT	NT	No	NT	NT	NT	NT	NT	NT
MEX-013	DEM30523	Yes	No	MetOH	>2 ul/200 ul	NT	NT	No	NT	NT	NT	NT	NT	NT
				H2O	2 ul/200 ul	Yes	Yes	No	NT	No	No	NT	NT	Larger zone of inhibition + Ca^{2+}
S93	DEM20819	Yes	No	MetOH	>2 ul/200 ul	NT	NT	No	NT	NT	NT	NT	NT	NT
				H2O	>2 ul/200 ul	NT	NT	No	NT	NT	NT	NT	NT	NT
571.5	DEM30680	Yes	No	MetOH	>2 ul/200 ul	NT	NT	No	NT	NT	NT	NT	NT	NT
				H2O	>2 ul/200 ul	NT	NT	No	NT	NT	NT	NT	NT	NT
Q286	DEM21415	Yes	No	MetOH	>2 ul/200 ul	NT	NT	No	NT	NT	NT	NT	NT	NT
				H2O	>2 ul/200 ul	NT	NT	No	NT	NT	NT	NT	NT	NT
S1P1	DEM20508	Yes	Yes	MetOH	0.5 ul/200 ul	Yes	Yes	Yes	NT	No	No	NT	NT	NT
				H2O	>2 ul/200 ul	NT	NT	Yes	NT	NT	NT	NT	NT	NT
SI1.40	DEM30667	Yes	No	MetOH	>2 ul/200 ul	NT	NT	No	NT	NT	NT	NT	NT	Larger zone of inhibition + Ca^{2+}
				H2O	>2 ul/200 ul	NT	NT	No	NT	NT	NT	NT	NT	NT
S2P2	DEM20252	Yes	Yes	MetOH	2 ul/200 ul	Yes	No	Yes	NT	No	No	NT	NT	NT
				H2O	>2 ul/200 ul	NT	NT	Yes	NT	NT	NT	NT	NT	NT
NERCl1-45	DEM30994	Yes	Yes	MetOH	0.25 ul/200 ul	Yes	Yes	No	Yes	No	No	No	Yes	Division-independent NADA foci
				H2O	2 ul/200 ul	Yes	Yes	No	Yes	No	No	No	Yes	Division-independent NADA foci
SI1.28a	DEM30665	Yes	Yes	MetOH	>2 ul/200 ul	NT	NT	No	NT	NT	NT	NT	NT	Induced Lia + Ca^{2+}
				H2O	>2 ul/200 ul	NT	NT	No	NT	NT	NT	NT	NT	NT
A11r1	DEM30336	Yes	No	MetOH	>2 ul/200 ul	NT	NT	No	NT	NT	NT	NT	NT	Larger zone of inhibition + Ca^{2+}
				H2O	>2 ul/200 ul	NT	NT	No	NT	NT	NT	NT	NT	NT
MU1466	DEM10314	Yes	No	MetOH	>2 ul/200 ul	NT	NT	No	NT	NT	NT	NT	NT	NT
				H2O	>2 ul/200 ul	NT	NT	No	NT	NT	NT	NT	NT	NT
ID10(2)	DEM31717	Yes	Yes	MetOH	2 ul/200 ul	No	No	Yes	NT	No	No	NT	NT	NT
				H2O	>2 ul/200 ul	NT	NT	Yes	NT	NT	NT	NT	NT	NT
USA 49012	DEM32126	Yes	No	MetOH	>2 ul/200 ul	NT	NT	Yes	NT	NT	NT	NT	NT	NT
				H2O	>2 ul/200 ul	NT	NT	Yes	NT	NT	NT	NT	NT	NT
STS 43	DEM31526	Yes	Yes	MetOH	>2 ul/200 ul	NT	NT	No	NT	NT	NT	NT	NT	NT
				H2O	>2 ul/200 ul	NT	NT	No	NT	NT	NT	NT	NT	NT
MU1452	DEM10412	Yes	No	MetOH	>2 ul/200 ul	NT	NT	No	NT	NT	NT	NT	NT	NT
				H2O	>2 ul/200 ul	NT	NT	No	NT	NT	NT	NT	NT	NT
S21	DEM20758	Yes	No	MetOH	>2 ul/200 ul	NT	NT	Yes	NT	NT	NT	NT	NT	NT
				H2O	>2 ul/200 ul	NT	NT	Yes	NT	NT	NT	NT	NT	NT
A126	DEM30018	Yes	No	MetOH	>2 ul/200 ul	NT	NT	No	NT	NT	NT	NT	NT	NT
				H2O	>2 ul/200 ul	NT	NT	No	NT	NT	NT	NT	NT	NT

Lab Strain	DEM code	Lia induction	SigM induction	Extract	MIC (v/v)	Growth inhibitory (mid-log)	Lytic	Lia induction	SigM induction	Depolarisation	Permeabilisation	Lipid domain formation	Bulging	Oddities
MU1456	DEM10315	Yes	No	MetOH	>2 ul/200 ul	NT	NT	No	NT	NT	NT	NT	NT	NT
				H2O	>2 ul/200 ul	NT	NT	No	NT	NT	NT	NT	NT	NT
MU1579(1)	DEM10360	Yes	Yes	MetOH	>2 ul/200 ul	NT	NT	No	NT	NT	NT	NT	NT	NT
				H2O	>2 ul/200 ul	NT	NT	No	NT	NT	NT	NT	NT	NT
MR572	DEM10474	Yes	Yes	MetOH	1 ul/200 ul	No	No	Yes	NT	No	No	NT	NT	NT
				H2O	>2 ul/200 ul	NT	NT	No	NT	NT	NT	NT	NT	NT
A328	DEM30062	Yes	No	MetOH	0.125 ul/200 ul	No	No	No	No	No	No	Yes	No	MreB-independent lipid domains
				H2O	1 ul/200 ul	No	No	No	NT	No	No	NT	NT	NT
JL39(A)	DEM21278	Yes	Yes	MetOH	2 ul/200 ul	No	No	Yes	NT	No	No	NT	NT	NT
				H2O	>2 ul/200 ul	NT	NT	Yes	NT	NT	NT	NT	NT	NT
STS 48	DEM31404	Yes	No	MetOH	>2 ul/200 ul	NT	NT	No	NT	NT	NT	NT	NT	NT
				H2O	>2 ul/200 ul	NT	NT	Yes	NT	NT	NT	NT	NT	NT
ID10	DEM31717	Yes	Yes	MetOH	2 ul/200 ul	Yes	Yes	Yes	Yes	Yes	Yes	Yes	No	MreB-independent lipid domains
				H2O	>2 ul/200 ul	NT	NT	Yes	NT	NT	NT	NT	NT	NT
JL264	DEM21231	Yes	Yes	MetOH	2 ul/200 ul	Yes	Yes	Yes	NT	No	No	NT	NT	NT
				H2O	>2 ul/200 ul	NT	NT	Yes	NT	NT	NT	NT	NT	NT
ID4	DEM31723	Yes	Yes	MetOH	>2 ul/200 ul	NT	NT	Yes	NT	NT	NT	NT	NT	NT
				H2O	>2 ul/200 ul	NT	NT	Yes	NT	NT	NT	NT	NT	NT
ID10(1)	DEM31717	Yes	Yes	MetOH	>2 ul/200 ul	NT	NT	Yes	NT	NT	NT	NT	NT	NT
				H2O	>2 ul/200 ul	NT	NT	Yes	NT	NT	NT	NT	NT	NT
B12	DEM10811	Yes	No	MetOH	>2 ul/200 ul	NT	NT	No	NT	NT	NT	NT	NT	NT
				H2O	>2 ul/200 ul	NT	NT	Yes	NT	NT	NT	NT	NT	NT
ID9	DEM31728	Yes	Yes	MetOH	1 ul/200 ul	Yes	Yes	Yes	NT	No	No	NT	NT	NT
				H2O	>2 ul/200 ul	NT	NT	Yes	NT	NT	NT	NT	NT	NT
JL173	DEM21277	Yes	Yes	MetOH	>2 ul/200 ul	NT	NT	Yes	NT	NT	NT	NT	NT	NT
				H2O	>2 ul/200 ul	NT	NT	Yes	NT	NT	NT	NT	NT	NT
ID8	DEM31717	Yes	Yes	MetOH	1 ul/200 ul	Yes	Yes	Yes	NT	No	No	NT	NT	NT
				H2O	>2 ul/200 ul	NT	NT	No	NT	NT	NT	NT	NT	NT
ID6	DEM31725	Yes	No	MetOH	>2 ul/200 ul	NT	NT	No	NT	NT	NT	NT	NT	NT
				H2O	>2 ul/200 ul	NT	NT	Yes	NT	NT	NT	NT	NT	NT
ID5	DEM31723	Yes	Yes	MetOH	>2 ul/200 ul	NT	NT	Yes	NT	NT	NT	NT	NT	Larger zone of inhibtion + Ca^{2+}
				H2O	>2 ul/200 ul	NT	NT	Yes	NT	NT	NT	NT	NT	NT
SB8	DEM30444	Yes	Yes	MetOH	0.125 ul/200 ul	Yes	Yes	Yes	NT	Yes	Yes	NT	NT	NT
				H2O	2 ul/200 ul	Yes	Yes	Yes	NT	No	No	NT	NT	NT
SB431	DEM30486	Yes	Yes	MetOH	0.5 ul/200 ul	Yes	Yes	No	NT	Yes	Yes	NT	NT	NT
				H2O	>2 ul/200 ul	NT	NT	Yes	NT	NT	NT	NT	NT	NT
B29	DEM10828	Yes	Yes	MetOH	>2 ul/200 ul	NT	NT	Yes	NT	NT	NT	NT	NT	NT
				H2O	>2 ul/200 ul	NT	NT	No	NT	NT	NT	NT	NT	NT

Appendix I: Summary tables of Demuris Ltd strains and their methanolic and aqueous extracts. Depicted is screening with both *B. subtilis* reporter strains (P*ypuA*-*lacZ* and P*lial*-*lacZ*), minimum inhibitory concentration (MIC) determination, growth experiments, membrane depolarisation and permeabilisation (tested both fluorometrically and microscopically), changes in lipid domain organisation and cell morphology and finally any other oddities. Strains used: *B. subtilis* 168 (wild type), *B. subtilis* YuPA (*ypuA'-lacZ*), *B. subtilis* YvQI (*lial-lacZ*), *B. subtilis* HS553 (*msfGFP-mreB*) and *B. subtilis* KS60V *(ΔmreB Δmbl ΔmreBH)*.

References

Abellón-Ruiz, J., Kaptan, S.S., Baslé, A., Claudi, B., Bumann, D., Kleinekathöfer, U. and Van Den Berg, B. (2017) 'Structural basis for maintenance of bacterial outer membrane lipid asymmetry', *Nature Microbiology*, 2(12), pp. 1616–1623.

Abhayawardhane, Y. and Stewart, G.C. (1995) 'Bacillus subtilis possesses a second determinant with extensive sequence similarity to the escherichia coli mreB morphogene', *Journal of Bacteriology*, 177(3), pp. 765–773.

Abraham, E.P. and Chain, E. (1940) 'An enzyme from bacteria able to destroy penicillin', *Nature*, p. 837.

Aguilar, P.S., Hernandez-Arriaga, A.M., Cybulski, L.E., Erazo, A.C. and De Mendoza, D. (2001) 'Molecular basis of thermosensing: A two-component signal transduction thermometer in bacillus subtilis', *EMBO Journal*, 20(7), pp. 1681–1691.

Al-Dabbagh, B., Mengin-Lecreulx, D. and Bouhss, A. (2008) 'Purification and characterization of the bacterial UDP-GlcNAc:Undecaprenyl- phosphate GlcNAc-1-phosphate transferase WecA', *Journal of Bacteriology*, 190(21), pp. 7141–7146.

Allen, N.E., Hobbs, J.N. and Alborn, W.E. (1987) 'Inhibition of peptidoglycan biosynthesis in gram-positive bacteria by LY146032', *Antimicrobial Agents and Chemotherapy*, 31(7), pp. 1093–1099.

Allison, S.E., D'Elia, M.A., Arar, S., Monteiro, M.A. and Brown, E.D. (2011) 'Studies of the genetics, function, and kinetic mechanism of TagE, the wall teichoic acid glycosyltransferase in Bacillus subtilis 168', *Journal of Biological Chemistry*, 286(27), pp. 23708–23716.

Alnaseri, H., Arsic, B., Schneider, J.E.T., Kaiser, J.C., Scinocca, Z.C., Heinrichs, D.E. and McGavin, M.J. (2015) 'Inducible expression of a resistance-nodulation-division-type efflux pump in Staphylococcus aureus provides resistance to linoleic and arachidonic acids', *Journal of Bacteriology*, 197(11), pp. 1893–1905.

Alvarez-Marin, R., Aires-de-Sousa, M., Nordmann, P., Kieffer, N. and Poirel, L. (2017) 'Antimicrobial activity of octenidine against multidrug-resistant Gram-negative pathogens', *European Journal of Clinical Microbiology and Infectious Diseases*, 36(12), pp. 2379–2383.

Anagnostopoulos, C. and Spizizen, J. (1960) 'REQUIREMENTS FOR

TRANSFORMATION IN BACILLUS SUBTILIS', *Journal of Bacteriology*, 81(5), pp. 741–746.

Anoushiravani, M., Falsafi, T. and Niknam, V. (2009) 'Proton motive force-dependent efflux of tetracycline in clinical isolates of Helicobacter pylori', *Journal of Medical Microbiology*, 58(10), pp. 1309–1313.

Antai, S.P. and Crawford, D.L. (1981) 'Degradation of Softwood, Hardwood, and Grass Lignocelluloses by Two Streptomyces Strains', *Applied and Environmental Microbiology*, 42(2), p. 378.

Apfel, C.M., Takács, B., Fountoulakis, M., Stieger, M. and Keck, W. (1999) 'Use of genomics to identify bacterial undecaprenyl pyrophosphate synthetase: Cloning, expression, and characterization of the essential uppS gene', *Journal of Bacteriology*, 181(2), pp. 483–492.

Appelt, C., Wessolowski, A., Dathe, M. and Schmieder, P. (2008) 'Structures of cyclic, antimicrobial peptides in a membrane-mimicking environment define requirements for activity', *Journal of Peptide Science*, 14(4), pp. 524–527.

Aretz, W., Meiwes, J., Seibert, G., Vobis, G. and Wink, J. (2000) 'Friulimicins: Novel lipopeptide antibiotics with peptidoglycan synthesis inhibiting activity from Actinoplanes friuliensis sp. nov. I. Taxonomic studies of the producing microorganism and fermentation', *Journal of Antibiotics*, 53(8), pp. 807–815.

Arouri, A., Dathe, M. and Blume, A. (2009) 'Peptide induced demixing in PG/PE lipid mixtures: A mechanism for the specificity of antimicrobial peptides towards bacterial membranes?', *Biochimica et Biophysica Acta (BBA) - Biomembranes*, 1788(3), pp. 650–659.

Assadian, O. (2016) 'Octenidine dihydrochloride: Chemical characteristics and antimicrobial properties', *Journal of Wound Care*, 25(3 Suppl), pp. S3-6.

Attwell, R.W. and Colwell, R.R. (1981) 'Actinomycetes in New York Harbour sediments and dredging spoil', *Marine Pollution Bulletin*, 12(10), pp. 351–353.

Azad, M.A.K., Finnin, B.A., Poudyal, A., Davis, K., Li, Jian, Li, Jinhua, Hill, P.A., Nation, R.L. and Velkov, T. (2013) 'Polymyxin B induces apoptosis in kidney proximal tubular cells', *Antimicrobial Agents and Chemotherapy*, 57(9), pp. 4329–4335.

Baba, T., Ara, T., Hasegawa, M., Takai, Y., Okumura, Y., Baba, M., Datsenko, K.A.,

Tomita, M., Wanner, B.L. and Mori, H. (2006) 'Construction of Escherichia coli K-12 in-frame, single-gene knockout mutants: The Keio collection', *Molecular Systems Biology*, 2.

Bach, J.N. and Bramkamp, M. (2013) 'Flotillins functionally organize the bacterial membrane', *Molecular Microbiology*, 88(6), pp. 1205–1217.

Ball, L.J., Goult, C.M., Donarski, J.A., Micklefield, J. and Ramesh, V. (2004) 'NMR structure determination and calcium binding effects of lipopeptide antibiotic daptomycin', *Organic and Biomolecular Chemistry*, 2(13), pp. 1872–1878.

Baltz, R.H., Miao, V. and Wrigley, S.K. (2005) 'Natural products to drugs: daptomycin and related lipopeptide antibiotics', *Natural Product Reports*, 22(6), pp. 717–741.

Band, V.I. and Weiss, D.S. (2015) 'Mechanisms of Antimicrobial Peptide Resistance in Gram-Negative Bacteria.', *Antibiotics (Basel, Switzerland)*, 4(1), pp. 18–41.

Barns, K.J. and Weisshaar, J.C. (2013) 'Real-time attack of LL-37 on single Bacillus subtilis cells', *Biochimica et Biophysica Acta - Biomembranes*, 1828(6), pp. 1511–1520.

Baumgart, T., Hunt, G., Farkas, E.R., Webb, W.W. and Feigenson, G.W. (2007) 'Fluorescence probe partitioning between Lo/Ld phases in lipid membranes', *Biochimica et Biophysica Acta - Biomembranes*, 1768(9), pp. 2182–2194.

Beall, B., Lowe, M. and Lutkenhaus, J. (1988) 'Cloning and characterization of Bacillus subtilis homologs of Escherichia coli cell division genes ftsZ and ftsA', *Journal of Bacteriology*, 170(10), pp. 4855–4864.

Belley, A., Neesham-Grenon, E., McKay, G., Arhin, F.F., Harris, R., Beveridge, T., Parr, T.R. and Moeck, G. (2009) 'Oritavancin kills stationary-phase and biofilm Staphylococcus aureus cells in vitro', *Antimicrobial Agents and Chemotherapy*, 53(3), pp. 918–925.

Bentley, S.D., Chater, K.F., Cerdeño-Tárraga, A.M., Challis, G.L., Thomson, N.R., James, K.D., Harris, D.E., Quail, M.A., Kieser, H., Harper, D., Bateman, A., Brown, S., Chandra, G., Chen, C.W., Collins, M., Cronin, A., Fraser, A., Goble, A., Hidalgo, J., Hornsby, T., Howarth, S., Huang, C.H., Kieser, T., Larke, L., Murphy, L., Oliver, K., O'Neil, S., Rabbinowitsch, E., Rajandream, M.A., Rutherford, K., Rutter, S., Seeger, K., Saunders, D., Sharp, S., Squares, R., Squares, S., Taylor, K., Warren,

T., Wietzorrek, A., Woodward, J., Barrell, B.G., Parkhill, J. and Hopwood, D.A. (2002) 'Complete genome sequence of the model actinomycete Streptomyces coelicolor A3(2)', *Nature*, 417(6885), pp. 141–147.

Van Den Berg Van Saparoea, H.B., Lubelski, J., Van Merkerk, R., Mazurkiewicz, P.S. and Driessen, A.J.M. (2005) 'Proton motive force-dependent Hoechst 33342 transport by the ABC transporter LmrA of Lactococcus lactis', *Biochemistry*, 44(51), pp. 16931–16938.

Bernhardt, T.G. and De Boer, P.A.J. (2005) 'SlmA, a nucleoid-associated, FtsZ binding protein required for blocking septal ring assembly over chromosomes in E. coli', *Molecular Cell*, 18(5), pp. 555–564.

Bertani, B. and Ruiz, N. (2018) 'Function and biogenesis of lipopolysaccharides', *EcoSal Plus*, 8(1).

Bhattacharyya, T., Sharma, A., Akhter, J. and Pathania, R. (2017) 'The small molecule IITR08027 restores the antibacterial activity of fluoroquinolones against multidrug-resistant Acinetobacter baumannii by efflux inhibition', *International Journal of Antimicrobial Agents*, 50(2), pp. 219–226.

Bhavsar, A.P., Truant, R. and Brown, E.D. (2005) 'The TagB protein in Bacillus subtilis 168 is an intracellular peripheral membrane protein that can incorporate glycerol phosphate onto a membrane-bound acceptor in vitro', *Journal of Biological Chemistry*, 280(44), pp. 36691–36700.

Bi, E. and Lutkenhaus, J. (1991) 'FtsZ ring structure associated with division in Escherichia coli', *Nature*, 354(6349), pp. 161–164.

Bibb, M.J. (2005) 'Regulation of secondary metabolism in streptomycetes', *Current Opinion in Microbiology*, 8(2), pp. 208–215.

Bishop, R.E. (2019) 'Phospholipid middle management', *Nature Microbiology*, 4(10), pp. 1608–1609.

Bisicchia, P., Noone, D., Lioliou, E., Howell, A., Quigley, S., Jensen, T., Jarmer, H. and Devine, K.M. (2007) 'The essential YycFG two-component system controls cell wall metabolism in Bacillus subtilis', *Molecular Microbiology*, 65(1), pp. 180–200.

Bisson-Filho, A.W., Hsu, Y.P., Squyres, G.R., Kuru, E., Wu, F., Jukes, C., Sun, Y., Dekker, C., Holden, S., VanNieuwenhze, M.S., Brun, Y. V. and Garner, E.C. (2017)

'Treadmilling by FtsZ filaments drives peptidoglycan synthesis and bacterial cell division', *Science*, 355(6326), pp. 739–743.

Blattner, F.R., Plunkett, G., Bloch, C.A., Perna, N.T., Burland, V., Riley, M., Collado-Vides, J., Glasner, J.D., Rode, C.K., Mayhew, G.F., Gregor, J., Davis, N.W., Kirkpatrick, H.A., Goeden, M.A., Rose, D.J., Mau, B. and Shao, Y. (1997) 'The complete genome sequence of Escherichia coli K-12', *Science*, pp. 1453–1462.

Bloch, K. (1963) 'The biological synthesis of unsaturated fatty acids.', *Biochemical Society Symposia*, 24, pp. 1–16.

Blondelle, S.E., Pérez-Payá, E. and Houghten, R.A. (1996) 'Synthetic combinatorial libraries: Novel discovery strategy for identification of antimicrobial agents', *Antimicrobial Agents and Chemotherapy*, pp. 1067–1071.

Boaretti, M., Canepari, P., Lleò, M.D.M. and Satta, G. (1993) 'The activity of daptomycin on enterococcus faecium protoplasts: Indirect evidence supporting a novel mode of action on lipoteichoic acid synthesis', *Journal of Antimicrobial Chemotherapy*, 31(2), pp. 227–235.

de Boer, P.A.J., Crossley, R.E. and Rothfield, L.I. (1989) 'A division inhibitor and a topological specificity factor coded for by the minicell locus determine proper placement of the division septum in E. coli', *Cell*, 56(4), pp. 641–649.

Bohnert, J.A., Karamian, B. and Nikaido, H. (2010) 'Optimized Nile red efflux assay of AcrAB-TolC multidrug efflux system shows competition between substrates', *Antimicrobial Agents and Chemotherapy*, 54(9), pp. 3770–3775.

Boix-Lemonche, G., Lekka, M. and Skerlavaj, B. (2020) 'A Rapid Fluorescence-Based Microplate Assay to Investigate the Interaction of Membrane Active Antimicrobial Peptides with Whole Gram-Positive Bacteria', *Antibiotics*, 9(2).

Booth, I.R. and Blount, P. (2012) 'The MscS and MscL families of mechanosensitive channels act as microbial emergency release valves', *Journal of Bacteriology*, pp. 4802–4809.

Bouhss, A., Trunkfield, A.E., Bugg, T.D.H. and Mengin-Lecreulx, D. (2008) 'The biosynthesis of peptidoglycan lipid-linked intermediates', *FEMS Microbiology Reviews*, 32(2), pp. 208–233.

Boylan, R.J., Mendelson, N.H., Brooks, D. and Young, F.E. (1972) 'Regulation of the

Bacterial Cell Wall: Analysis of a Mutant of Bacillus subtilis Defective in Biosynthesis of Teichoic Acid', *Journal of Bacteriology*, 110(1), pp. 281–290.

Breukink, E. and de Kruijff, B. (2006) 'Lipid II as a target for antibiotics', *Nature Reviews Drug Discovery*, 5(4), pp. 321–323.

Brown, D.A. (2002) 'Isolation and use of rafts.', *Current protocols in immunology / edited by John E. Coligan ... [et al.]*, Chapter 11(1), pp. 11.10.1-11.10.23.

Bruni, G.N. and Kralj, J.M. (2020) 'Membrane voltage dysregulation driven by metabolic dysfunction underlies bactericidal activity of aminoglycosides', *eLife*, 9, pp. 1–25.

Budiardjo, S.J., Stevens, J.J., Calkins, A.L., Ikujuni, A.P., Wimalasena, V.K., Firlar, E., Case, D.A., Biteen, J.S., Kaelber, J.T. and Slusky, J.S. (2022) 'Colicin E1 opens its hinge to plug TolC', *eLife*, 11.

Bull, A.T., Asenjo, J.A., Goodfellow, M. and Gómez-Silva, B. (2016) 'The Atacama Desert: Technical Resources and the Growing Importance of Novel Microbial Diversity', *Annual Review of Microbiology*, pp. 215–234.

Butler, E.K., Davis, R.M., Bari, V., Nicholson, P.A. and Ruiz, N. (2013) 'Structure-function analysis of MurJ reveals a solvent-exposed cavity containing residues essential for peptidoglycan biogenesis in Escherichia coli', *Journal of Bacteriology*, 195(20), pp. 4639–4649.

Buttress, J.A., Halte, M., te Winkel, J.D., Erhardt, M., Popp, P.F. and Strahl, H. (2022) 'A guide for membrane potential measurements in Gram-negative bacteria using voltage-sensitive dyes', *bioRxiv*, p. 2022.04.30.490130.

Cao, G., Zhong, C., Zong, G., Fu, J., Liu, Z., Zhang, G. and Qin, R. (2016) 'Complete Genome Sequence of Streptomyces clavuligerus F613-1, an Industrial Producer of Clavulanic Acid', *Genome announcements*, 4(5).

Cao, M., Wang, T., Ye, R. and Helmann, J.D. (2002) 'Antibiotics that inhibit cell wall biosynthesis induce expression of the Bacillus subtilisσW and σM regulons', *Molecular Microbiology*, 45(5), pp. 1267–1276.

Carballido-López, R., Formstone, A., Li, Y., Ehrlich, S.D., Noirot, P. and Errington, J. (2006) 'Actin Homolog MreBH Governs Cell Morphogenesis by Localization of the Cell Wall Hydrolase LytE', *Developmental Cell*, 11(3), pp. 399–409.

Cascales, E., Gavioli, M., Sturgis, J.N. and Lloubes, R. (2000) 'Proton motive force drives the interaction of the inner membrane TolA and outer membrane Pal proteins in Escherichia coli', *Molecular Microbiology*, 38(4), pp. 904–915.

Catucci, L., Depalo, N., Lattanzio, V.M.T., Agostiano, A. and Corcelli, A. (2004) 'Neosynthesis of Cardiolipin in Rhodobacter sphaeroides under Osmotic Stress', *Biochemistry*, 43(47), pp. 15066–15072.

Chen, R., Guttenplan, S.B., Blair, K.M. and Kearns, D.B. (2009) 'Role of the σD-Dependent Autolysins in Bacillus subtilis Population Heterogeneity', *Journal of Bacteriology*, 191(18), p. 5775.

Chong, Z.S., Woo, W.F. and Chng, S.S. (2015) 'Osmoporin OmpC forms a complex with MlaA to maintain outer membrane lipid asymmetry in Escherichia coli', *Molecular Microbiology*, 98(6), pp. 1133–1146.

Clementi, E.A., Marks, L.R., Roche-Håkansson, H. and Håkansson, A.P. (2014) 'Monitoring changes in membrane polarity, membrane integrity, and intracellular ion concentrations in Streptococcus pneumoniae using fluorescent dyes', *Journal of Visualized Experiments*, 84(84), p. e51008.

Colavin, A., Shi, H. and Huang, K.C. (2018) 'RodZ modulates geometric localization of the bacterial actin MreB to regulate cell shape', *Nature Communications*, 9(1).

Coldham, N.G., Webber, M., Woodward, M.J. and Piddock, L.J.V. (2010) 'A 96-well plate fluorescence assay for assessment of cellular permeability and active efflux in Salmonella enterica serovar Typhimurium and Escherichia coli', *Journal of Antimicrobial Chemotherapy*, 65(8), pp. 1655–1663.

Cole, R.M., Popkin, T.J., Boylan, R.J. and Mendelson, N.H. (1970) 'Ultrastructure of a Temperature-Sensitive Rod− Mutant of Bacillus subtilis', *Journal of Bacteriology*, 103(3), pp. 793–810.

Conceição, T., de Lencastre, H. and Aires-de-Sousa, M. (2016) 'Efficacy of octenidine against antibiotic-resistant Staphylococcus aureus epidemic clones', *Journal of Antimicrobial Chemotherapy*, 71(10), pp. 2991–2994.

D'Elia, M.A., Henderson, J.A., Beveridge, T.J., Heinrichs, D.E. and Brown, E.D. (2009) 'The N-acetylmannosamine transferase catalyzes the first committed step of teichoic acid assembly in Bacillus subtilis and Staphylococcus aureus', *Journal of*

Bacteriology, 191(12), pp. 4030–4034.

D'Elia, M.A., Millar, K.E., Beveridge, T.J. and Brown, E.D. (2006) 'Wall teichoic acid polymers are dispensable for cell viability in Bacillus subtilis', *Journal of Bacteriology*, 188(23), pp. 8313–8316.

Damper, P.D. and Epstein, W. (1981) 'Role of the membrane potential in bacterial resistance to aminoglycoside antibiotics', *Antimicrobial Agents and Chemotherapy*, 20(6), pp. 803–808.

Datsenko, K.A. and Wanner, B.L. (2000) 'One-step inactivation of chromosomal genes in Escherichia coli K-12 using PCR products', *Proceedings of the National Academy of Sciences of the United States of America*, 97(12), p. 6640.

Debarbouille, M., Gardan, R., Arnaud, M. and Rapoport, G. (1999) 'Role of bkdR, a transcriptional activator of the SigL-dependent isoleucine and valine degradation pathway in Bacillus subtilis', *Journal of Bacteriology*, 181(7), pp. 2059–2066.

Debono, M., Barnhart, M., Carrell, C.B., Hoffmann, J.A., Occolowitz, J.L., Abbott, B.J., Fukuda, D.S., Hamill, R.L., Biemann, K. and Herlihy, W.C. (1987) 'A21978C, a complex of new acidic peptide antibiotics: Isolation, chemistry, and mass spectral structure elucidation', *The Journal of Antibiotics*, 40(6), pp. 761–777.

Deckers-Hebestreit, G. and Altendorf, K. (1996) 'The F0F1-type ATP synthases of bacteria: Structure and function of the F0 complex', *Annual Review of Microbiology*, pp. 791–824.

Dempwolff, F., Reimold, C., Reth, M. and Graumann, P.L. (2011) 'Bacillus subtilis MreB orthologs self-organize into filamentous structures underneath the cell membrane in a heterologous cell system', *PloS one*, 6(11).

Dempwolff, F., Schmidt, F.K., Hervás, A.B., Stroh, A., Rösch, T.C., Riese, C.N., Dersch, S., Heimerl, T., Lucena, D., Hülsbusch, N., Stuermer, C.A.O., Takeshita, N., Fischer, R., Eckhardt, B. and Graumann, P.L. (2016) 'Super Resolution Fluorescence Microscopy and Tracking of Bacterial Flotillin (Reggie) Paralogs Provide Evidence for Defined-Sized Protein Microdomains within the Bacterial Membrane but Absence of Clusters Containing Detergent-Resistant Proteins', *PLoS Genetics*, 12(6), p. 1006116.

Dimick, K.P. (1951) 'The Hemolytic Action of Gramicidin and Tyrocidin', *Experimental*

Biology and Medicine, 78(3), pp. 782–784.

Dion, M.F., Kapoor, M., Sun, Y., Wilson, S., Ryan, J., Vigouroux, A., van Teeffelen, S., Oldenbourg, R. and Garner, E.C. (2019) 'Bacillus subtilis cell diameter is determined by the opposing actions of two distinct cell wall synthetic systems', *Nature Microbiology*, 4(8), pp. 1294–1305.

Domínguez-Cuevas, P., Porcelli, I., Daniel, R.A. and Errington, J. (2013) 'Differentiated roles for MreB-actin isologues and autolytic enzymes in Bacillus subtilis morphogenesis', *Molecular Microbiology*, 89(6), p. 1084.

Domínguez-Escobar, J., Chastanet, A., Crevenna, A.H., Fromion, V., Wedlich-Söldner, R. and Carballido-López, R. (2011) 'Processive movement of MreB-associated cell wall biosynthetic complexes in bacteria', *Science*, 333(6039), pp. 225–228.

Domínguez-Escobar, J., Wolf, D., Fritz, G., Höfler, C., Wedlich-Söldner, R. and Mascher, T. (2014) 'Subcellular localization, interactions and dynamics of the phage-shock protein-like Lia response in Bacillus subtilis', *Molecular Microbiology*, 92(4), pp. 716–732.

Donohue-Rolfe, A.M. and Schaechter, M. (1980) 'Translocation of phospholipids from the inner to the outer membrane of Escherichia coli', *Proceedings of the National Academy of Sciences of the United States of America*, 77(4 I), pp. 1867–1871.

Donovan, C. and Bramkamp, M. (2009) 'Characterization and subcellular localization of a bacterial flotillin homologue', *Microbiology*, 155(6), pp. 1786–1799.

Dramsi, S., Magnet, S., Davison, S. and Arthur, M. (2008) 'Covalent attachment of proteins to peptidoglycan', *FEMS Microbiology Reviews*, 32(2), pp. 307–320.

Draper, L.A., Cotter, P.D., Hill, C. and Ross, R.P. (2015) 'Lantibiotic Resistance', *Microbiology and Molecular Biology Reviews : MMBR*, 79(2), p. 171.

Du, D., Wang-Kan, X., Neuberger, A., van Veen, H.W., Pos, K.M., Piddock, L.J.V. and Luisi, B.F. (2018) 'Multidrug efflux pumps: structure, function and regulation', *Nature Reviews Microbiology*, pp. 523–539.

Egan, A.J.F. (2018) 'Bacterial outer membrane constriction', *Molecular Microbiology*, pp. 676–687.

Eiamphungporn, W. and Helmann, J.D. (2008) 'The Bacillus subtilis sigma(M)

regulon and its contribution to cell envelope stress responses', *Molecular microbiology*, 67(4), pp. 830–848.

Ekiert, D.C., Bhabha, G., Isom, G.L., Greenan, G., Ovchinnikov, S., Henderson, I.R., Cox, J.S. and Vale, R.D. (2017) 'Architectures of Lipid Transport Systems for the Bacterial Outer Membrane', *Cell*, 169(2), pp. 273-285.e17.

Eldridge, G.R., Vervoort, H.C., Lee, C.M., Cremin, P.A., Williams, C.T., Hart, S.M., Goering, M.G., O'Neil-Johnson, M. and Zeng, L. (2002) 'High-throughput method for the production and analysis of large natural product libraries for drug discovery', *Analytical Chemistry*, 74(16), pp. 3963–3971.

Eliopoulos, G.M., Willey, S., Reiszner, E., Spitzer, P.G., Caputo, G. and Moellering, R.C. (1986) 'In vitro and in vivo activity of LY 146032, a new cyclic lipopeptide antibiotic', *Antimicrobial Agents and Chemotherapy*, 30(4), pp. 532–535.

Emami, K., Guyet, A., Kawai, Y., Devi, J., Wu, L.J., Allenby, N., Daniel, R.A. and Errington, J. (2017) 'RodA as the missing glycosyltransferase in Bacillus subtilis and antibiotic discovery for the peptidoglycan polymerase pathway', *Nature Microbiology*, 2.

van den Ent, F., Izoré, T., Bharat, T.A., Johnson, C.M. and Löwe, J. (2014) 'Bacterial actin MreB forms antiparallel double filaments.', *eLife*, 3, p. e02634.

Epand, R.F., Savage, P.B. and Epand, R.M. (2007) 'Bacterial lipid composition and the antimicrobial efficacy of cationic steroid compounds (Ceragenins)', *Biochimica et Biophysica Acta - Biomembranes*, 1768(10), pp. 2500–2509.

Epand, R.M., Walker, C., Epand, R.F. and Magarvey, N.A. (2016) 'Molecular mechanisms of membrane targeting antibiotics', *Biochimica et Biophysica Acta (BBA) - Biomembranes*, 1858(5), pp. 980–987.

Erikson, D. (1941) 'Studies on Some Lake-Mud Strains of Micromonospora', *Journal of Bacteriology*, 41(3), pp. 277–300.

Ernst, R., Ejsing, C.S. and Antonny, B. (2016) 'Homeoviscous Adaptation and the Regulation of Membrane Lipids', *Journal of Molecular Biology*, 428(24), pp. 4776–4791.

Espéli, O., Borne, R., Dupaigne, P., Thiel, A., Gigant, E., Mercier, R. and Boccard, F. (2012) 'A MatP–divisome interaction coordinates chromosome segregation with cell

division in E. coli', *The EMBO Journal*, 31(14), p. 3198.

Eylar, E.H., Madoff, M.A., Brody, O. V. and Oncley, J.L. (1962) 'The contribution of sialic acid to the surface charge of the erythrocyte.', *The Journal of biological chemistry*, 237(6), pp. 1992–2000.

Falk, S.P., Noah, J.W. and Weisblum, B. (2010) 'Screen for inducers of autolysis in Bacillus subtilis', *Antimicrobial Agents and Chemotherapy*, 54(9), pp. 3723–3729.

Favini-Stabile, S., Contreras-Martel, C., Thielens, N. and Dessen, A. (2013) 'MreB and MurG as scaffolds for the cytoplasmic steps of peptidoglycan biosynthesis', *Environmental Microbiology*, 15(12), pp. 3218–3228.

Feile, H., Porter, J.S., Slayman, C.L. and Kaback, H.R. (1980) 'Quantitative Measurements of Membrane Potential in Escherichia Coli', *Biochemistry*, 19(15), pp. 3585–3590.

Feng, X., Hu, Y., Zheng, Y., Zhu, W., Li, K., Huang, C.H., Ko, T.P., Ren, F., Chan, H.C., Nega, M., Bogue, S., López, D., Kolter, R., Götz, F., Guo, R.T. and Oldfield, E. (2014) 'Structural and Functional Analysis of Bacillus subtilis YisP Reveal a Role of its Product in Biofilm Production', *Chemistry & biology*, 21(11), p. 1557.

Finger, S., Kerth, A., Dathe, M. and Blume, A. (2015) 'The efficacy of trivalent cyclic hexapeptides to induce lipid clustering in PG/PE membranes correlates with their antimicrobial activity', *Biochimica et Biophysica Acta (BBA) - Biomembranes*, 1848(11), pp. 2998–3006.

Fischer, H.P., Brunner, N.A., Wieland, B., Paquette, J., Macko, L., Ziegelbauer, K. and Freiberg, C. (2004) 'Identification of antibiotic stress-inducible promoters: A systematic approach to novel pathway-specific reporter assays for antibacterial drug discovery', *Genome Research*, 14(1), pp. 90–98.

Flärdh, K. (2010) 'Cell polarity and the control of apical growth in Streptomyces', *Current Opinion in Microbiology*, 13(6), pp. 758–765.

Fluhler, E., Burnham, V.G. and Loew, L.M. (1985) 'Spectra, Membrane Binding, and Potentiometric Reponses of New Charge Shift Probes', *Biochemistry*, 24(21), pp. 5749–5755.

Formstone, A. and Errington, J. (2005) 'A magnesium-dependent mreB null mutant: implications for the role of mreB in Bacillus subtilis', *Molecular Microbiology*, 55(6),

pp. 1646–1657.

Fox, M.H. and Delohery, T.M. (1987) 'Membrane fluidity measured by fluorescence polarization using an EPICS V cell sorter', *Cytometry*, 8(1), pp. 20–25.

French, S., Farha, M., Ellis, M.J., Sameer, Z., Côté, J.P., Cotroneo, N., Lister, T., Rubio, A. and Brown, E.D. (2020) 'Potentiation of Antibiotics against Gram-Negative Bacteria by Polymyxin B Analogue SPR741 from Unique Perturbation of the Outer Membrane', *ACS Infectious Diseases*, 6(6), pp. 1405–1412.

Fujisawa, M., Kusumoto, A., Wada, Y., Tsuchiya, T. and Ito, M. (2005) 'NhaK, a novel monovalent cation/H+ antiporter of Bacillus subtilis', *Archives of microbiology*, 183(6), pp. 411–420.

Fujisawa, M., Wada, Y., Tsuchiya, T. and Ito, M. (2009) 'Characterization of Bacillus subtilis YfkE (ChaA): a calcium-specific Ca2+/H+ antiporter of the CaCA family', *Archives of microbiology*, 191(8), pp. 649–657.

Fukushima, T., Afkham, A., Kurosawa, S.I., Tanabe, T., Yamamoto, H. and Sekiguchi, J. (2006) 'A new D,L-endopeptidase gene product, YojL (renamed CwlS), plays a role in cell separation with LytE and LytF in Bacillus subtilis', *Journal of bacteriology*, 188(15), pp. 5541–5550.

Gamba, P., Veening, J.W., Saunders, N.J., Hamoen, L.W. and Daniel, R.A. (2009) 'Two-step assembly dynamics of the Bacillus subtilis divisome', *Journal of Bacteriology*, 191(13), pp. 4186–4194.

Ganchev, D.N., Hasper, H.E., Breukink, E. and de Kruijff, B. (2006) 'Size and Orientation of the Lipid II Headgroup As Revealed by AFM Imaging', *Biochemistry*, 45(19), pp. 6195–6202.

Garner, E.C., Bernard, R., Wang, W., Zhuang, X., Rudner, D.Z. and Mitchison, T. (2011) 'Coupled, circumferential motions of the cell wall synthesis machinery and MreB filaments in B. subtilis', *Science*, 333(6039), pp. 222–225.

Garwin, J.L., Klages, A.L. and Cronan, J.E. (1980) 'Beta-ketoacyl-acyl carrier protein synthase II of Escherichia coli. Evidence for function in the thermal regulation of fatty acid synthesis.', *Journal of Biological Chemistry*, 255(8), pp. 3263–3265.

El Ghachi, M., Bouhss, A., Blanot, D. and Mengin-Lecreulx, D. (2004) 'The bacA Gene of Escherichia coli Encodes an Undecaprenyl Pyrophosphate Phosphatase

Activity', *Journal of Biological Chemistry*, 279(29), pp. 30106–30113.

Gohrbandt, M., Lipski, A., Grimshaw, J.W., Buttress, J.A., Baig, Z., Herkenhoff, B., Walter, S., Kurre, R., Deckers-Hebestreit, G. and Strahl, H. (2022) 'Low membrane fluidity triggers lipid phase separation and protein segregation in living bacteria', *The EMBO Journal*, 41(5), p. e109800.

Gomes, R.C., Semêdo, L.T.A.S., Soares, R.M.A., Alviano, C.S., Linhares, L.F. and Coelho, R.R.R. (2000) 'Chitinolytic activity of actinomycetes from a cerrado soil and their potential in biocontrol', *Letters in applied microbiology*, 30(2), pp. 146–150.

Goodfellow, M. and Haynes, J.A. (1984) 'ACTINOMYCETES IN MARINE SEDIMENTS', in *Biological, Biochemical, and Biomedical Aspects of Actinomycetes*, pp. 453–472.

Goodfellow, M. and Williams, S.T. (1983) 'Ecology of actinomycetes.', *Annual review of microbiology*, pp. 189–216.

Greenspan, P. and Fowler, S.D. (1985) 'Spectrofluorometric studies of the lipid probe, nile red.', *Journal of lipid research*, 26(7), pp. 781–9.

Grein, F., Müller, A., Scherer, K.M., Liu, X., Ludwig, K.C., Klöckner, A., Strach, M., Sahl, H.G., Kubitscheck, U. and Schneider, T. (2020) 'Ca2+-Daptomycin targets cell wall biosynthesis by forming a tripartite complex with undecaprenyl-coupled intermediates and membrane lipids', *Nature Communications*, 11(1), pp. 1–11.

Gruszecki, W.I. and Strzałka, K. (2005) 'Carotenoids as modulators of lipid membrane physical properties', *Biochimica et Biophysica Acta (BBA) - Molecular Basis of Disease*, 1740(2), pp. 108–115.

Guzman, L.M., Belin, D., Carson, M.J. and Beckwith, J. (1995) 'Tight regulation, modulation, and high-level expression by vectors containing the arabinose P(BAD) promoter', *Journal of Bacteriology*, 177(14), pp. 4121–4130.

Hachmann, A.B., Sevim, E., Gaballa, A., Popham, D.L., Antelmann, H. and Helmann, J.D. (2011) 'Reduction in membrane phosphatidylglycerol content leads to daptomycin resistance in Bacillus subtilis', *Antimicrobial Agents and Chemotherapy*, 55(9), pp. 4326–4337.

Haest, C.W.M., De Gier, J., Op Den Kamp, J.A.F., Bartels, P. and Van Deenen, L.L.M. (1972) 'Changes in permeability of Staphylococcus aureus and derived

liposomes with varying lipid composition', *BBA - Biomembranes*, 255(3), pp. 720–733.

Haeusser, D.P., Garza, A.C., Buscher, A.Z. and Levin, P.A. (2007) 'The Division Inhibitor EzrA Contains a Seven-Residue Patch Required for Maintaining the Dynamic Nature of the Medial FtsZ Ring', *Journal of Bacteriology*, 189(24), p. 9001.

Hajduk, I. V., Mann, R., Rodrigues, C.D.A. and Harry, E.J. (2019) 'The ParB homologs, Spo0J and Noc, together prevent premature midcell Z ring assembly when the early stages of replication are blocked in Bacillus subtilis', *Molecular Microbiology*, 112(3), p. 766.

Hamedi, J., Poorinmohammad, N. and Papiran, R. (2017) 'Growth and life cycle of actinobacteria', in *Biology and Biotechnology of Actinobacteria*, pp. 29–50.

Harder, K.J., Nikaido, H. and Matsuhashi, M. (1981) 'Mutants of Escherichia coli that are resistant to certain beta-lactam compounds lack the ompF porin', *Antimicrobial agents and chemotherapy*, 20(4), pp. 549–552.

Hashimoto, M., Ooiwa, S. and Sekiguchi, J. (2012) 'Synthetic lethality of the lytE cwlO genotype in Bacillus subtilis is caused by lack of D, L-endopeptidase activity at the lateral cell wall', *Journal of Bacteriology*, 194(4), pp. 796–803.

Heckels, J.E., Lambert, P.A. and Baddiley, J. (1977) 'Binding of magnesium ions to cell walls of Bacillus subtilis W23 containing teichoic acid or teichuronic acid', *The Biochemical journal*, 162(2), pp. 359–365.

Helander, I.M. and Mattila-Sandholm, T. (2000) 'Fluorometric assessment of Gram-negative bacterial permeabilization', *Journal of Applied Microbiology*, 88(2), pp. 213–219.

Helmann, J.D. (2002) 'The extracytoplasmic function (ECF) sigma factors', *Advances in Microbial Physiology*, pp. 47–110.

Helmann, J.D. and Moran, C.P. (2014) 'RNA Polymerase and Sigma Factors', in *Bacillus subtilis and Its Closest Relatives*. John Wiley & Sons, Ltd, pp. 287–312.

Helmke, E. (1981) 'Growth of actinomycetes from marine and terrestrial origin under increased hydrostatic pressure.', *Zentralbl. Bakteriol. Suppl.*, 11, pp. 321–327.

Henzler Wildman, K.A., Lee, D.K. and Ramamoorthy, A. (2003) 'Mechanism of lipid bilayer disruption by the human antimicrobial peptide, LL-37', *Biochemistry*, 42(21),

pp. 6545–6558.

Herbold, D.R. and Glaser, L. (1975) 'Bacillus subtilis N-acetylmuramic acid L-alanine amidase.', *Journal of Biological Chemistry*, 250(5), pp. 1676–1682.

Van Der Heul, H.U., Bilyk, B.L., McDowall, K.J., Seipke, R.F. and Van Wezel, G.P. (2018) 'Regulation of antibiotic production in Actinobacteria: new perspectives from the post-genomic era', *Natural Product Reports*, 35(6), pp. 575–604.

Higashi, Y., Strominger, J.L. and Sweeley, C.C. (1967) 'Structure of a lipid intermediate in cell wall peptidoglycan synthesis: a derivative of a C55 isoprenoid alcohol.', *Proceedings of the National Academy of Sciences of the United States of America*, 57(6), pp. 1878–1884.

Hirota, Y., Ryter, A. and Jacob, F. (1968) 'Thermosensitive mutants of E. coli affected in the processes of DNA synthesis and cellular division.', *Cold Spring Harbor symposia on quantitative biology*, 33, pp. 677–693.

Hladky, S.B. and Haydon, D.A. (1972) 'Ion transfer across lipid membranes in the presence of gramicidin A. I. Studies of the unit conductance channel', *BBA - Biomembranes*, 274(2), pp. 294–312.

Hobbs, J.K., Miller, K., O'Neill, A.J. and Chopra, I. (2008) 'Consequences of daptomycin-mediated membrane damage in Staphylococcus aureus', *Journal of Antimicrobial Chemotherapy*, 62(5), pp. 1003–1008.

Höltje, J.-V. (1998) 'Growth of the stress-bearing and shape-maintaining murein sacculus of Escherichia coli', *Microbiology and molecular biology reviews : MMBR*, 62(1), pp. 181–203.

Horsburgh, M.J. and Moir, A. (1999) 'σM, an ECF RNA polymerase sigma factor of Bacillus subtilis 168, is essential for growth and survival in high concentrations of salt', *Molecular Microbiology*, 32(1), pp. 41–50.

Hosoi, S., Mochizuki, N., Hayashi, S. and Kasai, M. (1980) 'Control of membrane potential by external H+ concentration in Bacillus subtilis as determined by an ion-selective electrode', *Biochimica et Biophysica Acta (BBA) - Biomembranes*, 600(3), pp. 844–852.

Hover, B.M., Kim, S.H., Katz, M., Charlop-Powers, Z., Owen, J.G., Ternei, M.A., Maniko, J., Estrela, A.B., Molina, H., Park, S., Perlin, D.S. and Brady, S.F. (2018)

'Culture-independent discovery of the malacidins as calcium-dependent antibiotics with activity against multidrug-resistant Gram-positive pathogens', *Nature Microbiology*, 3(4), pp. 415–422.

Huber, F.M., Pieper, R.L. and Tietz, A.J. (1988) 'The formation of daptomycin by supplying decanoic acid to Streptomyces roseosporus cultures producing the antibiotic complex A21978C', *Journal of Biotechnology*, 7(4), pp. 283–292.

Hübner, N.O., Siebert, J. and Kramer, A. (2010) 'Octenidine Dihydrochloride, a Modern Antiseptic for Skin, Mucous Membranes and Wounds', *Skin Pharmacology and Physiology*, 23(5), pp. 244–258.

Hughes, G.W., Hall, S.C.L., Laxton, C.S., Sridhar, P., Mahadi, A.H., Hatton, C., Piggot, T.J., Wotherspoon, P.J., Leney, A.C., Ward, D.G., Jamshad, M., Spana, V., Cadby, I.T., Harding, C., Isom, G.L., Bryant, J.A., Parr, R.J., Yakub, Y., Jeeves, M., Huber, D., Henderson, I.R., Clifton, L.A., Lovering, A.L. and Knowles, T.J. (2019) 'Evidence for phospholipid export from the bacterial inner membrane by the Mla ABC transport system', *Nature Microbiology*, 4(10), pp. 1692–1705.

Hussain, S., Wivagg, C.N., Szwedziak, P., Wong, F., Schaefer, K., Izoré, T., Renner, L.D., Holmes, M.J., Sun, Y., Bisson-Filho, A.W., Walker, S., Amir, A., Löwe, J. and Garner, E.C. (2018) 'Mreb filaments align along greatest principal membrane curvature to orient cell wall synthesis', *eLife*, 7.

Imada, C., Sakata, K., Terahara, T. and Kobayashi, T. (2014) 'Isolation of alginate lyase-producing actinomycetes from the marine environment and purification of lyase', *Nippon Suisan Gakkaishi (Japanese Edition)*, 80(3), pp. 371–378.

Infectious Diseases Society of America (IDSA) (2011) 'Combating Antimicrobial Resistance: Policy Recommendations to Save Lives', *Clinical Infectious Diseases*, 52, pp. S397–S428.

Iwasaki, H., Shimada, A. and Ito, E. (1986) 'Comparative studies of lipoteichoic acids from several Bacillus strains', *Journal of Bacteriology*, 167(2), pp. 508–516.

Iwasaki, H., Shimada, A., Yokoyama, K. and Ito, E. (1989) 'Structure and glycosylation of lipoteichoic acids in Bacillus strains', *Journal of Bacteriology*, 171(1), pp. 424–429.

Jaffe, A., Chabbert, Y.A. and Semonin, O. (1982) 'Role of porin proteins OmpF and

OmpC in the permeation of beta-lactams', *Antimicrobial agents and chemotherapy*, 22(6), pp. 942–948.

Jan, K.M. and Chien, S. (1973) 'Role of Surface Electric Charge in Red Blood Cell Interactions', *Journal of General Physiology*, 61(5), pp. 638–654.

Janas, T., Chojnacki, T., Swiezewska, E. and Janas, T. (1994) 'The effect of undecaprenol on bilayer lipid membranes.', *Acta biochimica Polonica*, 41(3), pp. 351–8.

Jansen, K.B., Inns, P.G., Housden, N.G., Hopper, J.T.S., Kaminska, R., Lee, S., Robinson, C. V., Bayley, H. and Kleanthous, C. (2020) 'Bifurcated binding of the OmpF receptor underpins import of the bacteriocin colicin N into Escherichia coli', *Journal of Biological Chemistry*, 295(27), pp. 9147–9156.

Jay, A.G. and Hamilton, J.A. (2017) 'Disorder Amidst Membrane Order: Standardizing Laurdan Generalized Polarization and Membrane Fluidity Terms', *Journal of Fluorescence*, 27(1), pp. 243–249.

Jeans, E., Holleyman, R., Tate, D., Reed, M. and Malviya, A. (2018) 'Methicillin sensitive staphylococcus aureus screening and decolonisation in elective hip and knee arthroplasty', *Journal of Infection*, 77(5), pp. 405–409.

Jimmy, S., Saha, C.K., Kurata, T., Stavropoulos, C., Oliveira, S.R.A., Koh, A., Cepauskas, A., Takada, H., Rejman, D., Tenson, T., Strahl, H., Garcia-Pino, A., Hauryliuk, V. and Atkinson, G.C. (2020) 'A widespread toxin−antitoxin system exploiting growth control via alarmone signaling', *Proceedings of the National Academy of Sciences of the United States of America*, 117(19), pp. 10500–10510.

Johnson, A.S., van Horck, S. and Lewis, P.J. (2004) 'Dynamic localization of membrane proteins in Bacillus subtilis', *Microbiology*, 150(9), pp. 2815–2824.

Johnston, D.W. and Cross, T. (1976) 'Actinomycetes in lake muds: dormant spores or metabolically active mycelium?', *Freshwater Biology*, 6(5), pp. 465–470.

Jolliffe, L.K., Doyle, R.J. and Streips, U.N. (1981) 'The energized membrane and cellular autolysis in Bacillus subtilis', *Cell*, 25(3), pp. 753–763.

Jones, L.J.F., Carballido-López, R. and Errington, J. (2001) 'Control of Cell Shape in Bacteria: Helical, Actin-like Filaments in Bacillus subtilis', *Cell*, 104(6), pp. 913–922.

Jones, N.C. and Osborn, M.J. (1977) 'Translocation of phospholipids between the

outer and inner membranes of Salmonella typhimurium', *Journal of Biological Chemistry*, 252(20), pp. 7405–7412.

Jorasch, P., Wolter, F.P., Zähringer, U. and Heinz, E. (1998) 'A UDP glucosyltransferase from Bacillus subtilis successively transfers up to four glucose residues to 1,2-diacylglycerol: expression of ypfP in Escherichia coli and structural analysis of its reaction products', *Molecular Microbiology*, 29(2), pp. 419–430.

Jordan, S., Junker, A., Helmann, J.D. and Mascher, T. (2006) 'Regulation of LiaRS-Dependent Gene Expression in Bacillus subtilis: Identification of Inhibitor Proteins, Regulator Binding Sites, and Target Genes of a Conserved Cell Envelope Stress-Sensing Two-Component System', *Journal of Bacteriology*, 188(14), p. 5153.

Jordan, S., Rietkötter, E., Strauch, M.A., Kalamorz, F., Butcher, B.G., Helmann, J.D. and Mascher, T. (2007) 'LiaRS-dependent gene expression is embedded in transition state regulation in Bacillus subtilis', *Microbiology*, 153(8), pp. 2530–2540.

Jung, D., Rozek, A., Okon, M. and Hancock, R.E.W. (2004) 'Structural transitions as determinants of the action of the calcium-dependent antibiotic daptomycin', *Chemistry and Biology*, 11(7), pp. 949–957.

Jurėnas, D., Fraikin, N., Goormaghtigh, F. and Van Melderen, L. (2022) 'Biology and evolution of bacterial toxin–antitoxin systems', *Nature Reviews Microbiology 2022*, pp. 1–16.

Kaiser, R.D. and London, E. (1998) 'Location of diphenylhexatriene (DPH) and its derivatives within membranes: comparison of different fluorescence quenching analyses of membrane depth', *Biochemistry*, 37(22), pp. 8180–8190.

Kamio, Y. and Nikaido, H. (1976) 'Outer Membrane of Salmonella Typhimurium: Accessibility of Phospholipid Head Groups to Phospholipase C and Cyanogen Bromide Activated Dextran in the External Medium', *Biochemistry*, 15(12), pp. 2561–2570.

Kamischke, C., Fan, J., Bergeron, J., Kulasekara, H.D., Dalebroux, Z.D., Burrell, A., Kollman, J.M. and Miller, S.I. (2019) 'The acinetobacter baumannii mla system and glycerophospholipid transport to the outer membrane', *eLife*, 8.

Kaneda, T. (1977) 'Fatty acids of the genus Bacillus: An example of branched chain preference', *Bacteriological Reviews*, 41(2), pp. 391–418.

Kaneda, T. (1991) 'Iso- and anteiso-fatty acids in bacteria: biosynthesis, function, and taxonomic significance.', *Microbiological Reviews*, 55(2), p. 288.

Kawai, Y., Asai, K. and Errington, J. (2009) 'Partial functional redundancy of MreB isoforms, MreB, Mbl and MreBHp in cell morphogenesis of Bacillus subtilis', *Molecular Microbiology*, 73(4), pp. 719–731.

Kawai, Y., Daniel, R.A. and Errington, J. (2009) 'Regulation of cell wall morphogenesis in Bacillus subtilis by recruitment of PBP1 to the MreB helix', *Molecular Microbiology*, 71(5), pp. 1131–1144.

Kawai, Y., Marles-Wright, J., Cleverley, R.M., Emmins, R., Ishikawa, S., Kuwano, M., Heinz, N., Bui, N.K., Hoyland, C.N., Ogasawara, N., Lewis, R.J., Vollmer, W., Daniel, R.A. and Errington, J. (2011) 'A widespread family of bacterial cell wall assembly proteins', *The EMBO Journal*, 30(24), pp. 4931–4941.

Kawai, Y., Mercier, R. and Errington, J. (2014) 'Bacterial cell morphogenesis does not require a preexisting template structure', *Current Biology*, 24(8), pp. 863–867.

Kelesidis, T. and Falagas, M.E. (2015) 'The safety of polymyxin antibiotics', *Expert Opinion on Drug Safety*, 14(11), pp. 1687–1701.

Kelkar, D.A. and Chattopadhyay, A. (2007) 'The gramicidin ion channel: A model membrane protein', *Biochimica et Biophysica Acta (BBA) - Biomembranes*, 1768(9), pp. 2011–2025.

Kepplinger, B., Morton-Laing, S., Seistrup, K.H., Marrs, E.C.L., Hopkins, A.P., Perry, J.D., Strahl, H., Hall, M.J., Errington, J. and Allenby, N.E.E. (2018) 'Mode of Action and Heterologous Expression of the Natural Product Antibiotic Vancoresmycin', *ACS Chemical Biology*, 13(1), pp. 207–214.

Kiriyama, Y., Yazawa, K., Tanaka, T., Yoshikawa, R., Yamane, H., Hashimoto, M., Sekiguchi, J. and Yamamoto, H. (2014) 'Localization and expression of the Bacillus subtilis DL-endopeptidase LytF are influenced by mutations in LTA synthases and glycolipid anchor synthetic enzymes', *Microbiology*, 160(12), pp. 2639–2649.

Klieneberger-Nobel, E. (1947) 'The life cycle of sporing Actinomyces as revealed by a study of their structure and septation.', *Journal of general microbiology*, 1(1), pp. 22–32.

Kobayashi, K., Ehrlich, S.D., Albertini, A., Amati, G., Andersen, K.K., Arnaud, M.,

Asai, K., Ashikaga, S., Aymerich, S., Bessieres, P., Boland, F., Brignell, S.C., Bron, S., Bunai, K., Chapuis, J., Christiansen, L.C., Danchin, A., Débarbouillé, M., Dervyn, E., Deuerling, E., Devine, K., Devine, S.K., Dreesen, O., Errington, J., Fillinger, S., Foster, S.J., Fujita, Y., Galizzi, A., Gardan, R., Eschevins, C., Fukushima, T., Haga, K., Harwood, C.R., Hecker, M., Hosoya, D., Hullo, M.F., Kakeshita, H., Karamata, D., Kasahara, Y., Kawamura, F., Koga, K., Koski, P., Kuwana, R., Imamura, D., Ishimaru, M., Ishikawa, S., Ishio, I., le Coq, D., Masson, A., Mauël, C., Meima, R., Mellado, R.P., Moir, A., Moriya, S., Nagakawa, E., Nanamiya, H., Nakai, S., Nygaard, P., Ogura, M., Ohanan, T., O'Reilly, M., O'Rourke, M., Pragai, Z., Pooley, H.M., Rapoport, G., Rawlins, J.P., Rivas, L.A., Rivolta, C., Sadaie, A., Sadaie, Y., Sarvas, M., Sato, T., Saxild, H.H., Scanlan, E., Schumann, W., Seegers, J.F.M.L., Sekiguchi, J., Sekowska, A., Séror, S.J., Simon, M., Stragier, P., Studer, R., Takamatsu, H., Tanaka, T., Takeuchi, M., Thomaides, H.B., Vagner, V., van Dijl, J.M., Watabe, K., Wipat, A., Yamamoto, H., Yamamoto, M., Yamamoto, Y., Yamane, K., Yata, K., Yoshida, K., Yoshikawa, H., Zuber, U. and Ogasawara, N. (2003) 'Essential Bacillus subtilis genes', *Proceedings of the National Academy of Sciences of the United States of America*, 100(8), pp. 4678–4683.

Koburger, T., Hübner, N.O., Braun, M., Siebert, J. and Kramer, A. (2010) 'Standardized comparison of antiseptic efficacy of triclosan, PVP–iodine, octenidine dihydrochloride, polyhexanide and chlorhexidine digluconate', *Journal of Antimicrobial Chemotherapy*, 65(8), pp. 1712–1719.

Kondejewski, L.H., Farmer, S.W., Wishart, D.S., Kay, C.M., Hancock, R.E. and Hodges, R.S. (1996) 'Modulation of structure and antibacterial and hemolytic activity by ring size in cyclic gramicidin S analogs.', *The Journal of biological chemistry*, 271(41), pp. 25261–8.

Kourtesi, C., Ball, A.R., Huang, Y.-Y., Jachak, S.M., Mariano, D., Vera, A., Khondkar, P., Gibbons, S., Hamblin, M.R. and Tegos, G.P. (2013) 'Microbial Efflux Systems and Inhibitors: Approaches to Drug Discovery and the Challenge of Clinical Implementation', *The Open Microbiology Journal*, (7), pp. 34–52.

Kucherak, O.A., Oncul, S., Darwich, Z., Yushchenko, D.A., Arntz, Y., Didier, P., Mély, Y. and Klymchenko, A.S. (2010) 'Switchable Nile Red-Based Probe for Cholesterol and Lipid Order at the Outer Leaflet of Biomembranes', *Journal of the American Chemical Society*, 132(13), pp. 4907–4916.

Kumar, P., Kizhakkedathu, J.N. and Straus, S.K. (2018) 'Antimicrobial Peptides: Diversity, Mechanism of Action and Strategies to Improve the Activity and Biocompatibility In Vivo.', *Biomolecules*, 8(1), p. 4.

Kurata, T., Saha, C.K., Buttress, J.A., Mets, T., Brodiazhenko, T., Turnbull, K.J., Awoyomi, O.F., Oliveira, S.R.A., Jimmy, S., Ernits, K., Delannoy, M., Persson, K., Tenson, T., Strahl, H., Hauryliuk, V. and Atkinson, G.C. (2022) 'A hyperpromiscuous antitoxin protein domain for the neutralization of diverse toxin domains', *Proceedings of the National Academy of Sciences of the United States of America*, 119(6).

Kurita, K., Kato, F. and Shiomi, D. (2020) 'Alteration of Membrane Fluidity or Phospholipid Composition Perturbs Rotation of MreB Complexes in Escherichia coli', *Frontiers in Molecular Biosciences*, 7, p. 364.

Kuru, E., Hughes, H.V., Brown, P.J., Hall, E., Tekkam, S., Cava, F., De Pedro, M.A., Brun, Y. V. and Vannieuwenhze, M.S. (2012) 'In situ probing of newly synthesized peptidoglycan in live bacteria with fluorescent D-amino acids', *Angewandte Chemie - International Edition*, 51(50), pp. 12519–12523.

Labischinski, H., Barnickel, G., Bradaczek, H., Naumann, D., Rietschel, E.T. and Giesbrecht, P. (1985) 'High state of order of isolated bacterial lipopolysaccharide and its possible contribution to the permeation barrier property of the outer membrane.', *Journal of bacteriology*, 162(1), pp. 9–20.

Lacriola, C.J., Falk, S.P. and Weisblum, B. (2013) 'Screen for Agents That Induce Autolysis in Bacillus subtilis', *Antimicrobial Agents and Chemotherapy*, 57(1), p. 229.

Lakey, J.H. and Ptak, M. (1988) 'Fluorescence Indicates a Calcium-Dependent Interaction between the Lipopeptide Antibiotic LY146032 and Phospholipid Membranes', *Biochemistry*, 27(13), pp. 4639–4645.

Lam, C., Hildebrandt, J., Schütze, E. and Wenzel, A.F. (1986) 'Membrane-disorganizing property of polymyxin b nonapeptide', *Journal of Antimicrobial Chemotherapy*, 18(1), pp. 9–15.

Lamers, R.P., Cavallari, J.F. and Burrows, L.L. (2013) 'The Efflux Inhibitor Phenylalanine-Arginine Beta-Naphthylamide (PAβN) Permeabilizes the Outer Membrane of Gram-Negative Bacteria', *PLOS ONE*, 8(3), p. e60666.

Lamsa, A., Liu, W.T., Dorrestein, P.C. and Pogliano, K. (2012) 'The Bacillus subtilis

cannibalism toxin SDP collapses the proton motive force and induces autolysis', *Molecular microbiology*, 84(3), pp. 486–500.

Langhorst, M.F., Reuter, A. and Stuermer, C.A.O. (2005) 'Scaffolding microdomains and beyond: The function of reggie/flotillin proteins', *Cellular and Molecular Life Sciences*, pp. 2228–2240.

Langley, K.E., Hawrot, E. and Kennedy, E.P. (1982) 'Membrane assembly: Movement of phosphatidylserine between the cytoplasmic and outer membranes of Escherichia coli', *Journal of Bacteriology*, 152(3), pp. 1033–1041.

LaPlante, K.L. and Mermel, L.A. (2009) 'In vitro activities of telavancin and vancomycin against biofilm-producing Staphylococcus aureus, S. epidermidis, and Enterococcus faecalis strains.', *Antimicrobial agents and chemotherapy*, 53(7), pp. 3166–9.

Lazarevic, V. and Karamata, D. (1995) 'The tagGH operon of Bacillus subtilis 168 encodes a two-component ABC transporter involved in the metabolism of two wall teichoic acids', *Molecular Microbiology*, 16(2), pp. 345–355.

Lazarevic, V., Margot, P., Soldo, B. and Karamata, D. (1992) 'Sequencing and analysis of the Bacillus subtilis lytRABC divergon: a regulatory unit encompassing the structural genes of the N-acetylmuramoyl-L-alanine amidase and its modifier', *Journal of General Microbiology*, 138(9), pp. 1949–1961.

Lee, J., Kim, S., Sim, J.-Y., Lee, D., Kim, H.H., Hwang, J.S., Lee, D.G., Park, Z.-Y. and Kim, J. II (2019) 'A potent antibacterial activity of new short d-enantiomeric lipopeptide against multi drug resistant bacteria', *Biochimica et Biophysica Acta (BBA) - Biomembranes*, 1861(1), pp. 34–42.

Leive, L. (1965) 'Release of lipopolysaccharide by EDTA treatment of E., coli', *Biochemical and Biophysical Research Communications*, 21(4), pp. 290–296.

Levin, P.A., Margolis, P.S., Setlow, P., Losick, R. and Sun, D. (1992) 'Identification of Bacillus subtilis genes for septum placement and shape determination', *Journal of bacteriology*, 174(21), pp. 6717–6728.

Llamas, M.A., Ramos, J.L. and Rodriguez-Herva, J.J. (2000) 'Mutations in Each of the tol Genes of Pseudomonas putida Reveal that They Are Critical for Maintenance of Outer Membrane Stability', *Journal of Bacteriology*, 182(17), p. 4764.

Lomovskaya, O., Warren, M.S., Lee, A., Galazzo, J., Fronko, R., Lee, M., Blais, J., Cho, D., Chamberland, S., Renau, T., Leger, R., Hecker, S., Watkins, W., Hoshino, K., Ishida, H. and Lee, V.J. (2001) 'Identification and characterization of inhibitors of multidrug resistance efflux pumps in Pseudomonas aeruginosa: novel agents for combination therapy', *Antimicrobial agents and chemotherapy*, 45(1), pp. 105–116.

Lopez, C.S., Alice, A.F., Heras, H., Rivas, E.A. and Sánchez-Rivas, C. (2006) 'Role of anionic phospholipids in the adaptation of Bacillus subtilis to high salinity', *Microbiology*, 152(3), pp. 605–616.

López, C.S., Heras, H., Ruzal, S.M., Sánchez-Rivas, C. and Rivas, E.A. (1998) 'Variations of the envelope composition of Bacillus subtilis during growth in hyperosmotic medium.', *Current microbiology*, 36(1), pp. 55–61.

López, D. and Kolter, R. (2010) 'Functional microdomains in bacterial membranes', *Genes and Development*, 24(17), pp. 1893–1902.

Lovering, A.L., Safadi, S.S. and Strynadka, N.C.J. (2012) 'Structural perspective of peptidoglycan biosynthesis and assembly', *Annual Review of Biochemistry*, pp. 451–478.

Lubelski, J., Konings, W.N. and Driessen, A.J.M. (2007) 'Distribution and physiology of ABC-type transporters contributing to multidrug resistance in bacteria', *Microbiology and molecular biology reviews : MMBR*, 71(3), pp. 463–476.

Lutkenhaus, J.F., Wolf-Watz, H. and Donachie, W.D. (1980) 'Organization of genes in the ftsA-envA region of the Escherichia coli genetic map and identification of a new fts locus (ftsZ).', *Journal of Bacteriology*, 142(2), p. 615.

Ma, D., Cook, D.N., Alberti, M., Pon, N.G., Nikaido, H. and Hearst, J.E. (1993) 'Molecular cloning and characterization of acrA and acrE genes of Escherichia coli', *Journal of bacteriology*, 175(19), pp. 6299–6313.

Ma, D., Cook, D.N., Alberti, M., Pon, N.G., Nikaido, H. and Hearst, J.E. (1995) 'Genes acrA and acrB encode a stress-induced efflux system of Escherichia coli', *Molecular microbiology*, 16(1), pp. 45–55.

MacLeod, C.M. (1940) 'The inhibition of the bacteriostatic action of sulfonamide drugs by substances of animal and bacterial origin', *Journal of Experimental Medicine*, 72(3), pp. 217–232.

Magnuson, K., Jackowski, S., Rock, C.O., Cronan, J.E. and Jr (1993) 'Regulation of fatty acid biosynthesis in Escherichia coli.', *Microbiological reviews*, 57(3), pp. 522–42.

Malanovic, N., Buttress, J.A., Vejzovic, D., Ön, A., Piller, P., Kolb, D., Lohner, K. and Strahl, H. (2022) 'Disruption of the Cytoplasmic Membrane Structure and Barrier Function Underlies the Potent Antiseptic Activity of Octenidine in Gram-Positive Bacteria', *Applied and Environmental Microbiology*, 88(10).

Malanovic, N., Ön, A., Pabst, G., Zellner, A. and Lohner, K. (2020) 'Octenidine: Novel insights into the detailed killing mechanism of Gram-negative bacteria at a cellular and molecular level', *International Journal of Antimicrobial Agents*, 56(5), p. 106146.

Malinverni, J.C. and Silhavy, T.J. (2009) 'An ABC transport system that maintains lipid asymmetry in the gram-negative outer membrane', *Proceedings of the National Academy of Sciences of the United States of America*, 106(19), pp. 8009–8014.

Margot, P. and Karamata, D. (1992) 'Identification of the structural genes for N-acetylmuramoyl-l-alanine amidase and its modifier in Bacillus subtilis 168: inactivation of these genes by insertional mutagenesis has no effect on growth or cell separation', *MGG Molecular & General Genetics*, 232(3), pp. 359–366.

Margot, P., Mauël, C. and Karamata, D. (1994) 'The gene of the N-acetylglucosaminidase, a Bacillus subtilis 168 cell wall hydrolase not involved in vegetative cell autolysis.', *Molecular microbiology*, 12(4), pp. 535–45.

Margot, P., Pagni, M. and Karamata, D. (1999) 'Bacillus subtilis 168 gene lytF encodes a γ-D-glutamate-meso-diaminopimelate muropeptidase expressed by the alternative vegetative sigma factor, σ(D)', *Microbiology*, 145(1), pp. 57–65.

Mariano, G., Trunk, K., Williams, D.J., Monlezun, L., Strahl, H., Pitt, S.J. and Coulthurst, S.J. (2019) 'A family of Type VI secretion system effector proteins that form ion-selective pores', *Nature Communications*, 10(1).

Marquez, L.M., Helmann, J.D., Ferrari, E., Parker, H.M., Ordal, G.W. and Chamberlin, M.J. (1990) 'Studies of sigma D-dependent functions in Bacillus subtilis', *Journal of Bacteriology*, 172(6), pp. 3435–3443.

Marr, A.G. and Ingraham, J.L. (1962) 'EFFECT OF TEMPERATURE ON THE COMPOSITION OF FATTY ACIDS IN ESCHERICHIA COLI', *Journal of bacteriology*,

84(6), pp. 1260–1267.

Marshall, R.L., Lloyd, G.S., Lawler, A.J., Element, S.J., Kaur, J., Ciusa, M.L., Ricci, V., Tschumi, A., Kühne, H., Alderwick, L.J. and Piddock, L.J.V. (2020) 'New multidrug efflux inhibitors for gram-negative bacteria', *mBio*, 11(4), pp. 1–19.

Martinez-Corral, R., Liu, J., Prindle, A., Süel, G.M. and Garcia-Ojalvo, J. (2019) 'Metabolic basis of brain-like electrical signalling in bacterial communities', *Philosophical Transactions of the Royal Society B: Biological Sciences*, 374(1774).

Mascher, T., Margulis, N.G., Wang, T., Ye, R.W. and Helmann, J.D. (2003) 'Cell wall stress responses in Bacillus subtilis: the regulatory network of the bacitracin stimulon', *Molecular Microbiology*, 50(5), pp. 1591–1604.

Mascher, T., Zimmer, S.L., Smith, T.A. and Helmann, J.D. (2004) 'Antibiotic-inducible promoter regulated by the cell envelope stress-sensing two-component system LiaRS of Bacillus subtilis', *Antimicrobial Agents and Chemotherapy*, 48(8), pp. 2888–2896.

Matsumoto, K., Kusaka, J., Nishibori, A. and Hara, H. (2006) 'Lipid domains in bacterial membranes', *Molecular microbiology*, 61(5), pp. 1110–1117.

Matsuzaki, K., Sugishita, K., Ishibe, N., Ueha, M., Nakata, S., Miyajima, K. and Epand, R.M. (1998) 'Relationship of Membrane Curvature to the Formation of Pores by Magainin 2', *Biochemistry*, 37(34), pp. 11856–11863.

Mattick, A.T.R., Hirsch, A. and Berridge, N.J. (1947) 'FURTHER OBSERVATIONS ON AN INHIBITORY SUBSTANCE (NISIN) FROM LACTIC STREPTOCOCCI', *The Lancet*, 250(6462), pp. 5–8.

Mbamala, E.C., Ben-Shaul, A. and May, S. (2005) 'Domain formation induced by the adsorption of charged proteins on mixed lipid membranes.', *Biophysical journal*, 88(3), pp. 1702–14.

McAuley, S., Huynh, A., Czarny, T.L., Brown, E.D. and Nodwell, J.R. (2018) 'Membrane activity profiling of small molecule B. subtilis growth inhibitors utilizing novel duel-dye fluorescence assay', *MedChemComm*, 9(3), p. 554.

McCarthy, A.J. (1987) 'Lignocellulose-degrading actinomycetes', *FEMS Microbiology Reviews*, 3(2), pp. 145–163.

Medema, M.H., Blin, K., Cimermancic, P., De Jager, V., Zakrzewski, P., Fischbach,

M.A., Weber, T., Takano, E. and Breitling, R. (2011) 'AntiSMASH: Rapid identification, annotation and analysis of secondary metabolite biosynthesis gene clusters in bacterial and fungal genome sequences', *Nucleic Acids Research*, 39(SUPPL. 2), p. W339.

Meeske, A.J., Riley, E.P., Robins, W.P., Uehara, T., Mekalanos, J.J., Kahne, D., Walker, S., Kruse, A.C., Bernhardt, T.G. and Rudner, D.Z. (2016) 'SEDS proteins are a widespread family of bacterial cell wall polymerases', *Nature*, 537(7622), pp. 634–638.

Meeske, A.J., Sham, L.T., Kimsey, H., Koo, B.M., Gross, C.A., Bernhardt, T.G. and Rudner, D.Z. (2015) 'MurJ and a novel lipid II flippase are required for cell wall biogenesis in Bacillus subtilis', *Proceedings of the National Academy of Sciences of the United States of America*, 112(20), pp. 6437–6442.

De Mendoza, D., Klages Ulrich, A. and Cronan, J.E. (1983) 'Thermal regulation of membrane fluidity in Escherichia coli. Effects of overproduction of beta-ketoacyl-acyl carrier protein synthase I.', *Journal of Biological Chemistry*, 258(4), pp. 2098–2101.

Mengin-Lecreulx, D., Allen, N.E., Hobbs, J.N. and van Heijenoort, J. (1990) 'Inhibition of peptidoglycan biosynthesis in Bacillus megaterium by daptomycin.', *FEMS microbiology letters*, 57(3), pp. 245–8.

Migocki, M.D., Freeman, M.K., Wake, R.G. and Harry, E.J. (2002) 'The Min system is not required for precise placement of the midcell Z ring in Bacillus subtilis', *EMBO Reports*, 3(12), p. 1163.

Mileykovskaya, E. and Dowhan, W. (2000) 'Visualization of phospholipid domains in Escherichia coli by using the cardiolipin-specific fluorescent dye 10-N-nonyl acridine orange', *Journal of Bacteriology*, 182(4), pp. 1172–1175.

Mitchell, P. (1961) 'Coupling of phosphorylation to electron and hydrogen transfer by a chemi-osmotic type of mechanism', *Nature*, 191(4784), pp. 144–148.

Mohammadi, T., Karczmarek, A., Crouvoisier, M., Bouhss, A., Mengin-Lecreulx, D. and den Blaauwen, T. (2007) 'The essential peptidoglycan glycosyltransferase MurG forms a complex with proteins involved in lateral envelope growth as well as with proteins involved in cell division in Escherichia coli.', *Molecular microbiology*, 65(4), pp. 1106–21.

Morin, N., Lanneluc, I., Connil, N., Cottenceau, M., Pons, A.M. and Sablé, S. (2011) 'Mechanism of Bactericidal Activity of Microcin L in Escherichia coli and Salmonella enterica', *Antimicrobial Agents and Chemotherapy*, 55(3), p. 997.

Moriya, S., Rashid, R.A., Rodrigues, C.D.A. and Harry, E.J. (2010) 'Influence of the nucleoid and the early stages of DNA replication on positioning the division site in Bacillus subtilis', *Molecular microbiology*, 76(3), pp. 634–647.

Muheim, C., Götzke, H., Eriksson, A.U., Lindberg, S., Lauritsen, I., Nørholm, M.H.H. and Daley, D.O. (2017) 'Increasing the permeability of Escherichia coli using MAC13243', *Scientific Reports*, 7(1).

Mulkins Phillips, G.J. and Stewart, J.E. (1974) 'Distribution of hydrocarbon utilizing bacteria in Northwestern Atlantic waters and coastal sediments', *Canadian Journal of Microbiology*, 20(7), pp. 955–962.

Müller, A., Wenzel, M., Strahl, H., Grein, F., Saaki, T.N. V., Kohl, B., Siersma, T., Bandow, J.E., Sahl, H.-G., Schneider, T. and Hamoen, L.W. (2016) 'Daptomycin inhibits cell envelope synthesis by interfering with fluid membrane microdomains', *Proceedings of the National Academy of Sciences*, 113(45), pp. E7077–E7086.

Muraih, J.K., Pearson, A., Silverman, J. and Palmer, M. (2011) 'Oligomerization of daptomycin on membranes', *Biochimica et biophysica acta*, 1808(4), pp. 1154–1160.

Murakami, S., Nakashima, R., Yamashita, E., Matsumoto, T. and Yamaguchi, A. (2006) 'Crystal structures of a multidrug transporter reveal a functionally rotating mechanism', *Nature*, 443(7108), pp. 173–179.

Murray, C.J., Ikuta, K.S., Sharara, F., Swetschinski, L., Robles Aguilar, G., Gray, A., Han, C., Bisignano, C., Rao, P., Wool, E., Johnson, S.C., Browne, A.J., Chipeta, M.G., Fell, F., Hackett, S., Haines-Woodhouse, G., Kashef Hamadani, B.H., Kumaran, E.A.P., McManigal, B., Agarwal, R., Akech, S., Albertson, S., Amuasi, J., Andrews, J., Aravkin, A., Ashley, E., Bailey, F., Baker, S., Basnyat, B., Bekker, A., Bender, R., Bethou, A., Bielicki, J., Boonkasidecha, S., Bukosia, J., Carvalheiro, C., Castañeda-Orjuela, C., Chansamouth, V., Chaurasia, S., Chiurchiù, S., Chowdhury, F., Cook, A.J., Cooper, B., Cressey, T.R., Criollo-Mora, E., Cunningham, M., Darboe, S., Day, N.P.J., De Luca, M., Dokova, K., Dramowski, A., Dunachie, S.J., Eckmanns, T., Eibach, D., Emami, A., Feasey, N., Fisher-Pearson, N., Forrest, K., Garrett, D., Gastmeier, P., Giref, A.Z., Greer, R.C., Gupta, V., Haller, S., Haselbeck, A., Hay, S.I.,

Holm, M., Hopkins, S., Iregbu, K.C., Jacobs, J., Jarovsky, D., Javanmardi, F., Khorana, M., Kissoon, N., Kobeissi, E., Kostyanev, T., Krapp, F., Krumkamp, R., Kumar, A., Kyu, H.H., Lim, C., Limmathurotsakul, D., Loftus, M.J., Lunn, M., Ma, J., Mturi, N., Munera-Huertas, T., Musicha, P., Mussi-Pinhata, M.M., Nakamura, T., Nanavati, R., Nangia, S., Newton, P., Ngoun, C., Novotney, A., Nwakanma, D., Obiero, C.W., Olivas-Martinez, A., Olliaro, P., Ooko, E., Ortiz-Brizuela, E., Peleg, A.Y., Perrone, C., Plakkal, N., Ponce-de-Leon, A., Raad, M., Ramdin, T., Riddell, A., Roberts, T., Robotham, J.V., Roca, A., Rudd, K.E., Russell, N., Schnall, J., Scott, J.A.G., Shivamallappa, M., Sifuentes-Osornio, J., Steenkeste, N., Stewardson, A.J., Stoeva, T., Tasak, N., Thaiprakong, A., Thwaites, G., Turner, C., Turner, P., van Doorn, H.R., Velaphi, S., Vongpradith, A., Vu, H., Walsh, T., Waner, S., Wangrangsimakul, T., Wozniak, T., Zheng, P., Sartorius, B., Lopez, A.D., Stergachis, A., Moore, C., Dolecek, C. and Naghavi, M. (2022) 'Global burden of bacterial antimicrobial resistance in 2019: a systematic analysis', *The Lancet*, 399(10325), pp. 629–655.

Nakamura, S. and Minamino, T. (2019) 'Flagella-driven motility of bacteria', *Biomolecules*, 9(7).

Nation, R.L., Rigatto, M.H.P., Falci, D.R. and Zavascki, A.P. (2019) 'Polymyxin Acute Kidney Injury: Dosing and Other Strategies to Reduce Toxicity.', *Antibiotics (Basel, Switzerland)*, 8(1).

Nation, R.L., Velkov, T. and Li, J. (2014) 'Colistin and polymyxin B: Peas in a pod, or chalk and cheese?', *Clinical Infectious Diseases*. Oxford University Press, pp. 88–94.

Neuhaus, F.C. and Baddiley, J. (2003) 'A continuum of anionic charge: structures and functions of D-alanyl-teichoic acids in gram-positive bacteria.', *Microbiology and molecular biology reviews : MMBR*, 67(4), pp. 686–723.

Nikaido, H. (1996) 'Multidrug efflux pumps of gram-negative bacteria.', *Journal of bacteriology*, 178(20), pp. 5853–9.

Nikaido, H. (2003) 'Molecular basis of bacterial outer membrane permeability revisited.', *Microbiology and molecular biology reviews : MMBR*, 67(4), pp. 593–656.

Nikaido, H., Rosenberg, E.Y. and Foulds, J. (1983) 'Porin channels in Escherichia coli: studies with beta-lactams in intact cells.', *Journal of Bacteriology*, 153(1), p. 232.

Nishino, K., Nikaido, E. and Yamaguchi, A. (2009) 'Regulation and physiological

function of multidrug efflux pumps in Escherichia coli and Salmonella', *Biochimica et Biophysica Acta (BBA) - Proteins and Proteomics*, 1794(5), pp. 834–843.

Normand, P., Lapierre, P., Tisa, L.S., Gogarten, J.P., Alloisio, N., Bagnarol, E., Bassi, C.A., Berry, A.M., Bickhart, D.M., Choisne, N., Couloux, A., Cournoyer, B., Cruveiller, S., Daubin, V., Demange, N., Francino, M.P., Goltsman, E., Huang, Y., Kopp, O.R., Labarre, L., Lapidus, A., Lavire, C., Marechal, J., Martinez, M., Mastronunzio, J.E., Mullin, B.C., Niemann, J., Pujic, P., Rawnsley, T., Rouy, Z., Schenowitz, C., Sellstedt, A., Tavares, F., Tomkins, J.P., Vallenet, D., Valverde, C., Wall, L.G., Wang, Y., Medigue, C. and Benson, D.R. (2007) 'Genome characteristics of facultatively symbiotic Frankia sp. strains reflect host range and host plant biogeography', *Genome Research*, 17(1), pp. 7–15.

O'Riordan, K. and Lee, J.C. (2004) 'Staphylococcus aureus Capsular Polysaccharides', *Clinical Microbiology Reviews*. Clin Microbiol Rev, pp. 218–234.

Ocaktan, A., Yoneyama, H. and Nakae, T. (1997) 'Use of fluorescence probes to monitor function of the subunit proteins of the MexA-MexB-oprM drug extrusion machinery in Pseudomonas aeruginosa', *The Journal of biological chemistry*, 272(35), pp. 21964–21969.

Ohnishi, R., Ishikawa, S. and Sekiguchi, J. (1999) 'Peptidoglycan hydrolase LytF plays a role in cell separation with CwlF during vegetative growth of Bacillus subtilis.', *Journal of bacteriology*, 181(10), pp. 3178–84.

Ohnishi, Y., Ishikawa, J., Hara, H., Suzuki, H., Ikenoya, M., Ikeda, H., Yamashita, A., Hattori, M. and Horinouchi, S. (2008) 'Genome sequence of the streptomycin-producing microorganism Streptomyces griseus IFO 13350', *Journal of bacteriology*, 190(11), pp. 4050–4060.

Ohniwa, R.L., Kitabayashi, K. and Morikawa, K. (2013) 'Alternative cardiolipin synthase Cls1 compensates for stalled Cls2 function in *Staphylococcus aureus* under conditions of acute acid stress', *FEMS Microbiology Letters*, 338(2), pp. 141–146.

Okazaki, T. and Okami, Y. (1972) 'Studies on marine microorganisms. II: Actinomycetes in sagami bay and their antibiotic substances', *The Journal of Antibiotics*, 25(8), pp. 461–466.

Okuda, S., Sherman, D.J., Silhavy, T.J., Ruiz, N. and Kahne, D. (2016) 'Lipopolysaccharide transport and assembly at the outer membrane: The PEZ

model', *Nature Reviews Microbiology*. NIH Public Access, pp. 337–345.

Oliynyk, M., Samborskyy, M., Lester, J.B., Mironenko, T., Scott, N., Dickens, S., Haydock, S.F. and Leadlay, P.F. (2007) 'Complete genome sequence of the erythromycin-producing bacterium Saccharopolyspora erythraea NRRL23338', *Nature biotechnology*, 25(4), pp. 447–453.

Omardien, S., Drijfhout, J.W., Vaz, F.M., Wenzel, M., Hamoen, L.W., Zaat, S.A.J. and Brul, S. (2018) 'Bactericidal activity of amphipathic cationic antimicrobial peptides involves altering the membrane fluidity when interacting with the phospholipid bilayer', *Biochimica et Biophysica Acta - Biomembranes*, 1860(11), pp. 2404–2415.

Oswald, F., Varadarajan, A., Lill, H., Peterman, E.J.G. and Bollen, Y.J.M. (2016) 'MreB-Dependent Organization of the E. coli Cytoplasmic Membrane Controls Membrane Protein Diffusion.', *Biophysical journal*, 110(5), pp. 1139–49.

Parasassi, T. and Gratton, E. (1995) 'Membrane lipid domains and dynamics as detected by Laurdan fluorescence', *Journal of fluorescence*, 5(1), pp. 59–69.

Parkinson, J.S. (1993) 'Signal transduction schemes of bacteria', *Cell*, 73(5), pp. 857–871.

Paulsen, I.T., Brown, M.H. and Skurray, R.A. (1996) 'Proton-dependent multidrug efflux systems.', *Microbiological Reviews*, 60(4), p. 575.

Pawlik, K., Kotowska, M., Chater, K.F., Kuczek, K. and Takano, E. (2007) 'A cryptic type I polyketide synthase (cpk) gene cluster in Streptomyces coelicolor A3(2)', *Archives of Microbiology*, 187(2), pp. 87–99.

Penyige, A., Matkó, J., Deák, E., Bodnár, A. and Barabás, G. (2002) 'Depolarization of the Membrane Potential by β-Lactams as a Signal to Induce Autolysis', *Biochemical and Biophysical Research Communications*, 290(4), pp. 1169–1175.

Perego, M., Glaser, P., Minutello, A., Strauch, M.A., Leopold, K. and Fischer, W. (1995) 'Incorporation of D-alanine into lipoteichoic acid and wall teichoic acid in Bacillus subtilis: Identification of genes and regulation', *Journal of Biological Chemistry*, 270(26), pp. 15598–15606.

Pereira, M.P., Schertzer, J.W., D'Elia, M.A., Koteva, K.P., Hughes, D.W., Wright, G.D. and Brown, E.D. (2008) 'The Wall Teichoic Acid Polymerase TagF Efficiently Synthesizes Poly(glycerol phosphate) on the TagB Product Lipid III', *ChemBioChem*,

9(9), pp. 1385–1390.

Petersohn, A., Brigulla, M., Haas, S., Hoheisel, J.D., Völker, U. and Heckler, M. (2001) 'Global analysis of the general stress response of Bacillus subtilis', *Journal of Bacteriology*, 183(19), pp. 5617–5631.

Petiti, M., Serrano, B., Faure, L., Lloubes, R., Mignot, T. and Duché, D. (2019) 'Tol Energy-Driven Localization of Pal and Anchoring to the Peptidoglycan Promote Outer-Membrane Constriction', *Journal of molecular biology*, 431(17), pp. 3275–3288.

PhysiologyWeb. (2005) 'Nernst Potential Calculator', Available at: https://www.physiologyweb.com/calculators/nernst_potential_calculator.html [Accessed 16 October 2022].

Pichler, G., Pux, C., Babeluk, R., Hermann, B., Stoiser, E., De Campo, A., Grisold, A., Zollner-Schwetz, I., Krause, R. and Schippinger, W. (2018) 'MRSA prevalence rates detected in a tertiary care hospital in Austria and successful treatment of MRSA positive patients applying a decontamination regime with octenidine', *European Journal of Clinical Microbiology and Infectious Diseases*, 37(1), pp. 21–27.

Piddock, L.J.V. (2006) 'Multidrug-resistance efflux pumps - Not just for resistance', *Nature Reviews Microbiology*, 4(8), pp. 629–636.

Pietiäinen, M., Gardemeister, M., Mecklin, M., Leskelä, S., Sarvas, M. and Kontinen, V.P. (2005) 'Cationic antimicrobial peptides elicit a complex stress response in Bacillus subtilis that involves ECF-type sigma factors and two-component signal transduction systems', *Microbiology*, 151(5), pp. 1577–1592.

Plé, C., Tam, H.K., Vieira Da Cruz, A., Compagne, N., Jiménez-Castellanos, J.C., Müller, R.T., Pradel, E., Foong, W.E., Malloci, G., Ballée, A., Kirchner, M.A., Moshfegh, P., Herledan, A., Herrmann, A., Deprez, B., Willand, N., Vargiu, A.V., Pos, K.M., Flipo, M. and Hartkoorn, R.C. (2022) 'Pyridylpiperazine-based allosteric inhibitors of RND-type multidrug efflux pumps', *Nature Communications 2022 13:1*, 13(1), pp. 1–11.

Pogmore, A.-R., Seistrup, K.H. and Strahl, H. (2018) 'The Gram-positive model organism Bacillus subtilis does not form microscopically detectable cardiolipin-specific lipid domains', *Microbiology*, 164(4), pp. 475–482.

Poole, K. (2004) 'Efflux-mediated multiresistance in Gram-negative bacteria', *Clinical Microbiology and Infection*, 10(1), pp. 12–26.

Popp, P.F., Benjdia, A., Strahl, H., Berteau, O. and Mascher, T. (2020) 'The Epipeptide YydF Intrinsically Triggers the Cell Envelope Stress Response of Bacillus subtilis and Causes Severe Membrane Perturbations', *Frontiers in Microbiology*, 11, p. 151.

Porrini, L., Cybulski, L.E., Altabe, S.G., Mansilla, M.C. and de Mendoza, D. (2014) 'Cerulenin inhibits unsaturated fatty acids synthesis in Bacillus subtilis by modifying the input signal of DesK thermosensor', *MicrobiologyOpen*, 3(2), pp. 213–224.

Powers, M.J., Simpson, B.W. and Stephen Trent, M. (2020) 'The mla pathway in acinetobacter baumannii has no demonstrable role in anterograde lipid transport', *eLife*, 9, pp. 1–21.

Prachayasittikul, V., Isarankura-Na-Ayudhya, C., Tantimongcolwat, T., Nantasenamat, C. and Galla, H.J. (2007) 'EDTA-induced membrane fluidization and destabilization: Biophysical studies on artificial lipid membranes', *Acta Biochimica et Biophysica Sinica*, 39(11), pp. 901–913.

Prindle, A., Liu, J., Asally, M., Ly, S., Garcia-Ojalvo, J. and Süel, G.M. (2015) 'Ion channels enable electrical communication in bacterial communities', *Nature*, 527(7576), pp. 59–63.

Radeck, J., Fritz, G. and Mascher, T. (2017) 'The cell envelope stress response of Bacillus subtilis: from static signaling devices to dynamic regulatory network', *Current Genetics*, 63(1), pp. 79–90.

Raetz, C.R. and Dowhan, W. (1990) 'Biosynthesis and function of phospholipids in Escherichia coli.', *The Journal of biological chemistry*, 265(3), pp. 1235–8.

Raetz, C.R.H. and Whitfield, C. (2002) 'Lipopolysaccharide endotoxins', *Annual Review of Biochemistry*, pp. 635–700.

Rani, C. and Khan, I.A. (2016) 'UDP-GlcNAc pathway: Potential target for inhibitor discovery against M. tuberculosis', *European Journal of Pharmaceutical Sciences*, 83, pp. 62–70.

Rashid, M.H., Kuroda, A. and Sekiguchi, J. (1993) 'Bacillus subtilis mutant deficient in the major autolytic amidase and glucosaminidase is impaired in motility.', *FEMS*

Microbiology Letters, 112(2), pp. 135–140.

Ravi, J. and Fioravanti, A. (2021) 'S-layers: The Proteinaceous Multifunctional Armors of Gram-Positive Pathogens', *Frontiers in Microbiology*, p. 685.

Richmond, G.E., Chua, K.L. and Piddock, L.J.V. (2013) 'Efflux in Acinetobacter baumannii can be determined by measuring accumulation of H33342 (bis-benzamide)', *Journal of Antimicrobial Chemotherapy*, 68(7), p. 1594.

Rico, A.I., Krupka, M. and Vicente, M. (2013) 'In the Beginning, Escherichia coli Assembled the Proto-ring: An Initial Phase of Division', *The Journal of Biological Chemistry*, 288(29), p. 20830.

Riool, M., de Breij, A., Kwakman, P.H.S., Schonkeren-Ravensbergen, E., de Boer, L., Cordfunke, R.A., Malanovic, N., Drijfhout, J.W., Nibbering, P.H. and Zaat, S.A.J. (2020) 'Thrombocidin-1-derived antimicrobial peptide TC19 combats superficial multi-drug resistant bacterial wound infections', *Biochimica et Biophysica Acta (BBA) - Biomembranes*, 1862(8), p. 183282.

Rodrigues, C.D.A. and Harry, E.J. (2012) 'The Min System and Nucleoid Occlusion Are Not Required for Identifying the Division Site in Bacillus subtilis but Ensure Its Efficient Utilization', *PLoS Genetics*, 8(3).

Roth, B.L., Poot, M., Yue, S.T. and Millard, P.J. (1997) 'Bacterial viability and antibiotic susceptibility testing with SYTOX green nucleic acid stain.', *Applied and Environmental Microbiology*, 63(6).

Rotondi, K.S. and Gierasch, L.M. (2005) 'A well-defined amphipathic conformation for the calcium-free cyclic lipopeptide antibiotic, daptomycin, in aqueous solution', *Biopolymers - Peptide Science Section*, 80(2–3), pp. 374–385.

Rutledge, P.J. and Challis, G.L. (2015) 'Discovery of microbial natural products by activation of silent biosynthetic gene clusters', *Nature Reviews Microbiology*, pp. 509–523.

Sabnis, A., Hagart, K.L.H., Klöckner, A., Becce, M., Evans, L.E., Furniss, R.C.D., Mavridou, D.A.I., Murphy, R., Stevens, M.M., Davies, J.C., Larrouy-Maumus, G.J., Clarke, T.B. and Edwards, A.M. (2021) 'Colistin kills bacteria by targeting lipopolysaccharide in the cytoplasmic membrane', *eLife*, 10.

Sáenz, J.P., Grosser, D., Bradley, A.S., Lagny, T.J., Lavrynenko, O., Broda, M. and

Simons, K. (2015) 'Hopanoids as functional analogues of cholesterol in bacterial membranes', *Proceedings of the National Academy of Sciences of the United States of America*, 112(38), pp. 11971–11976.

Saita, E., Albanesi, D. and De Mendoza, D. (2016) 'Sensing membrane thickness: Lessons learned from cold stress', *Biochimica et Biophysica Acta (BBA) - Molecular and Cell Biology of Lipids*, 1861(8), pp. 837–846.

Salje, J., van den Ent, F., de Boer, P. and Löwe, J. (2011) 'Direct Membrane Binding by Bacterial Actin MreB', *Molecular Cell*, 43(3), pp. 478–487.

Salzberg, L.I. and Helmann, J.D. (2008) 'Phenotypic and Transcriptomic Characterization of Bacillus subtilis Mutants with Grossly Altered Membrane Composition', *Journal of Bacteriology*, 190(23), p. 7797.

Saraste, M. (1999) 'Oxidative phosphorylation at the fin de siecle', *Science*, pp. 1488–1493.

Sarges, R. and Witkop, B. (1965) 'Gramicidin A. V. The Structure of Valine- and Isoleucine-gramicidin A', *Journal of the American Chemical Society*, 87(9), pp. 2011–2020.

Sauermann, R., Rothenburger, M., Graninger, W. and Joukhadar, C. (2008) 'Daptomycin: A Review 4 Years after First Approval', *Pharmacology*, 81(2), pp. 79–91.

Scheffers, D.-J. and Pinho, M.G. (2005) 'Bacterial cell wall synthesis: new insights from localization studies', *Microbiology and molecular biology reviews : MMBR*, 69(4), pp. 585–607.

Scheinpflug, K., Krylova, O., Nikolenko, H., Thurm, C. and Dathe, M. (2015) 'Evidence for a novel mechanism of antimicrobial action of a cyclic R-,W-rich hexapeptide', *PLoS ONE*, 10(4).

Scheinpflug, K., Nikolenko, H., Komarov, I. V, Rautenbach, M. and Dathe, M. (2013) 'What Goes around Comes around-A Comparative Study of the Influence of Chemical Modifications on the Antimicrobial Properties of Small Cyclic Peptides.', *Pharmaceuticals (Basel, Switzerland)*, 6(9), pp. 1130–44.

Scheinpflug, K., Wenzel, M., Krylova, O., Bandow, J.E., Dathe, M. and Strahl, H. (2017) 'Antimicrobial peptide cWFW kills by combining lipid phase separation with

autolysis', *Scientific Reports*, 7(1), p. 44332.

Schindelin, J., Arganda-Carreras, I., Frise, E., Kaynig, V., Longair, M., Pietzsch, T., Preibisch, S., Rueden, C., Saalfeld, S., Schmid, B., Tinevez, J.Y., White, D.J., Hartenstein, V., Eliceiri, K., Tomancak, P. and Cardona, A. (2012) 'Fiji: an open-source platform for biological-image analysis', *Nature methods*, 9(7), pp. 676–682.

Schindler, B.D., Frempong-Manso, E., DeMarco, C.E., Kosmidis, C., Matta, V., Seo, S.M. and Kaatz, G.W. (2014) 'Analyses of Multidrug Efflux Pump-Like Proteins Encoded on the Staphylococcus aureus Chromosome', *Antimicrobial Agents and Chemotherapy*, 59(1), pp. 747–748.

Schirner, K. and Errington, J. (2009) 'The cell wall regulator σI specifically suppresses the lethal phenotype of mbl mutants in Bacillus subtilis', *Journal of Bacteriology*, 191(5), pp. 1404–1413.

Schirner, K., Marles-Wright, J., Lewis, R.J. and Errington, J. (2009) 'Distinct and essential morphogenic functions for wall- and lipo-teichoic acids in Bacillus subtilis', *The EMBO journal*, 28(7), pp. 830–842.

Schneider, J., Klein, T., Mielich-Süss, B., Koch, G., Franke, C., Kuipers, O.P., Kovács, Á.T., Sauer, M. and Lopez, D. (2015) 'Spatio-temporal Remodeling of Functional Membrane Microdomains Organizes the Signaling Networks of a Bacterium', *PLoS Genetics*, 11(4), p. e1005140.

Schuster, S., Bohnert, J.A., Vavra, M., Rossen, J.W. and Kern, W. V. (2019) 'Proof of an outer membrane target of the efflux inhibitor phe-Arg-β-naphthylamide from random mutagenesis', *Molecules*, 24(3), p. 470.

Scott, W.R.P., Baek, S. Bin, Jung, D., Hancock, R.E.W. and Straus, S.K. (2007) 'NMR structural studies of the antibiotic lipopeptide daptomycin in DHPC micelles', *Biochimica et Biophysica Acta - Biomembranes*. Biochim Biophys Acta, pp. 3116–3126.

Seeger, M.A., Von Ballmoos, C., Verrey, F. and Pos, K.M. (2009) 'Crucial role of Asp408 in the proton translocation pathway of multidrug transporter AcrB: Evidence from site-directed mutagenesis and carbodiimide labeling', *Biochemistry*, 48(25), pp. 5801–5812.

Seeger, M.A., Schiefner, A., Eicher, T., Verrey, F., Diederichs, K. and Pos, K.M.

(2006) 'Structural asymmetry of AcrB trimer suggests a peristaltic pump mechanism', *Science*, 313(5791), pp. 1295–1298.

Seistrup, K.H. (2018) *MreB Dependent Cell Envelope Homeostasis in Bacillus subtilis*. Newcastle University.

Seydlová, G., Sokol, A., Lišková, P., Konopásek, I. and Fišer, R. (2018) 'Daptomycin Pore Formation and Stoichiometry Depend on Membrane Potential of Target Membrane', *Antimicrobial Agents and Chemotherapy*, 63(1), pp. e01589-18.

Sharff, A., Fanutti, C., Shi, J., Calladine, C. and Luisi, B. (2001) 'The role of the TolC family in protein transport and multidrug efflux. ', *European Journal of Biochemistry*, 268(19), pp. 5011–5026.

Shrivastava, R. and Chng, S.S. (2019) 'Lipid trafficking across the Gram-negative cell envelope', *Journal of Biological Chemistry*, 294(39), pp. 14175–14184.

Shrivastava, R., Jiang, X. and Chng, S.S. (2017) 'Outer membrane lipid homeostasis via retrograde phospholipid transport in Escherichia coli', *Molecular Microbiology*, 106(3), pp. 395–408.

Siewert, G. and Strominger, J.L. (1967) 'BACITRACIN: AN INHIBITOR OF THE DEPHOSPHORYLATION OF LIPID PYROPHOSPHATE, AN INTERMEDIATE IN THE BIOSYNTHESIS OF THE PEPTIDOGLYCAN OF BACTERIAL CELL WALLS', *Proceedings of the National Academy of Sciences*, 57(3), pp. 767–773.

Silverman, J.A., Perlmutter, N.G. and Shapiro, H.M. (2003) 'Correlation of daptomycin bactericidal activity and membrane depolarization in Staphylococcus aureus', *Antimicrobial Agents and Chemotherapy*, 47(8), pp. 2538–2544.

Silvestro, L., Weiser, J.N. and Axelsen, P.H. (2000) 'Antibacterial and Antimembrane Activities of Cecropin A in Escherichia coli', *Antimicrobial Agents and Chemotherapy*, 44(3), p. 602.

Simons, K. and Ikonen, E. (1997) 'Functional rafts in cell membranes', *Nature*, 387(6633), pp. 569–572.

Singer, S.J. and Nicolson, G.L. (1972) 'The fluid mosaic model of the structure of cell membranes', *Science*, 175(4023), pp. 720–731.

Smart, O.S., Goodfellow, J.M. and Wallace, B.A. (1993) 'The pore dimensions of gramicidin A', *Biophysical Journal*, 65(6), pp. 2455–2460.

Smith, T.J., Blackman, S.A. and Foster, S.J. (2000) 'Autolysins of Bacillus subtilis: multiple enzymes with multiple functions', *Microbiology*, 146(2), pp. 249–262.

Soldo, B., Lazarevic, V. and Karamata, D. (2002) 'tagO is involved in the synthesis of all anionic cell-wall polymers in Bacillus subtilis 168', *Microbiology*, 148(7), pp. 2079–2087.

Spanova, M., Zweytick, D., Lohner, K., Klug, L., Leitner, E., Hermetter, A. and Daum, G. (2012) 'Influence of squalene on lipid particle/droplet and membrane organization in the yeast Saccharomyces cerevisiae', *Biochimica et Biophysica Acta (BBA) - Molecular and Cell Biology of Lipids*, 1821(4), pp. 647–653.

Stiefel, P., Schmidt-Emrich, S., Maniura-Weber, K. and Ren, Q. (2015) 'Critical aspects of using bacterial cell viability assays with the fluorophores SYTO9 and propidium iodide', *BMC Microbiology*, 15(1), pp. 1–9.

Storm, D.R. and Strominger, J.L. (1973) 'Complex Formation between Bacitracin Peptides and Isoprenyl Pyrophosphates', *Journal of Biological Chemistry*, 248(11), pp. 3940–3945.

Strahl, H., Bürmann, F. and Hamoen, L.W. (2014) 'The actin homologue MreB organizes the bacterial cell membrane.', *Nature communications*, 5, p. 3442.

Strahl, H. and Errington, J. (2017) 'Bacterial Membranes: Structure, Domains, and Function', *Annual Review of Microbiology*, 71(1), pp. 519–538.

Strahl, H. and Hamoen, L.W. (2010) 'Membrane potential is important for bacterial cell division.', *Proceedings of the National Academy of Sciences of the United States of America*, 107(27), pp. 12281–6.

Szczepaniak, J., Holmes, P., Rajasekar, K., Kaminska, R., Samsudin, F., Inns, P.G., Rassam, P., Khalid, S., Murray, S.M., Redfield, C. and Kleanthous, C. (2020) 'The lipoprotein Pal stabilises the bacterial outer membrane during constriction by a mobilisation-and-capture mechanism', *Nature Communications*, 11(1).

Tacconelli, E., Carrara, E., Savoldi, A., Harbarth, S., Mendelson, M., Monnet, D.L., Pulcini, C., Kahlmeter, G., Kluytmans, J., Carmeli, Y., Ouellette, M., Outterson, K., Patel, J., Cavaleri, M., Cox, E.M., Houchens, C.R., Grayson, M.L., Hansen, P., Singh, N., Theuretzbacher, U., Magrini, N., Aboderin, A.O., Al-Abri, S.S., Awang Jalil, N., Benzonana, N., Bhattacharya, S., Brink, A.J., Burkert, F.R., Cars, O., Cornaglia, G.,

Dyar, O.J., Friedrich, A.W., Gales, A.C., Gandra, S., Giske, C.G., Goff, D.A., Goossens, H., Gottlieb, T., Guzman Blanco, M., Hryniewicz, W., Kattula, D., Jinks, T., Kanj, S.S., Kerr, L., Kieny, M.P., Kim, Y.S., Kozlov, R.S., Labarca, J., Laxminarayan, R., Leder, K., Leibovici, L., Levy-Hara, G., Littman, J., Malhotra-Kumar, S., Manchanda, V., Moja, L., Ndoye, B., Pan, A., Paterson, D.L., Paul, M., Qiu, H., Ramon-Pardo, P., Rodríguez-Baño, J., Sanguinetti, M., Sengupta, S., Sharland, M., Si-Mehand, M., Silver, L.L., Song, W., Steinbakk, M., Thomsen, J., Thwaites, G.E., van der Meer, J.W., Van Kinh, N., Vega, S., Villegas, M.V., Wechsler-Fördös, A., Wertheim, H.F.L., Wesangula, E., Woodford, N., Yilmaz, F.O. and Zorzet, A. (2018) 'Discovery, research, and development of new antibiotics: the WHO priority list of antibiotic-resistant bacteria and tuberculosis', *The Lancet Infectious Diseases*, 18(3), pp. 318–327.

Takahashi, Y. and Nakashima, T. (2018) 'Actinomycetes, an Inexhaustible Source of Naturally Occurring Antibiotics', *Antibiotics*, 7(2), p. 45.

Takeuchi, Y. and Nikaido, H. (1981) 'Persistence of segregated phospholipid domains in phospholipid--lipopolysaccharide mixed bilayers: studies with spin-labeled phospholipids.', *Biochemistry*, 20(3), pp. 523–9.

Tantibhedhyangkul, W., Wongsawat, E., Matamnan, S., Inthasin, N., Sueasuay, J. and Suputtamongkol, Y. (2019) 'Anti-mycoplasma activity of daptomycin and its use for mycoplasma elimination in cell cultures of rickettsiae', *Antibiotics*, 8(3).

Tascón, I., Sousa, J.S., Corey, R.A., Mills, D.J., Griwatz, D., Aumüller, N., Mikusevic, V., Stansfeld, P.J., Vonck, J. and Hänelt, I. (2020) 'Structural basis of proton-coupled potassium transport in the KUP family', *Nature Communications*, 11(1), pp. 1–10.

Taylor, R.M., Scott, B., Taylor, S. and Palmer, M. (2017) 'An Acyl-Linked Dimer of Daptomycin Is Strongly Inhibited by the Bacterial Cell Wall', *ACS Infectious Diseases*, 3(7), pp. 462–466.

van Teeffelen, S., Wang, S., Furchtgott, L., Huang, K.C., Wingreen, N.S., Shaevitz, J.W. and Gitai, Z. (2011) 'The bacterial actin MreB rotates, and rotation depends on cell-wall assembly.', *Proceedings of the National Academy of Sciences of the United States of America*, 108(38), pp. 15822–7.

Tesson, B., Dajkovic, A., Keary, R., Marlière, C., Dupont-Gillain, C.C. and Carballido-López, R. (2022) 'Magnesium rescues the morphology of Bacillus subtilis mreB

mutants through its inhibitory effect on peptidoglycan hydrolases', *Scientific Reports*, 12(1), pp. 1–14.

Thackray, P.D. and Moir, A. (2003) 'SigM, an Extracytoplasmic Function Sigma Factor of Bacillus subtilis, Is Activated in Response to Cell Wall Antibiotics, Ethanol, Heat, Acid, and Superoxide Stress', *Journal of Bacteriology*, 185(12), p. 3491.

Thong, S., Ercan, B., Torta, F., Fong, Z.Y., Alvina Wong, H.Y., Wenk, M.R. and Chng, S.S. (2016) 'Defining key roles for auxiliary proteins in an ABC transporter that maintains bacterial outer membrane lipid asymmetry', *eLife*, 5.

Touzé, T., Tran, A.X., Hankins, J. V., Mengin-Lecreulx, D. and Trent, M.S. (2008) 'Periplasmic phosphorylation of lipid A is linked to the synthesis of undecaprenyl phosphate', *Molecular Microbiology*, 67(2), pp. 264–277.

Tsuchido, T., Svarachorn, A., Soga, H. and Takano, M. (1990) 'Lysis and aberrant morphology of Bacillus subtilis cells caused by surfactants and their relation to autolysin activity.', *Antimicrobial Agents and Chemotherapy*, 34(5), p. 781.

Tsukagoshi, N. and Aono, R. (2000) 'Entry into and release of solvents by Escherichia coli in an organic-aqueous two-liquid-phase system and substrate specificity of the AcrAB-TolC solvent-extruding pump', *Journal of Bacteriology*, 182(17), pp. 4803–4810.

Tu, Y. and Yan, B. (2012) 'High-throughput fractionation of natural products for drug discovery', *Methods in Molecular Biology*, 918, pp. 117–126.

Urban, A., Eckermann, S., Fast, B., Metzger, S., Gehling, M., Ziegelbauer, K., Rübsamen-Waigmann, H. and Freiberg, C. (2007) 'Novel whole-cell antibiotic biosensors for compound discovery', *Applied and Environmental Microbiology*, 73(20), pp. 6436–6443.

Vaara, M. (1993) 'Antibiotic-supersusceptible mutants of Escherichia coli and Salmonella typhimurium.', *Antimicrobial Agents and Chemotherapy*, 37(11), p. 2255.

Vaara, M. (2019) 'Polymyxins and their potential next generation as therapeutic antibiotics', *Frontiers in Microbiology*, 10, p. 1689.

Vaara, M. and Vaara, T. (1983) 'Polycations as outer membrane-disorganizing agents.', *Antimicrobial agents and chemotherapy*, 24(1), pp. 114–22.

Vance, J.E. (2015) 'Phospholipid Synthesis and Transport in Mammalian Cells',

Traffic, 16(1), pp. 1–18.

Vargiu, A. V., Ruggerone, P., Opperman, T.J., Nguyen, S.T. and Nikaido, H. (2014) 'Molecular mechanism of MBX2319 inhibition of Escherichia coli AcrB multidrug efflux pump and comparison with other inhibitors', *Antimicrobial agents and chemotherapy*, 58(10), pp. 6224–6234.

Verstraeten, N., Knapen, W.J., Kint, C.I., Liebens, V., Van den Bergh, B., Dewachter, L., Michiels, J.E., Fu, Q., David, C.C., Fierro, A.C., Marchal, K., Beirlant, J., Versées, W., Hofkens, J., Jansen, M., Fauvart, M. and Michiels, J. (2015) 'Obg and Membrane Depolarization Are Part of a Microbial Bet-Hedging Strategy that Leads to Antibiotic Tolerance', *Molecular Cell*, 59(1), pp. 9–21.

Wachi, M., Doi, M., Tamaki, S., Park, W., Nakajima-Iijima, S. and Matsuhashi, M. (1987) 'Mutant isolation and molecular cloning of mre genes, which determine cell shape, sensitivity to mecillinam, and amount of penicillin-binding proteins in Escherichia coli.', *Journal of bacteriology*, 169(11), pp. 4935–40.

Waggoner, A. (1976) 'Optical probes of membrane potential', *The Journal of Membrane Biology*, 27(1), pp. 317–334.

Wang, A.Y. and Cronan, J.E. (1994) 'The growth phase-dependent synthesis of cyclopropane fatty acids in Escherichia coli is the result of an RpoS(KatF)-dependent promoter plus enzyme instability.', *Molecular microbiology*, 11(6), pp. 1009–17.

Watkinson, R.J., Hussey, H. and Baddiley, J. (1971) 'Shared lipid phosphate carrier in the biosynthesis of teichoic acid and peptidoglycan', *Nature: New biology*, 229(2), pp. 57–59.

Watve, M.G., Tickoo, R., Jog, M.M. and Bhole, B.D. (2001) 'How many antibiotics are produced by the genus Streptomyces?', *Archives of microbiology*, 176(5), pp. 386–390.

Weart, R.B., Lee, A.H., Chien, A.C., Haeusser, D.P., Hill, N.S. and Levin, P.A. (2007) 'A metabolic sensor governing cell size in bacteria', *Cell*, 130(2), p. 335.

Wecke, J., Madela, K. and Fischer, W. (1997) 'The absence of D-alanine from lipoteichoic acid and wall teichoic acid alters surface charge, enhances autolysis and increases susceptibility to methicillin in Bacillus subtilis', *Microbiology*, 143(9), pp. 2953–2960.

Wenzel, M., Kohl, B., Münch, D., Raatschen, N., Albada, H.B., Hamoen, L., Metzler-Nolte, N., Sahl, H.G. and Bandow, J.E. (2012) 'Proteomic response of Bacillus subtilis to lantibiotics reflects differences in interaction with the cytoplasmic membrane', *Antimicrobial Agents and Chemotherapy*, 56(11), pp. 5749–5757.

Wenzel, M., Rautenbach, M., Vosloo, J.A., Siersma, T., Aisenbrey, C.H.M., Zaitseva, E., Laubscher, W.E., van Rensburg, W., Behrends, J.C., Bechinger, B. and Hamoen, L.W. (2018) 'The multifaceted antibacterial mechanisms of the pioneering peptide antibiotics tyrocidine and gramicidin S', *mBio*, 9(5), pp. e00802-18.

Van Wezel, G.P. and McDowall, K.J. (2011) 'The regulation of the secondary metabolism of Streptomyces: New links and experimental advances', *Natural Product Reports*, pp. 1311–1333.

Wiedemann, I., Benz, R. and Sahl, H.G. (2004) 'Lipid II-Mediated Pore Formation by the Peptide Antibiotic Nisin: a Black Lipid Membrane Study', *Journal of Bacteriology*, 186(10), p. 3259.

Wiegert, T., Homuth, G., Versteeg, S. and Schumann, W. (2001) 'Alkaline shock induces the Bacillus subtilis σw regulon', *Molecular Microbiology*, 41(1), pp. 59–71.

Wiegeshoff, F., Beckering, C.L., Debarbouille, M. and Marahiel, M.A. (2006) 'Sigma L is important for cold shock adaptation of Bacillus subtilis', *Journal of Bacteriology*, 188(8), pp. 3130–3133.

Wilmsen, H.U., Pugsley, A.P. and Pattus, F. (1990) 'Colicin N forms voltage- and pH-dependent channels in planar lipid bilayer membranes', *European Biophysics Journal*, 18(3), pp. 149–158.

te Winkel, J.D., Gray, D.A., Seistrup, K.H., Hamoen, L.W. and Strahl, H. (2016) 'Analysis of Antimicrobial-Triggered Membrane Depolarization Using Voltage Sensitive Dyes', *Frontiers in Cell and Developmental Biology*, 4, p. 29.

Wolf, D., Domínguez-Cuevas, P., Daniel, R.A. and Mascher, T. (2012) 'Cell envelope stress response in cell wall-deficient L-forms of Bacillus subtilis', *Antimicrobial Agents and Chemotherapy*, 56(11), pp. 5907–5915.

Wood, T.M. and Martin, N.I. (2019) 'The calcium-dependent lipopeptide antibiotics: Structure, mechanism, & medicinal chemistry', *MedChemComm*, pp. 634–646.

World Health Organization (WHO) (2017) *WHO publishes list of bacteria for which*

new antibiotics are urgently needed.

Wörmann, M.E., Corrigan, R.M., Simpson, P.J., Matthews, S.J. and Gründling, A. (2011) 'Enzymatic activities and functional interdependencies of Bacillus subtilis lipoteichoic acid synthesis enzymes', *Molecular microbiology*, 79(3), pp. 566–583.

Wright, A., Dankert, M., Fennessey, P. and Robbins, P.W. (1967) 'Characterization of a polyisoprenoid compound functional in O-antigen biosynthesis', *Proceedings of the National Academy of Sciences of the United States of America*, 57(6), pp. 1798–1803.

Wu, L.J. and Errington, J. (2004) 'Coordination of cell division and chromosome segregation by a nucleoid occlusion protein in Bacillus subtilis', *Cell*, 117(7), pp. 915–925.

Wu, M., Maier, E., Benz, R. and Hancock, R.E.W. (1999) 'Mechanism of Interaction of Different Classes of Cationic Antimicrobial Peptides with Planar Bilayers and with the Cytoplasmic Membrane of Escherichia coli', *Biochemistry*, 38(22), pp. 7235–7242.

Yamamoto, H., Kurosawa, S.I. and Sekiguchi, J. (2003) 'Localization of the Vegetative Cell Wall Hydrolases LytC, LytE, and LytF on the Bacillus subtilis Cell Surface and Stability of These Enzymes to Cell Wall-Bound or Extracellular Proteases', *Journal of Bacteriology*, 185(22), p. 6666.

Yang, L., Lu, S., Belardinelli, J., Huc-Claustre, E., Jones, V., Jackson, M. and Zgurskaya, H.I. (2014) 'RND transporters protect Corynebacterium glutamicum from antibiotics by assembling the outer membrane', *MicrobiologyOpen*, 3(4), pp. 484–496.

Yang, X., Lyu, Z., Miguel, A., McQuillen, R., Huang, K.C. and Xiao, J. (2017) 'GTPase activity-coupled treadmilling of the bacterial tubulin FtsZ organizes septal cell wall synthesis', *Science*, 355(6326), pp. 744–747.

Yoon, V. and Nodwell, J.R. (2014) 'Activating secondary metabolism with stress and chemicals', *Journal of Industrial Microbiology and Biotechnology*, pp. 415–424.

Yoshimura, M., Asai, K., Sadaie, Y. and Yoshikawa, H. (2004) 'Interaction of Bacillus subtilis extracytoplasmic function (ECF) sigma factors with the N-terminal regions of their potential anti-sigma factors', *Microbiology*, 150(3), pp. 591–599.

Yu, X.C. and Margolin, W. (1999) 'FtsZ ring clusters in min and partition mutants: role of both the Min system and the nucleoid in regulating FtsZ ring localization', *Molecular microbiology*, 32(2), pp. 315–326.

Zakharov, S.D., Eroukova, V.Y., Rokitskaya, T.I., Zhalnina, M. V., Sharma, O., Loll, P.J., Zgurskaya, H.I., Antonenko, Y.N. and Cramer, W.A. (2004) 'Colicin occlusion of OmpF and TolC channels: Outer membrane translocons for colicin import', *Biophysical Journal*, 87(6), pp. 3901–3911.

Zhang, J., Scoten, K. and Straus, S.K. (2016) 'Daptomycin Leakage Is Selective', *ACS Infectious Diseases*, 2(10), pp. 682–687.

Zhang, T., Muraih, J.K., MacCormick, B., Silverman, J. and Palmer, M. (2014) 'Daptomycin forms cation- and size-selective pores in model membranes', *Biochimica et Biophysica Acta (BBA) - Biomembranes*, 1838(10), pp. 2425–2430.

Zhang, W., Yang, F.K., Han, Y., Gaikwad, R., Leonenko, Z. and Zhao, B. (2013) 'Surface and tribological behaviors of the bioinspired polydopamine thin films under dry and wet conditions', *Biomacromolecules*, 14(2), pp. 394–405.

Zhang, Y.M. and Rock, C.O. (2008) 'Membrane lipid homeostasis in bacteria', *Nature Reviews Microbiology 2008 6:3*, 6(3), pp. 222–233.

Zhao, J., Wu, J. and Veatch, S.L. (2013) 'Adhesion stabilizes robust lipid heterogeneity in supercritical membranes at physiological temperature.', *Biophysical journal*, 104(4), pp. 825–34.

Zhou, Z., White, K.A., Polissi, A., Georgopoulos, C. and Raetz, C.R.H. (1998) 'Function of Escherichia coli MsbA, an essential ABC family transporter, in lipid A and phospholipid biosynthesis', *The Journal of biological chemistry*, 273(20), pp. 12466–12475.

Zielińska, A., Savietto, A., Borges, A. de S., Martinez, D., Berbon, M., Roelofsen, J.R., Hartman, A.M., de Boer, R., Van der Klei, I.J., Hirsch, A.K.H., Habenstein, B., Bramkamp, M. and Scheffers, D.J. (2020) 'Flotillin-mediated membrane fluidity controls peptidoglycan synthesis and mreb movement', *eLife*, 9, pp. 1–21.

Zilberstein, D., Agmon, V., Schuldiner, S. and Padan, E. (1984) 'Escherichia coli intracellular pH, membrane potential, and cell growth', *Journal of Bacteriology*, 158(1), pp. 246–252.